Přírodovědecká fakulta
Faculty of Science

Jihočeská univerzita v Českých Budějovicích
University of South Bohemia in České Budějovice

JOHANNES KEPLER UNIVERSITY LINZ

Submitted by
Matthias Guggenberger

Elaborated at
Institute of Organic Chemistry

Thesis Supervisor
Univ.-Prof. Dr. Norbert Müller

Thesis Co-Supervisors
Dr. Matthias Bechmann
Dr. Stefan Aichhorn

July 2016

Synthesis of fMLF and $\mathcal{R}$-Symmetry Decoupling in Solid State NMR

Master Thesis

to confer the academic degree of

Master of Science

in the Joint Master Programme

Biological Chemistry (SKZ: 066 863)

JOHANNES KEPLER UNIVERSITY LINZ
Altenbergerstraße 69
4040 Linz
Austria
www.jku.at
DVR 0093696

Sworn Declaration - Johannes Kepler University, Linz

I hereby declare under oath that the submitted Master's degree thesis has been written solely by me without any third-party assistance, information other than provided sources or aids have not been used and those used have been fully documented. Sources for literal, paraphrased and cited quotes have been accurately credited.
The submitted document here present is identical to the electronically submitted text document

*Place and Date:*_____ *Signature:*_____

Sworn Declaration - University of South Bohemia, České Budějovice

I hereby declare that I have worked on my master's thesis independently and used only the sources listed in the bibliography.
I hereby declare that, in accordance with Article 47b of Act No. 111/1998 in the valid wording, I agree with the publication of my master thesis, in full form to be kept in the Faculty of Science archive, in electronic form in publicly accessible part of the STAG database operated by the University of South Bohemia in České Budějovice accessible through its web pages. Further, I agree to the electronic publication of the comments of my supervisor and thesis opponents and the record of the proceedings and results of the thesis defence in accordance with aforementioned Act No. 111/1998. I also agree to the comparison of the text of my thesis with the Theses.cz thesis database operated by the National Registry of University Theses and a plagerism detection system.

*Place and Date:*_____ *Signature:*_____

Acknowledgement

First of all I want to thank Univ.-Prof. Dr. Norbert Müller for giving me the chance to work at the Institute of Organic Chemistry, his supervision and him being ready to discuss the current state of the work at any time. Not only for this but also for his personal efforts in establishing and maintaining the unique study program of biological chemistry he deserves my gratitude.
I am also very grateful to my co-supervisors Dr. Stefan Aichhorn, who accompanied me on the journey through the field of organic chemistry, and Dr. Matthias Bechmann, who, not for the first time, guided me in the realms of solid state NMR. Both of them were always patiently willing to answer my questions and discuss my ideas as well as supporting me with their experiences in any thinkable way.
I further want to acknowledge Christian Rückl for his HPLC work and Dr. Mario Waser for counselling on synthetic topics as well as all the other people working at the Institute of Organic Chemistry for all their support. It is invaluable to work within such great atmosphere.
Additionally, I must not forget Prof. RNDr. Libor Grubhoffer, CSc, who is the initiator and co-ordinator of biological chemistry on the Czech side. His personal commitment for the University of South Bohemia, the study program and its students is something I really appreciate.
One person that was always at my side keeping me motivated and happy is my beloved partner Jacqueline. It was her who helped me to overcome obstacles not only with her understanding but also with her ideas. For that and at least thousand other things I love you!
Huge thanks naturally go to my family which enabled me to study and which supports me in everything I do. They too kept me in a good mood by making me smile whenever possible.
Finally, I want to express my thanks to my friends for the time spent together and study colleagues for the same reason and the fruitful collaboration during studying.

Contents

Abbreviations

Table I.: A list of all used abbreviations and their corresponding meaning

Abbreviation	**Explanation**
AcN	Acetonitrile
Ar-	Aryl-
Boc	*tert*-Butylcarbonyl protecting group
BOMI	benzotriazol-1-yl-oxy-*N,N*-dimethylmethaniminium hexachloroantimonate
BOP	tris-(dimethylamino)phosphonium hexafluorophosphate
Bt	Benzotriazole
Bz	Denotes the Benzyl Group
CP	Cross Polarisation
cpd	composite pulse decoupling
CSA	Chemical Shielding Anisotropy
DCC	*N,N'*-Dicyclohexylcarbodiimide
DCM	Dichloromethane
DCU	*N,N'*-Dicyclohexylurea
DDC	Direct Dipolar Coupling
DIC	*N,N'*-Diisopropylcarbodiimide
EDT	ethanedithiol
FID	Free induction decay
DMF	*N,N'*-Dimethylformamide
DMSO	Dimethylsulfoxide
EDC	*N*-ethyl-*N'*-(3-dimethylaminopropyl)carbodiimide
EDDQ	2-ethoxy-1-ethoxycarbonyl-1,2-dihydroquinoline
eDUMBO	experimental Decoupling Under Mind Boggling Optimisation
EtOAc	Ethylacetate
EtOH	Ethanol
ESI	Electrospray ionisation
Fmoc group	Fluorenylmethoxycarbonyl protecting group
G or Gly	Glycine
HATU	*O*-(7-azabenzotriazol-1-yl)-1,1,3,3-tetramethyluronium hexafluorophosphate
HBTU	*O*-(benzotriazol-1-yl)-1,1,3,3-tetramethyluronium hexafluorophosphate
HIV	Human Immunodeficiency Virus
HOAt	1-Hydroxy-7-azabenzotriazole
HOBt	Hydroxybenzotriazole
HOSu	*N*-hydroxysuccinimide
HPLC	High Pressure Liquid Chromatography
HSQC	Heteronuclear Single Quantum Correlation
INEPT	Insensitive Nuclei Enhancement by Polarisation Transfer
L or Leu	Leucine
MAS	Magic Angle Spinning
M or Met	Methionine
fMLF	*N*-Formyl-Methioninyl-Leucyl-Phenylalanine

Continuation of *Table I*, the Abbreviations List

Abbreviation	**Explanation**
MS	Mass Spectrometry
MSNT	1-(Mesitylene-2-sulfonyl)-3-nitro-1,2,4-triazole
NMP	*N*-Methylpyrrolidone
NMR	Nuclear Magnetic Resonance
Oxyma	Ethyl 2-cyano-2-(hydroxyimino)acetate
pdb	Protein Data Bank
F or Phe	Phenylalanine
PG	Protecting Group
mRNA	messenger Ribonucleic acid
rRNA	ribosomal Ribonucleic acid
tRNA	transfer Ribonucleic acid
rf	radiofrequency
r.t.	room temperature
SW	Spectral Width
TBAF	tetrabutylammoniumfluorid
TBTU	*O*-(benzotriazol-1-yl)-1,1,3,3-tetramethyluronium tetrafluorborate
Tcl	Tool Command Language
TEA	Triethylamin
THF	Tetrahydrofuran
TIS	Triisopropylsilane
TLC	Thin Layer Chromatography
TFA	Trifluoroacetic acid
qTOF	quadrupole time-of-flight mass analyser
TPPI	Time Proportional Phase Incrementation
Z	Carboxybenzyl protecting group

Abstract

The following thesis describes the investigations on the chemical synthesis of the tripeptide fMLF and the implementation of solid state NMR pulse sequences that employ dipolar decoupling based on the $\mathcal{R}$ symmetry.

fMLF in its ^{13}C and ^{15}N labelled from is often used as a reference substance in solid state NMR. This requires the synthesis to be as efficient as possible, especially with respect to expensive isotopically labelled compounds. In order to fulfil this requirement, four different synthesis routes based on solid phase peptide synthesis with Fmoc Protection were examined. In the course of these investigations several caveats of the original synthesis sequence [1] were identified. Although no robust procedure for the full route was found, several reactions such as Fmoc protections or *N*-terminal formylyations were optimised for further use in a labelled synthesis. Together, with the findings about the other reactions of the synthesis these lay the foundations for further investigations that certainly will lead to the desired synthesis procedure.

In the field of solid state NMR the implementation of three pulse sequences, which use $\mathcal{R}$ symmetry based decoupling schemes, was undertaken. The first pulse sequence is a ^{1}H experiment that produces high resolution proton spectra [2, 3]. The basic functionality of the experiment was confirmed although further improvement is necessary to make it suitable for routine application.

The second sequence is a ^{13}C experiment that affords spectra in which the splittings caused by the heteronuclear J-coupling can be seen. Upon optimising the acquisition parameters, the results stated in [2] could be reproduced. Further tests on other samples than adamantane stayed fruitless.

The third experiment, insprired by [4], is a $\mathcal{R}$ decoupled version of the well-known INEPT experiment[5]. Simulations confirmed the concept. With parameters, obtained from these, an experiment was set up on the spectrometer. Although promising in the beginning, it turned out to be not functional, requiring further investigations.

Zusammenfassung

Die folgende Arbeit beschreibt die Untersuchungen zur chemischen Synthese des Tripeptids fMLF und die Implemtierung von Festkörper NMR Pulssequenzen, welche dipolare Enkopplung basierend auf der $\mathcal{R}$ Symmetrie verwenden.
fMLF, in seiner ^{13}C und ^{15}N markierten Form wird oft als Referenzsubstanz in der Festkörper NMR Spektroskopie benutzt. Dies verlangt eine Synthese, welche die teuren Isotopen markierten Verbindungen möglichst effizient nützt. Um diese Voraussetzung zu erfüllen wurden vier verschiedene Syntheserouten untersucht, welchen alle die Festphasenpeptidsynthese mit Fmoc Schützung zugrunde lag. Während dieser Untesuchungen wurden einige Probleme der originalen Syntheseroute [1] identifiziert. Obwohl keine robuste Vorschrift für die gesamte Synthese gefunden werden konnte, wurden einige Reaktionen wie die Fmoc Schützungen und die N-terminalen Formylierungen für eine zukünftige Verwendung mit markierten Edukten optimiert. Zusammen mit den Informationen über die restlichen Reaktionen der Synthese legen diese optimierten Reaktionen den Grundstein für weiterführende Experimente die sicherlich zur gewünschten Synthesevorschrift führen werden.
Im Festkörper NMR-Bereich wurden drei Pulssequenzen, welche $\mathcal{R}$ basierende Enkopplungsschmata beinhalten, implementiert und untersucht.
Die erste Pulssequenz ist ein Experiment, welches hochaulösende ^{1}H Spektren liefert [2, 3]. Die grundsätzlich Funktionsfähigkeit diese Experiments wurde bestätigt, wenngleich weitere Verbesserungen notwendig sind um es für Routineanwendungen zu nutzen.
Die zweite Sequenz ist ein ^{13}C Experiment Spektren produziert, die von der heteronuclearen J-Kopplung verursachte Aufspaltungen zeigen. Durch Optimierung der Aufnahmeparameter konnten die Ergebisse von [2] reproduziert werden. Weitere Tests an anderen Proben die kein Adamantan enthielten waren fruchtlos.
Das dritte Experiment, in Anlehnung an [4], ist eine $\mathcal{R}$ enkoppelte Form des bekannten INEPT Experiments. Durch Simulationen wurde dieses Konzept bestätigt. Mit den dabei optimierten Parametern wurde ein NMR experiment aufgesetzt. Obwohl, diese zu Beginn vielversprechende Ergebnisse lieferte wurde herausgefunden, dass es trotz allem nicht die erwartete Funktion erfüllte und wetere Untersuchungen notwendg sind.

Keywords

Solid Phase Peptide Synthesis, Solid State NMR, fMLF, $\mathcal{R}$ Symmetry, Formylation, Spectrum Simulation

Annotation

Guggenberger M., 2016. Synthesis of fMLF and $\mathcal{R}$-Symmetry Decoupling in Solid State NMR. (Master thesis in English) - 118p., Institute of Organic Chemistry, Johannes Kepler University, Linz, Austria.

1. Introduction and Theory

1.1. Peptide Synthesis

Peptides and proteins are the foundation of life as it is known on earth, being of fundamental importance for various biochemical functions in biological systems. Some of these are structural integrity, catalysis, storage, transport and signal transduction amongst others. They are constituted of a certain set of α-L-amino acids, which are connected by amide bonds forming chains consisting of a few up to thousands of single amino acid units. These amino acids have chemically different side chains that dictate the three dimensional structure of the folded protein giving rise to its function.
In living organisms (poly)peptides usually are synthesized by ribosomes, a macromolecular complex of protein and rRNA components. mRNA is employed to provide information on the sequences of the individual amino acids and tRNAs guide the incorporation of amino acids into the nascent peptide in order to correctly match the mRNA code. [6]
As not just in nature peptides are key players, there is a high interest for synthetically produced peptides and their derivatives. They are invaluable in several fields of research for instance in the study of proteases (as models for proteins) and peptide hormones [7], in solid state NMR as reference substance [1] (see *Section 1.1.4*) or as subject of structure elucidation [8] (in case the (poly)peptides are solid in their native fold) as well as in medicinal chemistry and molecular biology either for the elucidation of biochemical mechanisms [9] or as drugs. [10] Finally, peptides are often very complex assemblies and therefore some are still considered to be synthetic challenges [7].
In the following, an overview of important methods in peptide synthesis will be given.

1.1.1. Linking Amino Acids

The most crucial part of peptide synthesis is the actual creation of the amide bond, which connects amino acids. In organic chemistry, a huge variety of approaches to perform this reaction has been developed as it does not occur spontaneously, apart from high temperature conditions (160-180 °C), which are, however, considered as extremely undesirable in peptide synthesis. [7, 11]

1.1.1.1. General Approaches

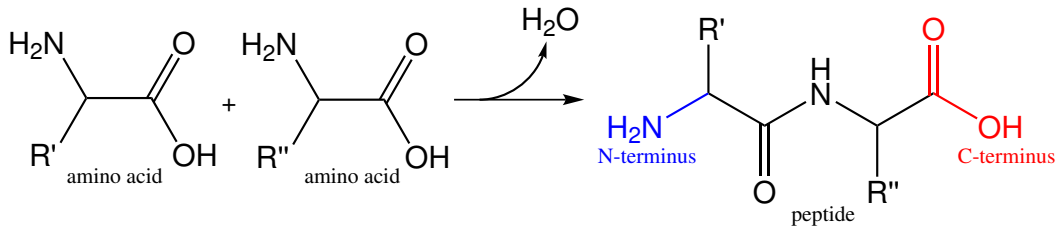

Figure 1.1.: Illustration of the condensation of two amino acids with the side chains R' and R'' to a dipeptide under formal elimination of water.

Acid Chlorides Basically, the principle behind all amino acid coupling procedures is the activation of the carboxyl group of one amino acid, which is then attacked by the amino group of the other amino acid giving rise to the amide bond. One of the simplest ways to activate the C-terminus of an amino acid or peptide is to convert it to a carboxylic acid chloride as it was actually done in the early days of peptide chemistry by Emil Fischer. [12] The reagents to form acyl chlorides such as thinoyl chloride, phosphorous oxichloride or phosphorous pentachloride inherit the drawback of forming HCl during the reaction, which has to be taken into account when using compounds susceptible to damage by acidic conditions. Additionally, these reagents may react with other parts of the amino acid such as side chain amide groups, which may be transformed into nitriles. Moreover, the actual coupling reaction with the amine is prone to side reactions. Examples among others are the cleavage of protecting groups, hydrolysis, intramolecular attack followed by cyclisation as well as racemisation under basic conditions.[1.1] The racemisation mechanism is thought to work via the generation of a ketene. This compound is prochiral and can react to different enantiomers, when treated with an amine (*Figure 1.2*).

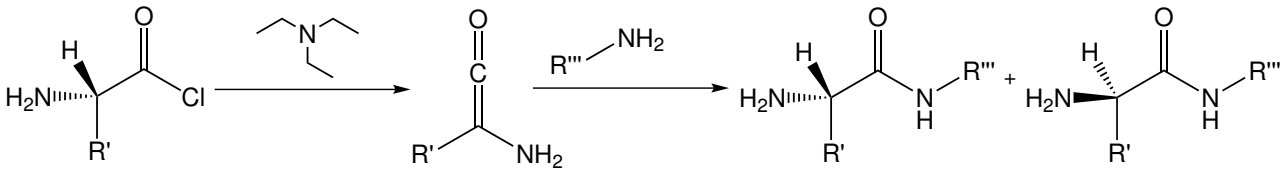

Figure 1.2.: Illustration of the racemisation of acyl chlorides reaction via a ketene intermediate. (Reproduced from [11])

It is obvious that the use of acid chlorides is problematic due to the high reactivity of the acid chlorides as well as the reagents used to generate them, which leads to various side reactions. [7, 11]

Azides Another way to form the amide bond, which stems from one of the pioneers of peptide chemistry, Theodor Curtius, is the azidation method. Although discovered over hundred years ago, it still is of significance as it exhibits several advantageous characteristics.[13] The preparation of the reactive azide is achieved by the reaction of an amino acid methyl ester with

[1.1] Basic condition are often desired during coupling in order to prevent protonation of the amino group by the evolving HCl and therefore reduction of its reactivity. [11]

hydrazine, which gives an intermediate hydrazide. This is subsequently converted to the azide via treatment with nirtous acid (or some alkyl nitrite) as shown in the following figure.

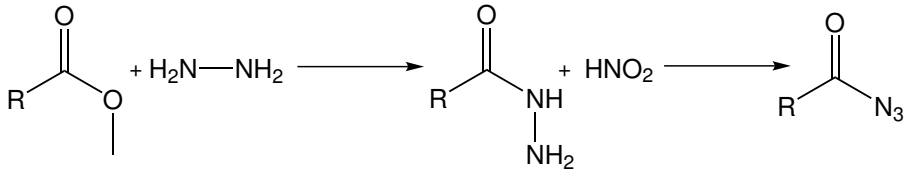

Figure 1.3.: Reaction scheme showing the process of amino acyl azide synthesis. (Reproduced from [11])

By treating the acyl azide with the amine functionality of an amino acid the peptide bond is established. One of most advantageous features of such conversions is that azides of peptides normally do not undergo racemisation, unless the conditions are too basic. Furthermore, a separate removal of the ester protecting group at the C-terminus can be avoided.
Nevertheless, the azide process also exhibits drawbacks, the most obvious being the fact that hydrazine is a very hazardous compound, being potentially carcinogenic on top of its very high acute toxicity.[14] Further, there is the possibility of side reactions predominantly in the form of the Curtius rearrangement. Upon this reaction the azide is converted to a isocyanate, whereby N_2 is formed. The isocyanate can be transformed in several ways, for instance to the corresponding amine accompanied by the evolution of CO_2 or with another amine to urea derivates (*Figure 1.4*).

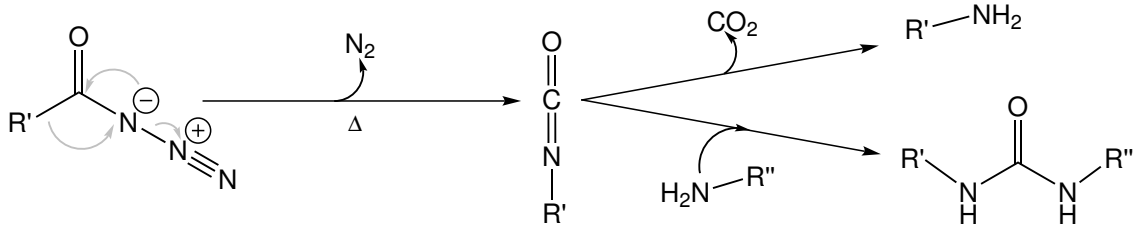

Figure 1.4.: Reaction pathway illustrating the Curtius rearrangement type of side reaction during azide coupling and two possible follow up reactions. The upper possibility shows the decarboxylation to the amine and the lower one the formation of an urea. [15]

One more inconvenience of the azide approach is that reaction times are usually very long (up to a few days) particularly at low temperatures, which are often used to minimize side reactions. In spite of these issues it is necessary to mention that this way of peptide synthesis is still not obsolete. Mainly in coupling reactions that show great vulnerability in terms of optical purity, the azide method is of practical significance. [7, 11, 15]

Anhydrides A further technique of establishing amide bonds is by activating the carboxylic acid moiety via anhydrides. This can be achieved utilizing either symmetric or mixed anhydrides. Both ways, however, have their caveats. [11]
Working with symmetric anhydrides, maximum yields of 50% can be achieved, when comparing it to the amount of amino acid initially used for the formation of the anhydride. Of course the

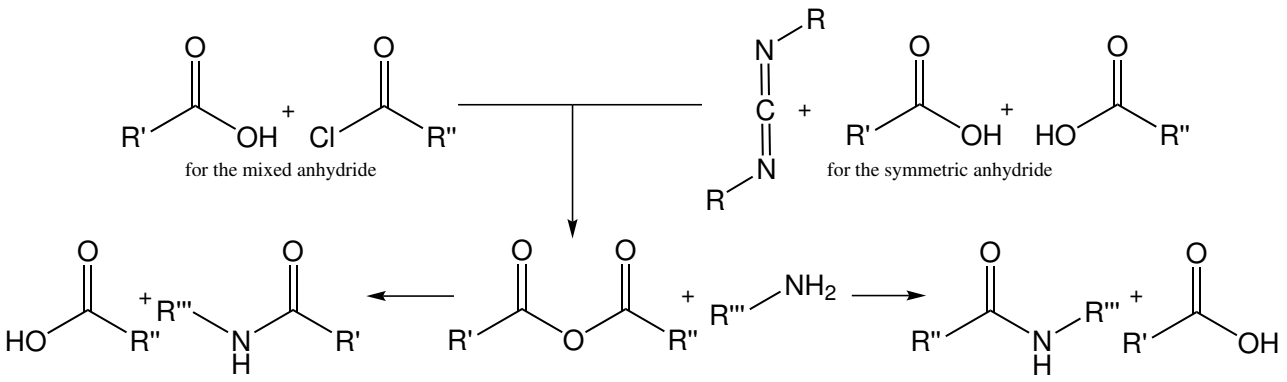

Figure 1.5.: Scheme illustrating the preparation of mixed (via acid chlorides e.g. ethyl chloroformate) and symmetric anhydrides (mediated by carbodiimides such as DCC; R' = R") as well as the challenges associated with them: If R' is equal to R" a symmetric anhydride is present where half of the acid does not react to an amide.
If R' is not equal to R" a mixed anhydride is present that theoretically allows the formation of two different products, whereby just one is desired. [7, 11, 15, 16]

rest of the amino acid is not lost. It can be recovered and reused. Nevertheless, this process is often rather expensive and time consuming.

Practically, a the symmetric anhydride is generated by treatment of two equivalents of carboxylic acid with one equivalent of DCC (*N,N'*-dicyclohexyl carbodiimide). Thereby first the *O*-acylisourea (see next section) is formed. This is then converted to the anhydride by a second molecule of acid, whereby DCU (*N,N'*-dicyclohexylurea) precipitates. Treatment with the desired amine gives the amide.

Concerning mixed anhydrides the problem of wasting half the starting material is not relevant as the anhydride is made with the desired acid and another one, which is just a kind of "leaving group". This would be the ideal case. In reality, however, it is rather difficult to direct the attack of the amine exclusively to the correct carbonyl center.

This is for instance achieved by using a sterically hindered species such a pivalic acid or by the generation of mixed carbonic anhydrides. The latter way works due to the different chemical nature of the two carbonyl groups, making the carboxyl site more prone to aminolysis.

For producing the mixed carbonic anhydride ethyl chloroformate or similar reagents are often used. The reaction is carried out in two steps. First the activation with the chloroformate is done in presence of a tertiary amine (e.g. *N*-Methylmorpholine) followed by the addition of the nucleophilic amine. The process is usually quite fast with the activation in the range of minutes and the actual coupling reaction in about one hour. It has to be carried out at low temperatures (-5 to -15 °C) to avoid side reactions.

One of the side reactions specific to this approach is the formation of urethane derivatives. These are generated by the attack of the amine at the wrong carbonyl group. This can lead to a 10% decrease in the peptide yield. Another minor source for urethanes originates from unconsumed chloroformate reagent (see *Figure 1.6*).

Furthermore, there are more sophisticated reagents (e.g. EDDQ) and variations (e.g. cyclic anhydrides, phosphoric/boronic acid derived anhydrides, carbodiimides *etc.*) based on the

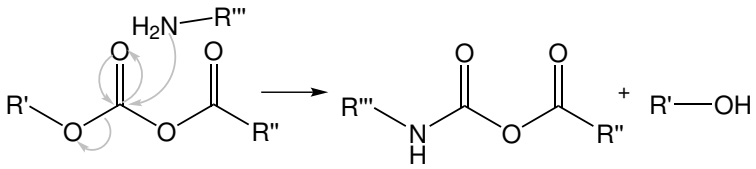

Figure 1.6.: The reaction generating the majority of the Urethane type side product in mixed carbonic anhydride coupling. The amine attacks the activated species at the carbonic acid carbonyl group leading to the undesired product. [16]

described approach that make it a very valuable and versatile tool in peptide chemistry. [7, 11, 15, 16]

Active Esters As the name of the active ester approach already suggests, this procedure relies on ester derivatives of the carboxylic acid group, which are reactive enough to undergo aminolysis. Hence, esters with methyl, ethyl or benzyl groups are not suitable as these would appear as protecting groups (see *Section 1.1.2*). The esters used for coupling purposes are groups with strong electron withdrawing capabilities. This increases the electrophilicity of the carbonyl carbon and makes it more susceptible to the nucleophilic attack of the amine. Additionally, in some species the anchimeric effect, the assistance of neighbouring groups in the reaction, contributes to their reactivity. Ester groups exhibiting these properties are substituted phenol compounds such as pentafluorophenol or *p*-nitrophenol or hydroxyl amine derivatives such as HOBt (Hydroxybenzotriazole).
Generally, the reactivity of most active esters is lower compared to other techniques (e.g. acid chlorides, anhydrides). Therefore, they are less prone to undesired side reactions. This also counts for racemisation.
The main way how to prepare active esters is via coupling by DCC or DIC (*N,N'*- diisopropylcarbodiimide). In many cases they are stable enough to be isolated and stored (e.g. pentafluorophenol esters).
All in all the active ester approach is a very useful one and integral part of several coupling methods which will be described in the following sections. [7, 11, 15, 16]

1.1.1.2. Carbodiimides - The Standard Method

The group of reagents, that are the *de facto* standard for the formation of peptide bonds are carbodiimides. There are several ways in which they are used. The most simple approach is just to activate the carboxylic acid directly with the carbodiimide. Thereby, an *O*-acylisourea derivative is formed which is then attacked by the amine (see *Figure 1.7*). Thereby, a urea species is generated when the isourea part of the activated molecule is displaced by the amine. The *O*-acylisourea species is a highly reactive compound and hence undergoes not only reaction with amines, as desired, but also transforms to several side products. One of these potential side reactions is the formation of symmetric anhydrides, which occurs in excess of the carboxylic acid. The superfluous carboxy groups attack the *O*-acylisourea leading to symmetric anhydrides.

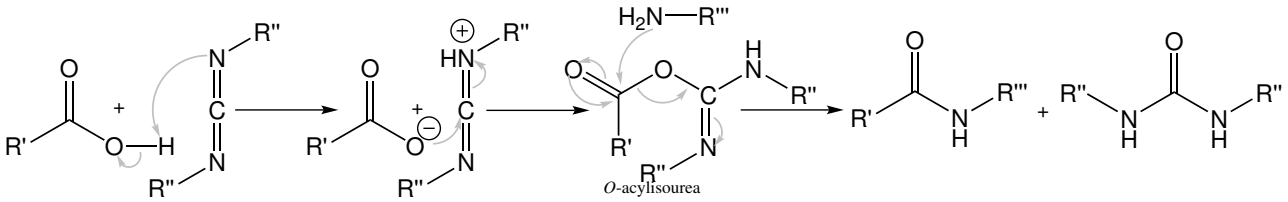

Figure 1.7.: Illustrating the activation using just carbodiimides followed by coupling to an amine. An intermediate *O*-acylisourea species of high reactivity is generated. It is transformed to the desired amide and an urea by-product upon nucleophilic attack of the amine. [15]

These products can further react with amines to the peptide and the free acid (see *Figure 1.5* - R' is equal to R''). This may be intended to happen when employing the symmetrical anhydride coupling method.

A side reaction which may pose a more serious problem to the formation of a peptide bond is the generation of *N*-acylurea. The mentioned compound forms upon intramolecular rearrangement and hampers the coupling reaction by being too unreactive to be able to undergo aminolysis. Hence, the yield is reduced and purification becomes more cumbersome.

In order to prevent this process, mixtures of the acid and the carbodiimide without the amines should be kept at 0°C. Additionally, DMF should be avoided as solvent as it speeds up the rearrangement reaction substantially.

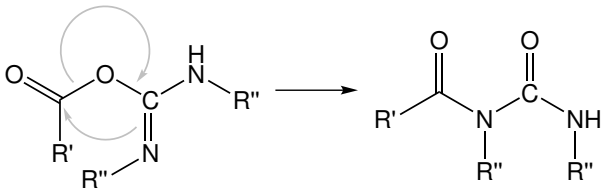

Figure 1.8.: Reaction scheme showing the intramolecular rearrangement of a highly activated *O*-acylisourea to an non reactive *N*-acylurea. (Reproduced from [15])

The last side reaction concerning direct *O*-acylisourea mediated coupling is the source of racemisation in this approach. It is the formation of oxazolone, as shown in the following figure.

It involoves the intramolecular nucleophilic attack of the tautomerized carbonyl group of the previous residue. Upon that a cyclic structure, the oxazolone, is formed.[1.2] The isourea part of the molecule acts as leaving group and is converted to the corresponding urea. Under mild basic condition this oxazolone can be deprotonated at the α-carbon, which leads to a conjugation stabilized anion. Reprotonation can occur from the one or the other side leading to a loss of optical purity. The oxazolone racemate itself is also reactive towards aminolysis, albeit slower. Hence, the desired amines are produced, however, without their chiral integrity.

Racemisation of this kind can be reduced using N-Terminal protection groups that are linked to the amino acid via a carbamate group and not directly via a simple amide bond. The reason for this is that the carbonyl group of a carbamate protecting group is less nucleophilic than

[1.2]Not only with carbodiimide activated acids oxazolone formation can take place. Also other activated species can undergo this side reaction, for instance acid chlorides.

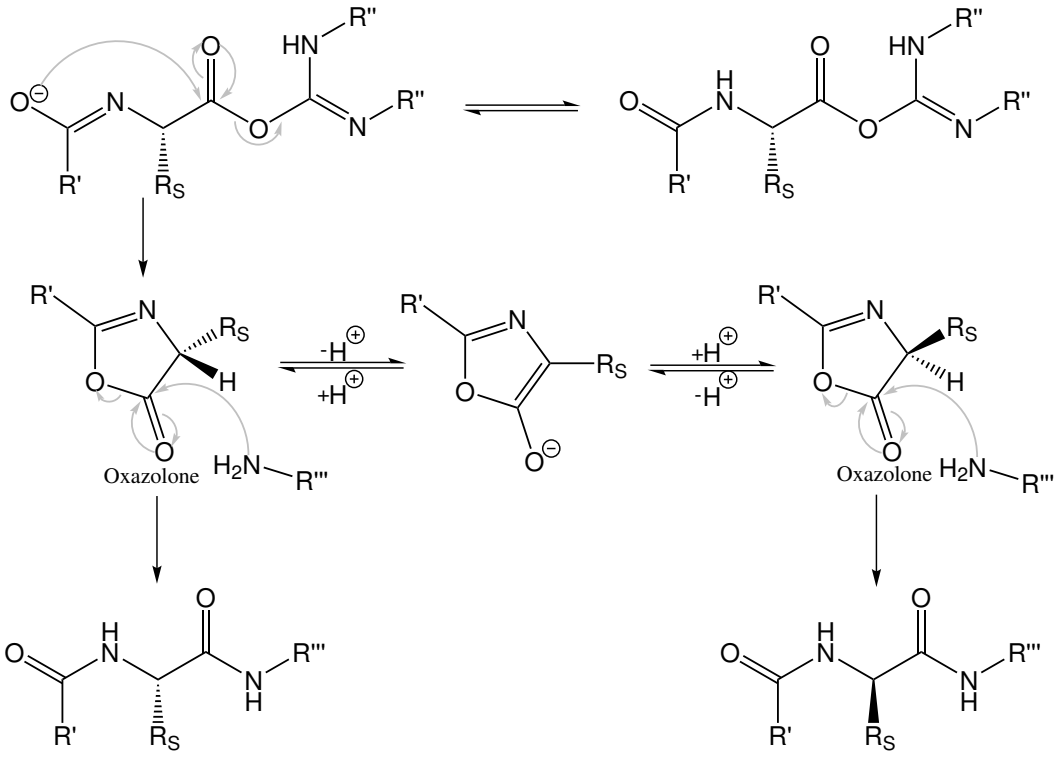

Figure 1.9.: Illustration of the racemisation pathway of an *O*-acylisourea via the oxazolone intermediate. [11, 15]
R_S ... amino acid side chain

the one of an amide. Examples of such protecting groups would be the Z and the Fmoc groups (see *Section 1.1.2*). [11, 15, 16]

Additives In order to circumvent side reactions, additives are employed. These are employed to produce activated carboxylic acid species, commonly activated esters, *in situ* that are further aminolysed, but are not as 'overreactive' as the corresponding *O*-acylisourea. Thereby the generation of the *O*-acylisourea is always the initial step. Subsequently, the reaction with the additive occurs. It is much faster than the side reactions, hence those are diminished. The most popular of these additives, namely HOBt, was introduced by König and Geiger in 1970. [17]

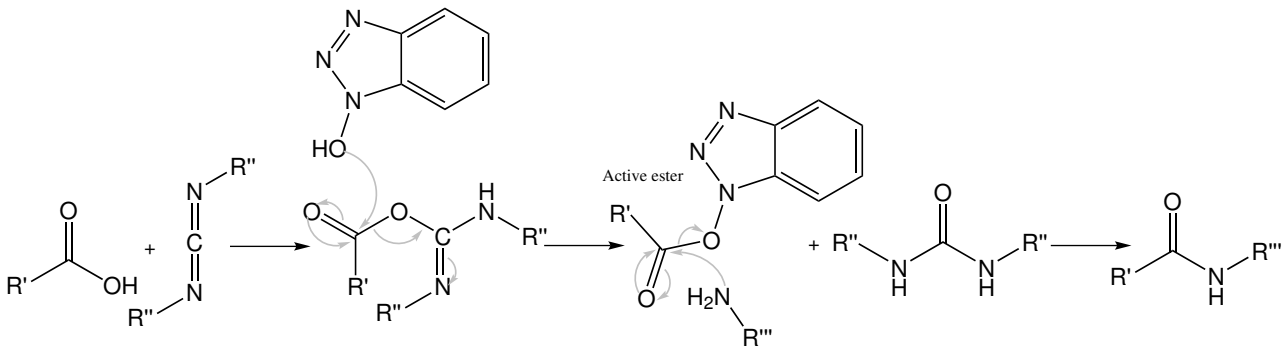

Figure 1.10.: Depiction of a coupling reaction using HOBt (Hydroxybenzotriazol) as additive, whereby an active ester is generated that is subsequently aminolysed. (Reproduced from [15])

However, there are dozens of other additives that have been found over time. Noteworthy exam-

ples are the rather expensive HOAt, which often leads to higher yields and lower racemisation when compared to other additives and Oxyma, which shows a similar performance as HOAt but is not consisting of rings with several nitrogens and hence is not considered an explosive. The reason for HOAt's superiority over HOBt comes from the interaction of the nitrogen in position seven (the only difference to HOBt) with the hydrogen of the attacking amine, which stabilizes conformation and increase reactivity (see *Figure 1.11 a.)*). Moreover, this N renders HOAt a better leaving group due to its electron withdrawing characteristics. [11, 15, 16]
Another additive for carbodiimide mediated couplings is *N*-hydroxysuccinimide (HOSu - *Figure 1.11 c.)*), which was already used before the introduction of HOBt and its derivatives. [17] This compound also reacts via the formation of an intermediate active ester by reaction with the *O*-acylisourea. In fact, *N*-hydroxysuccinimide esters can be easily purified and used in the multistep active esters procedure as described in *Section 1.1.1.1.* Despite the fact that HOSu esters tend to readily undergo side reactions and react slower than HOBt analogues, their major advantage is the water solubility of the reaction by-product. This facilitates purification of the product in many cases. [11, 15–17]
Summing up it is clear that the use of additives is a great enhancement for carbodiimide mediated amide couplings as it suppresses many side reactions and hence improves the efficiency of peptide synthesis. [11, 15, 16]

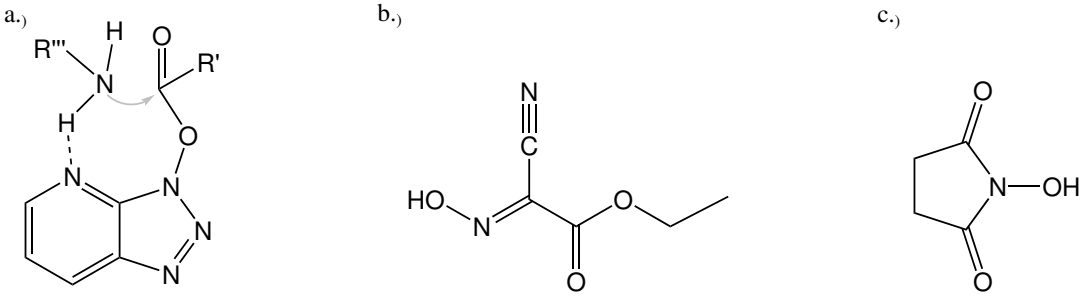

Figure 1.11.: a.) Structure of an HOAt ester and and the attack of an amine which is improved by the neighbouring group effect of HOAt [11], b.) Structure of Oxyma [16], c.) Structure of HOSu [15]

Urea solubility Another issue of the carbodiimide method in general is the urea by-product. Depending on the substituent of the carbodiimide the solubility of the resulting urea varies. DCC, which was used originally, is a sparingly soluble compound in most solvents. Therefore the majority of it can be mostly removed by filtration. However, often the compound cannot be completely removed and traces of it sometimes may not even be separated by column chromatography. Only TFA dissolves this urea, which makes it unsuitable for solid phase peptide synthesis according to the Fmoc strategy, which employs TFA as final cleavage reagent. The Boc strategy is feasable with this reagent, however, other carbodiimides have been found, of which the ureas show better solubility. One example would be DIC, which is soluble in DCM and hence is readily washed away in solid phase synthesis. Another example, which is suited for the use in solution phase chemistry, is EDC. It is soluble in aqueous solutions, and hence

easily separated during aqueous workup. [16]

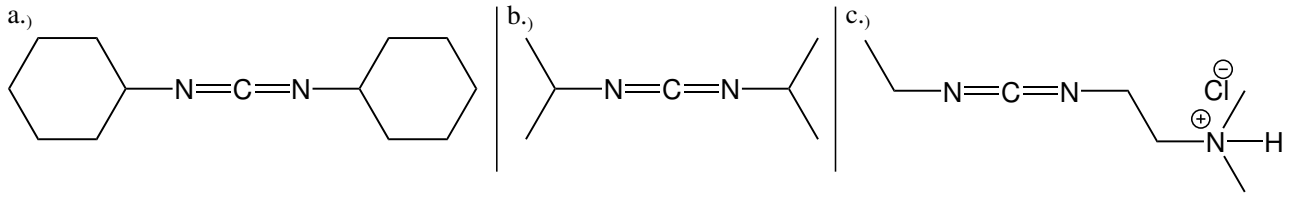

Figure 1.12.: Structures of different carbodiimides. Their corresponding ureas exhibit varying solubilities. a.) Structure of DCC, b.) Structure of DIC, c.) Structure of EDC hydrochloride [16]

Although all the carbodiimides are quite hazardous chemicals, being potent sensitizers, they are of immense value for peptide synthesis. They are the heart of the classical approach to form peptide bonds and still widely used due to their beneficial characteristics. [11, 15]

1.1.1.3. Phosphonium, Uronium and Iminium Type Reagents

A more sophisticated family of coupling reagents are the "-onium" reagents which can be classified according to their chemical nature as phosphonium, uronium or iminium type reagents. These reagents usually allow a one-pot peptide coupling, that involves activation of the carboxylic acid group and parallel liberation of a species (often HOBt or HOAt) which subsequently forms an active ester. This is then aminolysed yielding the desired peptide.

Phosphonium salts These coupling reagents have been developed since the 1970s with BOP being one of the pioneer compounds of this class. It consists of a HOBt and a tris(dimethylamine) phosphonium moiety. As counter ion hexfluorophosphate is used. A typical coupling reaction consists of a mixture of the acid, the amine and BOP in an inert, aprotic (preferrably non polar) solvent in the presence of two equivalents of base (eg. triethylamine). Additionally one equivalent of extra HOBt or HOAt is added to enhance the reaction.
Its main mode of action is thought to go via the attack of the carboxylate ion at positively charged phosphorous ion. Thereby, the HOBt moeity acts as a leaving group. The liberated HOBt then attacks the activated carboxyl group, initiating the transformation to the active ester, which is subsequently aminolysed.
Nonetheless, in BOP there is an alternative site, which seems for the attack of the carboxylate ion. It is one of the nitrogens of the triazole ring as shown in *Figure 1.14*. It would lead to a generation of the HOBt ester in one step, but the result would be same.
BOP mediated reactions are usually very efficient with hardly any side reactions occurring. Moreover, the workup is fairly facile as the product is easily cleaned from by-products. However, the main by-product Hexamethyl phosphoric triamide (HMPA) is a very hazardous substance. It is a potent toxin, causing genetic defects as well as cancer [18]. Hence, alternatives to BOP soon were developed. This led to a wide variety of different phosphonium reagents (see [16, p. 6572]), which all work in a similar way. [11, 15, 16]

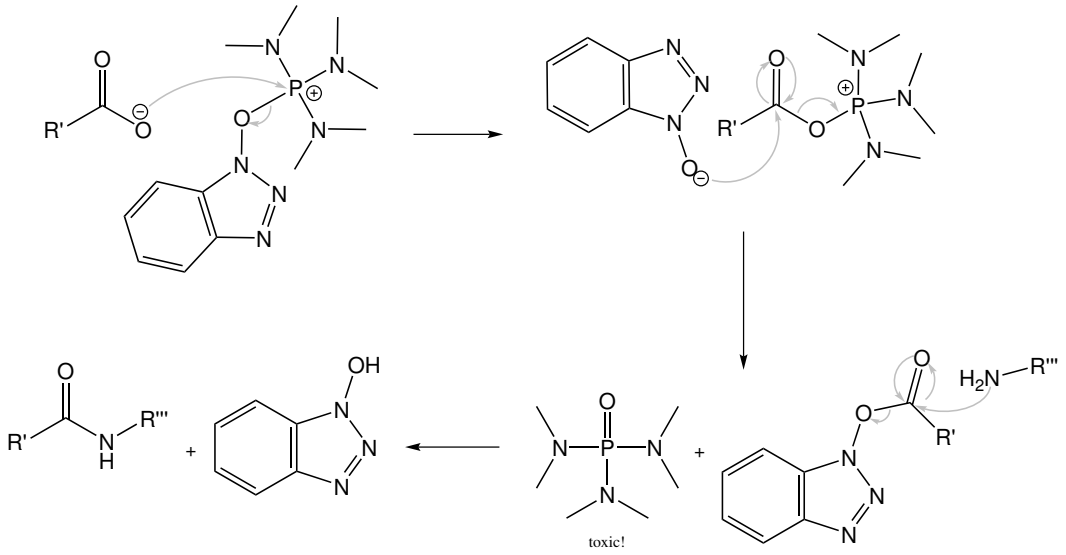

Figure 1.13.: Illustration of the proposed main reaction pathway in a BOP mediated coupling, which is analogous to most other phosphonium type reagents. (Reproduced from [15])

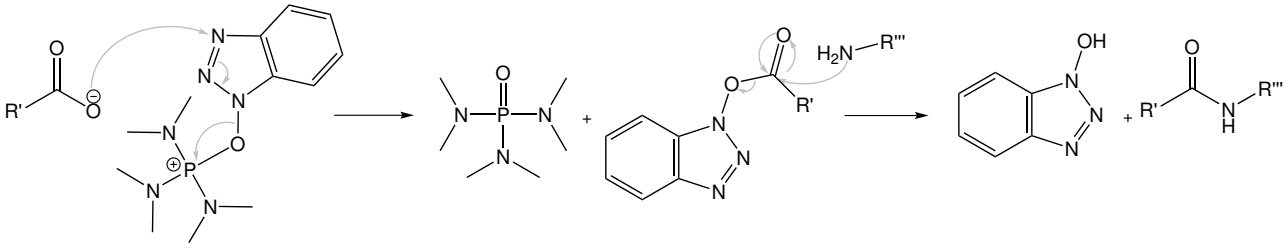

Figure 1.14.: Illustration of BOP mechanism with the alternative site for the attack of the deprotonated carboxylic acid. (Reproduced from [15])

Uronium salts The other big group of "-onium" reagents are the uronium (also called aminium) salts and their analogues, the iminium reagents. The methodology behind these coupling reagents is the same as for the phosphonium analogues. The carboxylic acid is activated and subsequently transformed to an active ester which is in turn aminolysed (see *Figure 1.15*). As a result their composition is quite similar to the phosphonium salts, with the difference that the phosphonium moiety is replaced by a group carrying an electron deficient carbon instead of the phosphorous. Further, these reagents are present in two different forms, the uronium and the guanidinium *N*-oxide form (*Figure 1.16*). In the crystalline state the latter form was found exclusively. This is the reason why they are nowadays often referred to as aminium salts. In solution, however, an equilibrium between these forms is postulated.

Generally, the performance of uronium reagents is superior compared to their phosphonium counterpart. However, they exhibit the potential to take part in a side reaction with the amine. Thereby, the amine attacks and a guanidine product is generated. As a result the amine group is blocked for further reactions. This side reaction can be reduced by addition of excess HOBt. Phosphonium reagents do not show this property and are therefore advantageous for some applications such as cyclisation reactions.

As for phosphonium salts, there is a range of different uronium salts (see [16, p. 6574 *et seq.*]),

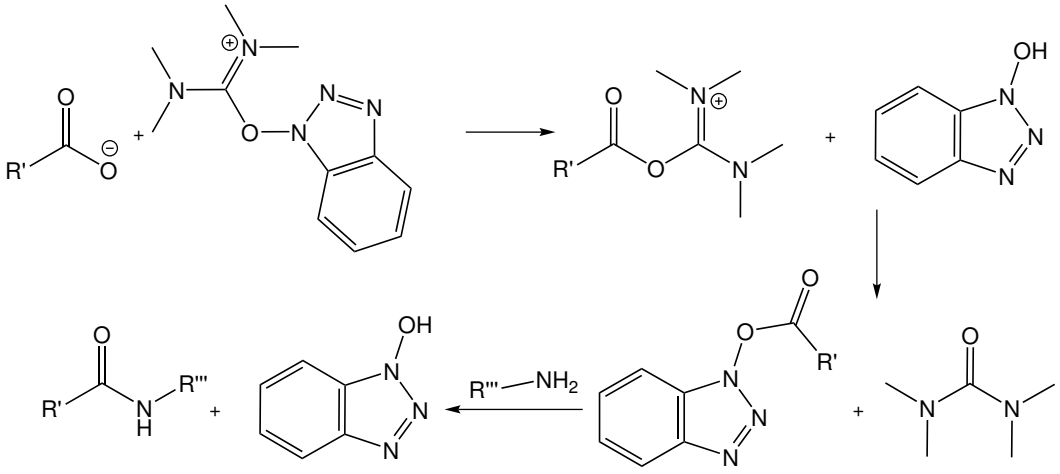

Figure 1.15.: Reaction scheme of HBTU mediated coupling, an exemplary uronium type reagent. (Reproduced from [11])

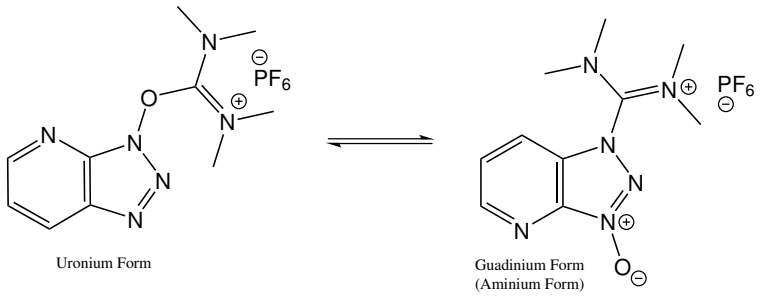

Figure 1.16.: The equilibrium of the different forms of HATU, another typical uronium salt. In the crystalline state the equilibrium if totally at the side of the guadinium form. (Reproduced from [11])

of which HBTU (also called TBTU if the counterion is tetrafluoroborate) and HATU are shown here as typical examples. It has to be noted that HATU is considered one of the most reactive coupling reagents of the uronium group, albeit also one of the most expensive.[11, 15, 16]

Iminium salts A group of coupling catalysts closely related to the uronium reagents are the iminium salts (or immonium salts as they are called in [15]). They generally are identical to uronium salts with the second amine group at the reactive carbon replaced by an other group which may be a simple hydrogen, an alkyl or an aryl group. Due to their similarity with uronium reagents they usually behave analogously. An example, the iminium salt BOMI is shown below. [11, 15]

1.1.1.4. Coupling with Benzotriazole

The final section is devoted to a relatively young method for amide bond formation. It is based on *N*-Acylbenzotriazoles as active species, which are stable enough to be stored under ambient conditions and react in partially aqueous solvents but reactive enough to be done at room temperature or below. This features allow for efficient couplings with amino acids devoid of C-terminal protection. Further, racemisation is efficiently suppressed if the reactions are performed at appropriate temperatures (the longer the peptide the colder). Successful

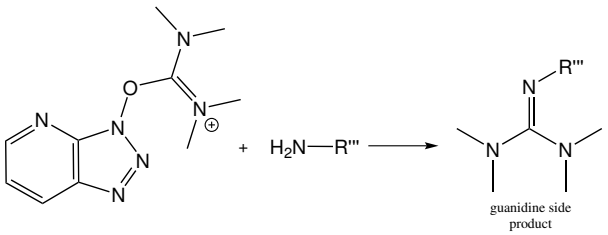

Figure 1.17.: The guadiniylation side reaction of uronium salts shown on the examole of HATU. (Reproduced from [11])

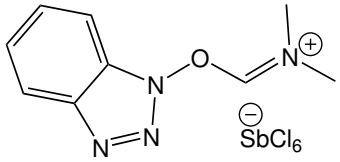

Figure 1.18.: Structure of BOMI a representative of the iminium salts.(Reproduced from [11])

multistep syntheses of peptides with up to seven amino acids in solution phase were reported, while it is also claimed to be suitable for solid phase synthesis.
Typical peptide synthesis using this method involves first the activation of a *N*-protected amino acid or peptide (Fmoc, Z and Boc are used) with benzotriazoles. This works via two ways, either with sulfonyl benzotriazoles for Boc-amino acids or benzotriazoles and thionylchloride for Z- and Fmoc- amino acids. Thereby, most types of side chain functionalities don't undergo side reactions and can be left unprotected. The next step is coupling of the generated species with a free unprotected amino acid or peptide in a water acetonitrile solution with triethylamine present (see *Figure 1.19*). The couplings often afford relatively pure products, hence not requiring extensive purification by chromatography. With all its advantages this approach seems to be very promising for the efficient synthesis of short peptide in solution. [16, 19, 20]

1.1.2. Protecting Groups

The necessity for protecting groups for amino acids is rather obvious, as otherwise the synthesis of defined peptides would be impossible. In order for a group to be usable for protection it has to fulfil several requirements. First of all the protection reaction is ought to be straightforward and efficient. Further, the protected species should withstand the conditions of the subsequent reactions and finally protecting groups should be removable in a clean and secure way, when it is not needed anymore. In case more than one functionality of a molecule has to be masked, it is desirable to use orthogonal protecting groups, meaning that the mechanism for the removal of one protecting group should different from the other one. This prevents competition between the deprotection reactions. In the following sections several basic protecting groups and their applications are presented. [21]

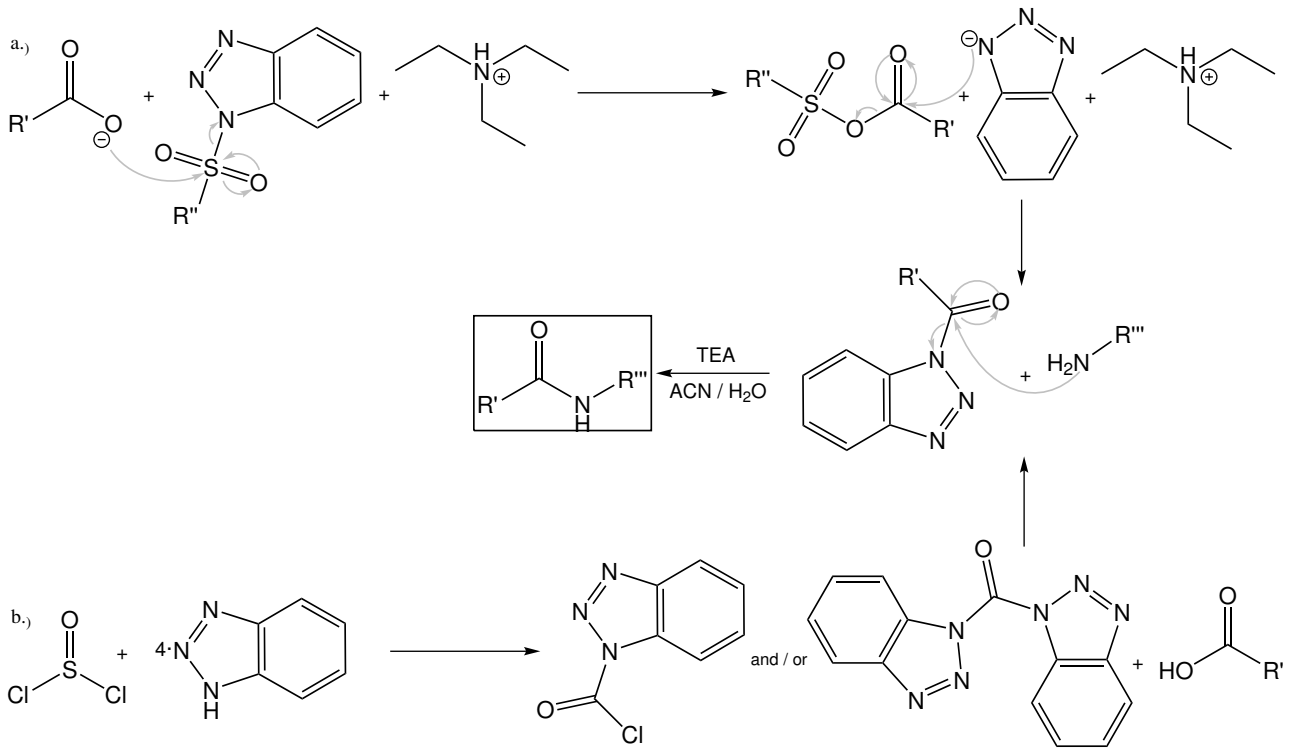

Figure 1.19.: This scheme shows the techniques to prepare the activated benzotriazole species, whereby a.) is used for Boc-protected compounds and b.) for Fmoc- and Z- protected ones. Further the subsequent coupling with an amine is depicted. [16]

1.1.2.1. C-Terminal protection

Special protection of the C-terminus of amino acids or peptides is applied mainly in liquid phase synthesis as in solid phase synthesis the carboxyl group forms the bridge to the resin and is thereby masked. In solution phase peptide synthesis it is not unconditionally necessary to protect the carboxyl group because the amine usually reacts faster. Nevertheless, it is strongly recommended to do so, mainly for solubility reasons. Moreover, transient side products may form without C-terminal protection that can lead to racemisation. [7, 21]

Methyl and Ethyl esters One of most simple ways to protect a carboxy group is to transform it into a methyl or ethyl ester. There are numerous procedures how to achieve this protection. One way is by treating the amino acid in the corresponding alcohol with HCl gas. Another approach would be the use of thionyl chloride in the alcohol amino acid suspension. Their blocking ability is described to be "excellent"[7], however, the removal of ethyl and methyl esters poses rather big difficulties in many cases. Although methyl esters can be transformed to azides for coupling or amides by ammonolysis, normal cleavage is done by saponification, which is accompanied by various side reactions. These may even result in the disintegration of the peptide backbone if serine residues are present. Also ethyl esters are removed by saponification, bringing along the same inconveniences as with methyl esters. Moreover, this deprotection reaction is slower as the ethyl ester is less susceptible to nucleophilic attack. A way to circumvent saponification for ethyl esters may be the use of enzymes such as thermolysine or carboxypep-

tidase Y.
Generally spoken, methyl and ethyl esters are very useful as long as their removal is not required at the end of the synthesis sequence.[7]

Benzyl esters A very popular group to protect the carboxy function in solution phase peptide synthesis is the benzyl group. Its preparation is done in a similar way as for the simple alkyl esters, using HCl, *p*-toluenesulfonic acid, [7] or thionylchloride. [22] In comparison to methyl or ethyl esters it is very easily and cleanly cleaved by catalytic hydrogenolysis. Thereby, it has to be mentioned that it is also possible to deprotect methionine containing peptides, although this amino acid has the potential to poison palladium catalysators as it contains sulfur in the form of a thioether. Using catalytic transfer hydrogenation with formic acid this doesn't pose an obstacle. [23] Additionally, there are other ways to deprotect the benzyl ester either by saponification or acidolysis with HBr in acetic acid. Moreover, it may be transformed to the hydrazide for subsequent azide coupling.
The benzyl ester was also the basis for the Merrifield resin, the first polymeric resin for solid phase peptide synthesis (see *Section 1.1.3*). It is based on benzyl chloride units. They react with the carboxy group of the first amino acid to establish the connection between the growing peptide chain and the resin via an benzyl ester linkage. [7, 21]

1.1.2.2. N-Terminal Protection

A topic crucial for all kinds of peptide synthesis approaches is the masking of the amine functionality, as an unprotected N-terminus of an activated amino acid would lead to a chain reaction with itself.
Most synthetic strategies require the peptide to be built from the C- to the N-Terminus. Hence deprotection of the latter has to be performed several times during the sequence. As a result deprotection conditions should be rather gentle in order not to harm the nascent peptide. Furthermore, N-terminal protection groups should suppress racemisation and enhance solubility of the peptide derivative in organic solvents.

The urethane type protecting groups Z and Fmoc The most widely used approach for protection of the α-amino group is by using urethane type protecting groups. One of their main advantages is their potential to suppress racemisation. As already discussed in *Section 1.1.1.2* this is due to their common feature, the carbamate moiety. It links the amino acid with the rest of the protecting group. Over time the pool of those rest groups has grown very diverse. It is this group that determines the individual characteristics of each kind of protecting group. The first ancestor of this class of protecting groups is the Z group. It is still widely used in solution phase chemistry. This is due to its facile introduction into amino acids, its stability towards basic and mild acidic conditions as well as the various methods with which it can be removed. For synthesis of Z-protected amino acids usually its corresponding acid chloride is

used. Its removal can be done using catalytic hydrogenation similarly to the benzyl ester or via various ways of acidolysis such as HF, TFA and thioanisole, HBr in acetic acid or BBr_3.

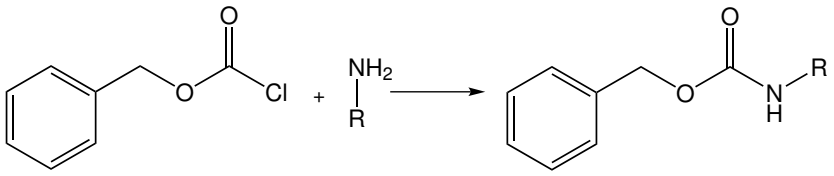

Figure 1.20.: Reaction scheme showing the protection of an amine with a Z group.[7]

One of the most popular protecting groups in solid phase synthesis is the Fmoc group. Similarly to the Z group it can be introduced via its acid chloride derivative in a fairly easy way. However, as a side reaction the formation of dipeptides may occur. It is stable towards acids but not towards bases. Hence, the Fmoc group is also cleaved under alkaline conditions. The standard way to do so is by secondary amines for instance piperidine in DMF. It is usually quite fast and works at room temperature via a β-elimination mechanism. Thereby, dibenzofulvene is generated, which is attacked by the secondary amine to form an adduct. Additionally, as in all urethane type deprotection reactions carbon dioxide is formed (*Figure 1.21*). Alternative ways of deprotection are catalytic hydrogenation which proceeds rather slow and cleavage with TBAF, which was also reported to be feasible. [7, 21, 24–26]

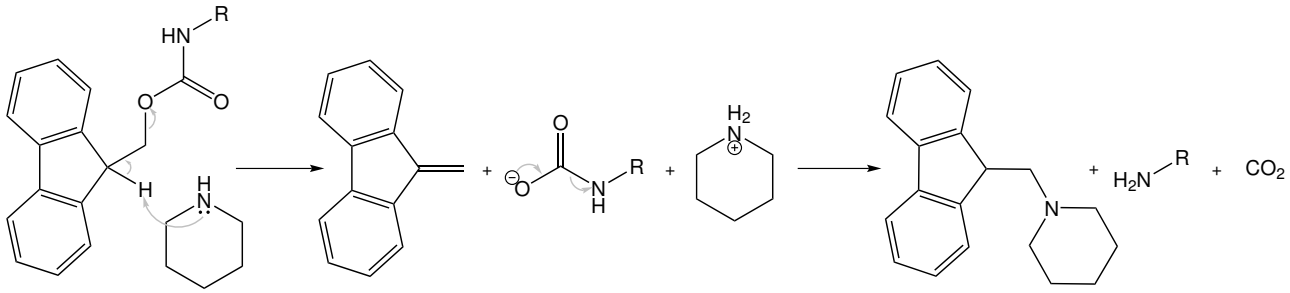

Figure 1.21.: The reaction pathway of the deprotection of the Fmoc group with piperidine. Thereby a dibenzofulvene adduct os formed as a result of the β-elimination.[25]

The Formyl-group The formyl group is a modification of the amino terminus that has also been proposed as a protecting group. It shows a high base stability, enduring saponification conditions, and is easily and cleanly cleaved by dilute acids. Additionally, one may use oxidation with hydrogen peroxide or nucleophiles such as aniline to remove this group. Although the formyl group exhibits favourable characteristics for a traditional peptide synthesis with C-terminal esterification, it was not used extensively. The reason therefore is that it does not inhibit racemisation very effectively. Only under very mild conditions peptides with retention of chiral purity were obtained. [7, 27]

Nevertheless, the formyl group is of interest for peptide synthesis as many bacterial peptides contain formylmethionine because peptide synthesis in bacteria is initiated with this residue.

This bacterial formyl-Met is enzymatically synthesized via donation of the formyl group by N^{10}-formyltetrahydrofolate to a special methionyl-tRNA. [6]
In the laboratory, fromyl amino acids are prepared by various ways, including the use of esters (e.g. *p*-nitrophenyl formate), coupling reagents (e.g. DCC) or mixed acetic formic anhydride. The last of these methods involves the generation of acetic formic anhydride from formic acid and an activated acetic acid species such as acetic anhydride. Subsequently, this reactive species is aminolysed giving the desired formyl amino acid in high yields without racemisation (*Figure 1.22*). [7, 27]

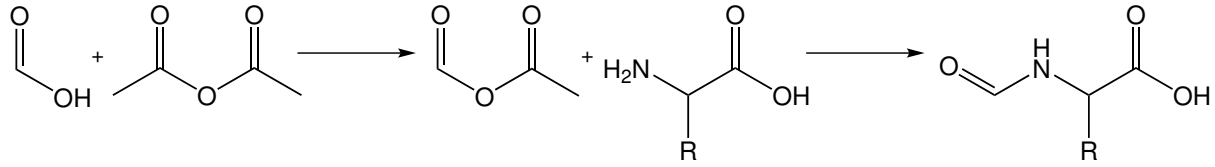

Figure 1.22.: Reaction scheme showing the formylation of an amino acid via the acetic formic anhydride process. [7, 27]

1.1.2.3. Side Chain Protection

A vast topic in peptide synthesis is the protection of side chain functionalities. These are rather diverse including carboxylic acids, (thio)alcohols, amines and amides, aromatic heterocycles, the guanidino group of arginine as well as a thioether of methionine.[7] For the performed synthetic work only methionine is relevant. Therefore this amino acid will be discussed, as a thorough description of this subject would go beyond the scope of this text.
Although, methionine is often not protected during peptide synthesis it may cause problems. One is the poisoning of palladium catalysts in hydrogenation reactions. Using enhanced conditions (see *Section 1.1.2.1 - Benzyl esters*) the need for protection may be avoided.
Further, there are two reactions that can occur easily on the thioether group of methionine. The first is oxidation of the sulfur atom to the corresponding sulfoxide. This occurs already upon extended contact to air or by oxidative cleavage of protecting groups and renders synthetic work and analytics more difficult due to the mixture of oxidized and unoxidized species. Moreover the generated sulfoxide is a chiral center, which means that diastereomers are formed. Fortunately, the oxidation is reversible. Reduction to the thioether can be achieved for instance by mercaptoethanol.
The second reaction is alkylation of the sulfur atom during acidolytic deprotection steps. Remarkably, this side reaction is avoided by oxidation of the thioether group with peracetic acid. When not needed anymore, the sulfoxide is reduced as described above. A disadvantage of using sulfoxide protection is the reduced solubility of sulfoxide compounds.
Another way of protection harnesses the alkylation side reaction and uses it to achieve methylation. This gives the dimethyl derivate of the thioether, which doesn't show a decreased solubility. Upon thiolysis with mercaptoethanol the original thioether is recovered independent on which methyl group is removed. [7]

1.1.3. Solid Phase Synthesis

Introduced by Merrifield in 1963, [28] the concept of solid phase synthesis has evolved over the decades to an invaluable synthetic strategy not only for peptides but also for DNA, oligosaccharides and small molecules. The key feature of this method is the use of solid supports, so-called resins, which are usually functionalized polymer beads. These functional groups are used to covalently attach molecules which are then modified in further synthesis steps. As soon as the synthesis is complete, the desired molecule is released from the resin. How this works in peptide synthesis is depicted in *Figure 1.23*.
Building molecules on solid support has several advantages over the solution phase approach. First and foremost purification of intermediate steps is highly simplified. The reaction solution can be easily filtered off and further purification is done simply by washing the beads. This also minimizes losses during purification, compared to conventional purification methods such as extraction or recrystallisation. Moreover, the time needed for those operations is reduced. Due to this overall increased efficiency, synthesis of long peptides with with several tens of amino acids has become feasible. [25, 28, 29]

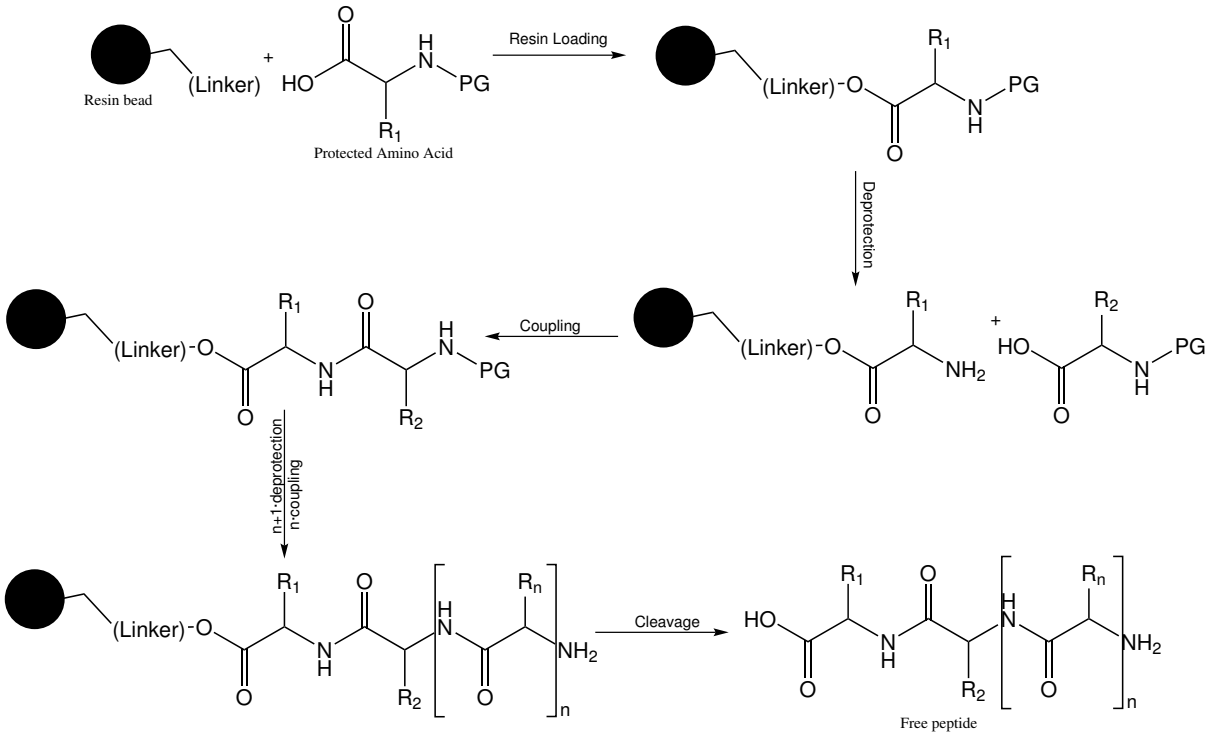

Figure 1.23.: Diagram illustrating the concept of solid phase peptide synthesis. An N-terminally protected amino acid is loaded onto the resin, optionally via a linker (e.g. the Wang linker). Subsequently, the protecting group (PG) is removed and a new protected amino acid (possibly side chain protected) is coupled to the existing one. The deprotecting-coupling cycle is repeated until all required amino acids are assembled. After a final deprotection the cleavage reaction is performed, to afford the free peptide. [25, 28, 29]

Apparatus In order to efficiently conduct the operations needed for solid phase synthsis, a specialised apparatus is to be used. Initially, Merrifield proposed a glass container with a porous

frit and a valve at the bottom. This makes removing reaction and washing solutions easier as no additional filter equipment is needed. Although still used today, there is an alternative to this apparatus in the form of syringes, which are equipped with discs made of pourous polypropylene. The concept behind this type of apparatus is the same as with the Merrifield reactor. Nowadays, syringes are more widely used because they are cheaper and if needed disposable. Further, exchanging liquids is performed in a straightforward manner by operating the plunger. One disadvantage of syringes is fatigue of the material (mostly polypropylene) as a result of prolonged solvent exposure.

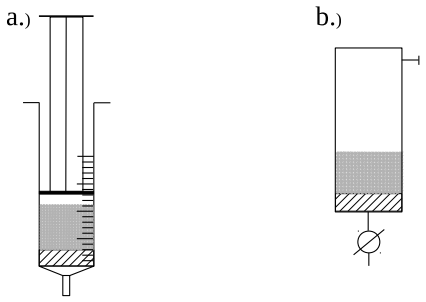

Figure 1.24.: Schemes of two kinds apparatuses used for manual solid phase peptide synthesis:
a.) Syringe equipped with a filter frit.
b.) Original fritted glass reaction vessel introduced by Merrifield.
In both drawings grey dots represent the resin and a striped box represents the filter frit. [29].

As already noticed by Merrifield [28], solid phase synthesis is not only suited for manual processing but also for automation. Methods to automate and paralellize solid phase synthesis firstly came up in the form of so-called blocks, which are assemblies of several reaction vessels (typically the syringe type) that allow simultaneous manipulations of the reactors. Further development resulted in fully automated synthesis robots, which are capable to perform multiple syntheses in a parallel fashion. This is for instance used with great success in the synthesis of oligonucleotides. [29]

1.1.3.1. The Wang resin, its loading and cleavage

While coupling and deprotection steps in a solid phase peptide synthesis are analogously performed to the solution phase approach, there are also reactions not needed in the solution phase. These involve mainly the resin and are outlined in the following lines on the example of the Wang resin.
As the original Merrifield resin, a chloromethylated copolymer made of styrene and divinylbenzene, requires rather harsh conditions to release the final peptide (eg. HF [30] or saponification with NaOH [28]). Hence, there was a search for modifications that allowed cleavage under milder conditions. This was accomplished by adding so-called linker groups to the resin (see *Figure 1.23*). One of these linkers is the Wang linker, a *p*-hydroxymethyl phenol unit directly connected to the Merrifield resin. It can be cleaved under milder conditions, with the most commonly employed method being treatment with TFA. Thereby, a full side chain deprotection

may also be achieved. During this reaction carbocations species are generated which may lead to undesired side reaction. In order to deactivate these species, nucleophilic compounds such as triethylsilane or thioanisole are added to the cleavage mixture. In addition to this approach there are many more ways to cleave the Wang resin. These include among others the Lewis acid $AlCl_3$, transesterifications with methanol catalysed by triethylamine and KCN as well as reductive cleavage using $LiAlH_4$. [30]

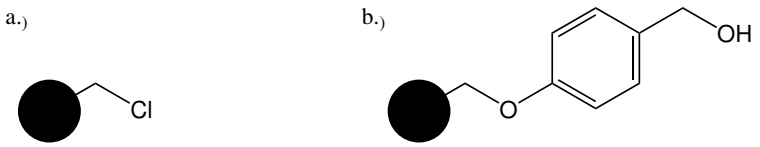

Figure 1.25.: Illustrations of the functional groups of the Merrifield (a.)) and Wang (b.)) resin. [30]

A further aspect of importance is the attachment of the first amino acid to the resin. A widely used approach is coupling via a carbodiimide in the presence of DMAP. This has the disavantage that it requires a big excess of protected amino acid (10 equivalents for instance in [Supplementary of 9]). Further, it is reported to be susceptible to racemisation. [31]
One of the alternatives to the above mentioned method is the use of the mesitylene sulfonic acid derivative MSNT (*Figure 1.26*) in presence of methylimidazole. This procedure gives excellent yields with a very low amount of racemisation. Moreover, only a twofold excess of protected amino acid compared to the resin capacity is necessary. [31] The disadvantages of this loading method, however, are the high moisture sensitivity and the high price of MSNT. [32]

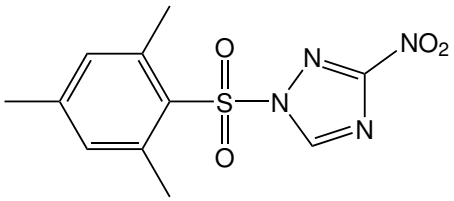

Figure 1.26.: The chemical Structure of MSNT. [31]

A reason for the popularity of the Wang resin, besides its comparably low cost, is its stability to various reaction conditions. It is stable towards highly basic conditions, even to organolithium compounds, as well as towards reducing conditions and organic radicals. Although it is cleaved by acid, a mildly acidic environment doesn't pose a problem. Apart from that it is not very tolerant to electrophilic and oxidating reagents.
Nevertheless, the Wang resin is extremely useful as solid support, which has been shown by numerous successful peptide and other kinds of syntheses. [30]

1.1.3.2. Colour Tests

One of the drawbacks of the solid phase approach is that reaction monitoring cannot be done in a straightforward way. Using traditional methods such as TLC would always require a preceding cleavage reaction in order to be applicable. This can be circumvented by specific colourimetric

tests. These are used to observe the appearence or vanishing of a particular functional group during a reaction. For this, a sample of the resin is treated with chemicals that give a colour reaction in the presence of a specific functional group. Such tests represent an easy way to reliably check the success of a synthesis step within a short period of time. Their disadvantage, however, is displayed in the fact that the resin beads used for the colourimetric test usually cannot be employed for further synthesis. This is especially undesirable if the synthesis is carried out on small scale or if the test requires a large quantity of resin.
In the following, two colour tests important for the present work are described. [29]

Test for free hydroxy groups The purpose of this test is checking the completeness of the loading of the Wang resin. Here, a small amount of resin is treated with triethylamin and diphenyldichlorosilane. If unreacted hydroxyl groups are present on the beads, this results in the formation of a polymer bound diphenylsilylchloride ether. Subsequently the beads are treated with a solution of an appropriate dye[1.3], which covalently attaches to the resin via the diphenylsilyl bridge. After washing away unreacted dye, the beads are inspected. If they are red, the loading of the resin is incomplete as free hydroxyl groups are present on the resin. If they are still white, loading was quantitative. [33, Supplementary of 1]

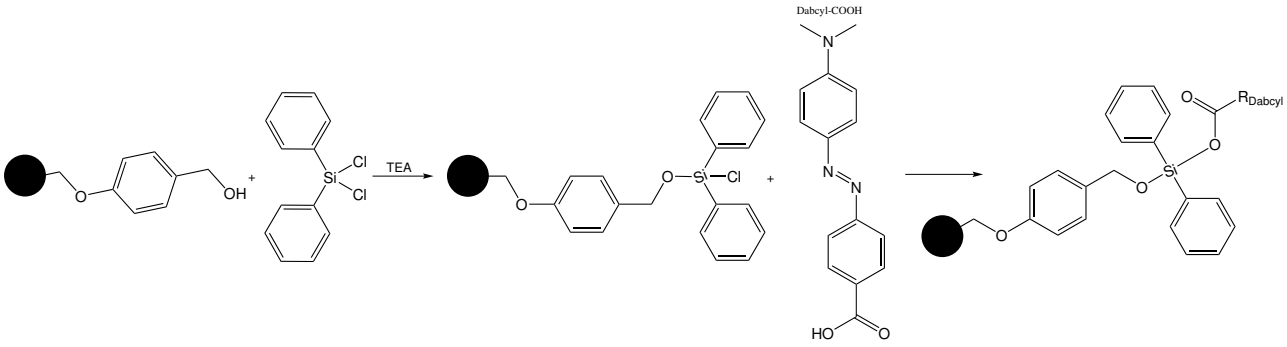

Figure 1.27.: Scheme showing the reactions behind the test for resin bound free hydroxyl groups. [33, Supplementary of 1]

Kaiser Test The Kaiser test is a method to detect primary amine groups on the resin. It is used to monitor coupling reactions and is based on the well-known chemistry of ninhydrin. The test involves treatment of a small sample of resin beads with a ninhydrin and a phenol solution (both in ethanol) as well as with a solution of KCN in pyridine. The phenol and pyridine enhance the rate of colour formation, whereas KCN serves as reducing agent, which also increases the quantity of colour and ensures reproducibility. The mixture is subsequently heated to 80°C. The evolution of blue colour indicates the presence of free primary amine groups, which are present in case of an incomplete coupling. This test still gives positive results if more than 99% of the amino groups are coupled.[34, 35, Supplementary of 1]

[1.3]Breitung *et al.* report using the so-called Dabcyl-COOH (*Figure 1.27*), whereas Burkett *et al.* recommend methyl red. Methyl red differs from Dabcyl-COOH just in that it has the carboxyl group in *ortho* position and not in *para*.

1.1.4. fMLF

General Aspects and Biological Function fMLF (sometimes called fMLP) is a tripeptide consisting of methionine, leucine and phenylalanine, whereby the methionine is *N*-formylated. It was originally isolated from culture media of gram negative bacteria such as *Escherichia coli*. [36, 37] This peptide and other formyl-peptides are produced by the cleavage of *N*-terminal signal sequences during the posttranslational modification of bacterial proteins.[1.4] Cleaving affords the short formyl-peptides in addition to the mature proteins. Thereby the ones stemming from membrane associated or secretory proteins are released into the surrounding media resulting in the enrichment of the formyl peptides in the bacteria's extracellular surrounding. [38]
The actual biological function of fMLF lies in its ability to induce chemotaxis in cells of the immune system such as neutrophils, monocytes and macrophages. These phagocytic cells follow the gradient of fMLF towards the bacteria, which release this chemotactic attractant. Further, fMLF triggers phagocytosis, the release of enzymes and the formation of free radicals, which are responses that counter the bacterial infection. These reactions to the presence of fMLF are initially elicited via binding to the human formyl peptide receptor. This receptor is a G-protein coupled one and it initiates a complex signalling cascade that regulates these defence mechanisms, via several effectors and second messengers. Additionally, there are several other cellular reactions to fMLF, for example actin polymerisation or the altering of cell shape. However, these are not fully understood yet. [37]
The ability of fMLF to recruit cells of the immune system is also of interest for medical applications. It may not only be of importance for fighting bacterial infections, but also for cancer therapy. Further, it was found that activating the formyl peptide receptor may even help in treating HIV. Therefore, fMLF and its receptor are intriguing targets for drug development. [36, 37]

Its use in solid state NMR Apart from its importance in biochemical research fMLF is also used as a standard sample in solid state NMR for setting up experiments and as model peptide. In the past this peptide was extensively studied with solid state NMR methods and it was found that fMLF is well suited for these purposes. Reasons therefore are the narrow linewidths of the ^{13}C and ^{15}N nuclei as well as a short T_1 relaxation time. Moreover, the molecule contains chemically very diverse groups that give rise to a broad variety of chemical shifts. This is advantageous for the set-up of correlation experiments. [1]

[1.4] The *N*-terminus of the nascent polypeptide is always formylated in bacteria due to the mechanism of translation (see *Section 1.1.2.2*). [6]

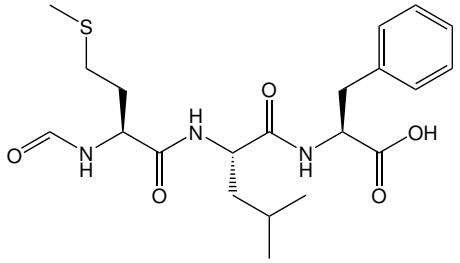

Figure 1.28.: The structure of fMLF. [1]

1.2. Solid State NMR

1.2.1. General Aspects of Solid State NMR

In contrast to liquid state NMR its counterpart in the solid state has to deal with orientation dependent spin interactions in addition to the isotropic chemical shielding and the J-coupling. These are mainly chemical shielding anisotropy, the dipolar and quadrupolar coupling. Commonly they are represented as tensors.

The chemical shielding anisotropy, CSA, is the anisotropic part of the chemical shielding, σ, which is in solution state NMR responsible for the isotropic chemical shielding. Chemical shielding arises from the electrons which surround the nucleus. These generate a secondary magnetic field in response to the B_0 field of the spectrometer. This secondary field may enforce or weaken the magnetic field experienced by the individual nuclei resulting in shifts of the resonance frequency. [40]

Dipolar Couplings originate from the interactions of the magnetic moments of the nuclei. This can be envisioned by two macroscopic magnets (which both have two poles) interacting with each other. The dipolar coupling is a through-space interaction that has no isotropic part and depends on distance and orientation of the molecules. In fact, one can directly relate the dipolar coupling constant, R_{DD}, to the internuclear distance, $r_{NN'}$, by the following equation:

$$R_{DD} = \frac{\mu_0}{4\pi} \cdot \frac{\hbar}{2\pi} \cdot \gamma_N \gamma_{N'} \cdot \frac{1}{r^3_{NN'}} \tag{1.1}$$

Thereby, μ_0 is the vacuum permeability constant, γ_N and $\gamma_{N'}$ are the gyromagnetic ratios of the nuclei N and N' and $\hbar$ is the reduced Planck constant. Although, homonuclear as well as heteronuclear dipolar couplings are a main sources of linebroadening (see below), they may be used to obtain information on molecular geometry. [40, 41]

All nuclei with a spin $> \frac{1}{2}$ exhibit an electric quadrupole moment. This comes from the charge distribution in nuclei. The quadrupole moment interacts with electric field gradients leading to the quadrupolar coupling. As the nuclei which are dealt with in this text are spin $\frac{1}{2}$ they will not discussed in further detail.

They are observable due to nature of the sample, usually a crystalline powder, which consists of separate crystallites ordered randomly in space. The molecules in the crystal lattice are restricted in motion. Hence, the anisotropic interactions are not averaged out by molecular tumbling (as it happens in liquids) and contribute to the spectra. Moreover, due to the random

orientation of the crystallites every one of those contributes differently to the overall signal. This yields very broad powder patterns and quickly produces excessive overlapping in the presence of several interaction signals. Nevertheless, powder patterns can be useful with suitable spin system.
The following section deals with the most popular method to reduce the linewidths of solid state NMR spectra. [40]

1.2.1.1. Magic Angle Spinning

The method of choice for removing or weakening the effect of anisotropic interactions in solid state NMR is magic angle spinning (MAS). Thereby, the sample is spun in a cylindrical rotor, whereby the rotor is set to the magic angle with respect to the B_0 field ($\Theta_R = \arctan(\sqrt{2}) \approx 54.74°$). The basic setup is shown in *Figure 1.29*. At the magic angle fast enough rotation causes the average orientation dependence of the spin interactions to go to zero. This means, that similar to the molecular motion in liquids, this rotation averages out anisotopic interactions such as CSA, heteronuclear (and at very high spinning speeds homonuclear) dipolar couplings. Further, linebroadening for signals from quadrupolar nuclei is reduced.

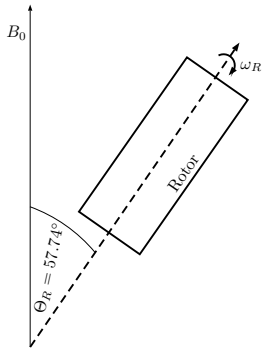

Figure 1.29.: Illustration of the basic concept of magic angle spinning. [40]

In order to fully remove any anisotropic contributions of a interaction from a spectrum the spinning rate has to be sufficiently fast, in practice three to four times faster than the magnitude of the interaction. If the spinning frequency is lower, sharp spinning sidebands are observed that have the same distance to the isotropic resonance as the spinning speed (in Hertz). The sidebands can be distinguished from the isotropic peak because they change position along with the speed.
Summing up, MAS is a very important technique in solid state NMR, being able to remove broad anisotropic signal components. With that it reduces overlapping signals and enables the generation of high resolution and high sensitivity spectra. [40]

1.2.1.2. Cross Polarisation

This section deals with another technique of solid state NMR. It is called cross polarisation (CP) and is used to transfer magnetisation from highly abundant (e.g. ^{1}H) spins, I, to low

abundant spins, S, (e.g. ^{13}C). The polarisation transfer is achieved by applying a contact pulse on both channels after a $\frac{\pi}{2}$ pulse on the highly abundant spins (*Figure 1.30*). This contact pulse induces a B_1 spin lock fields on both nuclei. In case the B_1 fields fulfil the Hartmann-Hahn condition (*Equation 1.2*) dipolar coupling interactions mediate the transfer of the polarisation.

$$\gamma_I B_1(I) = \gamma_S B_1(S) \tag{1.2}$$

In practice the Hartmann-Hahn match is achieved by setting the rf nutation frequencies, ω_1, to same values:

$$\omega_1(I) = \omega_1(S) \tag{1.3}$$

Under MAS, however, the Hartmann-Hahn condition is different:

$$(\omega_1(I) - \omega_1(S)) = \pm n\omega_R \tag{1.4}$$

Here ω_R is the spinning speed and n an integer with mostly with the values 1 or 2.

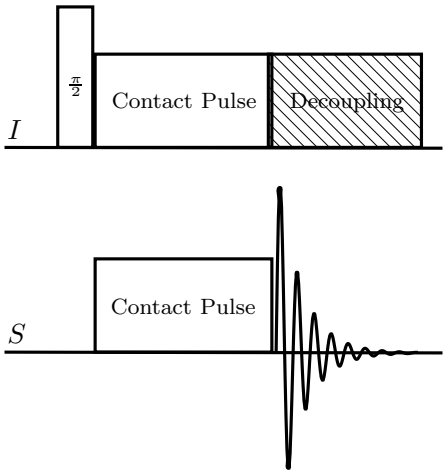

Figure 1.30.: A pulse sequence scheme showing the basic cross polarisation experiment. There are more sophisticated versions of this scheme such as the ramped CP, but they are not discussed here.
(Reproduced from [40])

Generally, CP is used for signal enhancement of dilute nuclei and due to shorter T_1 relaxation time, which comes along, the recycle delay and hence the experiment can be performed faster. Moreover, CP can be employed to gain distance information via spectral editing. Along with MAS cross polarisation is one of the most popular tools of solid state NMR. [40]

1.2.2. Symmetry Based Pulse Sequences in Solid State NMR

The basic concept behind pulse sequence design by means of symmetry criteria is that each kind of spin interaction possesses different rotational characteristics. A spin interaction Λ may be represented by three terms: A space term, for mechanical rotations of the sample molecules; a spin term, for rotations of the spin polarisations and a term for the rotations of the magnetic field. Each of these terms, which are expressed as spherical tensors, posess a (rotational) rank. It defines how a specific interaction behaves under one of the rotations. This means that each interaction possesses a set of distinct rotational ranks, a space rank l, a spin rank λ and a field

rank. The rotational ranks of the common spin interactions take integer values from 0 to 2, which corresponds to a rotational behaviour analogously to s-, p- and d-orbitals respectively (see *Figure 1.31*). [42]

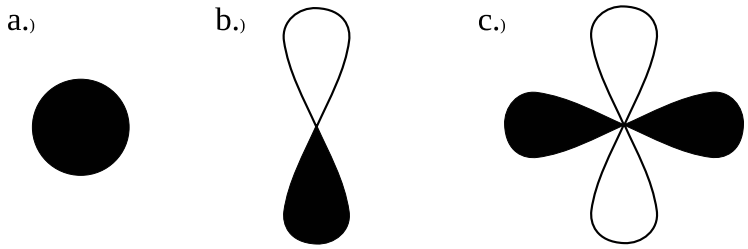

Figure 1.31.: The rotational ranks can be represented as spherical harmonic functions, similar to the visualisation of electronic orbitals in atoms or molecules:
a.) Rank 0, no change upon rotation (e.g. the field rank of the J-coupling).
b.) Rank 1, rotation causes change in a p-orbital like fashion (that means a 180° rotation causes a change of signs, e.g. λ of the chemical shielding anisotropy)
c.) Rank 2, rotation causes change similar to the d-orbital (a rotation of 90° causes sign inversion e.g. l of the Dipolar coupling) [42]

These spherical tensors of rank l or λ have a number of components m and μ, which can be calculated in the following way:

$$\text{Number of Components } m\text{: } 2 \cdot l + 1 \tag{1.5a}$$

$$\text{Number of Components } \mu\text{: } 2 \cdot \lambda + 1 \tag{1.5b}$$

Thereby, m and μ take the values:

$$m = -l, -l+1, \cdots, +l \tag{1.6a}$$

$$\mu = -\lambda, -\lambda+1, \cdots, +\lambda \tag{1.6b}$$

The relative position of the sample and its spin state are expressed via two sets of Euler angles [43] $\Omega_{RL} = \{\alpha_{RL}, \beta_{RL}, \gamma_{RL}\}$ and $\Omega_{rf} = \{\alpha_{rf}, \beta_{rf}, \gamma_{rf}\}$ respectively. [42] If the sample is now rotated mechanically and the spins are rotated by rf irradiation the two sets of Euler angles change over time, yielding two trajectories of Euler angles. Further, under spin and space rotation, the components of the tensors of a interaction can be viewed as superimposed giving the Hamiltonian:

$$\mathcal{H}^{\Lambda} = \sum_{m=-l}^{+l} \sum_{\mu=-\lambda}^{+\lambda} \mathcal{H}^{\Lambda}_{lm\lambda\mu} \tag{1.7}$$

It has to be noted that during MAS conditions components with the numbers $l = 2$ and $m = 0$ disappear as the corresponding reduced Wigner matrix element, [44] which is used to mathematically conduct the rotation operation, is zero. [42, 45]
When the spin and space part of the Hamiltonian are being synchronized by MAS and carefully designed pulse sequences, an average Hamiltonian can be generated which selectively allows or disallows combinations of rotational components. [42]

1.2.3. $\mathcal{R}$-Type Symmetry and its Applications in Homonuclear Decoupling

To achieve synchronisation, periodic symmetry relations are defined. These are unique for their respective symmetry class. There are two symmetry classes, namely $\mathcal{C}$ and $\mathcal{R}$. For the latter class, which will be treated exclusively in the following. The symmetry relations are for the space rotations are:

$$\alpha_{RL}\left(t+\frac{n\tau_r}{N}\right)=\alpha_{RL}\left(t\right)-\frac{2\pi n}{N} \tag{1.8a}$$

$$\beta_{RL}\left(t+\frac{n\tau_r}{N}\right)=\beta_{RL}\left(t\right) \tag{1.8b}$$

And for the spin rotations are:

$$\beta_{rf}\left(t+\frac{n\tau_r}{N}\right)=\beta_{rf}\left(t\right)\pm\pi \tag{1.8c}$$

$$\gamma_{rf}\left(t+\frac{n\tau_r}{N}\right)=\gamma_{rf}\left(t\right)-\frac{2\pi\nu}{N} \tag{1.8d}$$

They essentially relate periodic time points during a pulse sequence to each other, t and $t+\frac{n\tau_r}{N}$. Thereby, n, ν and N are integers, which are referred to as symmetry numbers. τ_r is the rotation period of the MAS defined as $\tau_r = |\frac{2\pi}{\omega_r}|$, with ω_r being the rotation frequency. As the spin relationships do not define the third Euler angle α_{rf}, there is not a single but several solutions to creating a synchronized pulse sequence. Nevertheless, general rules for establishing such pulse sequences can be deduced from the above relations. For a $\mathcal{R}$ sequence with its symmetry numbers n, ν and N, usually denoted as $\mathcal{R}N_n^\nu$, these rules are described in the following.

- $\mathcal{R}$ represents a block of rf pulses, which produces a spin rotation of 180° around the x-axis.
- $\mathcal{R}'$ is basically a normal $\mathcal{R}$ block with all the pulse phases inverted.
- The length of one $\mathcal{R}$ or $\mathcal{R}'$ block (Their lengths are equal!) has to be adjusted to fit N blocks in n rotational periods τ_r.
- One full sequence consists of $\frac{N}{2}$ $\mathcal{R}\mathcal{R}'$ blocks. Hence, N has to be even.
- Further, an additional phase shift, $\phi = \frac{\pi\nu}{N}$, is imposed onto each $\mathcal{R}$ block giving $\mathcal{R}_\phi\mathcal{R}'_{-\phi}$

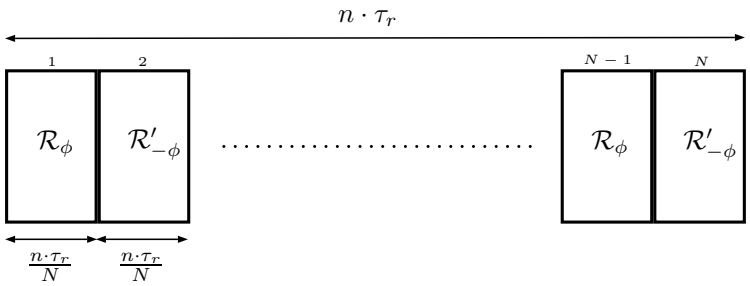

Figure 1.32.: Schematic representation of a basic $\mathcal{R}$ sequence according to the rules above. The angle ϕ is equal to $\frac{\pi\nu}{N}$. [42]

Using the above procedure a $\mathcal{R}$ type pulse sequence can be designed (see *Figure 1.32*), however without specific symmetry numbers the selectivity towards particular interactions cannot be established. To establish criteria for finding correct symmetry numbers, selection rules based on the average spin interaction Hamiltonian were formulated. The first step towards this is to approximate the effective interaction Hamiltonian $\overline{\mathcal{H}}$ using the Magnus expansion. [42, 46]

$$\overline{\mathcal{H}}(t^0) \cong \overline{\mathcal{H}}^{(1)}(t^0) + \overline{\mathcal{H}}^{(2)}(t^0) + \cdots \tag{1.9}$$

Thereby $\overline{\mathcal{H}}^{(1)}$ is the average Hamiltonian and $\overline{\mathcal{H}}^{(2)}$ its second order correction term. Further terms are then corrections of the third, fourth *etc.* order.

The average Hamiltonian can be rewritten as the sum of all the rotational components (see *Equation 1.7*):

$$\overline{\mathcal{H}}^{(1)}(t^0) = \sum_{lm\lambda\mu} = \overline{\mathcal{H}}^{(1)}_{lm\lambda\mu}(t^0) \tag{1.10}$$

With the symmetry relations from *Equation 1.8* one can derive selection rules that define under which combinations of symmetry numbers special rotational components are suppressed (*i.e.* when the average Hamiltonian, $\overline{\mathcal{H}}^{(1)}$, is zero). For the $\mathcal{R}$ symmetry class the first order rule is:

$$\overline{\mathcal{H}}^{(1)} = 0 \quad \text{if} \quad mn - \mu\nu \neq \frac{N}{2} Z_\lambda \tag{1.11}$$

Thereby, Z_λ is an arbitrary integer number, whose parity is equal to the rotational spin rank λ. This means that when λ is a even number Z_λ also has to be even and when it is uneven Z_λ has to be uneven.

Looking at the $\mathcal{R}6_1^3$ symmetry one gets for the homonuclear direct dipolar couplings, with the rotational components for example $\{l, m\lambda, \mu\} = \{2, -2, 2, 1\}$, $mn - \mu\nu = -2 \cdot 1 - 1 \cdot 3 = -5$. This is not equal to $\frac{6}{2} Z_\lambda$, with Z_λ being even, as it leads to $0, \pm 6, \pm 12, \ldots$ The other combinations of rotational components of the dipolar couplings lead to similar results except for some with $m = 0$, which would be allowed by the selection rule in *Equation 1.11*. These are, however, suppressed by magic angle spinning. Hence, dipolar couplings are not allowed by symmetry criteria.

When testing the isotropic chemical shifts, with the rotational components $\{l, m\lambda, \mu\} = \{0, 0, 1, -1\}$, for the same symmetry one gets $mn - \mu\nu = 0 \cdot 1 - (-1) \cdot 3 = 3$. This is equal to $\frac{N}{2} Z_\lambda = \frac{6}{2} \cdot 1 = 3$. As λ is uneven Z_λ also has to be uneven, which is fulfilled. Therefore, isotropic chemical shifts are symmetry allowed. [42]

Visualizing the symmetry properties of specific sequences is done with so-called space-spin selection diagrams. They are a straightforward way to show the results of the selection rule (*Equation 1.11*) for each kind of spin interaction. A diagram of that sort is made of two components. Firstly, there is a "wall" with holes which reflect the different values of $\frac{N}{2} Z_\lambda$. Secondly, there are branches which reflect $mn - \mu\nu$. Thereby, the first branching point in the diagram shows the possible values of mn (the space part) and the subsequent branches decrease or increase with the different values of $-\mu\nu$ (the spin part), creating all different values of $mn - \mu\nu$. When one of these numbers coincides with a value of $\frac{N}{2} Z_\lambda$ it is symmetry allowed and hence can grow through one of the holes in the wall. With that one can assess

at a glance if a specific interaction is allowed or not. The For the two interactions under $\mathcal{R}6_1^3$ symmetry, which were discussed above, such spin-space selection diagrams are shown in *Figure 1.33.*

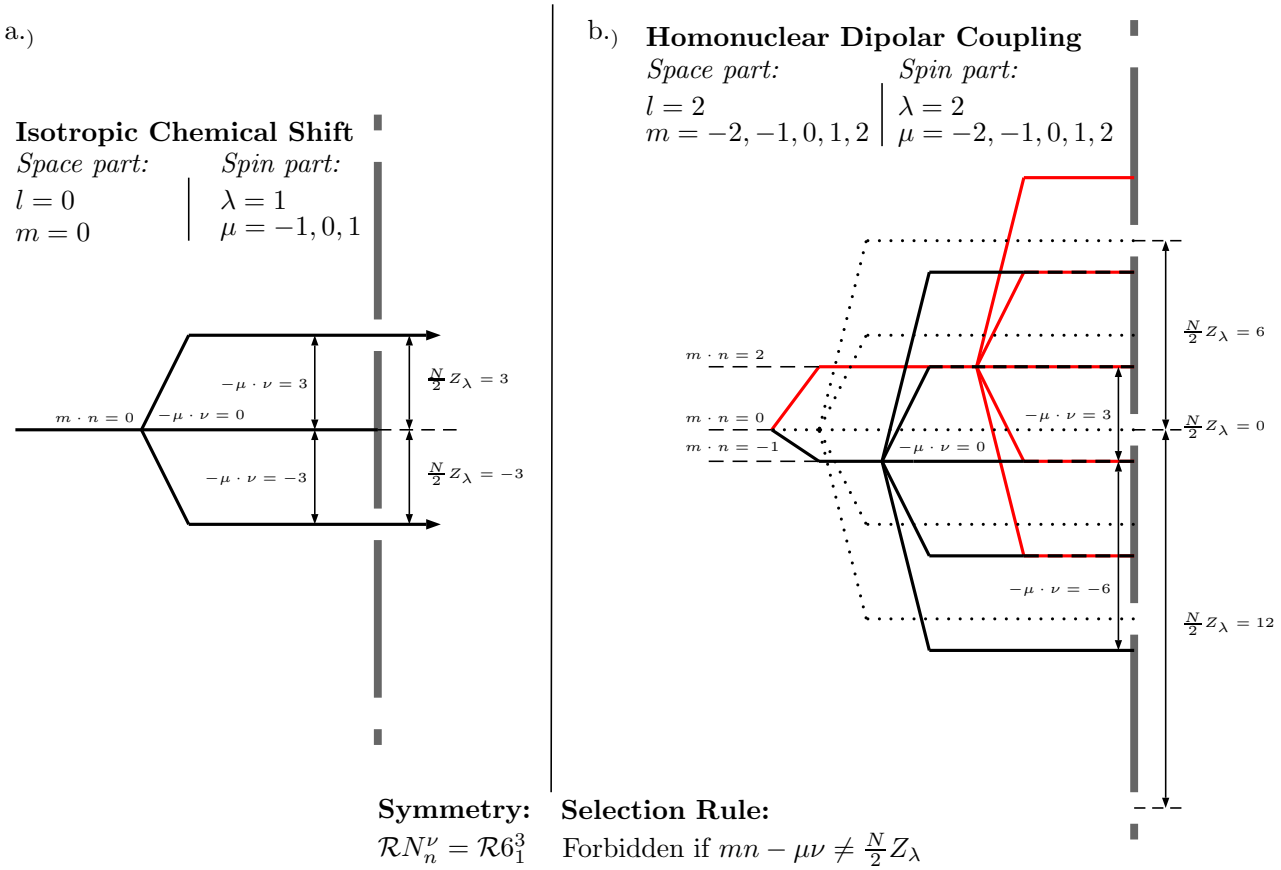

Figure 1.33.: This figure shows two exemplary spin-space selection diagrams of the $\mathcal{R}6_1^3$ symmetry. a.) depicts the isotropic chemical shift. It is symmetry allowed and hence, two branches find their way through the holes in the wall. b.) shows the homonuclear dipolar couplings. These are symmetry forbidden and therefore the red and black branches, which correspond to $m = 2$ and $m = -1$ respectively, are all blocked by the wall. (The other two values of m, -2 and 1, are not shown for better readability.) Some of the dotted lines are not blocked. These however, are suppressed by magic angle spinning as they belong to the space component $m = 0$ with the rank $l = 2$. [42]

In order to have a better approximation of the effective Hamiltonian not only the average Hamiltonian (the first term of the Magnus expansion) but also higher order terms may be incorporated. For these terms too, selection rules can be derived. They usually give a rough hint on the performance of a special symmetry. Nevertheless, the expressions get rather complicated with increasing order. This is exemplified by the selection rules for the second order term, $\overline{\mathcal{H}}^{(2)}_{l_2 m_2 \lambda_2 \mu_2 l_1 m_1 \lambda_1 \mu_1}$, which requires two sets of rotational components:

$$\overline{\mathcal{H}}^{(2)}_{l_2 m_2 \lambda_2 \mu_2 l_1 m_1 \lambda_1 \mu_1} = 0 \quad \text{if} \quad \begin{cases} m_1 n - \mu_1 \nu \neq \frac{N}{2} Z_{\lambda_1} \\ m_2 n - \mu_2 \nu \neq \frac{N}{2} Z_{\lambda_2} \\ (m_1 + m_2) n - (\mu_1 + \mu_2) \nu \neq \frac{N}{2} Z_{\lambda_1 + \lambda_2} \end{cases} \tag{1.12}$$

Here, all three conditions have to be fulfilled. Z_{λ_1} has the same parity as λ_1. Analogously, it works for Z_{λ_2}. $Z_{\lambda_1+\lambda_2}$ has the same parity as the sum of λ_1 and λ_2

There is a final point worth mentioning when discussing $\mathcal{R}$ and symmetry based pulse sequences in general. It is the presence of scaling factors. Each pulse sequence possesses a scaling factor that determines the magnitude of the terms which are allowed by symmetry criteria. It is always less than 1, which means that although undesired terms are suppressed also the desired ones are scaled down. Scaling factors can be either calculated [42] or determined experimentally (e.g. [2]) for a given pulse sequence. [42]
The following two sections are devoted to two pulse sequences that apply $\mathcal{R}$-type symmetry to achieve homonuclear dipolar decoupling.

1.2.3.1. ^{1}H Spectroscopy with $\mathcal{R}$ decoupling

Using $\mathcal{R}$ symmetries, that render the isotropic chemical shift and J-couplings allowed, but CSA and homonuclear dipolar couplings forbidden (*Figure 1.34*), experiments may be carried out which yield high resolution ^{1}H spectra. There are many $\mathcal{R}$ symmetries which can be employed to achieve this. Some are: $\mathcal{R}6_1^3$, $\mathcal{R}14_7^2$, $\mathcal{R}18_2^9$ or $\mathcal{R}16_3^8$. (For more comprehensive lists of the applicable symmetries see [47], [42] or [2].)

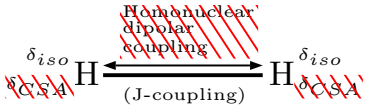

Figure 1.34.: Picture of two coupled ^{1}H atoms and which of their interactions are allowed or forbidden (crossed out in red) with the $\mathcal{R}$ symmetries for high resolution proton spectra. (Homonuclear J-coupling is allowed but not observed.)[2]

Pulse sequences for these proton spectra are shown in *Figure 1.35*. They are essentially 2D experiments in which the number of $\mathcal{R}\mathcal{R}'$ blocks is incremented by one block[1.5] during each evolution period. After Fourier transformation in both dimensions the projection along the direct dimension is done. This yields a spectrum of the indirect dimension, which contains the high resolution information on the isotropic proton shifts.[2, 47]
There are two versions of the pulse sequence depicted in *Figure 1.35*. Both rely on a composite π pulse, made up of three $\frac{\pi}{2}$ pulses as $\mathcal{R}$ element. This composite pulse is especially efficient when the rf-irradiation is done in an off resonant fashion. Therefore it was used for all the $\mathcal{R}$ based pulse sequences in this work.
a.) is the basic version and b.) an enhanced one. This has two pulses flanking the $\mathcal{R}$ block, which turns the decoupling field onto the z axis, as well as a an additional pulse before acquisition. It acts as a filter suppressing wrongly phased parts of the signal. Further TPPI is applied. Overall, these modifications enhance the lineshape of the spectra as well as their resolution. [3]

[1.5] It is possible to increment just one $\mathcal{R}\mathcal{R}'$ block, because it is not necessary to have full $\mathcal{R}$ cycles (which would take $\frac{N}{2}$ blocks or $\tau_r n$) in most practical applications, although theory would require it. This allows shorter time increments in t_1. [42]

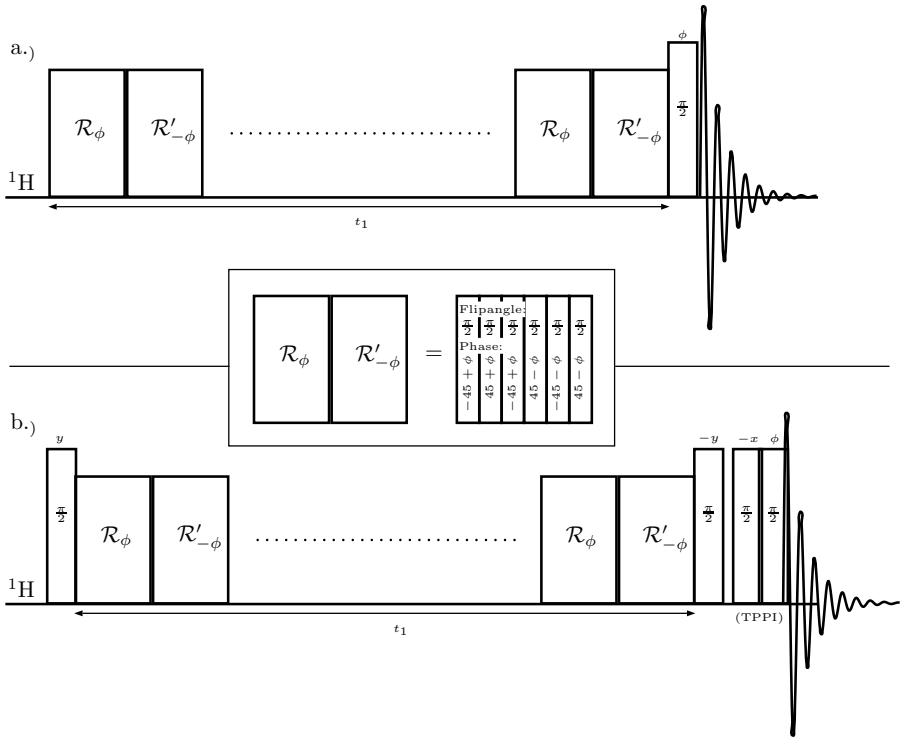

Figure 1.35.: Pulse sequence schemes for experiments giving high resolution ^{1}H spectra. One $\mathcal{R}$ block consists of three $\frac{\pi}{2}$ pulses with different phases, which form a composite π pulse (box in the middle). [2]
a.) shows a basic version of the sequence with t_1 incremented $\mathcal{R}$ decoupling followed by a phase cycled detection pulse. [2] b.) gives an enhanced version with two $\frac{\pi}{2}$ pulses flanking the decoupling block, an additional pulse before acquisition and TPPI. [3]

1.2.3.2. ^{13}C Spectroscopy with $\mathcal{R}$ decoupling

The pulse sequence below (*Figure 1.37*) gives one dimensional ^{13}C spectra. It is basically a pulse-acquire experiment with simultaneous $\mathcal{R}$ decoupling at the ^{1}H channel, for which the same symmetries as the proton experiment described in the previous section are used. Hence, influences of homonuclear dipoar couplings are suppressed and heteronuclear J-couplings are allowed. In case heteronuclear dipolar couplings are suppressed sufficiently by MAS in addition to the $\mathcal{R}$ decoupling, the symmetry allowed heteronuclear J-coupling can be observed. This has been shown in adamantane and used for calculating pulse sequence scaling factors. [2, 47]

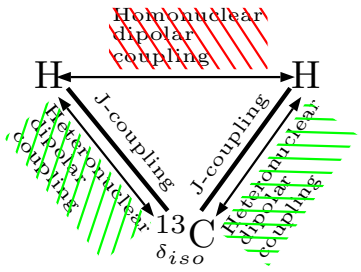

Figure 1.36.: Scheme showing the interactions between the nuclei of a CH_2 group Additionally, it shows which of them are suppressed by the described $\mathcal{R}$ sequences (crossed out in red) and which are suppressed by MAS (crossed out in green)[2]

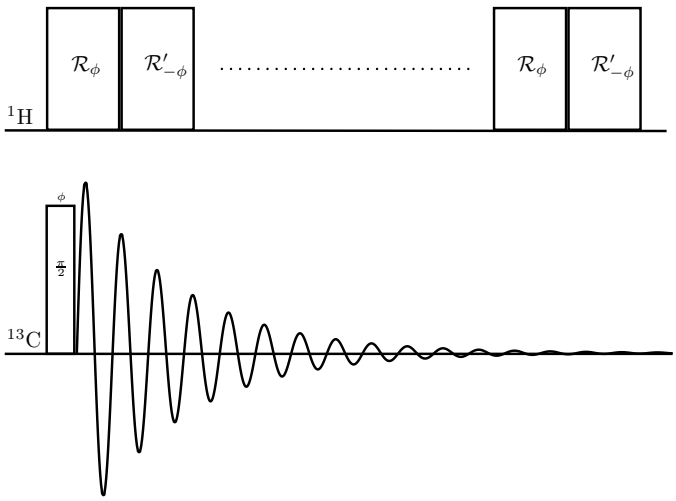

Figure 1.37.: Pulse sequence scheme showing the ^{13}C experiment, which allows observation of heteronuclear J-couplings. It consists of a simple one-pulse experiment, whereby the acquisition period is $\mathcal{R}$ decoupled. [2] A similar scheme using cross-polarisation for establishing the initial polarisation of the ^{13}C spins is also possible (see *Figure 1.30*). [47]

1.2.4. The INEPT experiment

This section deals with the INEPT experiment, a 1D pulse sequence which is originally and mostly used in solution state NMR, either on its own or as crucial building block in multi-dimensional spectroscopy (e.g. in the HSQC [4]). Two flavours of the INEPT are depicted in *Figure 1.38*. Both fulfil the same purpose, namely the enhancement of the signal of nuclei with a low gyromagnetic ratio, γ_S, by through bond polarisation transfer from a nucleus with a high gyromagnetic ratio, γ_I, (^{1}H) to the one with low γ_S (eg. ^{13}C or ^{15}N). The signal for such sequences is enhanced at least 4 times for ^{13}C, whereby it might be higher in practice.
This is brought about by initially exciting the protons and letting them evolve (including a refocussing pulse) under heteronuclear J-coupling for a period $\tau = \frac{1}{2J_{IS}}$. Thereby antiphase magnetisation is generated, which is transferred to the other nucleus by two simultaneous $\frac{\pi}{2}$ pulses on both channels. This transferred antiphase magnetisation is either detected directly (*Figure 1.38a.)*) or refocussed to give inphase lineshapes which do not vanish upon decoupling(*Figure 1.38b.)*). [5, 48]

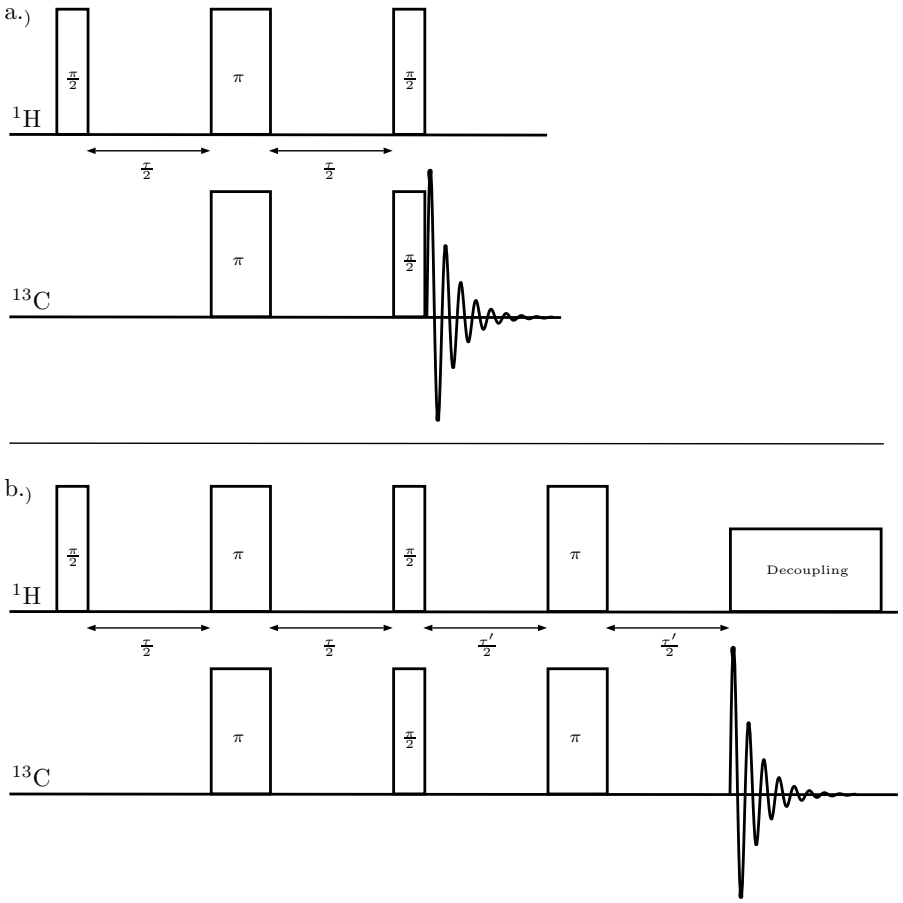

Figure 1.38.: Schemes of two versions of the INEPT experiment. a.) shows the original INEPT which gives antiphase lineshapes and is hence, not suited for decoupling during acquisition. [5] b.) presents the refocussed INEPT, which allows decoupling as it gives inphase lineshapes.[48]

In solid state NMR the INEPT technique is much more difficult to apply than in solution state due to the fact that ^{1}H transverse magnetisation is very short lived in most crystalline organic solids. The reason for that is the presence of dipolar couplings. Nevertheless, there have been attempts to implement a solid state INEPT experiment for instance using eDUMBO decoupling during the delay periods.[4]

Employing *R*-type decoupling schemes described in previous sections may also be an option for implementing the INEPT in solid state NMR. This would have the advantage that set up of such an experiment would be more straightforward as much less optimisation than in the eDUMBO approach would be necessary. Further, a new spectroscopic tool, possibly being the starting point for other INEPT based experiments such as the HSQC, would be provided for solid state NMR.

2. Objectives

The work performed during this master thesis was guided by several aims in the fields of peptide synthesis and solid state NMR, as described in the following lines.
The major goal of the synthetic work was to find an efficient and reliable route to produce fMLF in laboratory scale. The tripeptide fMLF is a standard sample in solid state NMR. Hence the route should be applicable for the synthesis of this peptide in ^{13}C and ^{15}N labelled form. For this the actual peptide synthesis as well as the protection of the amino acids was to be examined. As a starting point for the peptide assembling process the publication by Breitung and co-workers [1] was used. It already describes a solid phase synthesis of doubly labelled fMLF, however with already protected amino acids.
On the NMR side it was desired to implement the pulse sequences described in [47], [2] and [3] which employ a homonuclear decoupling scheme based on $\mathcal{R}$ symmetry pulse blocks. Further the applicability of of this decoupling method on the INEPT pulse sequence, which originally stems from liquid state NMR, was to be investigated. The impetus to do so came from a publication describing the INEPT experiment in solid state NMR using eDUMBO decoupling. [4]
As $\mathcal{R}$-type decoupling usually doesn't require the excessive optimisation normal for eDUMBO it would be beneficial to have an easily set up INEPT. Furthermore, a working INEPT implementation would open up the road to INEPT based multidimensional experiments such as the HSQC.

3. Experimental

3.1. Synthetic Investigations

The following sections give a detailed description of the synthetic work carried out. They will deal with the synthetic routes which were examined, the used apparatuses as well as the exact experimental procedures.

3.1.1. List of Chemicals

Table 3.I.: A list of all used Chemicals, their basic properties and their manufacturer. Trivial chemicals and solvents are omitted.

Chemical	**Sum Formula**	**Molar Mass [g mol^{-1}]**	**Purity**	**Source**
Acetic Acid (glacial)	$C_2H_4O_2$	60.05	100%	Merck
Acetic Anhydride	$C_4H_6O_3$	102.99	≥99%	Alfa Aesar
Acetonitrile	C_2H_3N	41.05	HPLC grade	VWR Chemicals
4-Aminobenzoic Acid	$C_7H_7NO_2$	137.14	99%	Alfa Aesar
1*H*-Benzotriazole	$C_8H_5N_3$	119.13	99%	Alfa Aesar
Benzyl Alcohol	C_7H_8O	108.14	>99%	ACROS
1-Butanol	$C_4H_{10}O$	74.12	99,8%	Sigma-Aldrich
Celite 454	-	-	-	Fluka
Citric acid	$C_6H_8O_7$	192.12	99.87%	Herba Chemosan
Dicyclohexylcarbodiimide	$C_{13}H_{22}N_2$	206.33	99%	Alfa Aesar
Diethylamine	$C_4H_{11}N$	73.14	>99	Alfa Aesar
Diisopropylcarbodiimide	$C_7H_{14}N_2$	126.20	99%	Alfa Aesar
N,N-Dimethylaniline	$C_8H_{11}N$	121.18	>99%	Merck-Suchardt
N,N-Dimethylformamide	C_3H_7NO	73.09	99.8%	Alfa Aesar
Dioxane	$C_4H_8O_2$	88.11	99.8%	Aldrich

[a] These chemicals were used for the production of the glycine polymorphs as described in *Section 3.2.3.*

Continuation of *Table 3.I*, the list of chemicals.

Chemical	**Sum Formula**	**Molar Mass [g mol^{-1}]**	**Purity**	**Source**
Diphenyldichlorosilane	$C_{12}H_{10}Cl_2Si$	253.20	97%	Alfa Aesar
Ethanedithiol	$C_2H_6S_2$	94.20	>98%	Alfa Aesar
Ethanol	C_2H_6O	46,07	analytical reagent grade	Fisher Scientific
Ethyl Formiate	$C_3H_6O_2$	74.08	99%	Merck-Suchardt
N-Ethyl-Morpholine	$C_6H_{13}NO$	115.18	>99.5%	Fluka
Fmoc-Chloride	$C_{15}H_{11}O_2Cl$	258.7	97%	Sigma-Aldrich
Fmoc-Leu	$C_{21}H_{23}NO_4$	353.43	>97%	Fluka
Formic acid	CH_2O_2	46.03	>99%	Merck
Glycine[a]	$C_2H_5O_2$	75.07	99%	Alfa Aesar
Hydrochloric acid	HCl	36.46	37%	VWR Chemicals
Hydrogen	H_2	2	-	Linde
Hydroxybenzotriazole (anhydrous)	$C_6H_5N_3O$	135.12	99%	molekula
Iron(II)sulfate	$FeSO_4 \cdot 7\,H_2O$	278.02	analytical grade	Merck
Leucine	$C_6H_{13}NO_2$	131.17	≥98%	Sigma-Aldrich
Methionine	$C_5H_{11}NO_2S$	149.2	97.7%	SERVA
N-Methylimidazole	$C_4H_6N_2$	82.11	>99%	Fluka
N-Methyl-pyrrolidone	C_5H_9NO	99.13	>99%	Fluka
MSNT	$C_{11}H_{12}N_4O_4S$	296.3	98%	Fluka
Ninhydrine	$C_9H_4O_3$	178.14	>99%	Fluka
Nitromethane	CH_3NO_2	61.04	synthesis grade	Aldrich
Palladium on Carbon	-	-	10% Pd	Fluka
Phenol	C_6H_6O	94.11	99%	Merck-Suchardt
Piperidine	$C_5H_{11}N$	85.15	98%	Fluka
Phenylalanine	$C_9H_{11}NO_2$	165.19	99%	Alfa Aesar
Potassium Cyanide	KCN	65.12	analytical grade	Merck
Potassium Carbonate	K_2CO_3	138.21	99%	Alfa Aesar
Potassium Nitrate[a]	KNO_3	101.11	analytical grade	Merck
Pyridine	C_5H_6N	79.10	99%	Fluka

[a] These chemicals were used for the production of the glycine polymorphs as described in *Section 3.2.3*.

Further continuation of *Table 3.I*, the list of chemicals.

Chemical	**Sum Formula**	**Molar Mass [g mol^{-1}]**	**Purity**	**Source**
Sodium Formate	CHO_2Na	68.01	analytical grade	Sigma-Aldrich
Sodium Hydrogencarbonate	$NaHCO_3$	84.01	100%	Herba Chemosan
Sodium Nitrite	$NaNO_2$	69.00	analytical grade	Merck
Sulfuric Acid	H_2SO_4	98.07	95-97%	J. T. Baker
Tetrahydrofuran	C_4H_8O	72.11	≥99%	ACROS
Thionyl Chloride	$SOCl_2$	118.96	>99%	Fluka
Triethylamine	$C_6H_{15}N$	101.19	≥99%	Sigma-Aldrich
Trifluoroacetic acid	$C_2HO_2F_3$	114.02	99%	Alfa Aesar
Triisopropylsilane	$C_9H_{22}Si$	158.36	99%	Sigma-Aldrich
Wang resin	-	0.6-1.0 mmol g^{-1}	-	Sigma-Aldrich
Z-Gly-Gly	$C_{12}H_{14}N_2O_5$	266.25	PURISS CHR	Fluka

[a] These chemicals were used for the production of the glycine polymorphs as described in *Section 3.2.3*.

3.1.2. Synthetic Routes

One of the main goals was to find an efficient and straightforward route for the synthesis of fMLF. The starting point for this investigation was the procedure published in [1], here called Route I. In succession, three additional synthesis routes were examined, which are all based to some degree on Route I. An overview of these routes is given in *Figure 3.1.*
The first steps of the syntheses are all quite similar and start with the loading of the first protected amino acid, Fmoc-Phe, onto the Wang resin. It is followed by deprotection and subsequent coupling of the second protected amino acid, Fmoc-Leu. At this point, a further deprotection step is required in Routes I, II and III, while in Route IV already the cleavage reaction is performed. From here on the routes are rather diverse and hence they will be described individually:

- Route I is continued by the coupling of Fmoc-Met followed by deprotection. The tripeptide is then formylated using Ethylformiate. Now fully assembled, fMLF is released from the resin, lyophilized and purified.
- In Route II formyl-Methionine is directly coupled to the dipeptide giving fMLF, which is also cleaved and subsequently purified. This route is the shortest in terms of the number of reaction steps.
- Route III as Route I carries on with the coupling of Fmoc-Met. Subsequently the protected tripeptide is cleaved off the resin and preliminarily purified. Then, the Fmoc group is removed by deprotection. Next, the formylation reaction is performed, affording fMLF ready for final purification.
- After the early cleavage, the dipeptide in Route IV is deprotected in solution phase and coupled without C-Terminal protection either to Fmoc-Met or formyl-Met. In case the former coupling step is performed, after preliminary purification, once again deprotection has to be done prior to the formylation reaction. The crude fMLF is then subjected to purification. If the formyl-Met was employed for coupling, purification could be done immediately after that.

Of these routes, I and II were performed as described. For Route III and IV it was investigated how to conduct single reaction steps that had not been needed in the other routes or improve the ones already used. This should ensure that these routes were actually feasible the way they were proposed.
In addition to the syntheses above it was tried to synthesize the peptide using solution phase synthesis exclusively. This was done with Fmoc amino acids and the benzyl ester of phenylalanine via the standard carbodiimide approach.

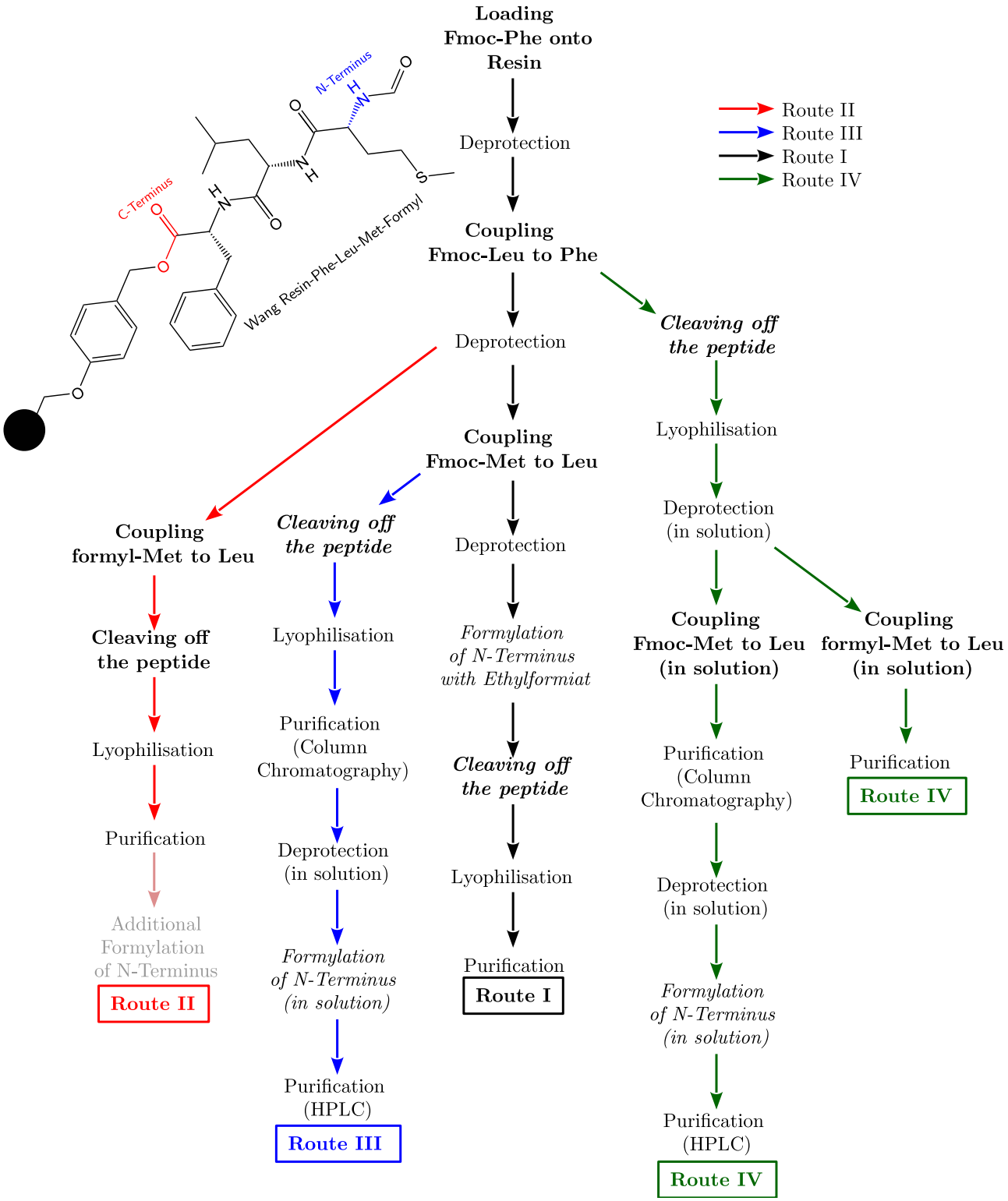

Figure 3.1.: Illustration of the four synthetic routes which were examined. They all are based on Route I, which was proposed by Breitung *et. al* [1]. Route I and II were fully carried out and in the case of Route III and IV their feasibility was tested.

3.1.3. Reaction Apparatus

As the available syringe based reactors (see *Section 1.1.3*) were too small for convenient usage, the solid phase peptide synthesis was carried out in alternative reaction apparatus. For most

steps of Route I (starting with the reaction in R_I - *III*) a Schlenk frit equipped with two Schlenk vessels was used (see *Figure 3.2 a.)*). It had the advantage that reaction and washing steps could be performed in the same vessel under inert conditions. Further, pressure or vacuum could be easily employed to accelerate filtration. Solutions were introduced via syringes through the gas valves. The drawback of this apparatus was that filtering during washing required turning it upside down, which resulted in many beads sticking to the walls of the container.

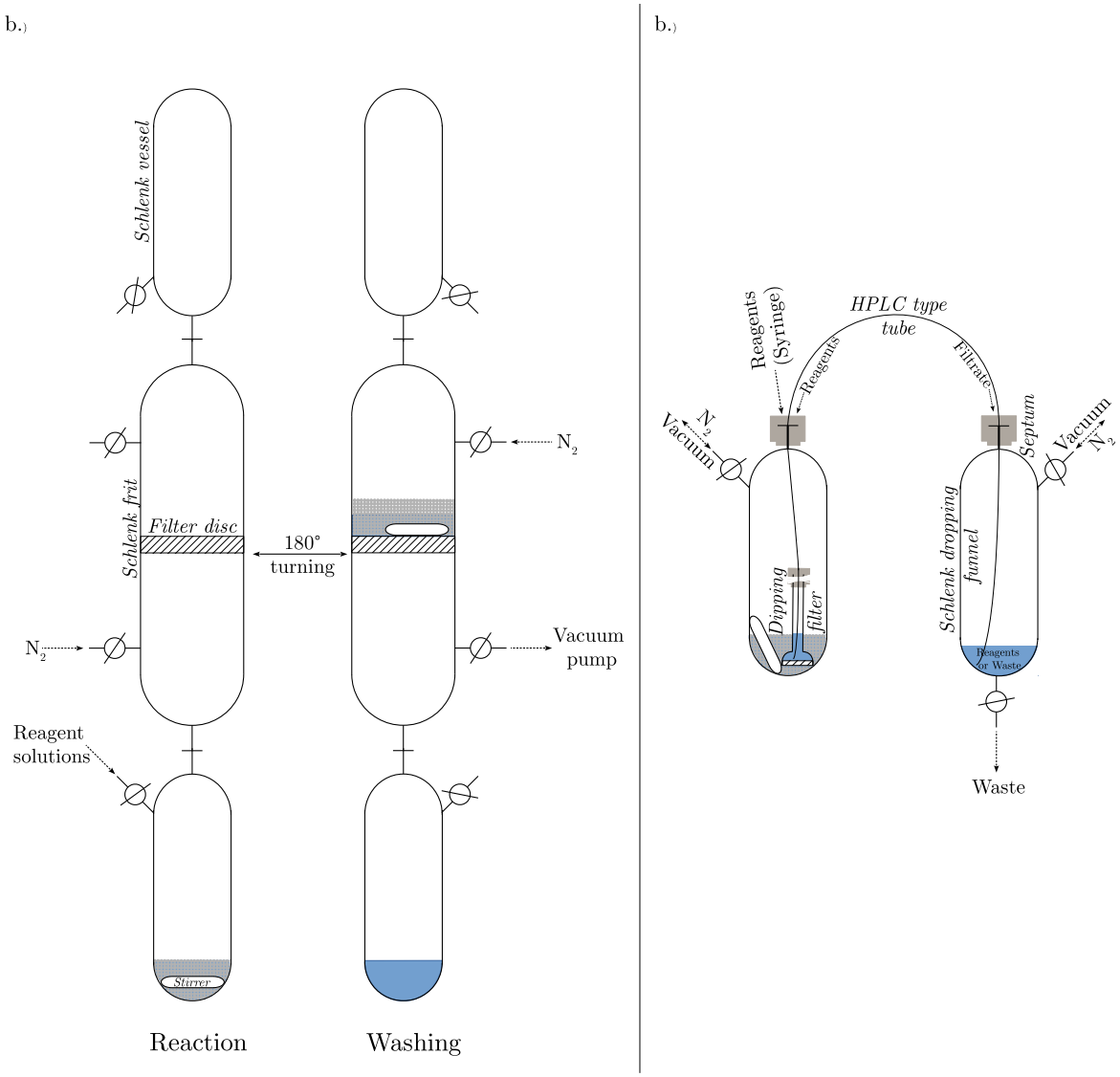

Figure 3.2.: Drawings of the apparatus used for solid phase synthesis. a.) The schlenk frit based apparatus in its reaction and filtration 'mode'. b.) The cannulation apparatus, constisting of Schlenk-type glassware connected with a HPLC tube which is fitted with a dipping filter. (The grey circles again symbolize the resin.)

As a result another apparatus for the synthesis along Route II was used. It consists of a Schlenk vessel and a Schlenk-type dropping funnel, which were connected via a HPLC tube. In order to seal the apparatus the tube was stuck through two septa. To make filtering feasible, one end of the tube was equipped with a dipping filter via a small septum and teflon tape. The filter was liftable not to disturb stirring. For a sketch of the apparatus see *Figure 3.2 b.)*
The apparatus was operated in following way: The resin was put into the Schlenk vessel with

the dipping filter. Reagents and washing solutions could be introduced directly with syringes or via the second vessel. Using N_2 or vacuum, solutions in the second container could be sucked or pressed through the tubing directly into the first one. If reversing the pressure or vacuum, removal of solutions from the resin was achieved, whereby the filter retained the beads in their original container. The bottleneck of this method was filtering off solvents which are rather viscous (for example NMP), because the filtration of these took usually extremely long. Moreover, too high N_2 pressure led to clogging of the filter as well as to untight septa.

3.1.4. Procedures

3.1.4.1. Auxiliary Reactions and Techniques

Aux - I: Synthesis of Ethylformate *According to [Supplementary of 49].* First 1.365 g (20.1 mmol) of sodium formate were dissolved in 60 mL ethanol. The solution was put on a ice/water bath and cooled for 20 minutes before adding 1.6 mL concentrated sulfuric acid during one minute. This was followed by flushing the reaction vessel three times with N_2 and removing the ice bath. The mixture was subsequently stirred for three days at room temperature. After that the reaction solution was distilled under atmospheric pressure with a Vigreux column. The resulting fractions were analysed using NMR[3.1] with $CDCl_3$ as solvent.

Yield	m [g]	n [mmol]	$\%_{\text{Theory}}$
Ethylformate	0.276	3.7	18.56

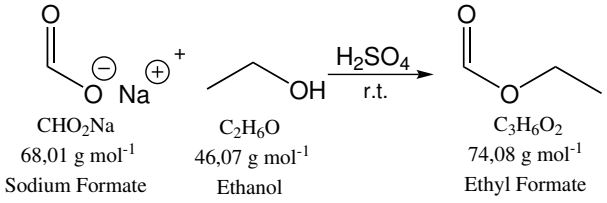

Characterisation - Ethylformate

Appearance: clear, slightly yellowish liquid

^{1}H-NMR (300 MHz, 298 K, $CDCl_3$, δ): 7.97 (s, 1H, **H**-C=O), 4.16 (q, *J*=7.2 Hz, 2H, -O-C**H$_2$**-CH_3), 1.23 (t, *J*=7.2 Hz, 3H, -O-CH_2-C**H$_3$**) [ppm]

Aux - II: Synthesis of Dabcyl-COOH *After [Supplementary of 1].* 1.374 g (10 mmol) of 4-amino benzoic acid were dissolved in 6 mL water and 2.5 mL HCl (12 M). The mixture was stirred and cooled on an ice/water bath. Then 1.393 g (20.2 mmol) $NaNO_2$ were dissolved in

[3.1] A typical NMR sample consisted of a few milligram of sample dissolved in about 600 µL of the desired deuterated solvent. In case dissolution was incomplete an ultrasonic sound bath or one or two drops of another deuterated solvent were used to facilitate dissolution.
The spectra were recorded at a Bruker 300 MHz Avance III spectrometer.
The spectra were referenced to their respective solvent signal, using the shift values published in [50].

3 mL H_2O. 1,26 mL of *N,N*-dimethylanilin were added and the mixture was stirred for 1 hour at 0°C. Subsequently, its pH was adjusted to 7 using saturated aqueous K_2CO_3 and HCl. The neutral suspension was filtered and the residue washed with water. As next step, the filter residue was then recrystallized from ethanol. The resulting product was dried and analysed by NMR (solvent: deuterated DMSO).

Yield	m [g]	n [mmol]	$\%_{\text{Theory}}$
Dabcyl-COOH	0.134	0.50	4.98

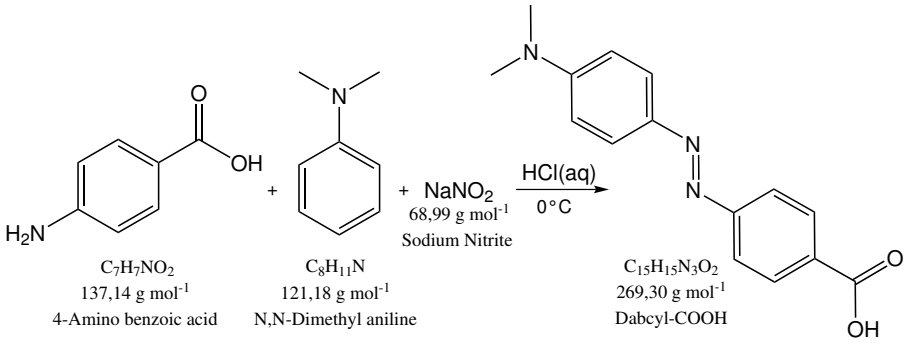

Characterisation - Dabcyl-COOH

Appearance: dark red powder

^{1}H-NMR (300 MHz, 298 K, DMSO-d_6, δ): 13.08 (broad s, 1H, O=C-O**H**), 8.07 (d, *J*=8.5 Hz, 2H, Ar-**H**), 7.83 (d, *J*=9.1 Hz, 4H, Ar-**H**), 6.86 (d, *J*=9.1 Hz, 2H, Ar-**H**), 3.08 (s, 6H, $-N(C\mathbf{H_3})_2$) [ppm]

Aux - III: Deprotection of Z-Gly-Gly for further use in R_{II} - XIII *In analogy to the procedure in [24, p.153-155].* 0.535 g (2 mmol) of Z-Gly-Gly were dissolved in 15 mL ethanol and 11 mL acetic acid. Dissolution had to be aided by ultrasonic sound irradiation and heat (60°C) treatment. After that the apparatus was flushed with N_2 and 0.092 g of Pd on C were added under stirring. After further flushing with N_2, five repeating freeze-pump-thaw cycles were conducted to remove oxygen. One such cycle consisted of following steps:

- Under a stream of gaseous N_2 the reaction suspension was frozen by immersion of the vessel in liquid N_2.
- Next, vacuum is applied for one minute to the reaction flask which is still in contact with N_2(l).
- Subsequently, the reaction mixture is thawed at room temperature under a stream of N_2(g).

After finishing the repeats, the N_2(g) was displaced with H_2(g) using a rubber balloon. The suspension was left stirring thoroughly for 3.5 hours at room temperature. This was followed

by displacing the H_2 with N_2 and filtering off the catalyst (under N_2), aided by the use of Celite 454. The residue was washed with methanol before being mixed with water to avoid spontaneous combustion of the catalyst. The solvent of the filtrate was then evaporated *in vacuo* at 35°C. The resulting precipitate was dried in the desiccator and analysed by NMR (solvent: D_2O).

Yield	m [g]	n [mmol]	$\%_{\text{Theory}}$
Gly-Gly	0.273	2.07	102.87

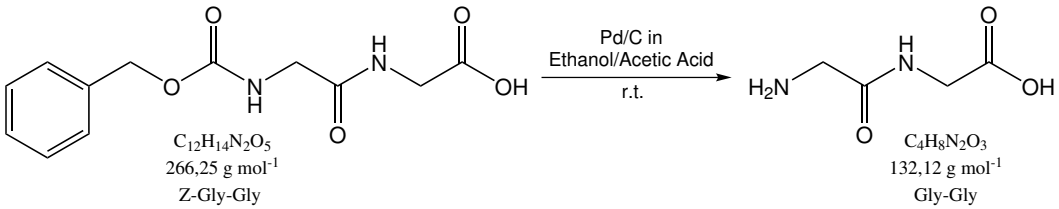

Characterisation - Gly-Gly

Appearance: greyish powder

^{1}H-NMR (300 MHz, 298 K, D_2O, δ): 3.85 (s, 4H, N−C**H_2**−C=O) [ppm]

Aux - IV: The Ninhydrin Stain The stain solution was prepared as described in [51]. 0.205 g (1.15 mmol) of ninhydrin were dissolved in a mixture 100 mL n-butanol, 0.5 mL acetic acid and 4.5 mL of H_2O. The stain was kept in the fridge wrapped in aluminium foil.
For a typical stain the (already UV-inspected) TLC plate was shortly immersed in the stain solution and heated either with a heat gun or in a drying oven at 80°C for a few minutes until the spots became visible.

3.1.4.2. Fmoc Protection of the Phe, Leu and Met

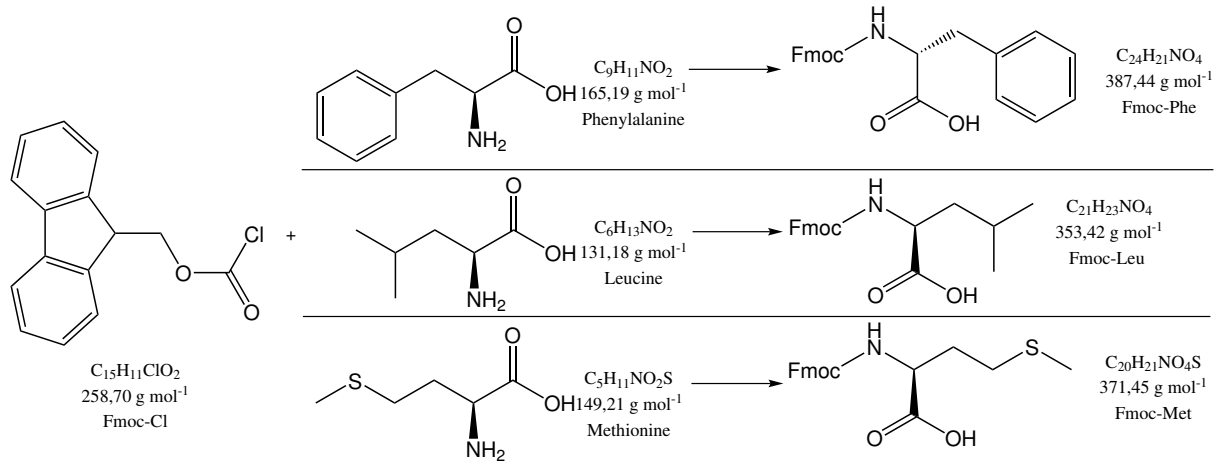

Prot - I, II and III: Synthesis of Fmoc-Phe, Fmoc-Leu and Fmoc-Met in Ethanol/Water *According to [52].* This approach of Fmoc protection was based on stirring Fmoc-chloride and the corresponding amino acid in a ethanol water solution (EtOH:H_2O=1:3[3.2]) at 60°C. Work-up involved extracting the aqueous phase with ethylacetate. The product resulting from the organic phase was examined by NMR (in various deuterated solvents). To enable further analysis, fractionation by column chromatography[3.3] was carried out in Prot - I and II. The product of Prot - III was analysed by MS[3.4] (solvent: methanol).
As the reactions did afford the desired products not at all or only in trace amounts, the details and variations of the single preparations are described in *Appendix A.1.*

Prot - IV and V: Synthesis of Fmoc-Phe and Fmoc-Leu, Microwave assisted *According to [53].* The second method to protect amino acids with the Fmoc group, which was tried, required a homogeneous suspension of Fmoc-Cl and the amino acid in water to be irradiated by microwaves. After irradiation and removal of the water the resulting residue was analysed by NMR (solvent: deuterated acetone) and MS (solvent: methanol).
The desired products were identified only in trace amounts and hence, details on the single reactions are given in *Appendix A.2.*

Prot - VI, VII and VIII: Synthesis of Fmoc-Phe, Bodanszky's method *In analogy to the procedure in [24, p.24-25].* Under stirring phenylalanine was dissolved in 3 mL of a 10% aqueous solution of Na_2CO_3. Next, 2 mL dioxane were added and the mixture was cooled on an ice/water bath. Upon that, the Fmoc-Cl was added portionwise. Subsequently, the reaction was stirred at 0°C under a N_2 atmosphere for four hours. Then stirring was continued at r.t. for at least over night. After that, the reaction mixture was treated with 60 mL of water and extracted two times with 10 mL of diethylether each. The resulting aqueous phase was acidified with concentrated HCl to pH 2 on an ice/water bath. Thereby a white precipitate occurred. In order to accomplish complete precipitation, the mixture was put into the fridge for several hours. After that the precipitate was filtered off and washed with water. The filter residue was dried in the desiccator and the filtrate was put once again into the fridge for several hours. In case a some more product precipitated, it was treated in the manner as the first crop of product. The product was analysed by NMR (solvents: deuterated aceton or $CDCl_3$) and MS (solvent: methanol). If necessary, recrystallisation from nitromethane was performed.

[3.2] Composition specifications of this format always refer to volume based concentrations (*i.e. V/V*).
[3.3] The stationary phase for column chromatography was silica in all cases.
[3.4] All MS investigations were performed with an ESI ion source and qTOF mass analyser. A typical MS ample was prepared by dissolving few crumbs of sample or a drop of the corresponding NMR sample in 1 mL methanol

Table 3.II.: A tabular compilation of the amounts of reagents used for the different preparations of Fmoc-Phe according to Bodanszky's procedure as well as the resulting yields.

Amounts for Fmoc-Phe	*Prot - VI*	*Prot - VII*	*Prot - VIII*
m_{Phe} [g]	0.166	0.166	0.166
n_{Phe} [mmol]	1	1	1
$m_{Fmoc\text{-}Cl}$ [g]	0.258	0.260	0.259
$n_{Fmoc\text{-}Cl}$ [mmol]	1	1	1
Yield Fmoc-Phe	*Prot - VI*	*Prot - VII*	*Prot - VIII*
m [g]	0.308	0.369	0.362
n [mmol]	0.79	0.95	0.93
$\%_{Theory}$	79.51	95.05	93.09

Characterisation - Fmoc-Phe (Prot - VI, VII and VIII)

Appearance: greyish-white powder

Melting Point: 184.9-186.1°C

^{1}H-NMR (300 MHz, 298 K, $CDCl_3$, δ): 7.77 (d, J=7.5 Hz, 2H, Ar_{Fmoc}-**H**), 7.55 (dd, 2H, J_1=7.2 Hz, J_2=3.0 Hz, Ar_{Fmoc}-**H**), 7.41 (t, J=7.4 Hz, 2H, Ar_{Fmoc}-**H**), 7.34-7.27 (m, 5H, $Ar_{Phe/Fmoc}$-**H**), 7.15 (d, J=6.5 Hz, 2H, Ar_{Phe}-**H**), 5.17 (d, J=8.14 Hz, 1H, N**H**), 4.76-4.65 (m, 1H, C_α-**H**), 4.51-4.32 (m, 2H, *Fmoc:* C$\mathbf{H_2}$), 4.21 (t, J=6.9 Hz, 1H, *Fmoc:* C**H**), 3.27-3.07 (m, 2H, *Phe:* C$\mathbf{H_2}$) [ppm]

MS (ESI, positive ion mode, qTOF, m/z): 388.1539 ($C_{24}H_{22}NO_4^+$, Fmoc-Phe)

Prot - IX, X and XI: Synthesis of Fmoc-Leu, Bodanszky's method *After the procedure in [24, p.24-25].* These experiments were carried out in the same fashion as described for Fmoc-Phe. The only differences were the usage of Leu and that the double amonuts of Na_2CO_3 as well as dioxane were applied for solubility reasons. This is also reflected in *Table 3.III.* The rest of the protocol was identical to the one stated above.

Table 3.III.: A list of the amounts of chemicals used for the different preparations of Fmoc-Leu according to Bodanszky's procedure as well as their corresponding yields.

Amounts for Fmoc-Leu	*Prot - IX*	*Prot - X*	*Prot - XI*
m_{Leu} [g]	0.133	0.134	0.132
n_{Leu} [mmol]	1	1	1
$m_{Fmoc\text{-}Cl}$ [g]	0.259	0.260	0.258
$n_{Fmoc\text{-}Cl}$ [mmol]	1	1	1
$V_{Na_2CO_3}$ [mL]	6	6	6
$V_{Dioxane}$ [mL]	4	4	4
Yield Fmoc-Leu	*Prot - IX*	*Prot - X*	*Prot - XI*
m [g]	0.287	0.311	0.316
n [mmol]	0.81	0.88	0.90
$\%_{Theory}$	79.77	86.16	89.23

Characterisation - Fmoc-Leu (Prot - IX, X and XI)

Appearance: white powder

Melting Point: 153.8-157.8°C

^{1}H-NMR (300 MHz, 298 K, $CDCl_3$, δ): 7.77 (d, *J*=7.5 Hz, 2H, Ar_{Fmoc}-**H**), 7.59 (d, *J*=8.1 Hz, 2H, Ar_{Fmoc}-**H**), 7.40 (t, *J*=7.4 Hz, 2H, Ar_{Fmoc}-**H**), 7.31 (t, *J*=7.3 Hz, 2H, Ar_{Fmoc}-**H**), 5.09 (d, *J*=8.5 Hz, 1H, N**H**), 4.5-4.36 (m, 3H, $C_{Fmoc}\mathbf{H_2}$, $C_{\alpha\text{-}Leu}$**H**), 4.23 (t, *J*=6.8 Hz, 1H, C_{Fmoc}**H**), 1.80-1.65 (m, 2H, C_αH−C$\mathbf{H_2}$−CH), 1.64-1.52 (m, 1H, CH_2−C**H**−$(CH_3)_2$), 0.97 (d, *J*=5.7 Hz, 6H, CH−(C$\mathbf{H_3}$)$_2$) [ppm]

Prot - XII and XIII: Synthesis of Fmoc-Met, Bodanszky's method *After the procedure in [24, p.24-25].* Also these syntheses were carried out identically to the ones described for the synthesis of Fmoc-Phe. Met was used for the reactions instead of Phe. Additionally, the amounts of solvents were varied as described in *Table 3.IV*.

Table 3.IV.: A compilation of the amounts of chemicals used for the different preparations of Fmoc-Met according to Bodanszky's procedure as well as the corresponding yields.

Amounts for Fmoc-Met	*Prot - XII*	*Prot - XIII*
m_{Met} [g]	0.150	0.225
n_{Met} [mmol]	1	1.5
$m_{Fmoc\text{-}Cl}$ [g]	0.260	0.390
$n_{Fmoc\text{-}Cl}$ [mmol]	1	1.5
$V_{Na_2CO_3}$ [mL]	3	4.5
$V_{Dioxane}$ [mL]	2	3
V_{H_2O} [mL]	60	110
$V_{Diethylether}$ [mL]	1x10, 1x20	1x15, 1x18
Yield Fmoc-Met	*Prot - XII*	*Prot - XIII*
m [g]	0.282	0.517
n [mmol]	0.76	1.39
$\%_{Theory}$	75.64	92.09

Characterisation - Fmoc-Met (Prot - XII and XIII)

Appearance: white, slightly yellowish powder

Melting Point: 128.5°C

^{1}H-NMR (300 MHz, 298 K, $CDCl_3$, δ): 7.77 (d, *J*=7.6 Hz, 2H, Ar_{Fmoc}-**H**), 7.59 (d, *J*=7.4 Hz, 2H, Ar_{Fmoc}-**H**), 7.41 (t, *J*=7.3 Hz, 2H, Ar_{Fmoc}-**H**), 7.32 (t, *J*=7.4 Hz, 2H, Ar_{Fmoc}-**H**), 5.39 (d, *J*=8.0 Hz, 1H, N**H**), 4.60-4.50 (m, 1H, $C_{\alpha\text{-}Leu}$**H**), 4.45 (d, *J*=6.8 Hz, 2H, C_{Fmoc}**H2**), 4.23 (t, *J*=6.6 Hz, 1H, C_{Fmoc}**H**), 2.57 (t, *J*=7.1 Hz, 2H, $CH_2-C\mathbf{H_2}-S$),
2.30-2.16 (m, 1H, $C_\alpha H-C\mathbf{H_2}-CH_2-S$), 2.11 (s, 3H, $S-C\mathbf{H_3}$),
2.07-1.98 (m, 1H, $C_\alpha H-C\mathbf{H_2}-CH_2-S$) [ppm]

3.1.4.3. General Procedures used for Solid Phase Peptide Synthesis Reactions

All the described solid phase reactions were carried out in and with oven dried instruments under Ar or N_2 atmosphere. The solvents were, if not already dry, dried with heat activated molecular sieves.

Gen - I: Resin Loading *According to the procedure in [1].* The resin loading reaction was initiated by swelling the Wang resin (capacity: 0.6-1.0 mmol g^{-1}) for 15 minutes in 1,5 mL of dry DCM. In a second reaction vessel Fmoc-Phe was dissolved in 3 mL DCM and 94 µL (1.18 mmol) *N*-methylimidazole. To that solution MSNT was added. After the dissolution of MSNT (after one minute) the mixture was transferred to the already swollen resin using a syringe. The resulting mixture was stirred under Ar atmosphere at room temperature over night. After that the resin was washed with DCM.

Gen - II: Fmoc Deprotection *According to the procedure in [1].* The removal of the Fmoc protection group was accomplished by stirring the (DMF washed) resin with three subsequent batches of 25% vol. piperidine in DMF at room temperature under N_2(g). The single reaction times were shortened from batch to batch (Typically, it was 15 minutes for the first, 10 minutes for the second and, 5 minutes for the last one.). Subsequently, the final batch of reaction solution was removed and the resin was washed with an appropriate solvent. Its choice depended on the following reaction.

Gen - III: Coupling to Extend the Peptide Chain *According to [1].* Initially, the coupling solution was prepared. To do so, the Fmoc-amino acid and HOBt were dissolved in NMP. Eventually, DIC was added. In the following, the coupling solution was applied to the resin. Under N_2 the reaction was stirred at room temperature over night. Then, the beads were washed with a suitable solvent (typically NMP).

Gen - IV: Cleaving off the Peptide *According to [1].* Removing the peptide from the solid support was done by applying a cleaveage solution to the dried resin. 2 mL cleavage solution consist of 1.88 mL TFA, 50 µL H_2O, 50 µL ethanedithiol and 20 µL triisoproylsilane. Three portions of cleavage solution were used. Each portion was stirred with the resin at r.t. under N_2 for 90 minutes and subsequently filtered off into H_2O. The resulting mixtures were then lyophilized.

Gen - V: Test for free -OH Groups *According to the supplementary of [1].* The test for free hydroxy groups (*Section 1.1.3.2*) was employed to assess the success of the resin loading. It was carried out in the following fashion. A dried sample (few mg) of the newly loaded resin (dried) and a control, consisting of unreacted resin, were treated each with 300 µL of 10% vol. triethylamine in DCM and 200 µL of diphenyldichlorosilane. The mixtures were shaken at r.t. for ten minutes and transferred to 2 mL syringes equipped with a filter frit. The supernatants were discarded and for each sample a mixture of 4 mg Dabcyl-COOH in 500 µL DMF was aspirated. The syringes were shaken again for ten minutes at ambient temperature. Next, the supernatant was discarded and the beads were washed five times with DMF. Further washing with DCM was continued until the supernatant remained colourless. The resulting colours of the beads (red indicates free -OH groups, white indicates none of them) were assessed bare eyed and microscopically.

Gen - VI: Kaiser Test *From the supplementary of [1].* In order to determine the success of coupling and deprotection reactions as well as the on-resin formylation, the Kaiser Test for free amine groups (*Section 1.1.3.2*) was performed. Typically, a small sample of resin was treated with 90 µL of a ninhydrin solution (0.054 g ninhydrin in 1 mL ethanol - 0.30 M), 90 µL of a phenol solution (0.808 g phenol in 0.2 mL ethanol - 42,95 M) and again 90 µL of

a KCN solution (20 µL of a 0.001 M aqueous KCN[3.5] solution in 980 µL pyridine - final KCN concentration: 0.02 mmol L^{-1}). The mixture was heated to 80°C for five minutes. After that, its colour was visually assessed. Strong blue colouring indicates the presence of free amine groups, which is the case when coupling occurred only partially. At least one control reaction (mostly negative with just the reagent solutions and from time to time positive with some sort of amine as sample) was always performed in parallel to the test with resin.

3.1.4.4. Synthesis of fMLF According to Route I

R_I - I: Coupling Fmoc-Phe to the Wang resin *According to [1].* The attachment of the first amino acid to the wang resin was accomplished as described in *Gen - I*. For 0.487 g Wang resin (capacity: 0.6-1.0 mmol g^{-1}), 0.254 g Fmoc-Phe (0.66 mmol) and 0.467 g MSNT (1.57 mmol) were employed. All other chemicals were used in the amounts stated in the general procedure. After the reaction the resin was washed seven times.
Subsequently, a small sample of resin was used to determine the success of the loading reaction with the test for free hydroxy groups as it is described in *Gen - V*.

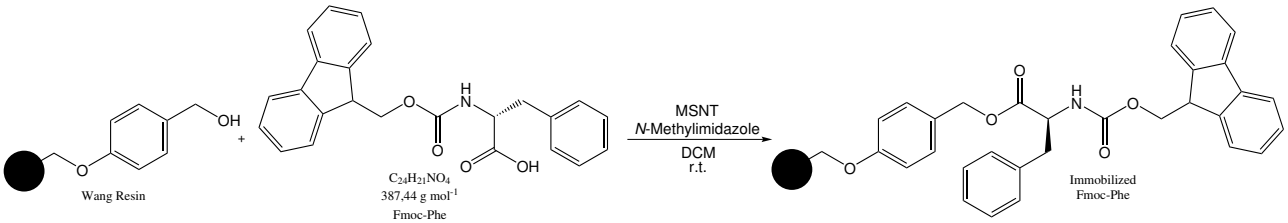

R_I - II: Deprotection of Fmoc-Phe and Coupling of Fmoc-Leu *According to [1].* In order to prepare the resin for the deprotection step it was washed five times with DMF. The reaction itself was conducted according to the general procedure *Gen - II*. 6 mL batches of piperidine solution were used and the reaction times were 20, 15 and 5 minutes, respectively. Subsequently the resin was washed five times with NMP
After the deprotection, the coupling reaction was performed as stated in *Gen - III*. The amounts of reagents are displayed in *Table 3.V.* As this reaction was performed in separate filtration and reaction apparatuses, additional 2 mL NMP were used for completely transferring the resin. After the reaction, the beads were washed five times with NMP.

Table 3.V.: The amounts of chemicals used in the coupling of Fmoc-Leu to resin bound Phe

	Fmoc-Leu		HOBt		DIC		V_{NMP} [mL]
	m [g]	n [mmol]	m [g]	n [mmol]	V [µL]	n [mmol]	
R_I - III	0.251	0.71	0.132	0.98	150	0.97	2.5

[3.5]KCN containing waste was treated with an aqueous solution of Fe(II)SO_4 for destruction purposes.

The success of the reaction was assessed using the Kaiser test, according to the procedure given in *Gen - VI*. As positive control substance pure Phenylalanine was used.

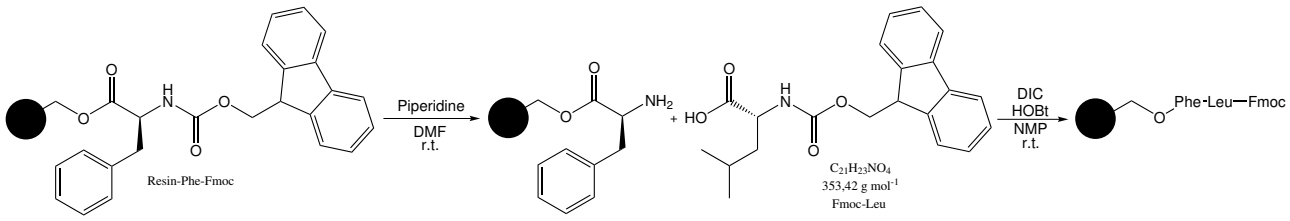

R_I - III: Deprotection of the Fmoc Dipeptide and Coupling of Fmoc-Met *According to [1].* The resin was washed 5 times with DMF and treatment of the resin with piperidine in DMF was performed as stated in *Gen - II*. 3-4 mL of piperidine solution per treatment step were used. The treatment time intervals were: 15, 10 and 5 minutes respectively.
After five times of washing the deprotected resin with NMP, coupling with Fmoc-Met was carried out. It was carried out to according to the general procedure *Gen - III*. The amounts of chemicals were are stated in *Table 3.VI.* HOBt was used in large excess by mistake.

Table 3.VI.: The amounts of chemicals used in the coupling of Fmoc-Met to the dipeptide

	Fmoc-Met		HOBt		DIC		V_{NMP} [mL]
	m [g]	n [mmol]	m [g]	n [mmol]	V [µL]	n [mmol]	
R_I - III	0.189	0.51	0.208	1.54	145	0.94	2.5

After the reaction, which was carried out at room temperature over night, the reaction solution was filtered off and the resin was washed five times with NMP. Subsequently, the Kaiser test was performed to check if the reaction had been working. This was done as stated in *Gen - VI*. As negative control, pure NMP was employed.

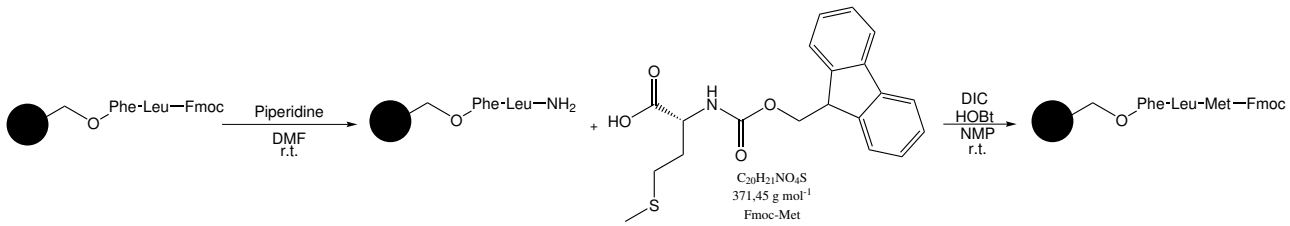

R_I - IV: Deprotection of the Fmoc Tripeptide and Formylation of the N-Terminus *According to [1].* Once again the resin was washed five times with DMF. Then, deprotection (*Gen - II*) was performed with 3 mL aliquots of the piperidine solution. The reaction times were 25, 10 and 5 minutes. After filtering off the last batch of piperidine solution, the resin was washed five times with DMF and subsequently, five times with DCM. Next, the resin was dried in the

apparatus under a stream of N_2 for 1.5 hours and then under vacuum for 1.5 hours. Additionally, a Kaiser test of the deprotected resin was performed for comparison purposes (*Gen - VI*). After the drying step, 7 mL of ethylformate were introduced. The mixture was stirred over night under N_2 at room temperature. Upon that, the ethylformate was removed and the resin was washed five times with DCM. A Kaiser test showed that the reaction had to be repeated. Hence, the resin was dried again *in vacuo* and additional 7 mL of ethylformate were applied to the resin. Stirring was conducted at r.t. under inert conditions for another night. Then, the DCM washings were repeated and a Kaiser test was performed. As a preparation for the next reaction, the resin was again dried for 2 hours and 20 minutes under water-jet pump vacuum and further 40 minutes under high vacuum.

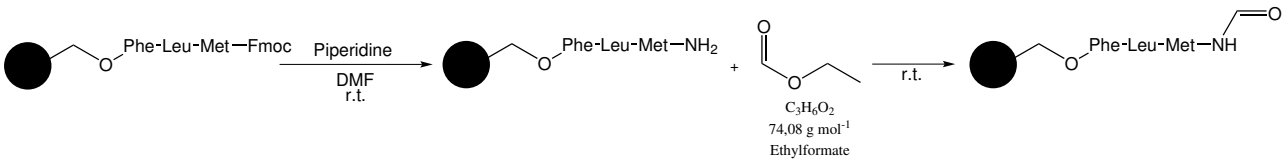

R_I - V: Cleaving fMLF off the resin *According to [1].* Releasing the peptide from the solid support was achieved as described in the general procedure *Gen - IV*. The first two aliquots of cleavage solution (4 mL each) were filtered into 10 mL portions of water. The third aliquot of cleavage (6 mL) solution was added to the aqueous mixture of the second one.

The two batches of cleavage solution were lyophilized, using a centrivugal evaporator, which was connected to a high vacuum pump via cooling trap. Aliquots of the solutions were filled in 1.5 mL Eppendorf vessels and frozen with liquid nitrogen. They were placed in the evaporator and evacuated with the high vacuum pump under rotation on liquid nitrogen. From time to time, the samples had to be refrozen. The lyophilized material was analysed by NMR (solvent: deuterated methanol) and MS (solvent: methanol).

The residue, coming from the first portion of cleavage solution was purified by normal phase column chromatography. Initially, the mobile phase was EtOAc:heptanes=2:3. This was then changed by adding 33% vol. acetone. From that it was changed to pure acetone and finally to pure methanol. The fractions were analysed by NMR (solvents: $CDCl_3$ or deuterated methanol).

The second fraction was subjected to another round of normal phase column chromatography. It was started with DCM:MeOH=6:1. Towards the end of the operation 30% vol. methanol was added to the mobile phase and for the last fractions pure methanol was used. Again the fractions were analysed by NMR[3.6] (solvent: deuterated methanol). The resulting data indicated that the product mainly consisted of unformylated MLF.

[3.6] With a sample of the product fraction a ^{13}C spectrum was recoded at a 700 MHz Bruker Avance III spectrometer.

Yield	m [mg]	n [mmol]	$\%_{\text{Theory}}$
Product of R_I - V (MLF)	17.8	0.043	13.73

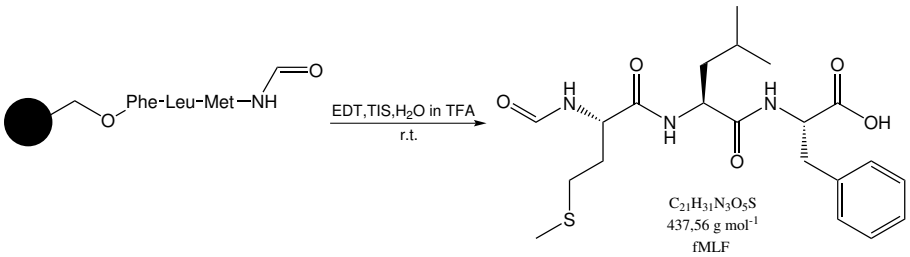

Characterisation - MLF (R_I - V)

Appearance: yellowish solid

[1]H-NMR (300 MHz, 298 K, Methanol-d_4, δ): 7.25-7.19 (m, 5H, Ar_{Phe}-**H**), 4.57-4.31 (m, 3H, $C_{\alpha\text{-Phe,Leu,Met}}$**H**), 3.20 (dd, 1H, J_1=13.7 Hz, J_2=5.0 Hz, C**H$_2$**−Ar_{Phe}), 3.01 (dd, 1H, J_1=13.7 Hz, J_2=6.5 Hz, C**H$_2$**-Ar_{Phe}), 2.55 (t, J=6.8 Hz, 2H, CH_2−C**H$_2$**−S−CH_3), 2.12-2.03 (m, 5H, C**H$_2$**−CH_2−S−C**H$_3$**), 1.70-1.60 (m, 1H, CH_2−C**H**−$(CH_3)_2$), 1.59-1.52 (m, 2H, C**H$_2$**−CH−$(CH_3)_2$), 0.97-0.89 (dd, 6H, J_1=10.2 Hz, J_2=6.1 Hz, CH_2−CH−(C**H$_3$**)$_2$) [ppm]

[13]C-NMR (176 MHz, 298 K, Methanol-d_4, δ): 177.3 (s, 1C, **C**=O), 173.3 (s, 1C, **C**=O), 173.1 (s, 1C, **C**=O), 139.2 (s, 1C, $\mathbf{C}_{q,\,Ar}$), 130.8 (s, 2C, $\mathbf{C}_{Ar}$), 129.2 (s, 2C, $\mathbf{C}_{Ar}$), 127.4 (s, 1C, $\mathbf{C}_{Ar}$), 57.0 (s, 1C, $\mathbf{C}_{\alpha}$), 53.9 (s, 1C, $\mathbf{C}_{\alpha}$), 53.7 (s, 1C, $\mathbf{C}_{\alpha}$), 41.9 (s, 1C, C−**C**H_2−C), 39.0 (s, 1C, C−**C**H_2−C), 32.8 (s, 1C, **C**H_2), 30.2 (s, 1C, **C**H_2), 25.8 (s, 1C, C−**C**H−$(CH_3)_2$), 23.4 (s, 1C, **C**H_3−CH−CH_3), 21.9 (s, 1C, CH_3−CH−**C**H_3), 15.2 (s, 1C, S−**C**H_3) [ppm]

3.1.4.5. Test Experiments for and Actual Synthesis of Route II

R_{II} - I, II, III, and IV: Test Reactions - Formylation of Met using Ethylformate *On the basis of the formylation reaction described in [1].* These trial reactions were performed in order to find optimal conditions for the formylation of methionine with ethylformate. Several reactions with different conditions (additional solvents, elevated temperature, basic and acidic pH) were performed. They all had in common that ethylformate was used in large excess compared to Met. Inn all reactions no useful amount of product was produced, although partial formylation occurred in some of them. Therefore, just the details on the reaction with the highest degree of formylation (R_{II} - IV) are given. The other reactions can be found in *Appendix A.3.*

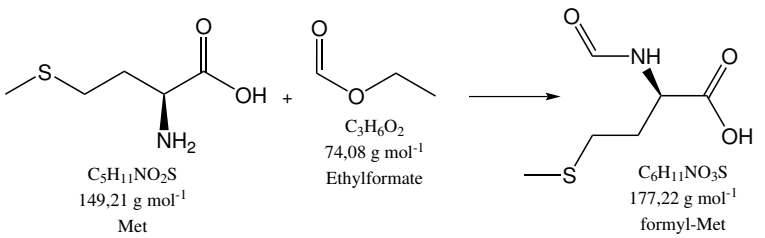

R_{II} - IV 0.151 g of Met (1.0 mmol) were dissolved in 3 mL Na_2CO_3 solution (10% in water). Then, 2 mL of ethylformat were added and the mixture was stirred for 2 days at r.t. under N_2(g). The solvents were removed *in vacuo* (70°C) and the residue was dried and examined by NMR in D_2O.

R_{II} - V, VI and VII: Formylation of Met - Formic Acetic Anhydride *Executed as described in [27].* In an inert (N_2) and dry Schlenk vessel, methionine was dissolved in formic acid. The mixture was cooled under stirring on an ice/water bath. Subsequently, acetic anhydride (0.7 mL) was dropped into the mixture via a syringe. Thereby, the temperature was monitored to be kept under 10°C. Subsequently, the solution was stirred for 1.5-3 hours at room temperature under N_2. After this period, 0.8 mL of ice cooled water were added to the reaction mixture. Next, the volatile components were removed *in vacuo* at 50°C, leaving behind the crude product. After drying, this was examined by NMR in D_2O. As a final step, the crude product was recrystallized from a minute amount of water, dried and again analysed by NMR in D_2O.

Table 3.VII.: Here the amounts of chemicals, which were varied in the preparations of formyl-Met according to the formic acetic anhydride method, are given Further the Yields of those reactions are given.

Amounts for formyl Met	R_{II} - V	R_{II} - VI	R_{II} - VII
m_{Met} [g]	0.148	0.155	0.155
n_{Met} [mmol]	1.0	1.0	1.0
$V_{Formic\ acid}$ [mL]	2.1	1.6	0.8
Yield formyl-Met	*R_{II} - V*	*R_{II} - VI*	R_{II} - VII
m [g]	0.121	0.143	0.166
n [mmol]	0.68	0.81	0.95
$\%_{Theory}$	68.81	78.10	91.10

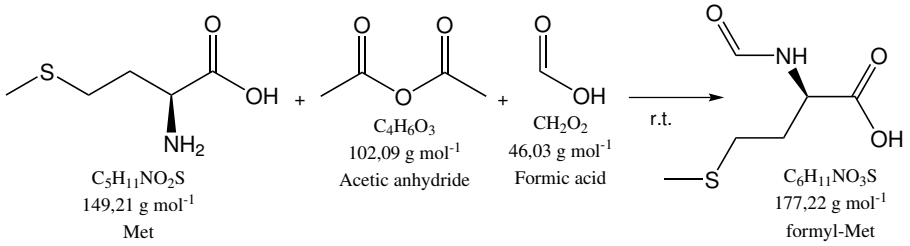

Characterisation - formyl-Met

Appearance: white, slightly brownish solid

[1]H-NMR (300 MHz, 298 K, D_2O, δ): 8.12 (s, 1H, **H**−C=O), 4.60 (dd, 1H, J_1=4.7 Hz, J_2=8.9 Hz, C_α**H**), 2.68-2.51 (m, 2H, C_αH−CH_2−C**H_2**−S), 2.26-2.13 (m, 1H, CH_2−C**H_2**−S), 2.09 (s, 3H, S−C**H_3**), 2.08-1.99 (m, 1H, CH_2−C**H_2**−S) [ppm]

R_{II} - VIII: Test Reaction - Solution Phase coupling of formyl-Met to Phe-OCH_3 *According to [27] and [24, p.145].* Initially, formyl-Met (0.121 g, 0.68 mmol), Phe-OCH_3·HCl (0.147 g, 0.68 mmol) and HOBt (0.092 g, 0.68 mmol) were dissolved in 0.72 mL of dry THF and 85.6 µL of *N*-ethylmorpholine. Subsequently, the mixture was put on an ice/water bath and DCC[3.7] (0.150 g 0.73 mmol) was added. The reaction mixture was stirred under inert conditions for one hour (N_2) at 0°C and then at room temperature for 75 minutes. After that, 2 more mL of THF were introduced to the reaction mixture in order to facilitate filtration which was subsequently carried out. The filter residue was washed with 4 mL THF. The THF phase (including the washing THF) was evaporated *in vacuo* at 32°C. The resulting residue was dissolved in a mixture of ethylacetate (3.4 mL) and saturated aqueous $NaHCO_3$ (1.7 mL). The phases were separated and the organic phase split into two halves. The first half was extracted once with 10% citric acid (1.7 mL), once with the $NaHCO_3$ (1.7 mL) and once with water (1.7 mL). The second half was treated in the same manner, however the extraction with citric acid was omitted. Next, each organic phase was diluted with 2 mL ethylacetate to facilitate the following drying of the solvent with Na_2SO_4. The dry phases were separately evaporated *in vacuo* (32°C) and dried under high vacuum. Finally, the products were anaysed by NMR (solvent: deuterated DMSO).

Yield	m [g]	n [mmol]	$\%_{Theory}$
formyl-Met-Phe-OCH_3	0.165	0.49	71.25

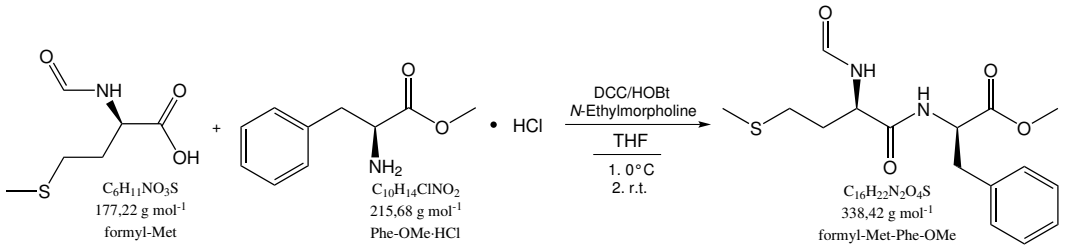

Characterisation - formyl-Met-Phe-OCH_3

Appearance: dark yellow, sticky solid

^{1}H-NMR (300 MHz, 298 K, DMSO-d_6, δ): 8.50 (d, *J*=7.7 Hz, 1H, N**H**), 8.27 (d, *J*=8.5 Hz, 1H, N**H**), 8.00 (s, 1H, **H**−C=O), 7.31-7.18 (m, 5H, Ar_{Phe}-**H**), 4.53-4.41 (m, 2H, $C_{\alpha\text{-Phe,Met}}$**H**), 3.58 (s, 3H, O=C−O−C**H$_3$**), 3.10-2.89 (m, 2H, CH_α−C**H$_2$**−Ar_{Phe}), 2.39 (t, *J*=7.9 Hz, 2H, CH_2−C**H$_2$**−S), 2.02 (s, 3H, S−C**H$_3$**), 1.92-1.69 (m, 2H, C_αH−C**H$_2$**−CH_2−S) [ppm]

^{13}C-NMR (75.45 MHz, 298 K, DMSO-d_6, δ): 171.8 (s, 1C, **C**=O), 170.9 (s, 1C, **C**=O), 160.9 (s, 1C, H−**C**=O), 137.1 (s, 1C, $\mathbf{C}_{q,Ar}$), 129.1 (s, 2C, $\mathbf{C}_{Ar}$), 128.3 (s, 2C, $\mathbf{C}_{Ar}$), 126.6 (s, 1C, $\mathbf{C}_{Ar}$), 53.6 (s, 1C, $\mathbf{C}_\alpha$H), 51.9 (s, 1C, $\mathbf{C}_\alpha$H), 50.1 (s, 1C, O=C−O−**C**H_3), 36.4 (s, 1C, **C**H_2−Ar), 32.3 (s, 1C, **C**H2-CH2-S), 29.2 (s, 1C, CH2-**C**H2-S), 14.6 (s, 1C, S-**C**H3) [ppm]

[3.7] DCC remnants were destroyed by letting them stand for several tens of minutes in a 6% ammonia solution

R_{II} - IX: Route II - Loading the Wang Resin with Fmoc-Phe *According to [1].* The reactions of Route II were carried out employing the cannulation apparatus described in *Section 3.1.3.*

The loading of the resin was performed in the same fashion as in *Gen - I*. 0.488 g Wang resin (capacity: 0.6-1.0 mmol g^{-1}), which was swollen for 25 minutes instead of 15 minutes, were used together with 0.254 g Fmoc-Phe (0.66 mmol) and 0.472 g MSNT (1.59 mmol). All other substances were used in the same amounts as stated in the general procedure. After the reaction the resin was washed five times with DCM.
A small sample of the resin was dried and tested for free hydroxy groups using the procedure described in *Gen - V*. Also, a positive control with unreacted Wang resin was performed. Finally, the resin was washed five times with DMF as preparation for the following deprotection reaction.

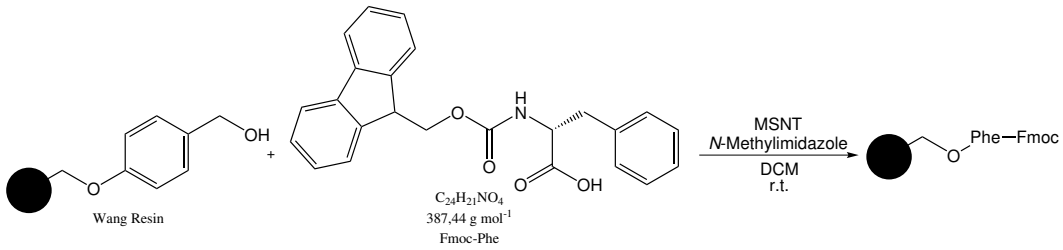

R_{II} - X: Route II - Deprotection of Fmoc-Phe and Coupling of Fmoc-Leu *According to [1].* After washing the resin five times with DMF deprotection according to the general procedure (*Gen - II*) was performed with 2.5 mL portions of piperidine solution. The first portion was stirred for 15 minutes, the second one for 10 minutes and the last one for 5 minutes. After removal of the last batch of reagent, the resin was washed five times with NMP.
During that, the coupling reaction according to *Gen - III* was prepared: Predried Fmoc-Leu (0.266 g, 0.75 mmol) and HOBt (0.134 g, 0.99 mmol) were dissolved in 2.5 mL NMP under N_2. Next, DIC (145 µL, 0.94 mmol) was added. Subsequently, this reaction solution was transferred to the washed resin and stirred at r.t. under inert conditions over night. In the following, the reaction solution was removed and the resin beads were washed five times with NMP. Using a small sample of the beads the Kaiser test was performed to assess the success of the coupling reaction. (For that purpose also a negative control with just the reagents was conducted.) The test was carried out as described in *Gen - VI*.

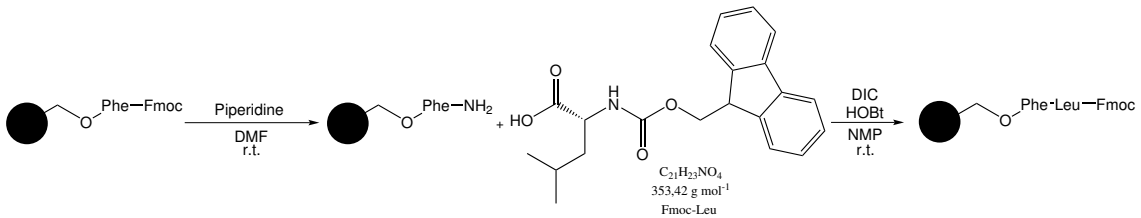

R_{II} - XI: Route II - Deprotection of Fmoc-Leu and Coupling of formyl-Met *According to [1, 27].* The first step was washing the resin five times with DMF. Then the standard deprotection

procedure (*Gen - II*) was performed. Three batches of piperidine solution (2.5 mL) were used. The reaction times were 15, 10 and 5 minutes. This was followed by five times washing with NMP.

Next, the coupling step with formyl-Met was carried out, similarly to the other couplings. Therefore, formyl-Met (0.166 g, 0.94 mmol) and HOBt (0.149 g 1.10 mmol) were dissolved in 2.5 mL of NMP (under N_2). Upon that, 145 µL DIC (0.94 mmol) were added. This coupling solution was then transferred via a syringe to the resin. The reaction was stirred over night at r.t. under N_2. After disposal of the reaction solution the resin was washed five times with NMP and subsequently, a Kaiser test was performed (*Gen - VI*; negative control: just the reagents) in order to confirm the success of the reaction. Finally, the resin was washed five times with DMF and then five times with DCM. To prepare for the cleavage reaction, the resin was dried *in vacuo* and in the desiccator.

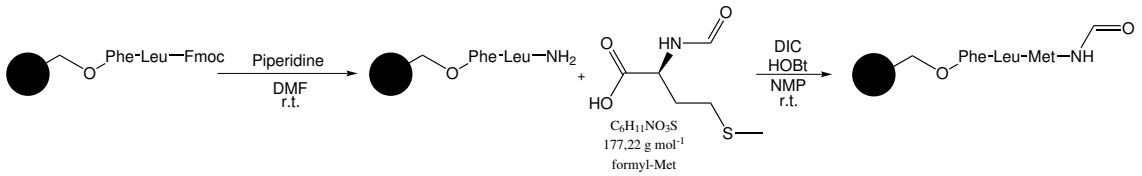

R_{II} - XII: Route II - Cleaving the Peptide Off the Resin *According to [1].* This step was carried out as already described in the general procedure *Gen - IV*. Three 2 mL portions of cleavage solution were employed to achieve cleavage. After the respective reaction time (1.5 hours each) the batches were filtered into one flask with 6 mL water.

Additionally, the resin was washed with water, which was kept separate from the cleavage mixtures. These two batches of liquid were then lyophilized as described in *R_I - V*. The samples were then analysed by NMR in deuterated acetone and acetonitrile. This showed that the product was unformylated MLF.

Yield	m [mg]	n [mmol]	$\%_{\text{Theory}}$
Product of R_{II} - XII (MLF)	49.1	0.12	37.77

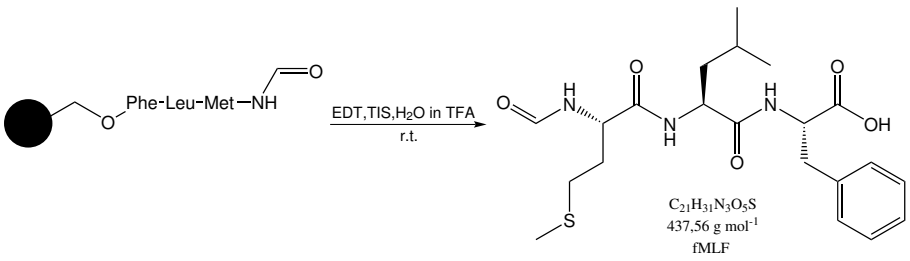

Characterisation - Product of R_{II} - XII (MLF)

Appearance: yellowish solid

^{1}H-NMR (300 MHz, 298 K, AcN-d_3, δ): 7.59-7.43 (m, 1H, N**H**), 7.42-7.32 (m, 1H, N**H**), 7.24-7.07 (m, 5H, Ar-**H**), 4.59-4.42 (m, 1H, C_α−**H**), 4.27-4.09 (m, 1H, C_α−**H**), 4.02-3.86 (m, 1H,

$C_\alpha-\mathbf{H}$), 2.45-2.35 (m, 2H, $Ch_2-C\mathbf{H_2}-S$), 1.94 (s, 3H, $-S-C\mathbf{H_3}$), 1.27-1.04 (m, 2H, $C\mathbf{H_2}-CH-(CH_3)_2$), 0.85-0.60 (m, 5H, $CH_2-CH-(C\mathbf{H_3})_2$) [ppm]

R_{II} - XIII: Test Reaction - Formylation of Gly-Gly with the Anhydride Approach *On the basis of [27].* The initial step was to dissolve the Gly-Gly dipeptide (0.135 g, 1.0 mmol) in formic acid (2 mL) while stirring. The solution was cooled on an ice/water bath. At a temperature not exceeding 10°C, acetic anhydride was added dropwise in (0.7 mL). Subsequently, the cooling bath was removed and the reaction was stirred at r.t. under N_2 for 3 hours. Next, it was poured into 0.8 mL of ice cold H_2O. Evaporation *in vacuo* at 28°C followed. After drying, the residue was examined by NMR (solvents: deuterated methanol and DMSO).

Yield	m [g]	n [mmol]	$\%_{\text{Theory}}$
formyl-Gly-Gly	0.161	1.00	98.37

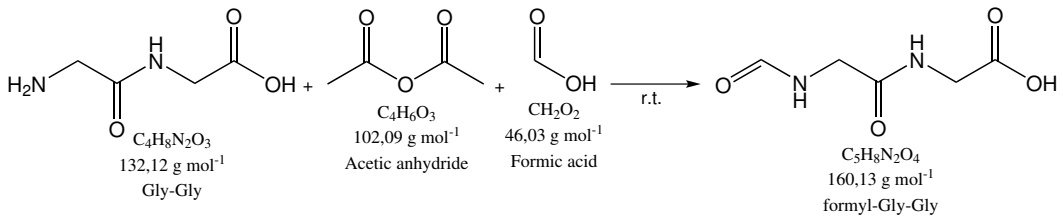

Characterisation - formyl-Gly-Gly

Appearance: greyish powder

^{1}H-NMR (300 MHz, 298 K, Methanol-d_4, δ): 8.17 (s, 1H, $\mathbf{H}-C=O$), 3.97 (s, 2H, $C_\alpha\mathbf{H_2}$), 3.94 (s, 2H, $C_\alpha\mathbf{H_2}$) [ppm]

The stability of the formyl-Gly-Gly Dipeptide A sample of the product (0.011 g, 0.67 mmol) in deuterated methanol (600 µL) was used to investigate the stability of the formyl group under various conditions (prolonged alcohol exposure at different temperatures as well as acidic environment). To do so, over a period of several weeks, standard ^{1}H spectra (32 scans) and occasionally standard HMBC spectra (6 scans) were recorded. In between the measurements, the sample was stored at room temperature and at 40.5°C after 11 days. After 28 days in total, the sample was treated with 150 µL TFA and measurements were continued for six further days.

R_{II} - XIV: Route II - Additional Formylation of the Cleaved Tripeptide *On the basis of [27].* As the *N*-formyl group of fMLF did not survive the cleavage and lyophilisation conditions, a further formylation attempt in solution was carried out. This reaction was generally performed as the previous formylation of Gly-Gly (*R_{II} - XIII*). First of all, the lyophilized residue (0.049 g) was dissolved in 0.25 mL formic acid. The mixture was cooled on an ice/water bath and 84 µL of acetic anhydride were added. Under a N_2 atmosphere, the mixture was stirred at room temperature for three hours. Upon that, the reaction solution was treated with 192 µL of

ice cooled water. Subsequently, the liquid components were removed by rotary evaporation *in vacuo* at 28°C as well as drying in the desiccator. The residue was analyzed by NMR in deuterated acetonitrile.

Next, this residue was purified by normal phase column chromatography. In the beginning the mobile phase was EtOAc:heptanes=1:2. This was then changed to EtOAc:heptanes=1:2. To this mobile phase 20% vol. acetonitrile was added later on. This was changed to 40 % vol. acetonitrile and after that EtOAc:AcN=1:1 was used. Upon that pure acetonitrile was used and finally on pure methanol was employed. The fractions were analysed with TLC with UV and ninhydrin detection. According to the TLCs the fractions were pooled evaporated and the residues were examined by NMR in deuterated acetonitril and methanol as well as with MS (solvent: methanol).

Upon that, the resulting product residue was further purified by HPLC using a reversed phase semi-preparative column (Nucleodur 100-7 C18ec 250x10 mm) and a 0.1% vol. aqueous TFA - methanol as the mobile phase (linear gradient from MeOH:TFA=1:4 to MeOH:TFA=9:1). The column was heated to 40°C and the flow rate was 3.0 mL min^{-1}. Detection was achieved with an UV detector. [54] The resulting fractions were evaporated and analysed by MS (in methanol).

Yield	m [g]	n [mmol]	$\%_{\text{Theory-Reaction}}$	$\%_{\text{Theory-Total Sequence}}$
fMLF	31.0	0.07	59.09	22.32

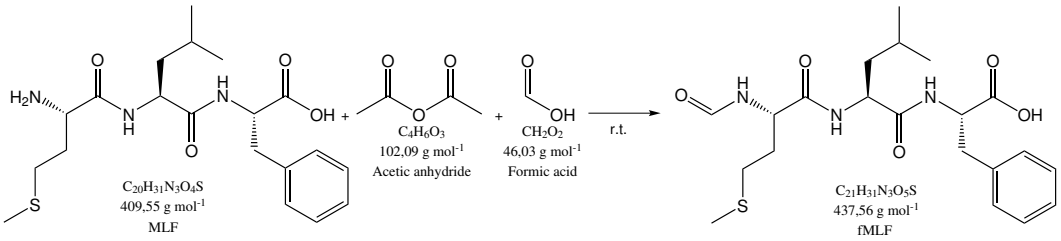

Characterisation - fMLF

After column chromatogrphy: *Appearance:* yellowish solid

^{1}H-NMR (300 MHz, 298 K, Methanol-d_4, δ): 8.11 (s, 1H, **H**−C=O), 7.27-7.11 (m, 5H, Ar−**H**), 4.64-4.51 (m, 1H, $C_{\alpha,Met}$**H**), 4.46-4.38 (m, 1H, $C_{\alpha,Phe}$**H**), 4.38-4.28 (m, 1H, $C_{\alpha,Leu}$**H**), 3.21 (dd, 1H, J_1=13.4 Hz, J_2=4.4 Hz, C_αH−C**H$_2$**−Ar), 3.07-2.96 (m, 1H, C_αH−C**H$_2$**−Ar), 1.91 (s, 3H, S−C**H$_3$**), 1.71-1.57 (m, 1H, CH_2−C**H**−$(CH_3)_2$), 1.56-1.40 (m, 1H, C**H$_2$**−CH−$(CH_3)_2$), 0.97-0.80 (m, 1H, CH_2−CH−(C**H$_3$**)$_2$) [ppm]

HPLC fraction 1: *MS (ESI, positive ion mode, qTOF, m/z):* 353.0268 , 401.0181 , 426.2056 ($C_{20}H_{32}N_3O_5S^+$, MLF-sulfoxide), 448.1873 ($C_{20}H_{31}N_3O_5SNa^+$, MLF-sulfoxide), 476.1818 ($C_{21}H_{31}N_3O_6SNa^+$, fMLF-sulfoxide), 490.1975 ($C_{22}H_{33}N_3O_6SNa^+$, *N*-Acetyl-MLF), 613.2668

HPLC Fraction 2: *MS (ESI, positive ion mode, qTOF, m/z):* 426,2055 ($C_{20}H_{32}N_3O_5S^+$, MLF-sulfoxide), 454.2001 ($C_{21}H_{32}N_3O_6S^+$, fMLF-sulfoxide), 476.1818 ($C_{21}H_{31}N_3O_6SNa^+$, fMLF-sulfoxide), 490.1974 ($C_{22}H_{33}N_3O_6SNa^+$, *N*-Acetyl-MLF), 492.1469

3.1.4.6. Test Reactions for Route III and IV

The following sections treat the reactions which were used to test the applicability of synthetic routes II and IV.

$R_{III\,IV}$ - I and II: Formylation of Met in Acetic acid *Based on the procedures and information in [27] and [55].* On an ice/water bath and under N_2 atmosphere formic acid and acetic anhydride were mixed and subsequently stirred at room temperature for 15 ($R_{III\,IV}$ - *I*) or 50 ($R_{III\,IV}$ - *II*) minutes. During that, methionine was mixed with acetic acid and cooled on an ice water bath. Next, the formic acid / acetic anhydride mixture was added to the Met suspension at 0°C. This was followed by stirring the mixture at r.t. for one hour. Thereby, the methionine dissolved. After that, 0.5 mL of ice cooled water were introduced. In $R_{III\,IV}$ - *II* 5 mL H_2O were used in addition to transfer the solution into a bigger vessel. Upon that the solvents were removed *in vacuo* at 30°C. After drying the residue in a desiccator, it was analysed with NMR in D_2O. (For the characterisation of the product see *Section 3.1.4.5.*)

Table 3.VIII.: The varying amounts of reagents for $R_{III\,IV}$ - I and II are given in this list as well as their resulting yields.

	Met		Formic Acid		Acetic Anhydride		$V_{\text{Acetic Acid}}$ [mL]
	m [g]	n [mmol]	V [µL]	n [mmol]	V [µL]	n [mmol]	
$R_{III\,IV}$ - *I*	0.150	1.0	120	3.18	380	4.02	2
$R_{III\,IV}$ - *II*	0.150	1.0	75	1.99	190	2.01	0.4

Yields: formyl-Met	m [g]	n [mmol]	$\%_{\text{Theory}}$
$R_{III\,IV}$ - *I*	0.200	1.13	112.47
$R_{III\,IV}$ - *II*	0.179	1.01	100.18

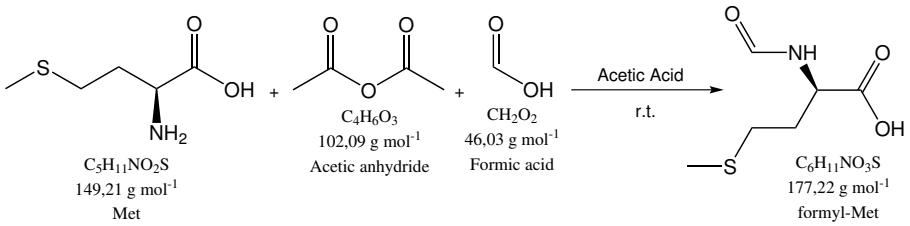

$R_{III\,IV}$ - III: Formylation of Gly-Gly in Acetic acid *Based on [27] and [55].* This experiment was conducted in the same way as $R_{III\,IV}$ - *I and II*. Acetic anhydride (94 µL, 0.99 mmol) and formic acid (38 µL, 1.01 mmol) were premixed for 30 minutes before being stirred with the suspension of Gly-Gly (0,067 g, 0.51 mmol) in 150 µL glacial acetic acid for one hour. The rest was performed identically to the above mentioned procedure. NMR experiments were recorded in D_2O. (For a characterisation of the product see R_{II} - *XIII.*)

Yield	m [g]	n [mmol]	$\%_{\text{Theory}}$
formyl-Gly-Gly	0.082	0.51	101.53

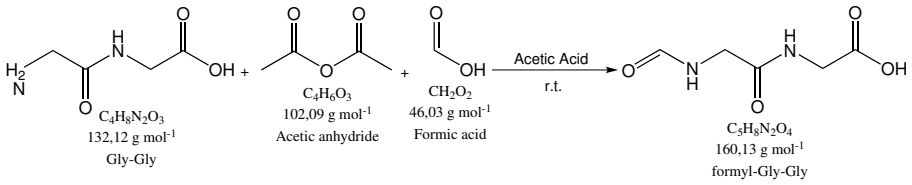

$R_{III\,IV}$ - IV Formylation of Met in One Equivalent of Formic acid *Based on [27].* This reaction was an attempt to achieve formylation without the use of formic acid in large excess or acetic acid as auxiliary solvent. Hence, just formic acid acetic anhydride and formic acid together with Met in equimolar amounts were used. However in the course of the reaction it became necessary to introduce acetic acid. The reaction did not afford an useful amount product. Details on the reaction can be found in *Appendix A.3*
(A reaction scheme can be found here: *R_{II} - V, VI and VII*)

$R_{III\,IV}$ - V: Solution Phase Deprotection of Fmoc-Leu *Based on [24, p.185-186] and [56]* Fmoc-Leu (0.177 g, 0.5 mmol) were dissolved in 10 mL acetonitrile. Subsequently, 1 mL of diethylamine was added. Under N_2 atmosphere and at room temperature the mixture was stirred for 1.5 hours. The volatile components were removed at a rotary evaporator *in vacuo* at 29°C. The residue was triturated with diethylether (12.5 mL). The insoluble fraction was filtered off, washed twice with 10 mL diethylether and dried in the desiccator. The ether phases were unified, evaporated and also dried. Finally, the residues were analysed by NMR (solvents: D_2O-insoluble, $CDCl_3$-ether phase)

Yield	m [g]	n [mmol]	$\%_{\text{Theory}}$
Leu	0.065	0.49	98.38

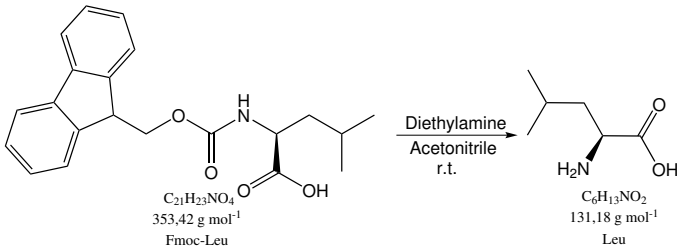

Characterisation - Leu

Appearance: greyish solid

^{1}H-NMR (300 MHz, 298 K, D_2O, δ): 3.75-3.67 (m, 1H, C_α**H**), 1.76-1.61 (m, 3H, C_αH-C**H2**-C**H**-(CH3)2), 0.94 (dd, 6H, J_1=6.2 Hz, J_2=3.4 Hz, $-CH_2-CH-(C\mathbf{H_3})_2$) [ppm]

Characterisation - 9-Methylene-9*H*-flourene

Appearance: yellowish solid

^{1}H-NMR (300 MHz, 298 K, $CDCl_3$, δ): 7.77 (d, J=7.6 Hz, 2H, Ar−**H**), 7.73 (d, J=7.2 Hz, 2H, Ar−**H**), 7.42 (td, 2H, J_1=7.5 Hz, J_2=1.3 Hz, Ar−**H**), 7.34 (td, 2H, J_1=7.5 Hz, J_2=1.2 Hz, Ar−**H**), 6.11 (s, 2H, C=C**H$_2$**) [ppm]

$R_{III\,IV}$ - VI: Solution Phase Coupling of Fmoc-Leu with Phe *According to [17]* Fmoc-Leu (0.195 g, 0.55 mmol) and HOBt (0.102 g, 0.76 mmol) were dissolved in 2 mL dry DMF. Next, the mixture was cooled on an ice/water bath. DCC (0.116 g, 0.66 mmol) was dissolved in 0.5 mL DMF and also cooled at 0°C under a nitrogen atmosphere. The cold DCC solution was then added to the amino acid/HOBt solution, which was then stirred for one hour at 0°C and one hour at room temperature. Upon that, phenylalanine (0.082 g, 0.50 mmol) was added and stirring was continued over night. This was followed by filtering the reaction mixture and washing the residue with 2 mL DMF to remove the DCU. The DMF phase was treated with 30 mL water and put into the fridge for 4 hours to ensure complete precipitation. The extremely fine precipitate was filtered off using a filter funnel (porosity 4) and high vacuum. After drying the residue was analysed by MS in (solvent: methanol) and NMR (solvent: deuterated methanol).

Yield	m [g]	n [mmol]	$\%_{\text{Theory}}$
Fmoc-Leu-Phe	0.281	0.56	112.86

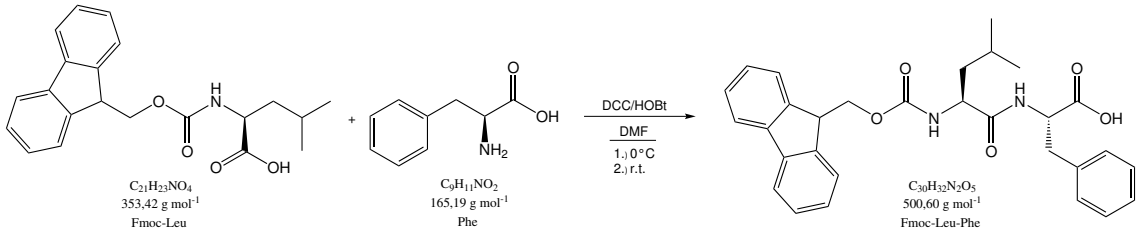

Characterisation - Fmoc-Leu-Phe

Appearance: light grey solid

^{1}H-NMR (300 MHz, 298 K, $CDCl_3$, δ): 7.77 (d, J=7.5 Hz, 2H, Ar_{Fmoc}−**H**), 7.64-7.53 (m, 2H, Ar_{Fmoc}−**H**), 7.32 (t, J=7.4 Hz, 2H, Ar_{Fmoc}−**H**), 7.24 (t, J=7.4 Hz, 2H, Ar_{Fmoc}−**H**), 7.19-7.03 (m, 5H, Ar_{Phe}−**H**), 4.79-4.63 (m, 1H, $C_{\alpha-Phe}$**H**), 4.36-4.18 (m, 3H, $C_{\alpha-Leu}$**H**, C_{Fmoc}**H$_2$**), 4.17-3.98 (m, 1H, C_{Fmoc}**H$_2$**), 3.24-3.09 (m, 1H, C**H$_2$**−Ar), 3.04-2.94 (m, 1H, C**H$_2$**−Ar), 0.98-0.79 (m, 6H, CH−(C**H$_3$**)$_2$) [ppm]

MS (ESI, positive ion mode, qTOF, m/z): 225.1963 ($C_{13}H_{25}N_2O^+$, DCU), 247.1782 ($C_{13}H_{24}N_2ONa^+$, DCU), 376.1520 ($C_{21}H_{23}NO_4Na^+$, Fmoc-Leu), 449.3845 ($C_{26}H_{49}N_4O^+_2$, 2 x DCU - aggregate), 501.2377 ($C_{30}H_{33}N_2O_5^+$, Fmoc-Leu-Phe), 523.2196 ($C_{30}H_{32}N_2O_5Na^+$, Fmoc-Leu-Phe)

$R_{III\,IV}$ - VII: Deprotection of Fmoc-Leu-Phe in solution *Based on [56] and [24, p.185-186]* The product of *$R_{III\,IV}$ - VI* (0.281 g) was dissolved in 8 mL of acetonitrile and treated with 0.8 mL of piperidine at room temperature. The mixture was stirred under a N_2 atmosphere for 1.5 hours. This was followed by evaporating the solvents *in vacuo* at 30°C. The residue was triturated with diethylether (12.5 mL). The resulting residue is filtered and washed twice (10 mL each) with diethylether.

After initial NMR experiments in D_2O and deuterted methanol, the residue was retriturated with 10 mL diethylether. The previous ether phase was evaporated and also retriturated with 15 mL diethylether. The resulting residue was again examined by NMR in deuterated DMSO. In another attempt to purify the product, all product components were unified and dissolved in a mixture of ethylacetate and water. Seven drops of triethylamine were added. The phases were mixed, separated and evaporated. The following residues were analysed by NMR in deuterated DMSO.

No product could be detected.

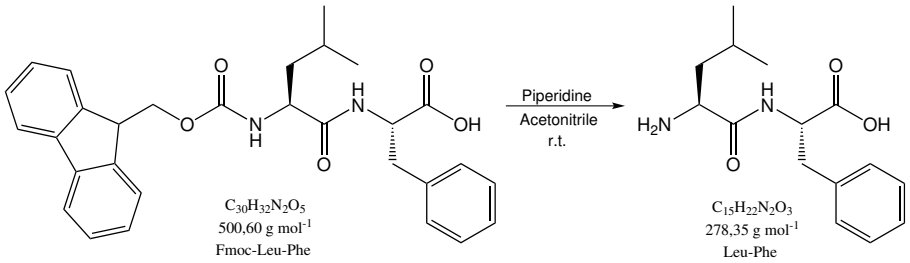

$R_{III\,IV}$ - VIII: Preparation of Fmoc-Met-Bt *According to [57].* 1*H*-Benzotriazole (0.477 g, 4.0 mmol) was dissolved in 3 mL of dry THF. To that solution 74 µL thionyl chloride (1,0 mmol) were added. The mixture was stirred at 40°C and under N_2 atmosphere for 20 minutes and subsequently cooled on an ice/water bath. To this cold solution, Fmoc-Met (0.372 g, 1.0 mmol) dissolved in 1 mL THF, was added dropwise. Next, the mixture was stirred at room temperature under nitrogen for 2 hours. Upon that, the reaction solution was filtered and the filter residue washed with 2 mL of THF. The filtrate was concentrated *in vacuo* at 30°C and then diluted with 20 mL ethylacetate. This organic phase was washed three times with 10 mL saturated aqueous Na_2CO_3 solution and once with 10 mL saturated aqueous NaCl solution. The combined aqueous layers were reextracted with 10 mL of ethylacetate. The unified organic phases were dried over Na_2SO_4 and evaporated *in vacuo* at 30°C. The product was examined with NMR in deuterated DMSO.

Yield	m [g]	n [mmol]	$\%_{\text{Theory}}$
Fmoc-Met-Bt	0.427	0.90	90.11

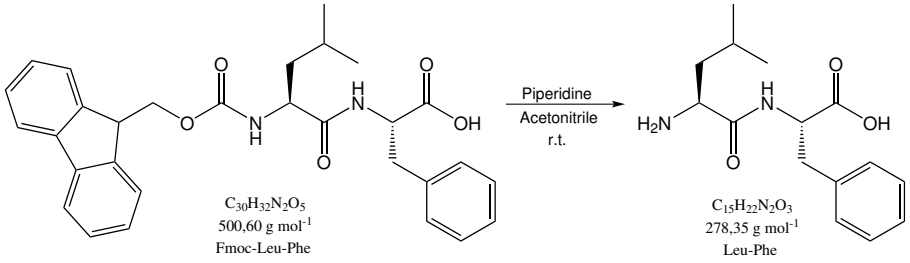

Characterisation - Fmoc-Met-Bt

Appearance: yellowish solid

^{1}H-NMR (300 MHz, 298 K, DMSO-d_6, δ): 8.32-8.27 (m, 2H, N**H**), 8.23 (d, J=8.2 Hz, 1H, Ar_{Bt}-**H**), 7.89 (d, J=7,6 Hz, 3H, Ar-**H**), 7.81 (t, J=7.6 Hz, 1H, Ar-**H**), 7.72 (d, J=7.1 Hz, 2H, Ar-**H**), 7.65 (t, J=7.8 Hz, 1H, Ar-**H**), 7.46-7.29 (m, 7H, Ar-**H**), 5.69-5.59 (m, 1H, C_α**H**$-Ch_2-Ch_2$), 4.43 (d, J=7.0 Hz, 2H, $C_{Fmoc}H_2$), 4.22-4.28 (m, 1H, C_{Fmoc}H), 2.71-2.58 (m, 2H, CH_2-C**H$_2$**$-S$), 2.33-2.19 (m, 1H, $C_\alpha H-C$**H$_2$**$-CH_2-S$), 2.18-2.08 (m, 1H, $C_\alpha H-C$**H$_2$**$-CH_2-S$), 2.06 (s, 3H, $-S-C$**H$_3$**) [ppm]

$R_{III\,IV}$ - IX: Coupling of Leu with Fmoc-Met-Bt *According to [57].* Leucine (0.131 g 1.0 mmol) was dissolved in 10 mL water and 4 mL acetonitril[3.8]. Next, 140 µL triethylamine (1.01 mmol) were added. The mixture was stirred at room temperature till the Leu was dissolved fully. Then it was transferred to the flask with Fmoc-Met-Bt (0.427 g, 0.9 mmol). Stirring was continued at r.t. and under N_2 for 3 hours. The acetonitrile was evaporated at 30°C *in vacuo* at the rotary evaporator. To the rest of the mixture was extracted twice with 15 mL ethylacetate. The unified organic phases were washed twice with 6 M HCl and dried over Na_2SO_4. Next, the ethylacetate was evaporated and the residue dried in the desiccator before analysis by NMR in deuterated DMSO.

No product could be detected.

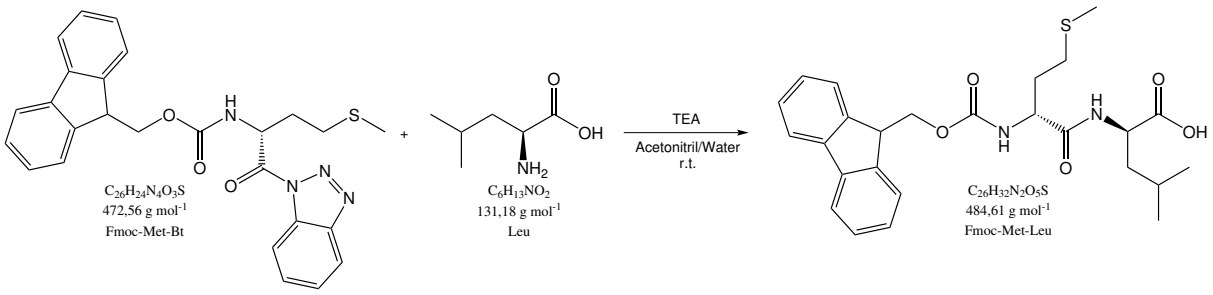

3.1.4.7. The Liquid Phase Approach

The following paragraphs describe the attempt of synthesizing fMLF by solution phase chemistry. For that the benzyl ester was used for C-terminal protection and the Fmoc-group for N-Terminal protection, as Fmoc-amino acids were readily available.

[3.8] This was a mistake, it should have been 4 mL water and 10 mL acetonitrile according to [57].

Sol - I and II: Benzylester of Phe *On the basis of the procedures given in [22, 58].* Phenylalanine was suspended in benzyl alcohol under N_2 and cooled on an ice/water bath to 0°C in Sol - I and on an ice/water/NaCl bath to -10°C in Sol - II. Next, thionyl chloride was dropped into the cold stirred suspension during ten minutes. The mixture was subsequently subjected to ultrasonic sound for five hours. Thereby, the ultrasonic sound bath heated up (maximal values from 45 to 50°C) and had to be cooled from time to time with small portions of ice. The following step was the addition of dry diethylether (Sol - I: 4 mL; Sol - II: 40 mL) in order to precipitate the product. In order to achieve full precipitation, the mixture was put into the fridge over night. Then, the precipitate was filtered off and washed with ether. As in Sol - I, more precipitation occurred, more batches of product were obtained. The purities of these were assessed by NMR in D_2O. In Sol - II the mother liquor was extracted 3 times with 10 mL water. The aqueous phase was evaporated and analysed by NMR in D2O and MS in methanol.

Table 3.IX.: The varying amounts of reagents for Sol - I and Sol - II, the preparations of the benzyl ester of Phe as well as their resulting yields.

	Phe		Benzyl alcohol		Thionylchloride	
	m [g]	n [mmol]	V [mL]	n [mmol]	V [mL]	n [mmol]
Sol - I	0.166	1.0	6.25	60	1	13.8
Sol - II	0.660	4.0	25	240	4	55.1

Yields: Phe-OBz	m [g]	n [mmol]	$\%_{Theory}$
Sol - I	0.188	0.64	64.25
Sol - II	0.947	3.25	81.34

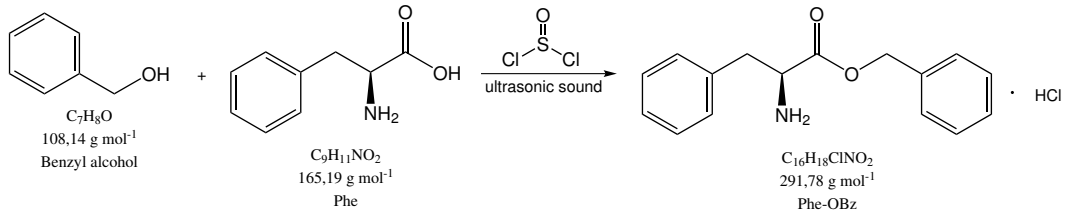

Characterisation - Phe-OBz

Appearance: white, slightly grey powder

^{1}H-NMR (300 MHz, 298 K, D_2O, δ): 7.48-7.42 (m, 3H, Ar−**H**), 7.42-7.36 (m, 2H, Ar−**H**), 7.36-7.31 (m, 3H, Ar−**H**), 7.19-7.12 (m, 2H, Ar−**H**), 5.27 (dd, 2H, J_1=12.0 Hz, J_2=19.4 Hz, −O−C**H$_2$**−Ar), 4.44 (t, J=6.6 Hz, 1H, C_α**H**−CH_2), 3.27 (d, J=6.4 Hz, 2H, C**H$_2$**−Ar) [ppm]

Sol - III: Coupling of Phe-OBz with Fmoc-Leu Followed by Deprotection *According to [24, p.145;185-186] and [56].* This short sequence consisted of DCC / HOBt mediated coupling of PheOBz to Fmoc-Leu and subsequent deprotection of the Fmoc group using diethylamine in acetonitrile. Already the first reaction gave a product which was not unambiguously identifiable

to be the desired one. Nevertheless, the deprotection was performed, affording no product at all. Details on the experimental procedures are shown in *Appendix A.4*.

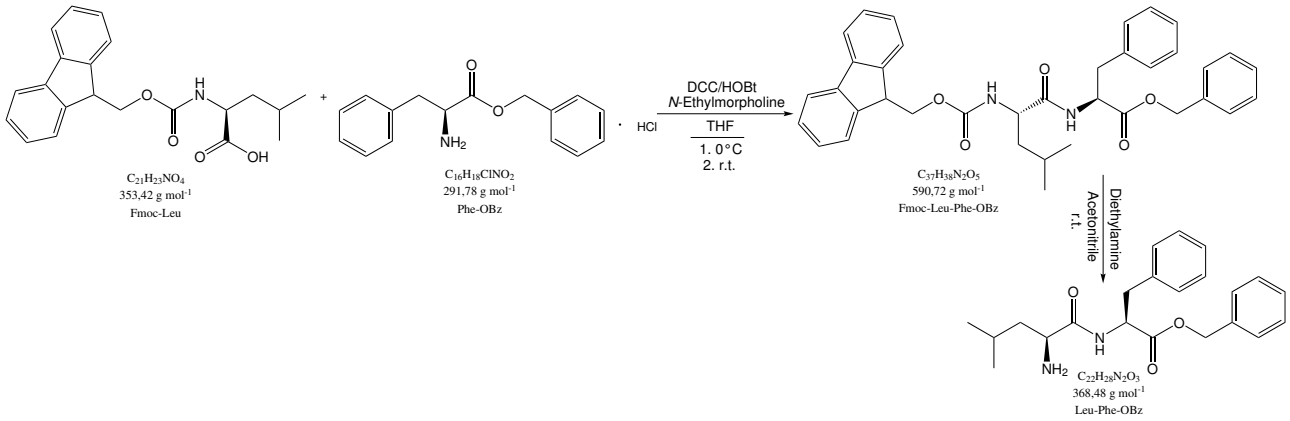

Sol - IV: Coupling of Phe-OBz with Fmoc-Leu, Alternative Protocol *According to [17]* Phe-OBz (0.296 g, 1.02 mmol), Fmoc-Leu (0.389 g, 1.10 mmol), and HOBt (0.207 g 1.53 mmol) were dissolved in 4 mL dry DMF under N_2. Subsequently, 125.2 µL *N*-ethylmorpholine (1.00 mmol) were added and the mixture was cooled to 0°C. This was treated with an ice-cold solution of DCC (0,232 g, 1.12 mmol) in 1 mL DMF. The reaction was stirred for one hour at 0°C and one further hour at room temperature. Next, the reaction solution is filtered to remove DCU. Thereby, 7 mL of DMF are used for washing purposes. The combined DMF phases were treated with 40 mL water. To ensure complete precipitation, the mixture was kept in the fridge over night. The precipitate was filtered off and washed with water. The filter residue was transferred to a mortar and ground with 6.5 mL of saturated aqueous $NaHCO_3$. The suspension was filtered and the residue was washed with water and dried in the desiccator. The dry product was then examined by NMR in deuterated DMSO and MS (solvent: methanol).

Yield	m [g]	n [mmol]	$\%_{\text{Theory}}$
Fmoc-Leu-Phe-OBz	0.757	1.28	126.19

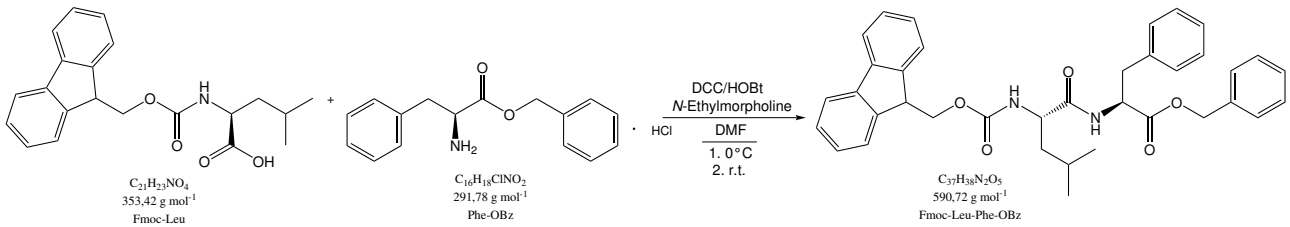

Characterisation - Fmoc-Leu-Phe-OBz

Appearance: light grey powder

^{1}H-NMR (300 MHz, 298 K, DMSO-d_6, δ): 8.38 (d, *J*=7.51 Hz, 1H, N**H**), 7.89 (d, *J*=7.1 Hz, 2H, Ar-**H**), 7.72 (d, *J*=7.4 Hz, 2H, Ar-**H**), 7.47-7.38 (m, 3H, Ar-**H**), 7.36-7.27 (m, 6H, Ar-**H**), 7.27-7.19 (m, 5H, Ar-**H**), 5.04 (dd, 2H, J_1=12.9 Hz, J_2=15.5 Hz, −O−C**H$_2$**−Ar), 4.57-4.46 (m, 1H, $C_{\alpha\text{–Phe}}$**H**), 4.31-4.25 (m, 1H, C_{Fmoc}**H**), 4.25-4.17 (m, 2H, C_{Fmoc}**H$_2$**), 4.11-4.01 (m, 1H, $C_{\alpha\text{–Phe}}$**H$_2$**), 3.07-2.94 (m, 2H, C**H$_2$**−Ar), 0.82 (dd, 6H, J_1=6.6 Hz, J_2=9.4 Hz, CH_2−CH−(C**H$_3$**)$_2$) [ppm]

MS (ESI, positive ion mode, qTOF, m/z): 225.1962 ($C_{13}H_{25}N_2O^+$, DCU), 247.1782 ($C_{13}H_{24}N_2ONa^+$, DCU), 354.2539 ($C_{21}H_{24}NO_4^+$, Fmoc-Leu), 376.1519 ($C_{21}H_{23}NO_4Na^+$, Fmoc-Leu), 449.3845 ($C_{26}H_{49}N_4O_2^+$, 2 x DCU - aggregate), 462.3107 , 613.2666 ($C_{37}H_{38}N_2O_5Na^+$, Fmoc-Leu-Phe-OBz)

Sol - V: Deprotection of Fmoc-Leu-Phe-OBz *According to [24, p.185-186]* The residue of *Sol - IV* (0.236 g, 0.4 mmol) was dissolved in 8 mL DMF. Next, 0.8 mL piperidine were added. The reaction mixture was stirred for 1.5 hours at room temperature under N_2. As attempting evaporation *in vacuo* at 30°C was in vain, the solution was treated with an excess of water and kept in the fridge over night to ensure complete precipitation. The precipitate was filtered off and washed with water. Next, it was triturated with 10 mL of heptanes. After a further filtration step, the residue was washed with 5 mL heptanes and dried. Finally, the product as well as the evaporated heptanes phase were analysed with NMR (solvent: deuterated DMSO). These indicated the product to be Leu-Phe and not Leu-Phe-OBz.

Yield	m [g]	n [mmol]	$\%_{Theory}$
Sol - V (Leu-Phe)	0.071	0.25	63.73

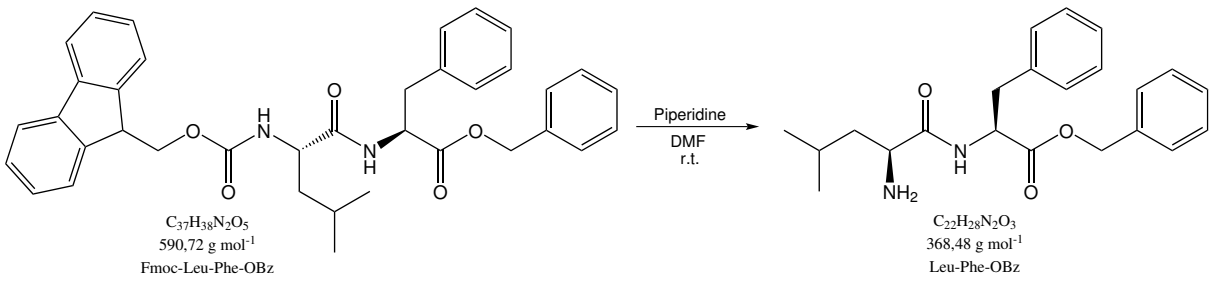

Characterisation - Sol - V (Leu-Phe)

Appearance: greyish powder

^{1}H-NMR (300 MHz, 298 K, DMSO-d_6, δ): 8.09 (d, *J*=12.0 Hz, 2H, N**H**), 7.32-7.18 (m, 4H, Ar_{Phe}−**H**), 7.18-7.09 (d, *J*=, Hz, 2H, Ar_{Phe}−**H**)4.16 (s, 1H, $C_{\alpha\text{–Phe}}$**H**), 3.51-3.43 (m, 1H, $C_{\alpha\text{–Leu}}$**H**), 3.13 (dd, 1H, J_1=3.4 Hz, J_2=13.2 Hz, C**H$_2$**−Ar), 2.82 (dd, 1H, J_1=4.7 Hz, J_2=13.4 Hz, C**H$_2$**−Ar), 0.61 (dd, 6H, J_1=6.5 Hz, J_2=10.0 Hz, CH−(C**H$_3$**)$_2$) [ppm]

3.2. Solid State NMR studies

The work in the field of solid state NMR consisted mainly of implementation of the experiments described in the introduction. Thereby, the first step was to obtain a well-behaving simulation of the desired experiment. This simulation was then in a second step transformed into an actual pulse program, which was examined on the spectrometer.

3.2.1. Simulations

Simulations were carried out with the SIMPSON software package (Version 3.1) [59], which is a program dedicated to solid state NMR, but also suitable for liquid state NMR. It is used by applying an input script, which is written in Tcl (`https://www.tcl.tk/`). In this script all necessary information, on the spin system, the setup of the 'virtual spectrometer', the pulse sequence and the data processing are given. From that SIMPSON generates data mostly in the form of FIDs or spectra. These were analysed using specialised tools such as SIMPLOT, which is a part of the SIMPSON distribution, jsnmr (`http://nmr.au.dk/software/jsnmr/`) or GSim (`https://sourceforge.net/projects/gsim/`). Further, MATLAB (`http://uk.mathworks.com/products/matlab/index.html`) and Octave (`https://www.gnu.org/software/octave/`) were employed to examine and process more complex datasets.
In order to extract correct dipolar coupling constants from PDB files, which is needed when modelling spin systems after real molecules, another program called SIMMOL (Version 1.0)[60] was used. It is also operated via Tcl input scripts and produces SIMPSON spin systems.

3.2.1.1. Illustration with a minimal SIMPSON example

This section illustrates the usage of SIMPSON by Tcl scripts (native Tcl commands are bold, SIMPSON ones are blue and underlined) via a practical example.[3.9] The following code represents the simulation of a $\mathcal{R}$-decoupled ^{13}C experiment as it was introduced in *Section 1.2.3.2.*

```
1  spinsys {
2   channels 1H 13C
3   nuclei 1H 13C 1H
4   shift 1 3p 7p 1 20 30 0
5   shift 2 1000 20p 0.5 0 50 0
6   shift 3 4p 5p 0.3 90 0 12
7   dipole 1 2 -5000 0 0 0
8   dipole 3 2 -5000 0 109 0
9   dipole 1 3 -20000 0 144 0
10  jcoupling 1 2 150 10 0.9 0 60 0
11  jcoupling 3 2 150 15 0.5 0 0 0
```

[3.9] Although this example shows a 1D experiment also 2D experiments are fully feasible with SIMPSON. Even higher dimensional experiments should be doable, although data processing would need to be done with external software.

```
}
par {
 spin_rate 20000
 proton_frequency 500e6
 np 1000
 crystal_file rep168
 gamma_angles 15
 start_operator Inz
 detect_operator I2p
 verbose 1101
 variable n 1.0
 variable N 6.0
 variable ny 3.0
 variable NumberPulsesRRp 6.0
}
proc pulseq {} {
 global par
 maxdt 5
 #Pulse sequence begins
 pulse 5 0 0 50000 $par(phi)
 #Acquisition under R decoupling
 acq
 for {set i 1} {$i < $par(np)} {incr i } {
  for { set p 1 } {$p <= [ expr $par(N) / 2 ] } { incr p } {
   #R block
   pulse $par(tPulse90) $par(ampPulse90) [ expr -45 + $par(phi) ] 0 0
   pulse $par(tPulse90) $par(ampPulse90) [ expr +45 + $par(phi) ] 0 0
   pulse $par(tPulse90) $par(ampPulse90) [ expr -45 + $par(phi) ] 0 0
   #R' block
   pulse $par(tPulse90) $par(ampPulse90) [ expr +45 - $par(phi) ] 0 0
   pulse $par(tPulse90) $par(ampPulse90) [ expr -45 - $par(phi) ] 0 0
   pulse $par(tPulse90) $par(ampPulse90) [ expr +45 - $par(phi) ] 0 0
  }
 acq
 }
}
proc main {} {
 #Further declaration of variables of the par{} block
 global par
 set par(tauRot)   [ expr 1.0e6 / $par(spin_rate) ]
 set par(tRblock) [ expr ($par(n) / $par(N)) * $par(tauRot)  ]
 set par(tPulse90)  [ expr $par(tRblock) / (0.5* $par(NumberPulsesRRp) ) ]
 set par(tPulse360) [ expr $par(tPulse90) *4.0  ]
 set par(ampPulse90) [ expr ((1.0 / $par(tPulse360) )*1.0e6) ]
 set par(tdwell) [ expr 6.0* $par(tPulse90) *( $par(N) /2) ]
 set par(sw) [ expr int(1.0e6/ $par(tdwell)) ]
 set par(phi) [ expr (180/ $par(N))* $par(ny) ]
```

```
59 #The actual simulation command followed by processing the dataset f.
60 set f [fsimpson]
61 faddlb $f 20 0
62 fsave $f $par(name).dat -xreim
63 fsave $f $par(name).fid
64 fzerofill $f 1024
65 fft $f
66 fsave $f $par(name).fdat -xreim
67 fsave $f $par(name).spe
68 funload $f
69 }
```

Generally, a SIMPSON input script[3.10] consists of four blocks, the `spinsys {}`, the `par{}`, the `proc pulseq {} {}` and the `proc main {} {}` block. All blocks allow standard Tcl expressions. In `spinsys` all the information on the spin system is given as well as the rf channels, which are declared first (*Line 2*). The other lines deal with the amount and order of nuclei (*Line 3*) and their interactions (*Lines 4-11*), whereby values for isotropic, anisotropic components and the corresponding Euler angles can be supplied.
The `par` section contains parameters concerning the 'virtual spectrometer' such as the MAS frequency (`spin_rate`), the spectrometer frequency, (`proton_frequency`) and the size of the FID (`np`). Further, the starting magnetisation and the operators which should be detected are specified (*Line 19 and 20*) as well as the number of sample crystallites (`crystal_file` and `gamma_angles`). Additionally, user defined variables can be set in this section with `variable` (In this case the symmetry numbers and the number of pulses during a $\mathcal{RR}'$ block). The last imporant command in this block is `verbose` which is a binary string that sets how much information shoud be displayed on the terminal.
The next section, `proc pulseq`, holds as the name indicates the information on the pulse sequence. The most basic commands which are needed for that are `pulse`, which exerts a pulse of a special duration and a for each channel unique amplitude and phase, `delay`, for a delay (not shown in the example) and `acq`, which detects one point of the FID. In order to produce useful pulse sequences these commands are often combined with native Tcl language constructs.
The last block, `proc main`, actually executes the simulation with `'set <DatasetName> [fsimpson ]'` (*Line 60*). Before that additional variables can be declared (*Lines 51-58* - Here, amongst others, pulse lengths, amplitude, spectral width and dwell time). After the execution command, the data generated by the simulation are saved to files with `fsave` and processed, whereby `faddlb` applies an exponential decay to the FID mimicking relaxation, `fzerofill`, performs zero filling and `fft` does the fourier transformation. Finally, `funload` closes the dataset and concludes the simulation (*Line 68*).
Additionally, SIMPSON input scripts containing just the `proc main` block can be used to process already existing datasets. To do so the dataset can be loaded with `fload`from a file and the standard processing commands followed by saving commands can be applied.

[3.10] It is required to save such a script as `'<InputScriptName>.in'`

A more detailed description of SIMPSON can be found in [59].

3.2.2. NMR Experiments

All solid state NMR experiments were performed on a Bruker 500 MHz instrument. It consisted of a Spectrospin Magnet, an Avance III console and a 3.2 mm MAS 1H/BB probe head. Frequency filters were mounted on the corresponding rf channels before the preamplifier except for $\mathcal{R}$-decoupled ^{1}H experiments.
A typical setup of the spectrometer involved adjusting the magic angle with a KBr sample and calibrating the ^{1}H and ^{13}C 90° pulses with adamantane (Typical values: ^{1}H - 2.1 µs at 136 W, ^{13}C - 3.1 µs at 110 W). These were then used as reference pulses for all other pulses. Shimming was carried out by assessing the linewidths of the ^{13}C resonances of adamantane. If needed CP was set up on adamantane too.
The spectra were referenced to the resonances of adamantane (^{1}H: 1.2 ppm and ^{13}C: 38.5 ppm; the higher shifted peak).
Data were analysed using Bruker's TopSpin (version 3.2). (`https://www.bruker.com/de/products/mr/nmr/nmr-software/software/topspin/overview.html`)
The following tables give experimental parameters of typical examples of the already described experiments. The corresponding Bruker pulse programs are given in the *Appendix B*.

Table 3.X.: A list of typical experimental parameters of the two versions of the $\mathcal{R}$-decoupled ^{1}H pulse sequence.

Parameter	**$\mathcal{R}$-decoupled ^{1}H-Basic**	**$\mathcal{R}$-decoupled ^{1}H-Improved**
$\mathcal{R}$ Symmetry	$\mathcal{R}6_1^3$	$\mathcal{R}6_1^3$
MAS frequency, CNST31 [Hz]	14000	20000
Spectral width, SWH [Hz]	100000	100000
Spectral width indirect dimension, CNST18 [Hz]	21000	30000
Size of FID, TD	1024	1024
Size of indirect dimension, TD F1	512	512
Dwell time, DW [µs]	5	5
Dwell time indirect dimension, INF1 [µs]	23.81	16.67
Acquisition time, AQ [s]	0.00512	0.00512
Recycle Delay, D1 [s]	6	5
Pre-scan delay, DE [µs]	10	10
Reciever gain, RG	8	8
^{1}H Transmitter Offset, O1 [Hz]	15500	14957
Length of a 90° ^{1}H Pulse, P1 [µs]	3.97	2.78
Power level of the ^{1}H channel, PLW1 [W]	38.1	77.6

Table 3.XI.: A list of typical experimental parameters of $\mathcal{R}$-decoupled ^{13}C and $\mathcal{R}$-decoupled INEPT pulse sequences.

Parameter	**$\mathcal{R}$-decoupled ^{13}C**	**$\mathcal{R}$-decoupled INEPT**
$\mathcal{R}$ Symmetry	$\mathcal{R}6_1^3$	$\mathcal{R}6_1^3$
MAS frequency, CNST31 [Hz]	18000	17920
Spectral width, SWH [Hz]	10080.65	10080.65
Size of FID, TD	2048	4096
Dwell time, DW [µs]	49.60	49.60
Acquisition time, AQ [s]	0.1015808	0.2031616
Recycle Delay, D1 [s]	5.0	5.0
Pre-scan delay, DE [µs]	6.50	6.50
Reciever gain, RG	128	128
^{13}C Transmitter Offset, O1 [Hz]	5372.45	5028.20
^{1}H Transmitter Offset, O2 [Hz]	14750	4222.88
Length of a 90° ^{13}C Pulse, P1 [µs]	2.9	3.1
Length of a 90° ^{1}H Pulse, P2 [µs]	-	3.1
Length of cpd Decoupling, PCPD2 [µs]	3.09	16
Power level of the ^{13}C channel, PLW1 [W]	110	110
Power level of the ^{1}H channel, PLW2 [W]	-	68.5
Power level of cpd decoupling, PLW12 [W]	63	10.3
cpd-Program	mg_RDec	spinal64

3.2.3. Growth of Glycine Polymorphs

As the available glycine consisted of a mixture of polymorphs, pure polymorphs had to be crystallized in order to have well defined NMR samples.

Cryst - I: The α and γ Polymorphs of Glycine

α-Glycine *According to [61].* 10 mL of 18 MΩ water were saturated with glycine under stirring for 45 minutes at room temperature. The solution was decanted from the remaining solid and subsequently filtered into a well of a clean six-welled tissue culture plate using a syringe with a 5 µm filtertip. The plate was set aside with the lid a little bit open to aid evaporation. After seven days a big crystal (0,802 g 10.7 mmol) had formed and was harvested. It was taken out of the mother liquor dried with tissue paper and further dried in the desiccator. It was morphologically similar to the ones depicted in [61].

γ-Glycine *According to [61].* To a 0.1 g mL^{-1} solution of NaCl (0.707 g of NaCl in 7 mL of 18 MΩ water) 2.206 g glycine were added according to the solubility table given in [61]. The mixture was stirred for 45 minutes at room temperature until everything had dissolved.

Next, the solution was filtered into another well of the tissue culture plate in the same way as described above. After setting it aside for thirteen days the small crystal (0.655 g, 8.7 mmol) were harvested and dried in the described manner.

As published in [62]. Equimolar amounts of KNO_3 (3.034 g, 30 mmol) and glycine (2.254 g, 30 mmol) were dissolved in a minimum amount of 18 MΩ water (8 mL in total) under 30 minute stirring at room temperature. The solution was filtered in the shown way into a third well of the tissue culture plate. After leaving it to crystallize for 29 days, the crystals (1.302 g, 17.3 mmol) were harvested in the already described fashion.

Cryst - II: The α Polymorph of Glycine according to the Bruker Method *As described in [63, p.79].* First 50 mL of 18 MΩ water were saturated at room temperature (21.5°C) with glycine.
10 mL of this solution were filtered into a well of a six-welled tissue cultivation dish and set aside for crystallisation according to the method described in *Cryst - I*. The crystals were harvested after nine days (1.302 g, 17.3 mmol).
The rest of the solution was precipitated with acetone. The white precipitate was filtered off and washed with acetone, whereby some more precipitation occurred in the mother liquor. After filtering off this second batch of precipitate the α-glycine was predried with vacuum from the water jet pump, followed by drying in the desiccator and under high vacuum (4.389 g, 58.5 mmol).

4. Results and Discussion

4.1. Synthesis of fMLF

4.1.1. Auxiliary Reactions

4.1.1.1. Aux - I: Synthesis of Ethylformate

The reaction was performed as described in the supplementary of [49]. Distillation gave two fractions, of which the first, boiling between 58 and 73°C (*Figure 4.1*), contained the product with an excess of ethanol (EtOFormate:EtOH=1:5, see *Figure 4.2*, at 3.60 and 1.14 ppm). The second one consisted entirely of ethanol as the NMR showed. The yield of 18.6% (ethanol impurities are already taken into account) is low although in accordance with the literature, where it was stated with 12%. The small discrepancy between the yields may be explained by the usage of radioactive tritium labelled compounds in [49].
The purpose of this reaction was to examine the efficiency of synthesizing small amounts of ethylformate, which would be desirable for isotopicly labelled synthesis runs according to Route I. However, the low yield and the difficult purification of such small reaction volumes, led to no further investigation of this topic. Additionally, the method of formylation with ethylformate was later shown to be unsuitable for the required needs.

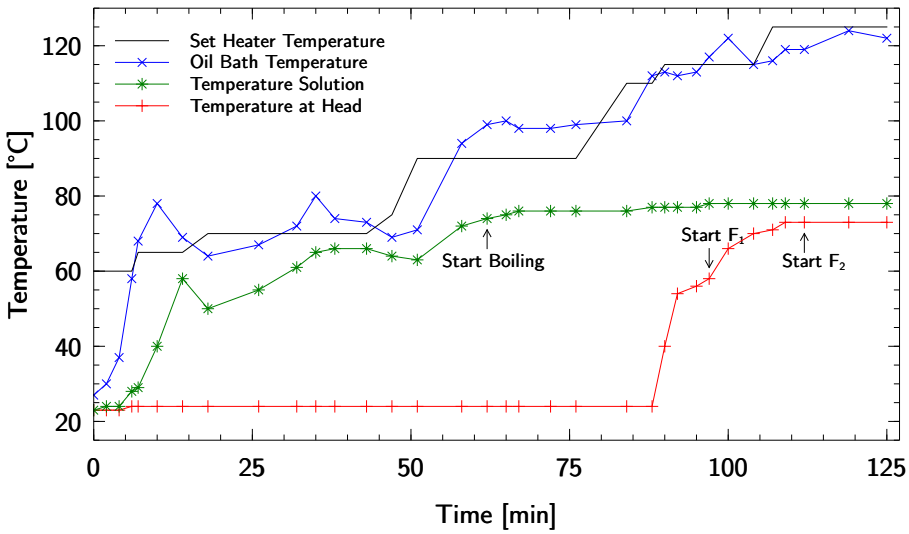

Figure 4.1.: Diagram, showing the different parameters monitored during distillation of Aux - I. Additionally, the start of boiling as well as the starts of the fractions are marked.

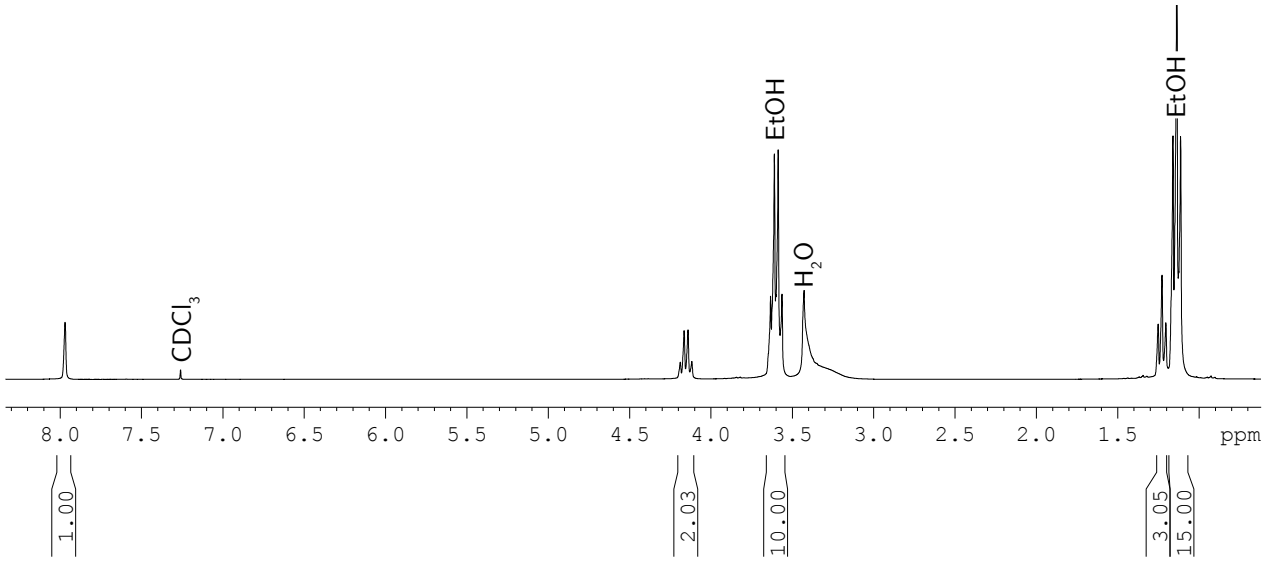

Figure 4.2.: 300 MHz ^{1}H NMR spectrum of the product of Aux - I, ethylformate, with excessive ethanol impurities at 3.60 and 1.14 ppm. (Solvent: $CDCl_3$)

4.1.1.2. Aux - II: Synthesis of Dabcyl-COOH

The reaction was carried out as stated in the supplementary of [1]. During work-up adjusting the pH to 7 proved rather difficult due to the dark colour of the reaction mixture, which may have contributed to the low yield of 4.98% of the theory (0.134 g, 0.50 mmol) after recrystallisation. This is not in correspondance with the 78% reported in [1]. Moreover, attempts to recover more product from the initial reaction solution were fruitless. Hence, it is probable that the reaction conditions were not chosen optimally, perhaps the reaction duration of one hour was too short. Nevertheless, the synthesis yielded more than enough Dabcyl-COOH, the colour inducing reagent in the test for free hydroxy groups (*Gen - V*), for performing this test as often as required. Furthermore, the product turned out to be rather pure, as the absence of intense impurity peaks in the NMR spectrum shows.

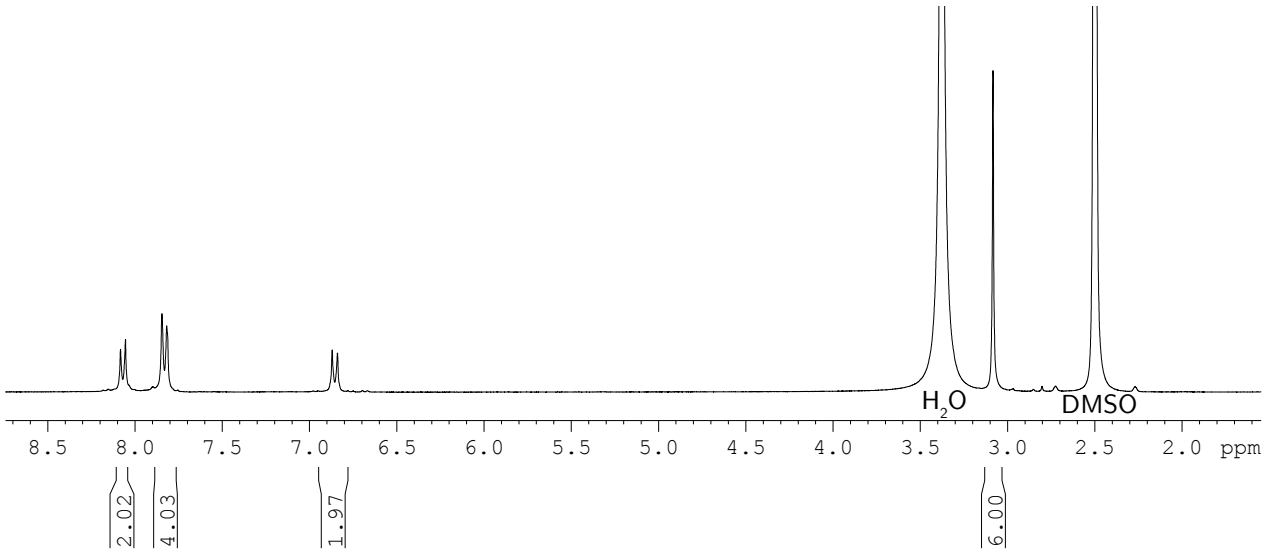

Figure 4.3.: 300 MHz ^{1}H NMR spectrum of recrystallized Dabcyl-COOH (Solvent: DMSO$-d_6$)

4.1.1.3. Aux - III: Deprotection of Z-Gly-Gly for further use in R_{II} - XIII

The deprotection of Z-Gly-Gly was conducted on the basis of Bodanszky's protocol, [24, p.153-155]. As the educt did not readily dissolve in ethanol, acetic acid, heat and ultrasonic sound were employed to bring about dissolution. No further difficulties were encountered and the product in the form of a greyish powder was obtained. Comparing the chemical shifts of reference spectra of glycine [64] and glycylglycine [65] with an NMR spectrum of the product (*Figure 4.4*) confirmed its chemical nature. Using the shift values published in [50] the big impurity peak at 2.05 ppm was identified as acetic acid. The majority of acetic acid was removed by further drying and resulted in a final yield of 102.87% (0.273 g, 2.07 mmol). Although it contained still some acetic acid as the yield suggests, the product was used as intended in *R_{II} - XIII* and additionally, in *$R_{III\,IV}$ - III*.

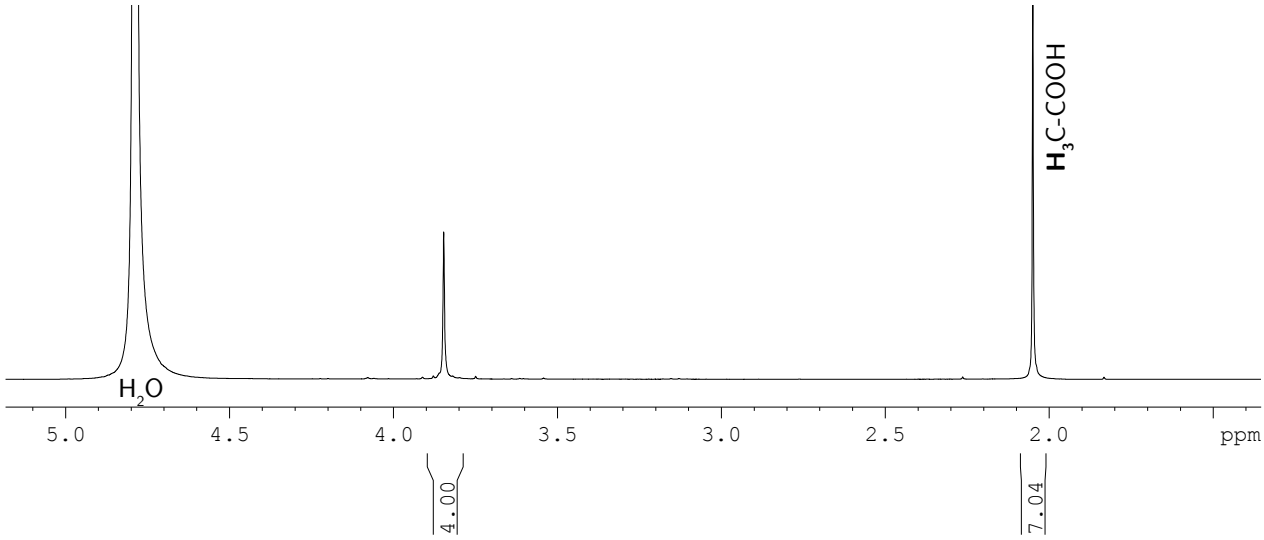

Figure 4.4.: 300 MHz NMR ^{1}H spectrum of Gly-Gly with a big acetic acid impurity at 2.05 ppm. (Solvent: D_2O)

4.1.2. Fmoc-protection of the desired Amino Acids

Three different approaches were tried to achieve Fmoc protection of Phe, Leu and Met, the needed amino acids.

The first one, based on [52], employs 25% vol. ethanol in water as solvent (at 60°C). Several attempts to conduct Fmoc protections (*Prot - I, II and III*) according to this procedure failed. The reason therefore is most probably that the amino acids used in [52], namely Glycine, Alanine and Proline, are several times more soluble under the above mentioned conditions than the ones used for the experiments in the current work. This is exemplified by comparing the solubility values of glycine (11.36 g glycine per 100 g Solvent) with leucine (1.32 g leucine per 100 g Solvent) or phenylalanine (1.86 g phenylalanine per 100 g Solvent) in a 20% vol. aqueous ethanol solution at 25.1°C. [66] Alanine also used in [52] shows a solubility similar to glycine under almost identical conditions: 7.09 g alanine per 100 g Solvent in a 25% vol. aqueous ethanol

solution at 25°C. [67]
The second method, described in [53], relies on microwave irradiation of a homogenous suspension of the amino acid and Fmoc-Cl in water. The desired Fmoc-amino acids (*Prot - IV and V*) were obtained in such low quantities that they could be detected only by MS within a mixture of several side products and the educt (*Figure 4.5*). This was probably due to highly unoptimized microwave irradiation conditions and a non functional temperature control in the available microwave instrument.

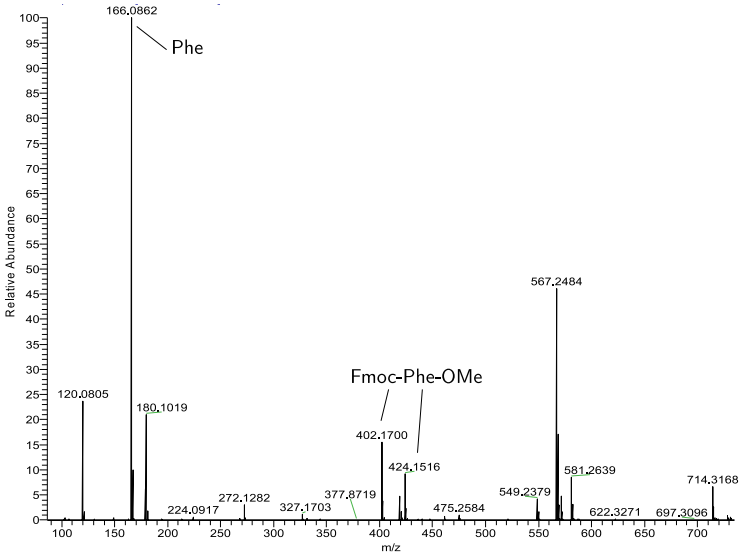

Figure 4.5.: MS spectrum (ESI ion source, positive mode; qTOF mass analyzer; solvent. methanol) of the product of Prot - IV. The educt, Phe (166.0862 m/z), and the product, Fmoc-Phe, detected as methyl ester (402.1700 m/z and its Na adduct at 424.1516 m/z), are marked. Details can be found in *Appendix A.2*.

In order to find an usable procedure for Fmoc-protection, a third method was tested. It is published in [24, p.24-25] and lets Fmoc-Cl and the amino acid react in a mixture of aqueous Na_2CO_3 with Dioxane, and is performed at low temperatures (0°C and r.t.). Except for adjusting the amount of solvent for each individual amino acid, the literature procedure was followed accurately. It proved to be very effective for the protection of all three amino acids (Fmoc-Phe: *Prot - VI, VII and VIII*, Fmoc-Leu: *Prot - IX, X and XI* and Fmoc-Met: *Prot - XII and XIII*), with yields ranging from 75 to 95%. The chemical nature and purity of the products was confirmed by NMR (and MS in case of *Prot - VI*).
The reaction products were often pure enough to allow further usage without prior recrystallisation. This is illustrated by the low abundance of impurity peaks in the NMR spectra (*Figure 4.6*).
The Fmoc-protected amino acids, which had been prepared this way, were used for the following peptide synthesis reactions. Moreover, this protection method seems to be very promising when it comes to synthesizing fMLF in isotopically labelled, because it easily affords pure protected amino acids in high yields.

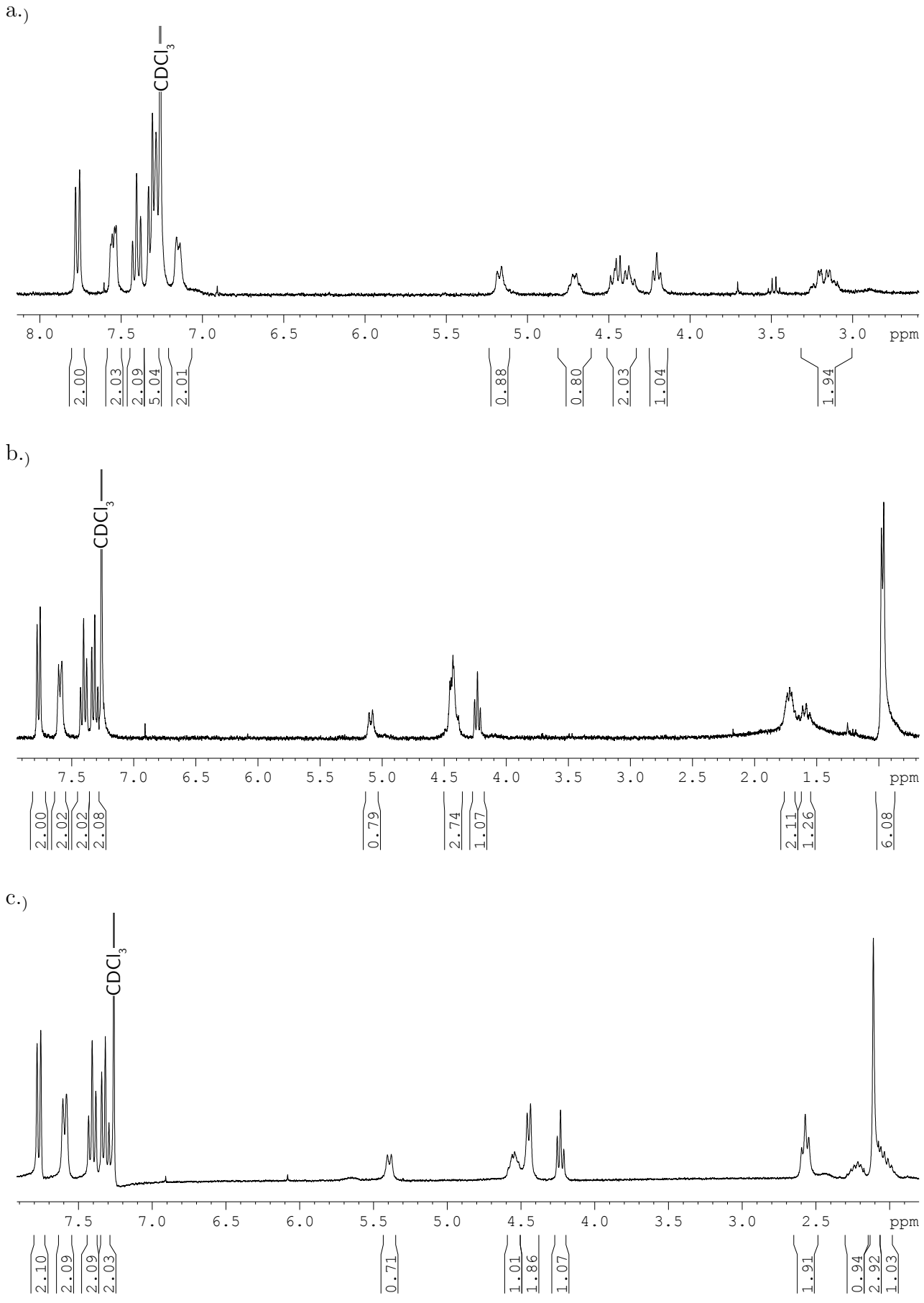

Figure 4.6.: 300 MHz ^{1}H NMR spectra of a.) Fmoc-Phe, b.) Fmoc-Leu, and c.) Fmoc-Met. The spectra were recorded with samples taken from not recrystallized product. (solvent: $CDCl_3$)

4.1.3. Synthesis of fMLF - Route I

After successful protection of the required amino acids, the first attempt of building fMLF was undertaken. This was done following the procedure published in [1].

4.1.3.1. R_I - I: Resin Loading

The first reaction in the sequence (R_I - I) was attaching Fmoc-Phe to the Wang resin. It was carried out as described and the test for free -OH groups (Gen - V) confirmed the complete loading of the resin. Initially, false negative results were obtained for the positive control sample. This was due to washing the resin after the diphenyldichlorosilane treatment with a solution containing triethylamine, that had not been dried before.[4.1] The water in the washing solution caused the destruction of the reactive silyl chloride ether on the resin, whereupon the Dabcyl-COOH could not couple to the resin. [33] Omitting the washing step resolved the issue and correct results were gained, although using dry reagents would be best practice for future tests. A picture showing exemplary results of a sample of fully loaded and a control consisting of unloaded resin is given in *Figure 4.7*.

Figure 4.7.: Comparison of the outcomes of the test for free -OH groups with unloaded Wang resin (labelled with '**CONTROL**') and Fmoc-Phe loaded Wang resin (labelled with '**SAMPLE**')

4.1.3.2. R_I - II and III: Coupling of Further Amino Acids

The next step in the synthesis sequence was the elongation of the peptide chain via repeated deprotection and coupling reactions. For that the resin had to be transferred to an apparatus that allowed performing the many filtration steps in an easy manner. Originally, syringes with frits or filter tips were intended to be used. As both ways proved insufficient with the equipment available (too small frits, immediate clogging of filter tips) and even led to a substantial loss of the resin (by using a solvent incompatible filter tip) alternatives were sought.
The first attempt was to use a separate filter funnel and a conventional reaction vessel. This approach however sufferd from various drawbacks including no permanent maintenance of inert conditions, the need for higher amounts of solvents and the possibility of resin loss during transfer from the filter funnel to the resin and back.
Therefore, from the second deprotection reaction on the whole synthesis was carried out in a Schlenk frit based apparatus, which is described in *Section 3.1.3*.

[4.1] The same solution had been used before for the actual diphenyldichlorosilane reaction. However, the water present under these conditions immediately reacted with the excess of diphenyldichlorosilane and was thereby removed without causing harm.

The reactions themselves were carried out according to [1]. Deviations from this procedure were necessary only concerning the volumes of solvents and the piperidine deprotection solution. Further, the individual reaction times were often prolonged.
To check if the coupling reactions worked quantitatively, the Kaiser test was used as described in *Gen - VI*. This was confirmed for both couplings.
Remarkably, the test exhibited a slightly blue colour, even in negative control experiments, which were performed without the addition of a sample. This was further investigated by testing different samples (water, pyridine, isopropylamine, NMP and the protected resin), in order to find an explanation. Thereby, it was found that the test which contained pyridine as sample was slightly darker than the ones with NMP and fully protected resin (see *Figure 4.8* c.$_)$). This implied that the used pyridine, which was a major constituent of the Kaiser test reagents contained some ammonia or primary amine impurity. This notion was confirmed by the paper [34] that first described the reagent formulation that was later on used for the Kaiser test published in [35]. In that publication ([34]) it is recommended to clean pyridine from ammonia before use, which was not done in the current work. Nevertheless, it was possible to discern positive and negative results of the Kaiser test, when employing control experiments, which is illustrated by *Figure 4.8* a.$_)$ and b.$_)$. It shows the comparison of Fmoc-protected resin and deprotected one (a.$_)$) as well as protected resin and a control test with just the Kaiser test reagents (b.$_)$).

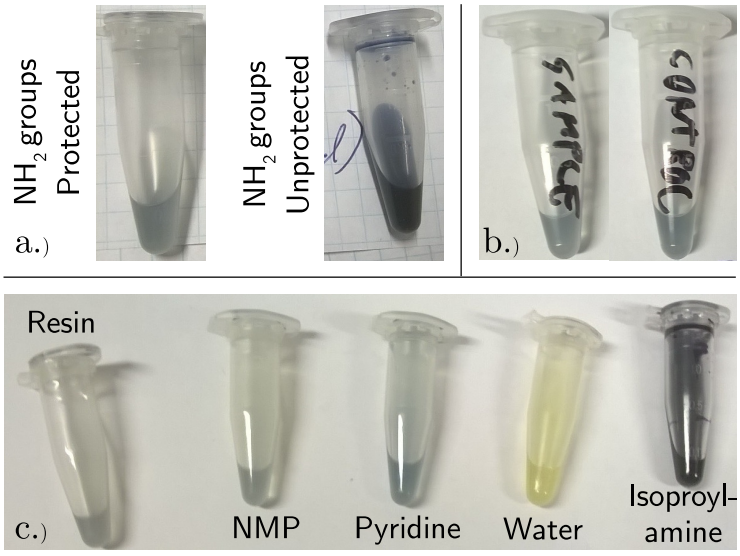

Figure 4.8.: Exemplary results of the Kaiser test.
a.$_)$ shows the test results for resin with and without free $-NH_2$ groups.
b.$_)$ compares Fmoc protected resin with a negative control experiment that involved just the test's reagents.
c.$_)$ shows the test solutions with different samples. some additional colour was produced with the pyridine containing sample, hinting amine impurities. NMP and the protected resin samples gave negative outcomes, whereas the isopropylamine sample resulted in a strongly positive. The sample containing H_2O stayed yelllow.

4.1.3.3. R_I - IV: N-Terminal Formylation with EthylFormate

With the peptide chain synthesized, the *N*-terminal modification was to be attached after a final deprotection step. This was conducted by treating the washed and dried resin with ethylformate as stated in [1] (the used amount of ethylformate was higher then required). The reaction again was checked for completeness employing the Kaiser test. It showed that the reaction only had occurred partially. Hence, the formylation step was repeated, however, without improving the outcome. At this point the synthesis sequence was continued according to [1] and no further attempts were made to enhance the formylation process, although it would be worth to do so, for instance by investigating the impact of ultrasonic sound treatment.

4.1.3.4. R_I - V: Cleavage and Purificatoion

Removing the peptide from the resin was conducted as described in [1], whereby the volumes of the portions of cleavage solution were increased. After that, the cleavage solution containing the peptide was lyophilized, which proved to be a little problematic as the centrifugal evaporator overheated with time. That led to very fast heating of the initially frozen samples, especially if their volumes were already low. Repeated cooling of the apparatus and refreezing of the samples improved the situation somewhat, but did not fully prevent occasional overheating of the samples.
NMR analysis of the lyophilized residues revealed the presence of the peptide in the residue that had resulted from the first batch of cleavage solution. However, the signal of the formyl group was not present, which confirmed the results of the Kaiser tests after the formylation reactions. As the sample was rather impure column chromatography was performed two times successively. The resulting product (17.8 mg, 0.043 mmol, 13.73%) fraction was still not fully pure, according to ^{1}H (*Figure 4.9*) and ^{13}C (*Figure C.1*) NMR spectra. Remarkably, a tiny peak at 8.10 ppm of the proton spectrum might correspond to a residual formyl or formic acid peak (*Figure 4.9*).
In an attempt to resolve the issue with the formyl group Route II was planned, tested and executed. It is described in the following chapter.

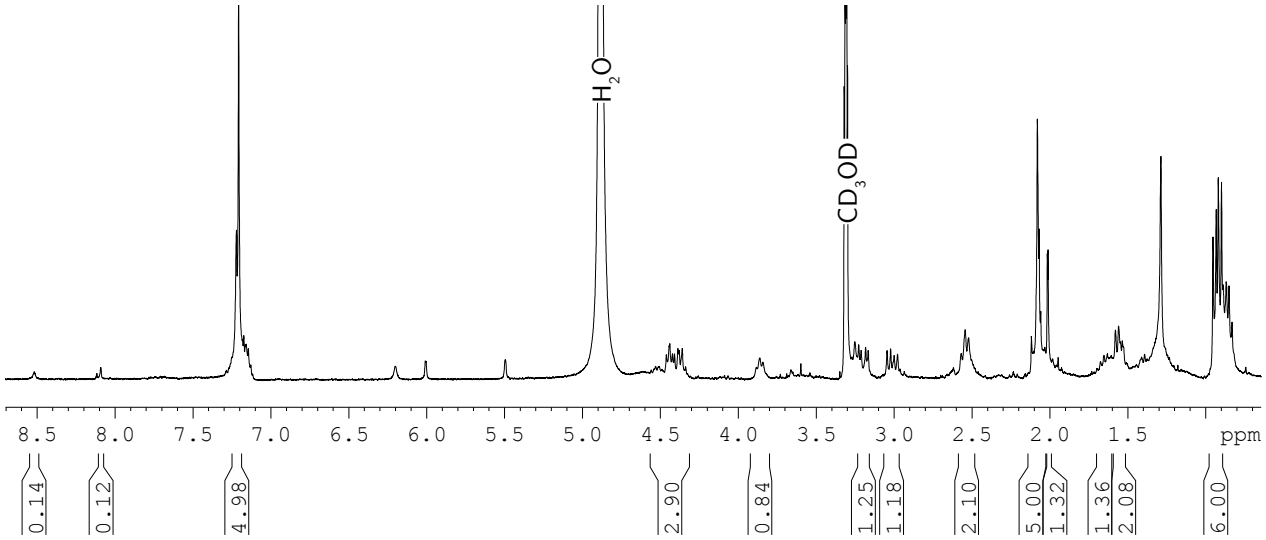

Figure 4.9.: 300 MHz NMR ^{1}H spectrum of the final purified product of Route I. (Solvent: methanol-d_4) Still the product is not clean. The peak at 8.10 ppm might correspond to the formyl group or formic acid.

4.1.4. Synthesis of fMLF - Test Reactions and Route II

4.1.4.1. R_{II} - I, II, III and IV: Test reactions - Formylating Met with Ethylformate

In order to improve the formylation of the *N*-terminus, several test reactions were carried out, which were based on formylation using ethylformate [1]. Methionine was used as educt because formyl-Met was needed for Route II and a working formylation of Met with ethylformate may have even enabled the successful completion of Route I. The reactions did differ in solvent, temperature and pH conditions. All of them did afford no or small fractions of the desired product. Reaction R_{II} - IV gave the best results with 33% formylation based on comparing the integral of the formyl peak with the one of the H_α of unformylated Met (see *Figure 4.10*). This reaction was carried out in a basic aqueous solvent at room temperature. Further optimisation of this reaction was not done because the formylation employing the formic acetic anhydride technique gave more promising results. Nevertheless, it would be interesting to try further variants of this reaction, perhaps employing an organic base such as triethylamine, to see if improvement was possible.

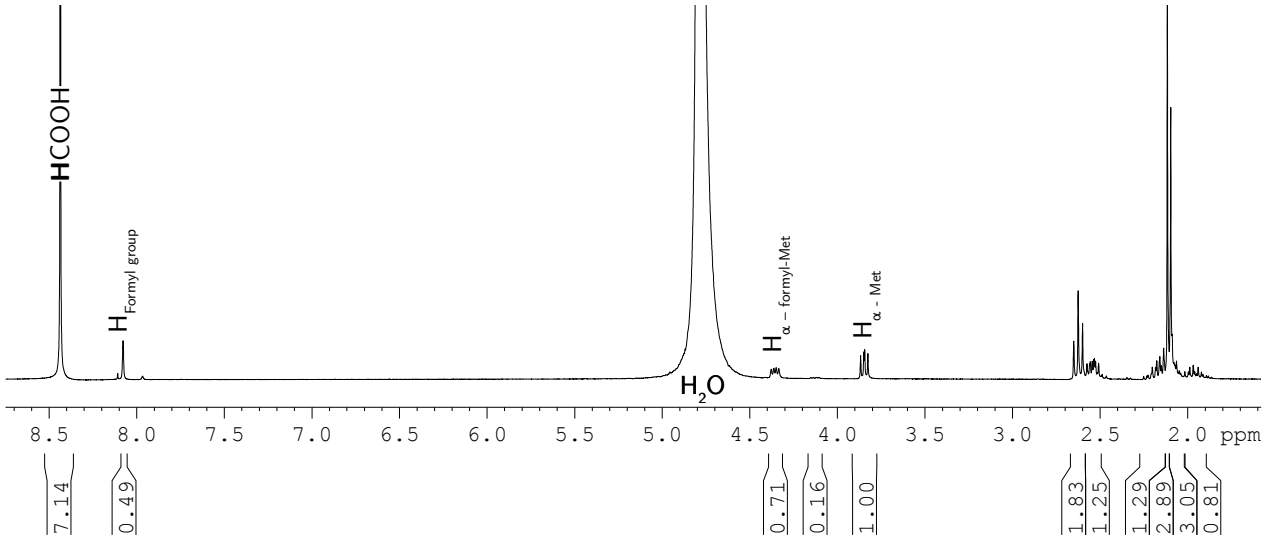

Figure 4.10.: 300 MHz NMR ^{1}H spectrum of the product of R_{II} - IV, partly formylated methionine. (Solvent: D_2O) A big formic acid impurity can be seen at 8.44 ppm. The degree of formylation was estimated by comparing the integrals of the formyl peak (8.08 ppm) and the H_α peak of Met.

4.1.4.2. R_{II} - V, VI and VII: Formylating Met using the Acetic Formic Anhydride Approach

An alternative to the ethylfomate based formylation is via aminolysis of formic acetic anhydride. The procedure used [27], involved *in situ* generation of this acivated species from formic acid and acetic anhydride, which immediately reacts with the amino acid. This approach gave rather high yields (68-91%) and after recrystallisation was pure enough for further use as shown by NMR (*Figure 4.18 a.)*).

In the different preparations the volume of formic acid was successively lowered to almost one third (0.8 mL per 1 mmol Met) of the original one in R_{II} - VII. With these low amounts of formic acid good results were obtained. This finding is important with respect to a synthesis with labelled compounds, as a minimal amount of ^{13}C labelled formic acid would heavily contribute to the cost efficiency of the synthesis.

4.1.4.3. R_{II} - VIII: Test reaction - Solution Phase coupling of formyl-Met to Phe-OCH_3

In order to test the feasibility of Route II it was checked if formyl-amino acids were useful educts of carbodiimide/HOBt mediated peptide couplings. This was done by coupling formyl-Met with the Methyl ester of Phe, which was available in sufficient amounts, employing the procedure published in [24, p.145]. The reaction gave the desired product, identified by proton and carbon NMR (for the carbon spectrum see *Figure C.2*), in 71.25% yield (0.165 g 0.49 mmol). Performing the work up in two variants, additionally showed, that the formyl group (stated to be acid labile in [27]) was stable to short exposure of dilute aqueous solutions of citric acid, as the proton spectra of both products are near to identical (*Figure 4.11*).

a.)

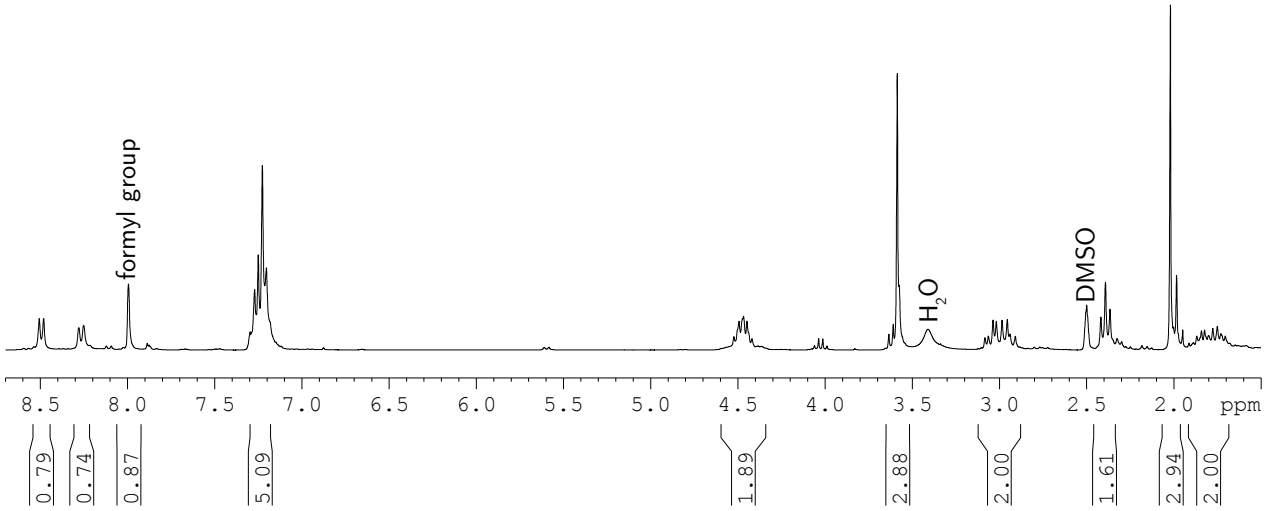

b.)

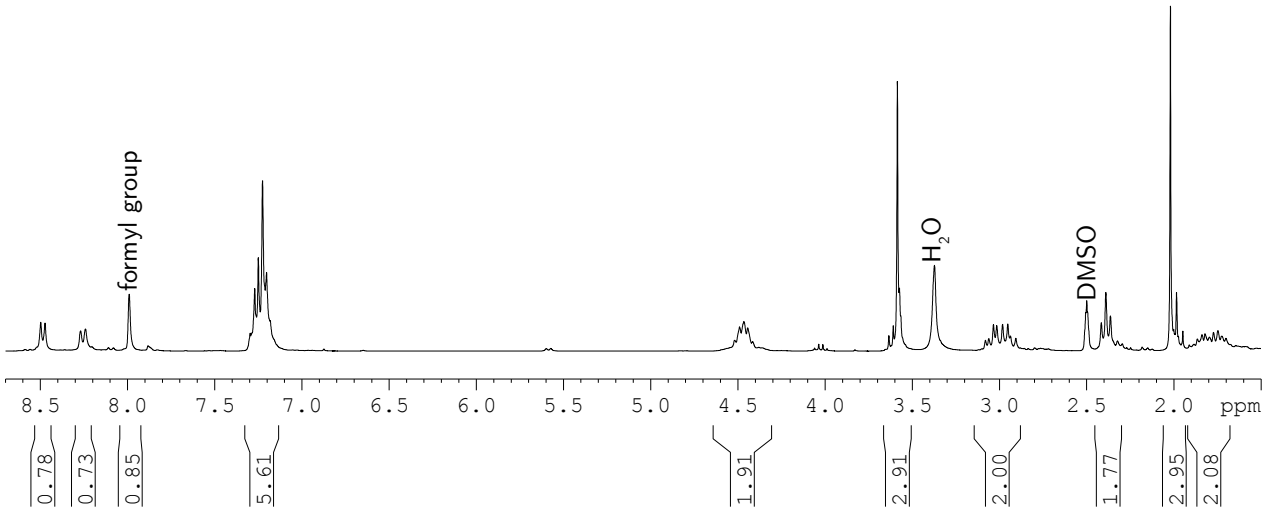

Figure 4.11.: 300 MHz NMR ^{1}H spectra formyl-Met-Phe-OCH_3. a.) was worked up with an aqueous 10% citric acid solution and for b.) this step was omitted. As the spectra are almost identical, it can be concluded that the citric acid did not harm the molecule especially the formyl group. (Solvent: DMSO)

4.1.4.4. R_{II} - IX, X, XI and XII: Solid Phase peptide Synthesis Along Route II

With the preliminary reactions confirming Route II, an actual synthesis run of was carried out. Therefore the cannulation apparatus (see *Section 3.1.3*) was used as the previous one required the transfer of resin between two parts of the apparatus. This often was accompanied by resin sticking to the walls of the vessel, which led to the need of larger amounts of solvents and reagents to wash the resin into the correct location. The cannulation apparatus had the advantage that the resin stayed in one place. However, its drawback was that filtration of some solvents (especially NMP) took very long, whereby too high pressure led to clogging of the filter and not to an increase of filtration speed.

Nevertheless, the full sequence was carried out in this apparatus. Up to the deprotection of Leu Route II is identical to Route I, and hence was performed according to [1] (R_{II} - IX,X and X). The subsequent reaction, the coupling of formyl-Met to Leu (R_{II} - XI) was performed under the usual conditions (stated in [1]) with fmoryl-Met instead of Fmoc-Met. The Kaiser test indicated the success of the reaction. Hence, cleavage was performed in the same way as in Route I, followed by lyophilisation as already described. Upon NMR investigation it was found that the formyl group was again missing. Obviously, it had been removed during the cleavage reaction by TFA.

4.1.4.5. R_{II} - XIII: Formylating Gly-Gly using the Acetic Formic Anhydride Approach

As the formyl group had been destroyed by the conditions of cleavage, it should be reintroduced by a reaction in solution. With this reaction the formylation of a peptide in solution phase with the well tried acetic formic anhydride method ([27]) was tested. It was performed in the same fashion than the formylation reactions with Met (*R_{II} - V, VI and VII*), however, with Gly-Gly instead of Met. The desired product was obtained in almost quantitative yield (0.161 g, 1.00 mmol, 98.37%) and high purity (*Figure 4.19 a.)*). Hence, the same procedure could be safely applied to the product of the cleavage reaction.

The Stability of the formyl-Gly-Gyl Dipeptide In [27] it is stated that formyl amino acids undergo alcoholysis and acidic hydrolysis. In order to get an idea about the conditions a formyl group tolerates, a stability test with formyl-Gly-Gly in deuterated methanol was performed at different temperatures and pH conditions over a period of 36 days. It was found that the formyl group was stable in pure methanol at room temperature and 40.5°C. However, it was very rapidly cleaved upon treatment with TFA. After over night exposure to the acid already 84% of the formyl group had been cleaved, based on the comparison of the integrals of the formyl peak before the acid treatment and one night after it. This outcome is rather remarkable because the procedure in [1] required prolonged TFA treatment for cleaving the formylated peptide off the resin. Hence, it explains also why no formyl group was present in products of both solid phase syntheses. The findings are illustrated in *Figure 4.12* and *Figure 4.13*. Additional supporting spectra can be found in *Figure C.3*.

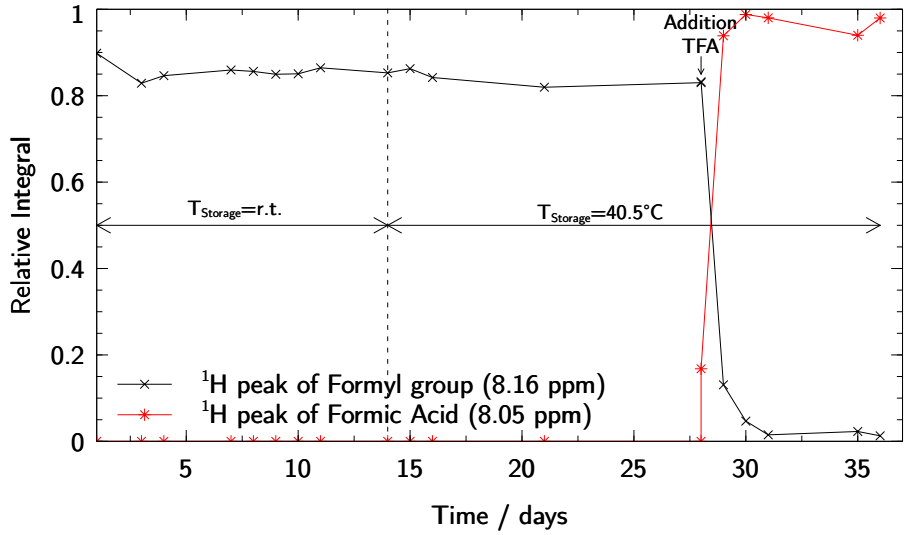

Figure 4.12.: This diagram shows the development of the integrals of the ^{1}H peak and the ^{1}H formic acid peak over the whole measurement period. The different conditions are also indicated in the plot. The decomposition of the formy group upon TFA treatment is exhibited by a pronounced drop of the formyl curve and a corresponding rise of the formic acid one.

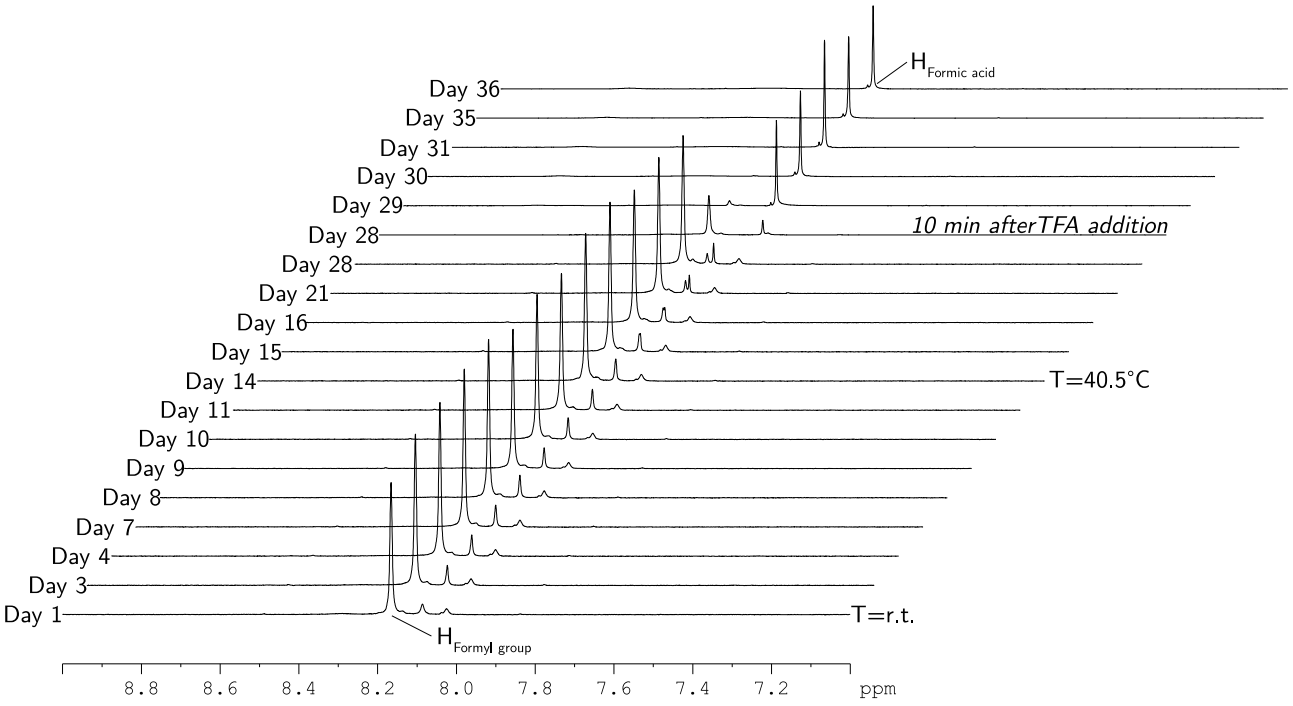

Figure 4.13.: A series of 300 MHz NMR ^{1}H NMR spectra of formyl-Gly-Gly in methanol$-d_4$. The spectra were recorded over a period of 36 days, whereby the conditions (temperature, pH) were changed as indicated to test the stability of the formyl group. The spectra show only the region around the formyl peak (8.16 ppm). They display the rapid conversion of the formyl group to formic acid (8.05 ppm) upon TFA treatment.

4.1.4.6. R_{II} - XIV: Additionally Formylating the Product of R_{II} - XII

After it was confirmed that the acetic formic anhydride technique was suitable for peptides (R_{II} - $XIII$) the same procedure ([27]) was employed to restore the formyl group of the product of R_{II} - XII, MLF. Purification with column chromatography afforded 31.0 mg of the desired

product (0.07 mmol 59.09% yield of the single reaction, 22.32% of the total synthesis sequence). It was, however, not pure according to NMR (*Figure 4.14*) and MS analysis (whereby the MS peaks showed the oxidation of the S in Met). Therefore HPLC was performed.

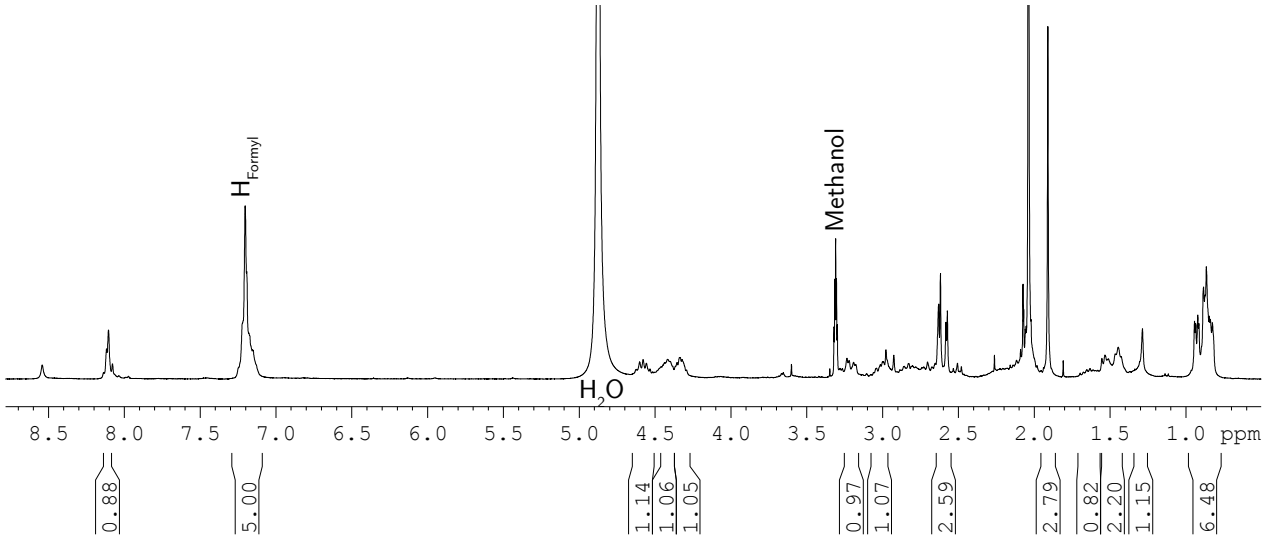

Figure 4.14.: 300 MHz NMR ^{1}H spectrum of fMLF, the product of R_{II} - XIV after column chromatography. (Solvent: Methanol$-d_4$) It is not free of impurities which led to further purification by HPLC.

With the conditions optimized, two fractions could be isolated. The first fraction was obtained after 23.52 min (relative peak area: 51.93%) and the second one after 25.62 min (relative peak area: 48.07%). The UV-vis spectra of the fractions were almost identical and revealed that both contained a peptide (backbone peak around 210 nm), of which a constituent was phenylalanine (Phe peak at 257 nm). Due to the low molar absorption coefficient of Phe the peak is not very intense. The UV spectra were interpreted with the help of [68].

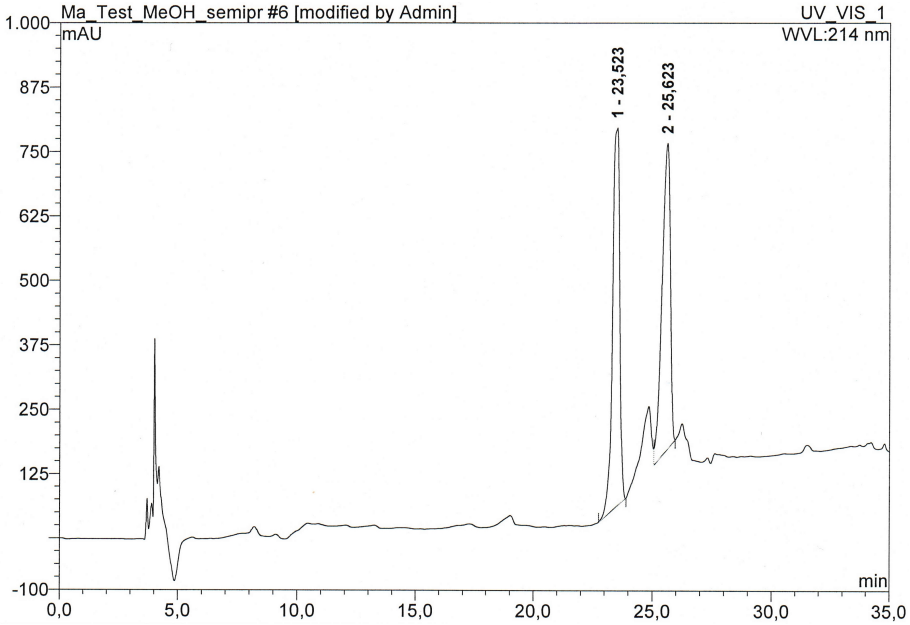

Figure 4.15.: Chromatogram of the product of R_{II} - XIV. Two fractions, with almost equal area were separated and collected. Detection was performed with an UV-vis detector at 214 nm

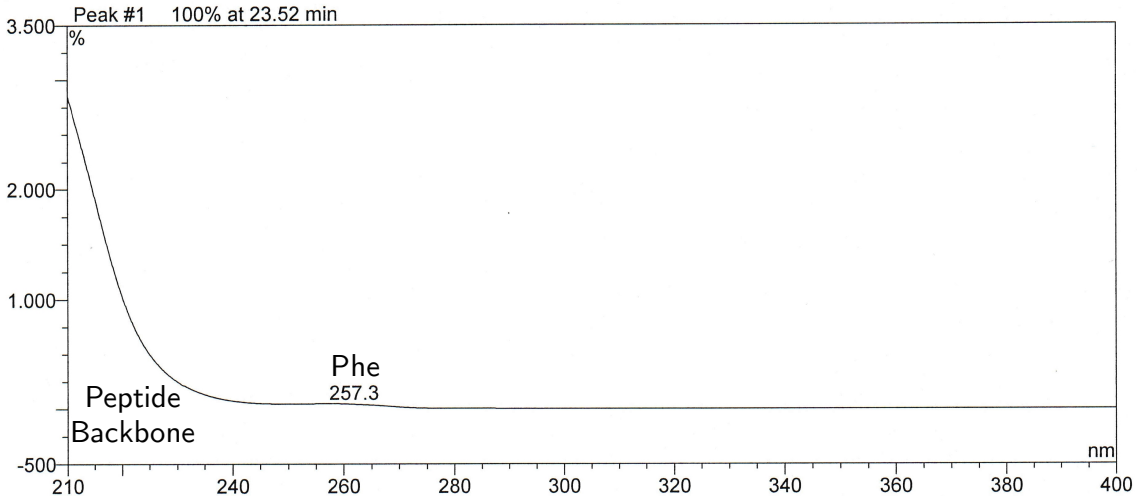

Figure 4.16.: UV vis spectrum of the first HPLC fraction (The spectrum of the second fraction looks essentially the same). The shoulder of a peak around 210 nm corresponds to the peptide backbone and the flat peak at 257 nm to the aromat in Phe.

In order to identify the compounds in the two fractions enough material was collected to perform a MS analysis. This revealed that both fractions contained a mixture of the same compounds, namely MLF, fMLF and *N*-Acetyl-MLF (*Figure 4.17*). In all these compounds the S of Met was oxidized to the sulfoxide. With this oxidation, which probably had occurred during a several week long period of standing at ambient conditions, a new chiral center had been created. This caused the formation of a racemic mixture of diastereomers, which probably is responsible for the two almost equally big peaks in the chromatogram corresponding to mixtures of the same masses in MS.
Furthermore the overall purification did not clean the sample completely as some not identifiable impurities were still observed.

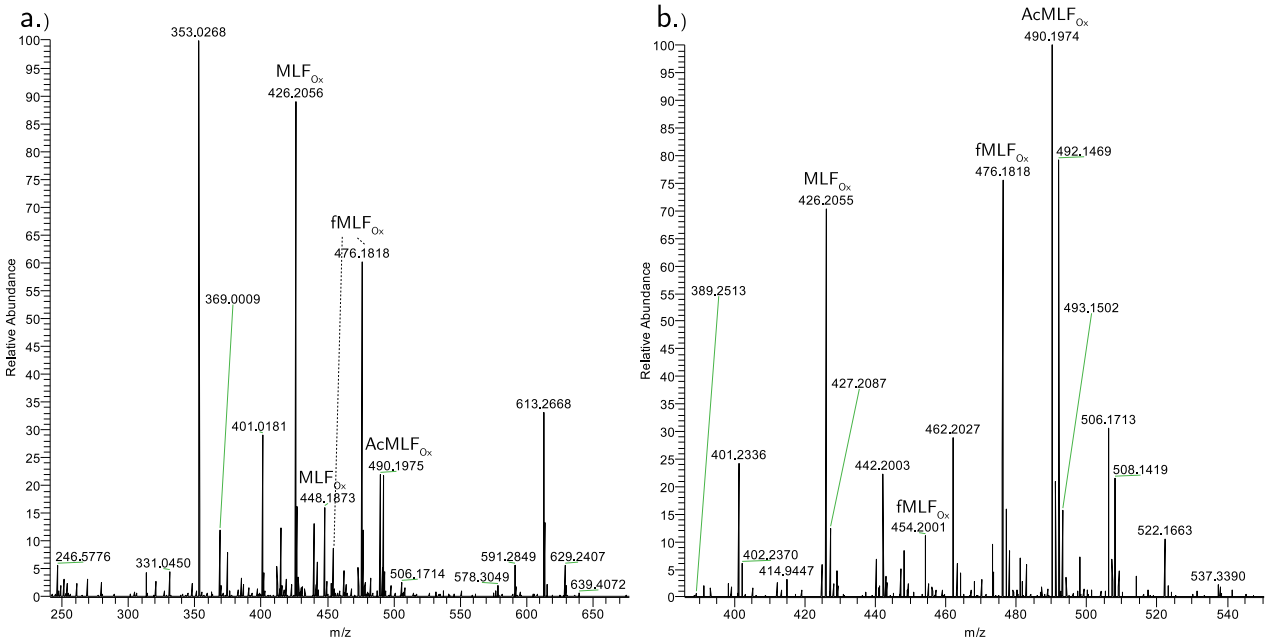

Figure 4.17.: Comparison of the MS spectra (ESI ion source, positive mode; qTOF mass analyser) of the two HPLC fractions. a.) corresponds to the first and b.) to the second fraction. In both spectra the same peptide derivatives are present. Moreover, several additional impurities are observed.
From these MS spectra no quantitative information can be obtained, as the calibration for that purpose was not performed.

4.1.5. Synthesis of fMLF - Test Reactions for Route III and IV

In order to enhance the synthesis sequence further and ensure that the formyl group was not harmed by subsequent reaction conditions Route III and IV were planned and reactions assessing their feasibility were conducted.

4.1.5.1. $R_{III\,IV}$ - I, II, III and IV: Formylation of reactions with a minimal amount of formic acid

The first issue to address was the formylation reaction. Using the acetic formic anhydride method formylation of peptides and amino acids posed no problem. However, the required amounts of formic acid were still very high, although they had been reduced already, especially in view of a synthesis with isotopically labelled compounds. A solution to that problem was found in a publication [55], whose topic was the synthesis and isolation of formic acetic anhydride and further formylation of amino acids. In this paper it was remarked that the formylation reaction was possible with acetic acid as solvent. Upon that a hybrid procedure based on [27] and [55] was tested ($R_{III\,IV}$ - I and II). The optimal procedure ($R_{III\,IV}$ - II) was performed in the following way: Formic acid (2 equivalents) and acetic anhydride (2 equivalents) were mixed to obtain the mixed anhydride. This solution was then introduced to a suspension of the Met (1 equivalent) in a minimal volume of glacial acetic acid. This means the consumption of formic acid was reduced from 0.8 mL to 75 µL per mmol of Met. As visible in *Figure 4.18* the resulting product does not substantially differ from the product obtained with the procedure of [27].

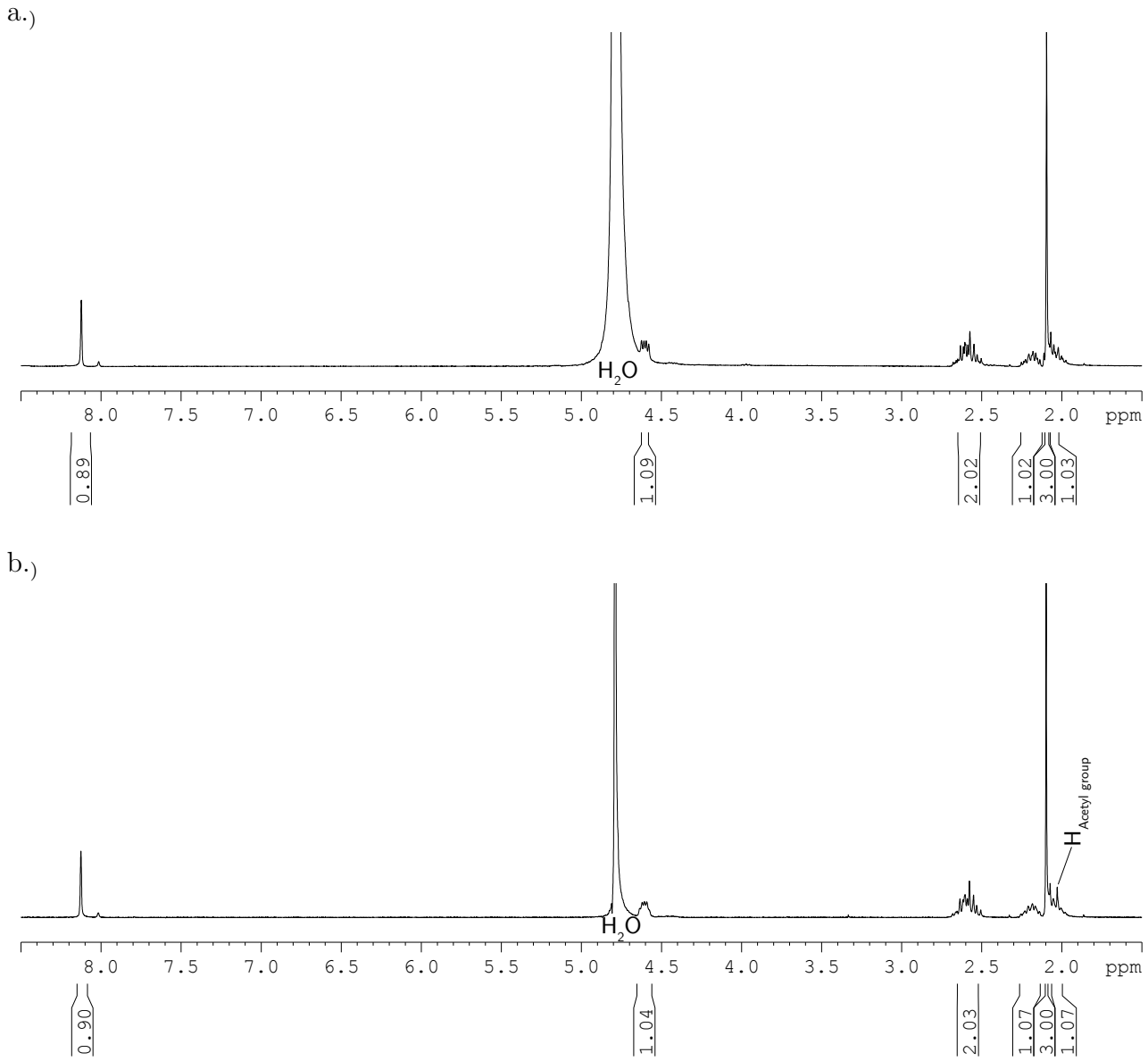

Figure 4.18.: 300 MHz NMR ^{1}H spectra of formyl-Met (Solvent: D_2O). a.) corresponds to the product of R_{II} - V (the huge excess of formic acid as solvent) and b.) corresponds to the product of $R_{III\,IV}$ - II (acetic acid as solvent). The spectra show hardly any differences, although the peak at 2.03 ppm in spectrum b.) suggests the occurrence of acetylation.

Also, the yield obtained was very good ($R_{III\,IV}$ - II: 0.179 g, 1.01 mmol, 100.18%). Nevertheless, the peak at 2.03 ppm (see *Figure 4.18b.)*) suggests that an acetylated side product was formed in small amounts.

The new formylation procedure was further tested with a peptide, namely Gly-Gly ($R_{III\,IV}$ - III). Although the reaction seems work also for this compound, acetylation did occur at a higher rate than with Met. This is illustrated by *Figure 4.19*, which compares ^{1}H NMR spectra of conventionally prepared formyl-Gly-Gly (R_{II} - $XIII$) and formyl-Gly-Gly prepared in acetic acid ($R_{III\,IV}$ - III). From the integrals of the second spectrum, *Figure 4.19* b.), the amount of acetylation was calculated to be 13.6%.

A reason for this high fraction of acetylated peptide is probably the low steric hindrance of glycine. It might be beneficial to conduct the reaction in a more sterically hindered acid (maybe propanoic acid or isobutyric acid). With acetic acid as the solvent formation of acetic anhydride from the mixed formic acetic anhydride may occur that gives the acetylated product. If such a product is formed with a sterically hindered solvent molecule aminolysis might be too slow to occur.
Further it might be of use to employ a mixed anhydride of pivalic acid for the reaction. These compounds are used in peptide coupling reactions because the attack of the amine occurs selectively at the non pivalic acid moiety of the mixed pivalic anhydride. [11] This might prevent the amino group (of Gly-Gly for example) from attacking at the wrong side of the anhydride.

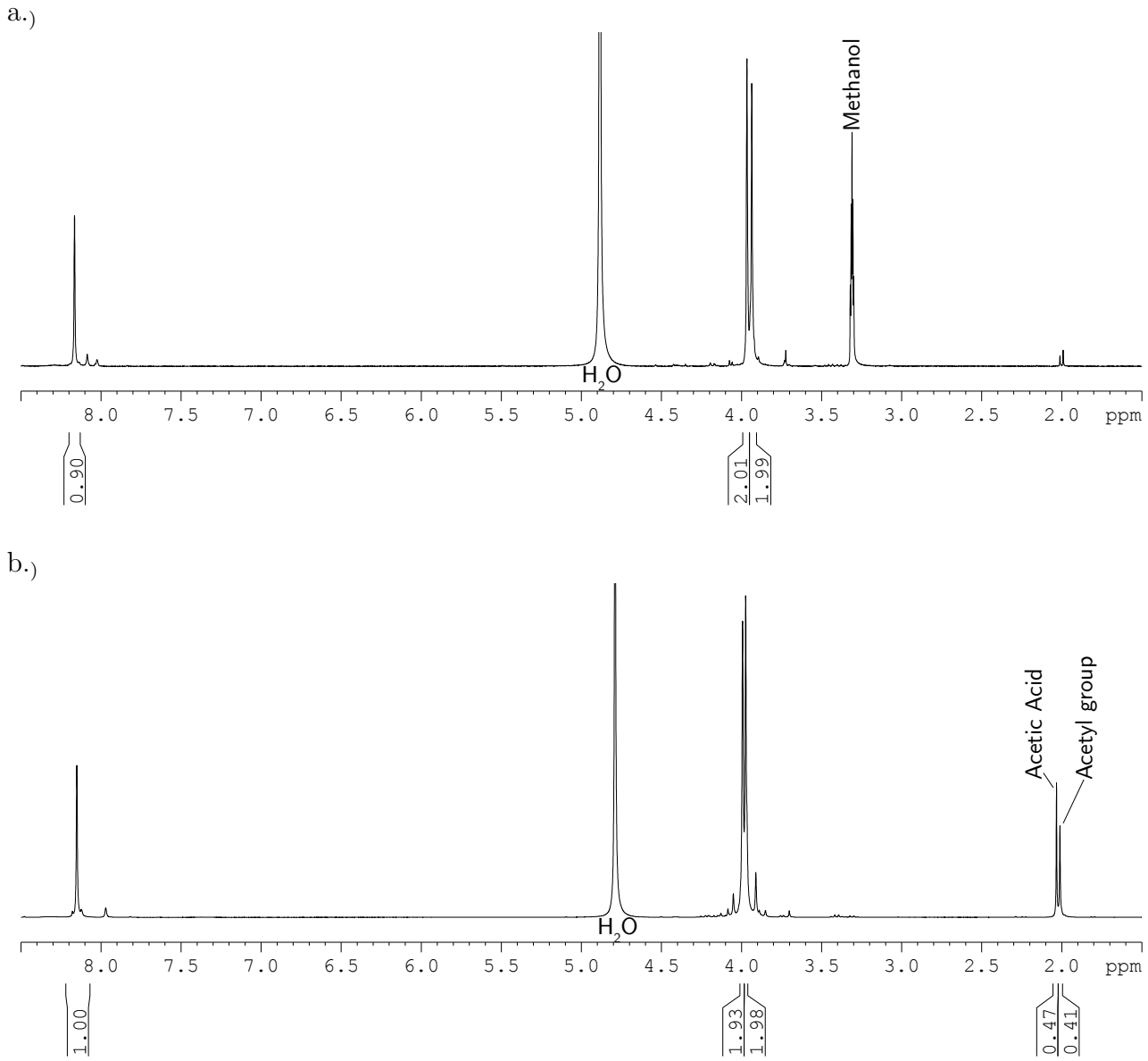

Figure 4.19.: 300 MHz NMR ^{1}H spectra of fromyl-Gly-Gly. a.) corresponds the product of R_{II} - *XIII*, prepared with formic acid as solvent (Solvent: methanol$-d_4$). b.) corresponds to the product of $R_{III\,IV}$ - *III*, which was prepared with acetic acid as solvent. (Solvent: D_2O) The peaks at 2.03 and 2.01 ppm correspond to acetic acid and acetyl-Gly-Gly impurities, respectively.

One further attempt to formylate Met was undertaken in $R_{III\,IV}$ - IV. Thereby, an equimolar mixture of the required reagents without any additional solvent was employed. As the mixture was not stirrable acetic acid was introduced afterwards. The product was heavily acetylated and not usable.

4.1.5.2. $R_{III\,IV}$ - V : Solution Phase Deprotection of Fmoc-Leu

Another requirement for being able to successfully conduct Routes III and IV are Fmoc-deprotection reactions in solution phase. This first preliminary experiment investigating this topic, the deprotection of Fmoc-Leu ($R_{III\,IV}$ - V) was conducted according to [24, p.185-186].

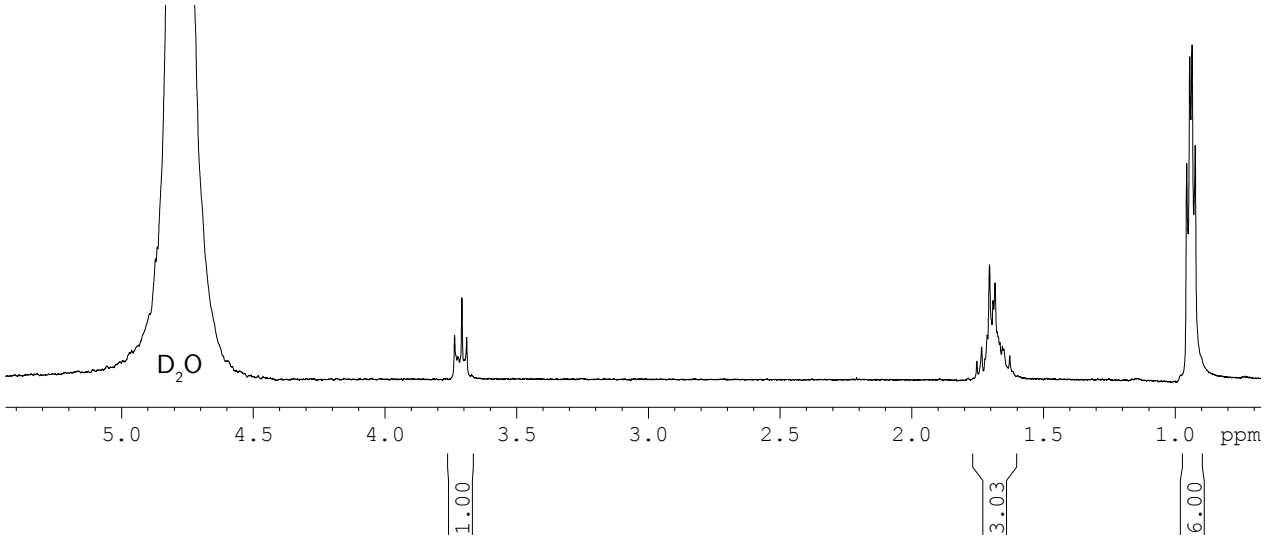

Figure 4.20.: 300 MHz NMR ^{1}H spectrum of Leucine, the product of $R_{III\,IV}$ - V. (Solvent: D_2O)

As solvent DMF was required. Because this solvent has a relatively high boiling point and is generally undesired, [56], it was replaced by acetonitrile as recommended by [56]. The product obtained was pure and identified by NMR as the expected one, namely leucine (see *Figure 4.20*). The yield was nearly quantitative (0.065 g 0.49 mmol 98.38%). Additionally, the evaporated trituration solution was analyzed by NMR. It was found that the expected by-product, 9-Methylene-9*H*-flourene, was also present almost purely (see *Figure C.4*).

4.1.5.3. $R_{III\,IV}$ - VI and VII : Solution Phase Coupling of Fmoc-Leu with Phe and Subsequent Deprotection

Another crucial transformation that is required for Route IV, is the coupling of a Fmoc-amino acid to a peptide that has no *C*-terminal protecting group. In [7, p.74] it is stated that *C*-terminal protection is no necessity by all means but strongly recommended. Hence, a DCC/HOBt mediated coupling of Fmoc-Leu with unprotected Phe, according to the preactivation method described in [17] was performed. The resulting product was highly impure, which is is reflected by the yield of 112.86% as well as the NMR, *Figure 4.21*, and MS, *Figure C.5*, spectra. Nevertheless, it was possible to identify the product with both methods. Further, experiments should target the efficiency of this transformation.

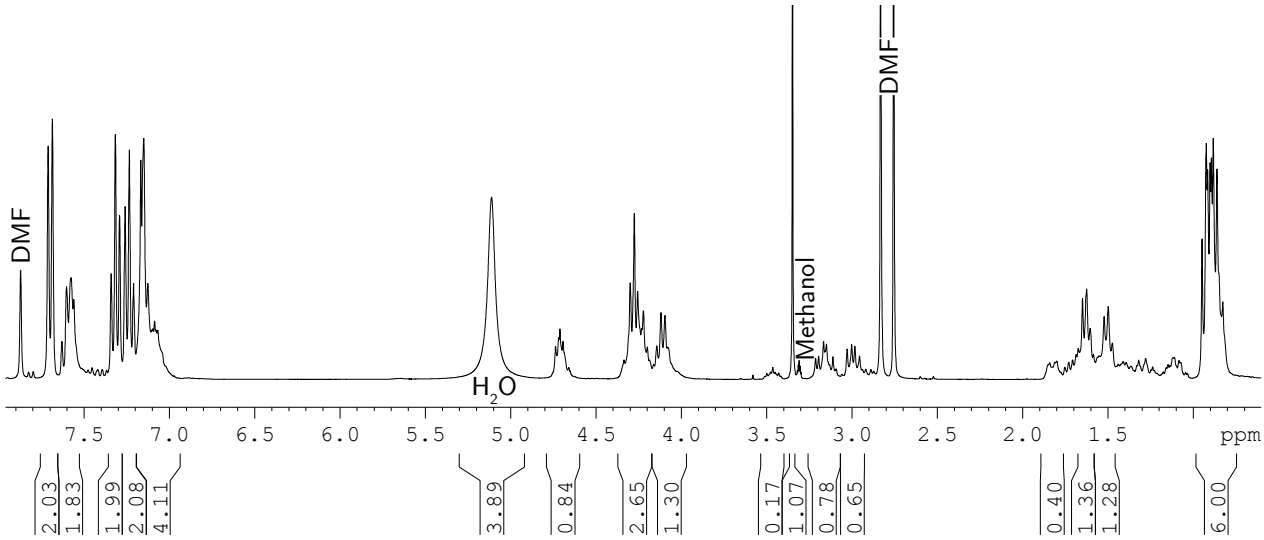

Figure 4.21.: 300 MHz NMR ^{1}H spectrum of the crude product of $R_{III\,IV}$ - VI, Fmoc-Leu-Phe. (Solvent: Methanol-d_4) The spectrum also shows several impuities, whereby the solvent of the reaction, DMF (at 7.87, 2.84 and 2.76 ppm), is very prominent. This was identified with the tables in [50].

Subsequently, the crude peptide product of $R_{III\,IV}$ - VI was deprotected in the same way as described in $R_{III\,IV}$ - *V* ([24, p.185-186] and [56]). The only difference was that piperidine was used instead of diethylamine.

Upon repeated trituration with diethylether (the work-up recommended in [24]) no clean product was obtained. Hence the residue was treated with an mixture of ethylacetate and water, to which a small amount of triethylamine was added. The purpose of the triethylamine was to deprotonate possible product peptide and direct it towards the acqueous phase. That approach gave a separation of apolar aromatic compounds, derivatives of the Fmoc-group (ethylacetate phase) and amino acid containing ones (water phase). Unfortunately, it was not possible to identify the desired peptide in the water phase, although the NMR spectra showed peaks corresponding to Phe and Leu. The integrals did not match at all and NH peptide backbone peaks, which should be visible in the used deuterated solvent, DMSO, were missing. From that, it can be concluded that the deprotection reaction or the subsequent work-up somehow damaged the peptide. This means that one requirement for the applicability of Route III and IV, the solution phase Fmoc deprotection of *C*-termially unprotected peptides is not met.

4.1.5.4. $R_{III\,IV}$ - VIII and IX: Coupling Fmoc-Met with Leu via the Benzotriazole Method

In addition to the carbodiimide mediated coupling an alternative approach, which is proven to work with *C*-terminal unprotected amino acids and peptides was tested. It is based on benzotriazole derivatives of *N*-terminal protected amino acids as the activated species. In a subsequent step these are aminolysed by an unprotected amino acid or peptide in aqueous solution.

The reactions to couple Fmoc-Met with Leu were performed as described in [57]. The first reaction, generating the active species, Fmoc-Met-Bt, gave a product in 90.11% yield (0.427 g,

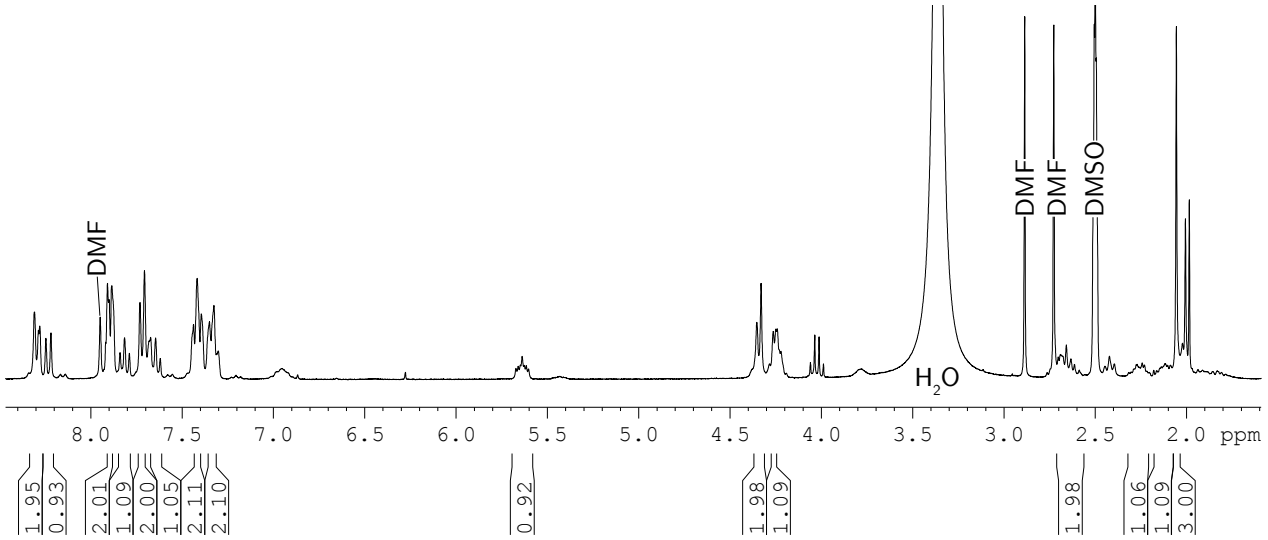

Figure 4.22.: 300 MHz NMR ^{1}H spectrum of the raw product of $R_{III\,IV}$ - VIII, Fmoc-Met-Bt. (Solvent: DMSO-d_6) This product was used for the following reaction without further purification, although it was not free of impurities. The origin of the DMF impurity is unclear, because this solvent was not used during the reaction.

0.90 mmol). Although, the proton NMR spectrum *Figure 4.22* of the product showed all peaks belonging to the product according to the reference spectrum in [57], it also exhibited several impurities. Thereby, it is was not traceable from where the DMF impurity came as this solvent was not used for the reaction.
Nevertheless, the raw product was used for the actual coupling reaction of Fmoc-Met-Bt with Leu without any additional purification measures. The coupling was performed as described in [57], with the exeption that the volumes of water and acetonitril were exchanged by mistake. This means that 10 mL water and 4 mL acetonitril were used as instead of 4 mL water and 10 ml acetonitril. This error might be the reason why no useful product could be obtained from the coupling reaction. With the excess of water the hydrolysis of Fmoc-Met-Bt was probably faster than the aminolysis. Unfortunately, time did not allow repeating the reactions to assess the performance of the coupling under correct conditions.

4.1.6. The Solution Phase Approach

In addition to the solid phase synthesis Routes it was tried to synthesize the fMLF using the traditional solution phase approach. The performed reactions are discussed in the following sections.

4.1.6.1. Sol - I and II: The Benzyl Ester of Phe

The first step in synthesizing the peptide along the solution phase route was to protect the *C*-terminus of Phe with a benzyl ester group. This transformation was achieved by combining the procedures stated in [22] and [58]. It involved thionyl chloride activating the carboxylic acid group of Phe, facilitating the attack of benzyl alcohol. The reaction was speeded up

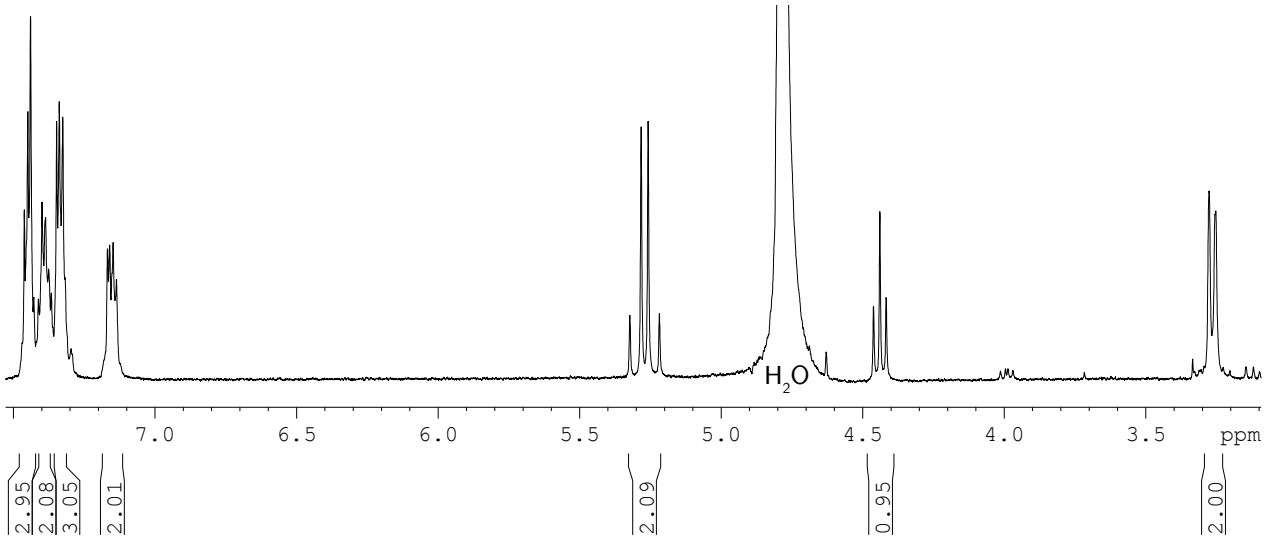

Figure 4.23.: 300 MHz NMR ^{1}H spectrum of Phe-OBz. It was produced in Sol - I. (Solvent:D_2O)

by ultrasonic sound irradiation. The products were obtained in accetptable yields (64.25% in Sol - I and 81.34% in Sol - II) and very high purity according to NMR analysis (*Figure 4.23*). Attempts to extract more product from the mother liquors afforded products that were not unambiguously identifiable as the desired species.

4.1.6.2. Sol - III, IV and V: Coupling Fmoc-Leu with Phe-OBz

The first attempt to perform the coupling of Fmoc Leu with the Benzyl ester of Phe was performed with DCC and HOBt according to the procedure stated in [24, p.145] (Sol - III). The resulting product was not identified as the desired one with full certainty. Nevertheless, it was used for the deprotection reaction in acetonitril and diethylamine (according to [24, p.185-186] and [56]). Dissolution was rather poor and the reaction yielded a product that could not at all be identified as the desired product.

Upon failing of the two previous reactions another attempt to couple and deprotect the mentioned amino acids was undertaken (Sol - IV). This time the coupling procedure of the publication introducing the DCC/HOBt method, [17], was followed. Thereby, 0.757 g (1.28 mmol 126.19%) of crude product was obtained. As the yield already suggests, the product was highly impure, which was confirmed by NMR (*Figure 4.24*) and MS (*Figure C.6*) analysis. The major fraction of these impurities is DCU, the by-product to which DCC is converted during the reaction. Nevertheless, Fmoc-Leu-Phe-OBz, could be identified by the mentioned methods. Therefore, a part of the product was used for the subsequent deprotection reaction (Sol - V).

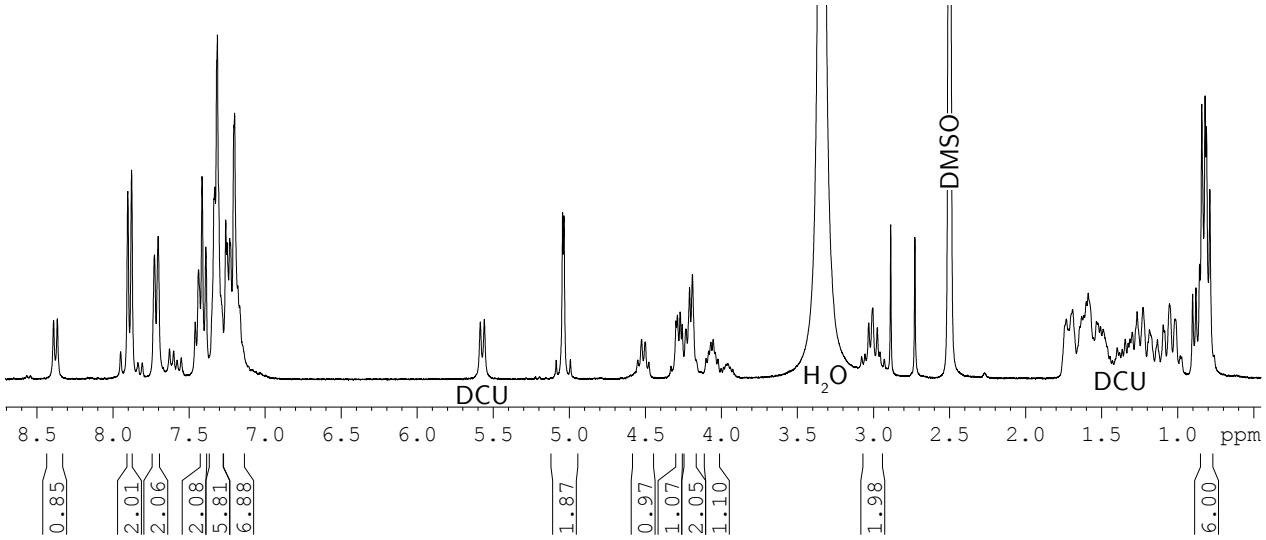

Figure 4.24.: 300 MHz NMR ^{1}H spectrum of the product of Sol - IV, Fmoc-Leu-Phe-OBz. (Solvent: DMSO-d_6) The region from 0.96 ppm to 1.78 ppm as well as the doublett at 5.57 ppm correspond the main impurity, DCU, the by-product to which DCC is converted. These peaks obscure some of the side chain signals of Leu.

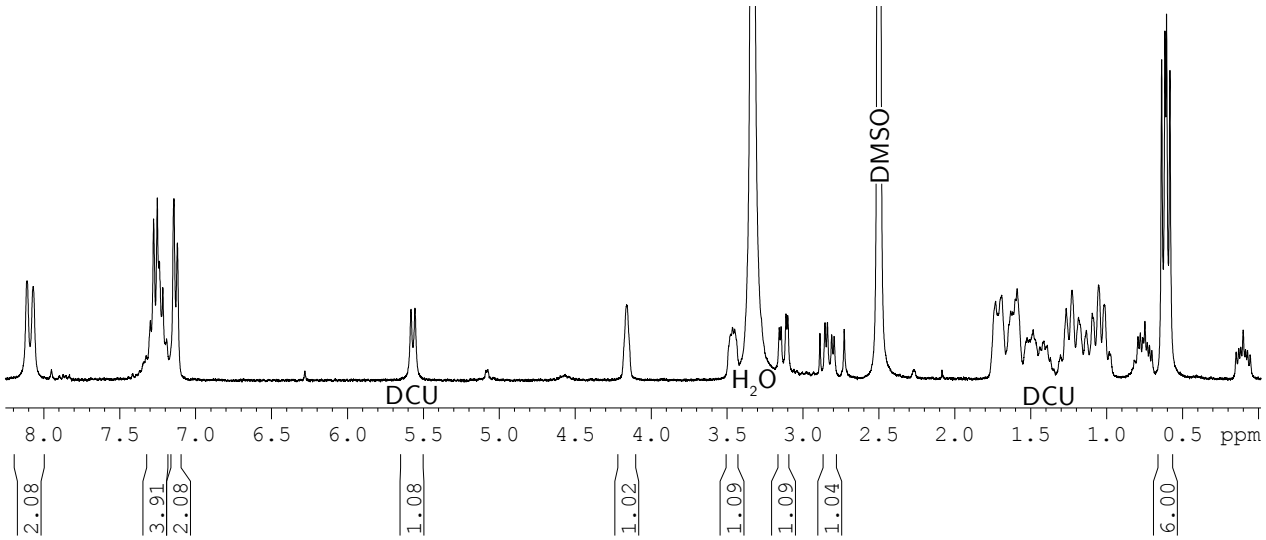

Figure 4.25.: 300 MHz NMR ^{1}H spectrum of the product of Sol - V. (Solvent: DMSO-d_6) Remarkably, the expected product is not observed as the the *C*-terminal benzyl ester group is missing. This can be seen by the small integral of the aromatic region as well as the (almost) complete absence of the C$\mathbf{H_2}$-peak at 5.08 ppm. Also here, the majority of impurity peaks (0.95-1.79 ppm, 5.57 ppm), hiding Leu side chain signals, are due to DCU.

This was achieved by the protocol stated in [24, p.185-186], with DMF as solvent and piperidine as base. Using DMF enabled the dissolution of the product in contrast to the previous deprotection reaction with acetonitril (Sol - III). The work-up, employing trituration with heptanes, successfully removed reaction by-products and hence, a peptide containing product residue was obtained (0.071 g, 0.25 mmol, 63.73%). Nonetheless, the chemical nature of the peptide derivative was not the expected one. Instead of Leu-Phe-OBz the NMR spectrum (*Figure 4.25*) indicated the presence of Leu-Phe (together with high amounts of DCU). The Aromatic region

exhibits a far to low integral for a benzyl group and the CH_2 signal normally observed is also hardly visible. Obviously, the benzyl ester had been removed in addition to the Fmoc group under the applied reaction conditions. As a result the synthesis sequence could not be continued. Due to time reasons the issue was not pursued further, although it would be interesting to perform additional experiments in order to clarify the phenomenon.

4.2. Solid state NMR investigations

The solid state NMR part focused on the implementation of three kinds of pulse sequences. For each simulations[4.2] as well as NMR experiments were conducted, which are discussed in the following sections.

4.2.1. $\mathcal{R}$ Decoupled ^{1}H Spectroscopy

One of the applications of $\mathcal{R}$ decoupling is in proton spectroscopy. Homonuclear dipolar decoupling by $\mathcal{R}$-schemes in the pulse sequences described in [2] and [3] allow the recording of high resolution ^{1}H spectra, which in solid state NMR is usually a rather tricky task due to the presence of large homonuclear dipolar interactions. [2] Initially, a basic version of the $\mathcal{R}$ decoupled proton-proton experiments (*Figure 1.35a.)*) as described in [2] was simulated. This was done by simulating the pulse sequence in its original 2D fashion and in a 1D fashion, that uses a theoretical shortcut and required less computional time. The 1D version simulates a sequence of individual $\mathcal{R}\mathcal{R}'$ blocks and after each block the z-magnetisation was determined.[4.3] After that the FID was not evolved but the next $\mathcal{R}\mathcal{R}'$ block was conducted (*Figure 4.26*). By comparing the resulting FID-like graphs of spin systems with and without homonuclear dipolar couplings, the performance of $\mathcal{R}$-type decoupling could be assessed. Further, it was verified that the fast 1D variant simulations give the same results as the full 2D simulations. To compare the two variants all initial points of the FIDs of a 2D dataset (for each t_1 increment there is one FID) were extracted and plotted accordingly. The results can be seen in *Figure 4.27.* a.) displays examples for the fast variant and b.) shows the corresponding ones for the 2D variant. The conditions under which these corrseponding simulations were performed (meaning the H_2 spin system, spectral width, MAS rate *etc.*) were identical to the fast variant. For each variant three graphs are depicted. The solid ones (red) correspond to simulations where only one J-coupling bewteen the two H spins was specified, the dashed lines (blue) correspond to simulation where one homonuclear dipolar coupling and one J-coupling were specified and the dotted ones (green) show simulations with both interactions (dipolar and J-coupling) but with wrong symmetry numbers. It can be seen that the graph with dipolar coupling is rather similar

[4.2] Exemplary SIMPSON input scripts can be found in *Appendix D.*
All simulations were carried out with a proton frequency of 500 MHz (leading to a carbon frequency of 125.76 MHz).

[4.3] In a real experiment only teansversal magnetisation, created e.g. by a $\frac{\pi}{2}$ pulse is detectable.

to the one without. However, without the correct symmetry this is not the case. Hence, the decoupling was proven indeed to suppress the effects of homonuclear dipolar couplings.

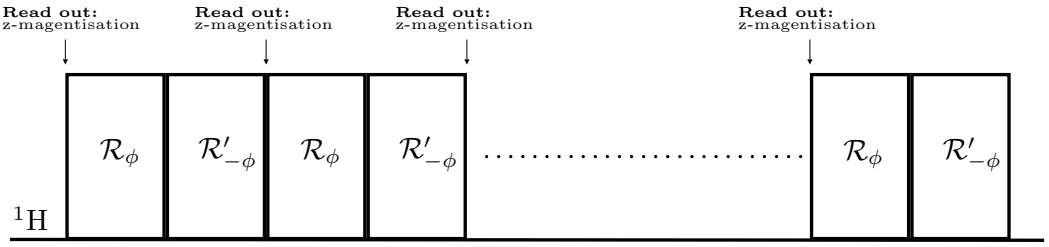

Figure 4.26.: This scheme illustrates how simulations of the fast variant were conducted. After each $\mathcal{R}\mathcal{R}'$ block the magnitude of the z-magnetisation was determined before the next block was performed.

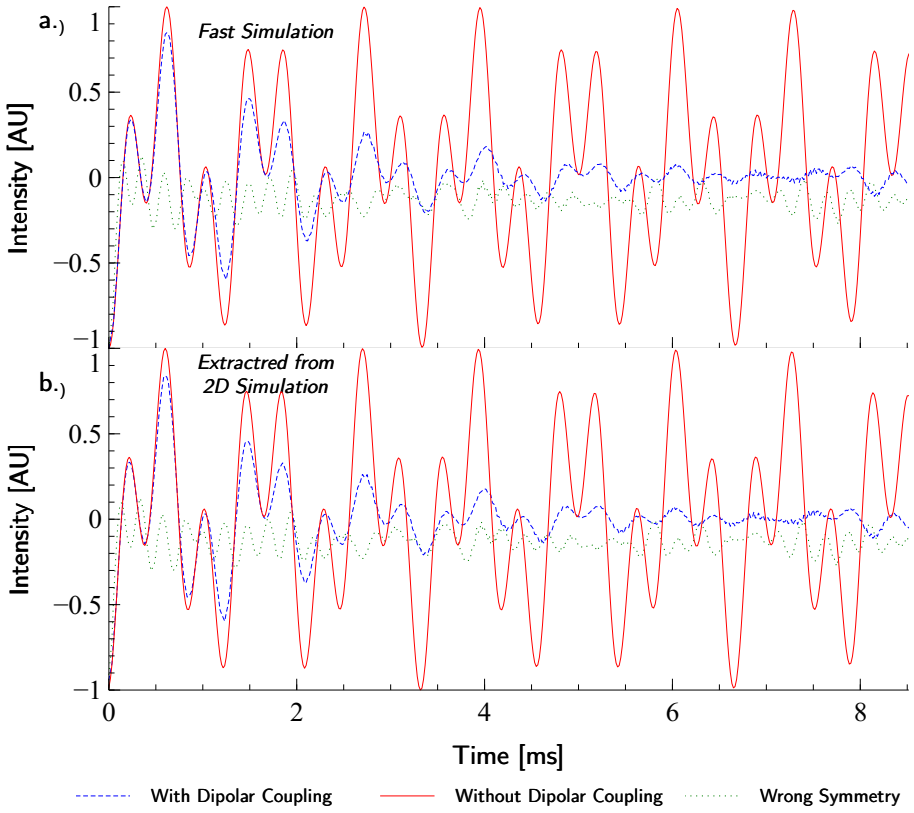

Figure 4.27.: a.) show the results of the fast variant simulations of a H_2 spin system (MAS: 20 kHz; SW: 60 kHz). The correctly decoupled (blue dashed) one exhibits a big similarity to the one without any dipolar couplings (red solid). The wrongly decoupled simulation (green dotted) differs just in one symmetry number from correctly decoupled one ($\mathcal{R}6_1^4$ instead of $\mathcal{R}6_1^3$). b.) shows the first points extracted from the FIDs of slow 2D simulations under the corresponding conditions. The graphs are identical to the ones obtained with the fast variant. This verifies, that both simulation types give the same results.

Spin System Details: *Nuclei:* $\delta_{iso}^{H_1}$=1.5 kHz, $\delta_{ansio}^{H_1}$=3.5 kHz, $\delta_{iso}^{H_2}$=4.0 kHz, $\delta_{ansio}^{H_2}$=1.5 kHz. *J-couplings:* $J_{iso}^{H_1H_2}$=7 Hz, $J_{aniso}^{H_1H_2}$=15 Hz. *Dipolar couplings:* $R_{DD}^{H_1H_1}$=20 kHz (Not set in the simulations depiced with solid (red) lines.).

High resolution ^{1}H spectra, were generated from the simulated 2D datasets. *Figure 4.28* shows several examples thereof. Spectra from the 2D simulations already mentioned above were

generated by taking the positive skyline projection[4.4] along the direct dimension of the fourier transformed 2D dataset (an example of such a 2D spectrum can be seen in *Figure 4.29*). The simulations with and without dipolar coupling are rather similar and the expected peaks are visible (together with their mirror images as no quadrature detection in the indirect dimension was performed). Their intensities, however, differ roughly by one order of magnitude, which is most probably due to non ideal decoupling. This is also illustrated by the curves shown in *Figure 4.27*. There the simulation with dipolar couplings starts to deviate from the one without diploar couplings after some time. A further intensity diminishing factor might be incomplete powder averaging due to a low number of simulated crystallites (fifty in this case), which nevertheless makes computation time shorter. In the spectrum with the wrong symmetry numbers no peaks are identifiable as expected. An additional spectrum exhibits the outcome of a simulation in which the decoupling power was set to zero and hence no decoupling at all was performed. It just shows a not very intense spike (compared to the other spectra) in the center of the spectrum, which actually comes from the rf transmitter ("transmitter spike"). The absence of any other signal is explained by the fact that just a single $\frac{\pi}{2}$ pulse is applied at each t_1 increment resulting basically in the repeated acquisition of the same experiment with increasing recycle delays. Consequently no modulation is encoded in the indirect dimension.

[4.4] For a skyline projection, just the maximal (minimal for a negative skyline projection) values of the respective rows or columns are selected. In contrast a sum projection takes the sums of the values over the entrie rows or columns.

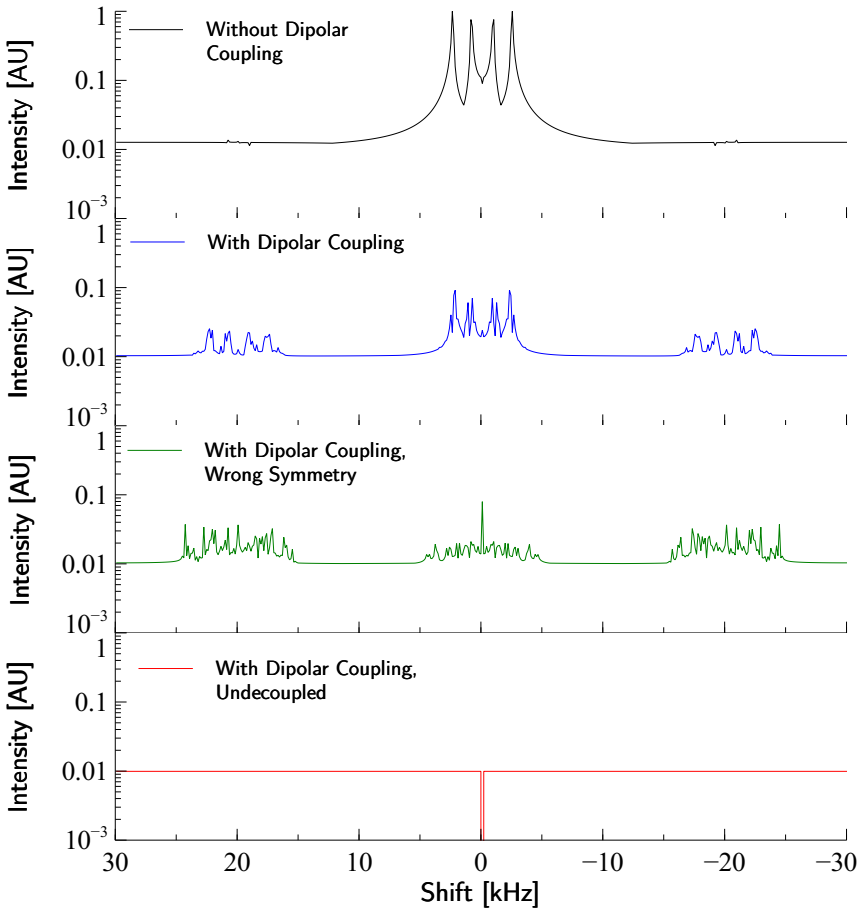

Figure 4.28.: Here, several simulated proton spectra generated from Fourier transformed 2D simulation datasets under several conditions (With and without dipolar couplings, with wrong symmetry numbers and with decoupling at all) are shown. The conditions (including the spin system) are the same as for the already above mentioned simulations (*Figure 4.27*, where also the details on the used spin system are stated.). The intensity differences have to be noted.

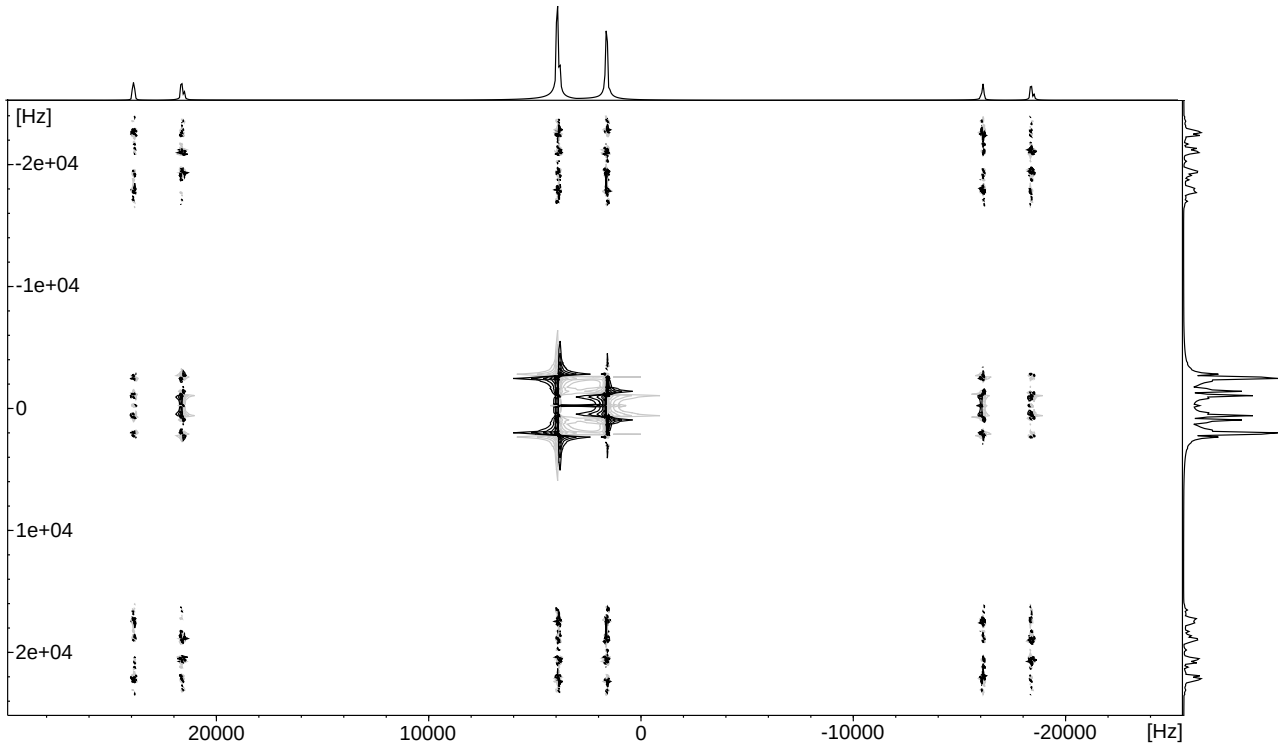

Figure 4.29.: Illustration of a simulated and Fourier transformed 2D dataset, which was used to create the proton spectrum (*Figure 4.28*) via positive skyline projection. This spectrum shows the simulation where correct $\mathcal{R}6_1^3$ decoupling was applied, with dipolar coupling enabled. (Details on the spin system can be found in the caption of *Figure 4.27*)

As the simulations gave reasonable results, the pulse program was implemented and tested on the spectrometer. The samples used were adamantane and α-glycine. The effect of variation of several experimental parameters was tested. It was found that the transmitter offset was crucial for recording useful spectra. It is therefore advisable to optimise this parameter for individual samples. Increasing or decreasing the amplitude of the pulses incrementally did not have any beneficial effect. Another aspect that was revealed to be very important was the application of window functions during processing. This is illustrated in *Figure 4.30*, which shows the same data (a spectrum of α-glycine) once processed with the QSINE window function and once without it. It is easily observable that the projection along the direct dimension is much better resolved, when the window function is applied.

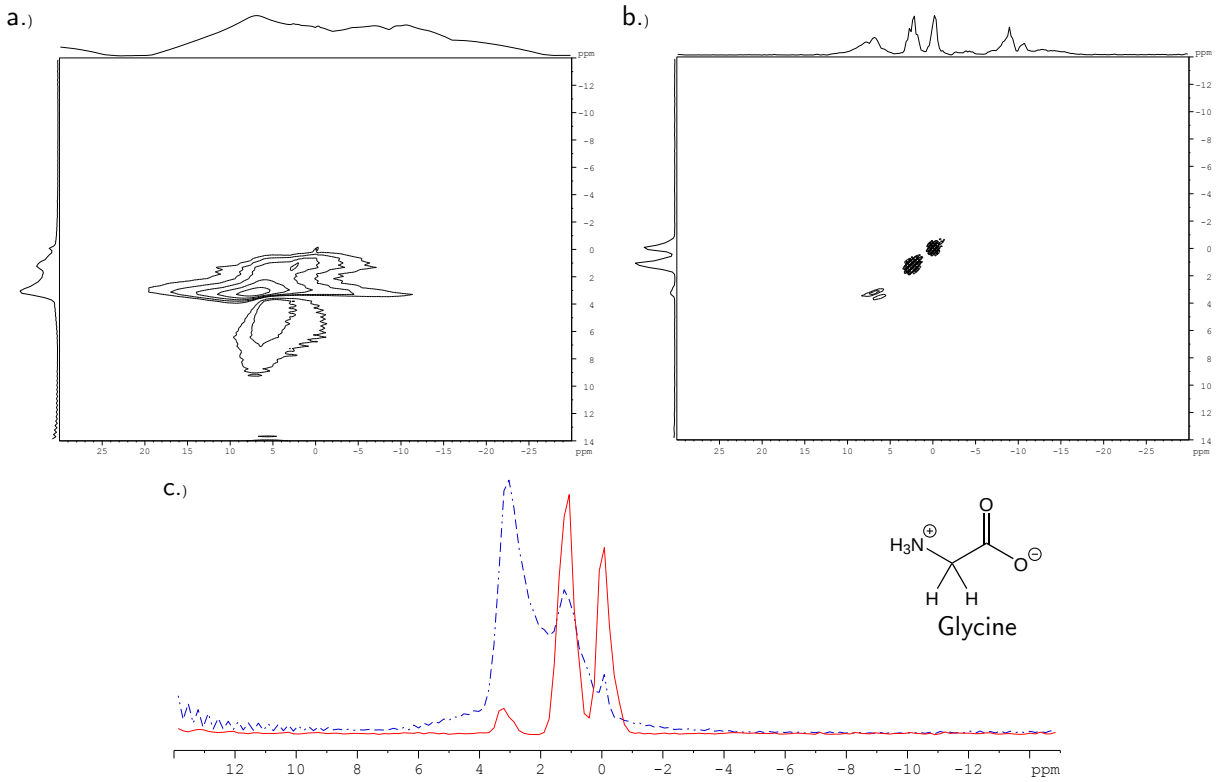

Figure 4.30.: Experimental 500 MHz ^{1}H NMR spectra (14 kHz MAS, Offset: 20.7 kHz, $\mathcal{R}6_1^3$) a.) shows a spectrum of α-glycine without a window function and b.) shows the same spectrum processed with the QSINE window function in both dimensions. The enhancement in resolution can be easily seen in the spectra as well as in the projections. c.) exhibits a direct comparison between the projections (solid: QSINE window function; dashed and dotted: no window function) as well as the chemical structure of glycine.

Although these spectra look quite promising, it was not possible to reproduce the glycine spectra shown in [2].[4.5] Most importantly, the $-NH_2$ peak (at 3.36 ppm, no extra scaling applied) has a different shift difference to the other peaks and depending on the processing method its intensity varies significantly. To that it has to be noted that the experiments in [2] were performed at higher MAS rates (25 kHz and 30 kHz), which leads to better heteronuclear dipolar decoupling and with a smaller rotor (2.5 mm instead of 3.2 mm), which results in performance enhancement due to a more homogeneous B_1 field.

In order to improve the performance of the pulse sequence, the changes stated in [3] were implemented (see *Section 1.2.3.1*). As before the sequence was firstly examined via simulations and then implemented on the spectrometer. For the simulations a realistic spin system with dipolar coupling constants extracted from the crystal structure of glycine was used. It consisted of three H and one C. Two H and the C formed the $C_\alpha H_2$] group and the third H should model the protons of the amino group. Isotropic chemical shift values were taken from a glycine spectrum [69]. Details on this spin system are given in the caption of *Figure 4.32*.

The following spectra (*Figure 4.31*) show the results for the basic (a.) - according to [2]) and

[4.5] In [2] the glycine spectra are depicted without scaling applied. Although not stated explicitly this can be deduced from the glycine spectra in [3], which show different shifts and where it explicitly stated that the spectra were scaled. Further, the shift of the single liquid state resonance in glycine (corresponding to C$\mathbf{H_2}$) is at 3.57 ppm [64], which does not correspond to the spectra of [2] but to the ones of [3].

the improved (b.) - according to [3]) pulse sequence. The simulations were performed with the glycine spin system described above, whereby just homonuclear dipolar couplings were enabled. Additionally, TPPI was omitted in order to simplify processing.
It is quite straightforward to identify b.), the improved pulse sequence, as the more efficient one when it comes to decoupling (The contour levels are set up in the same way for both spectra).

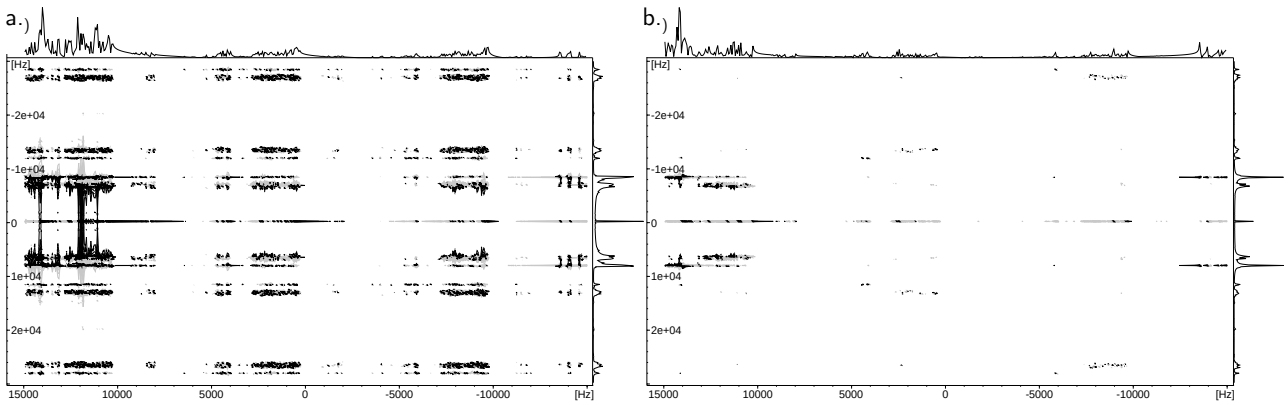

Figure 4.31.: Here two spectra are compared which were simulated under same conditions (same spin system derived from glycine, just homonuclear dipolar coupling enabled, 20 kHz MAS, spectral width 30 kHz, $\mathcal{R}6_1^3$) however with different pulse sequences. For a.) the pulse sequence of [2] was used and for b.) the improved one after [3] (without TPPI). It is rather obvious that the latter sequence produces cleaner spectra as well as better resolved projections. (The actual high resolution proton spectra, *i.e* the indirect projections, are better visible in *Figure 4.32*. Also the detailed spin system parameters are given there.)

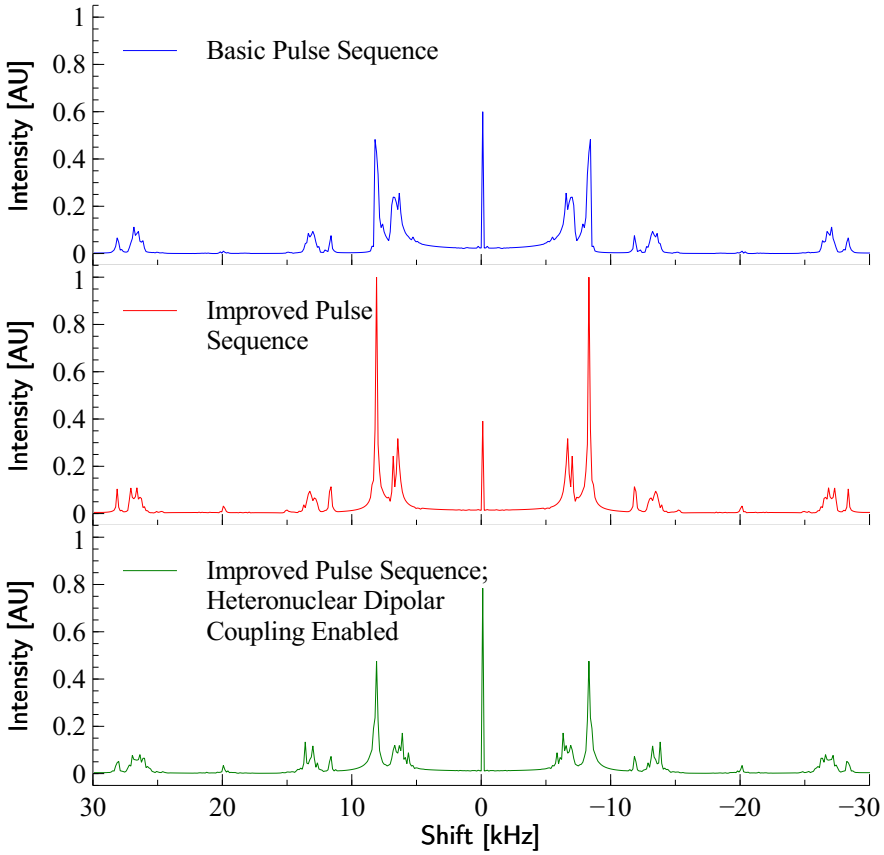

Figure 4.32.: These graphs of simulations compare the improved 2D proton pulse sequence with the basic one. Thereby, the higher effectivity of the former one is shown. Further a third spectrum shows the impact of the heteronuclear dipolar couplings on the simulations. These deteriorate the outcome as MAS of 20 kHz cannot fully average them out.
The spectra were generated from the 2D datasets shown in *Figure 4.31* except for the third one which was however also simulated under the same conditions as the other two. Just heteronuclear dipolar couplings were added.

Spin System Details: *Nuclei:* $\delta_{iso}^{C_1}$=5.4 kHz, $\delta_{ansio}^{C_1}$=0.0 kHz, $\delta_{iso}^{H_1}$=14.0 kHz, $\delta_{ansio}^{H_1}$=7.5 kHz, $\delta_{iso}^{H_2}$=11.9 kHz, $\delta_{ansio}^{H_2}$=5.0 kHz, $\delta_{iso}^{H_3}$=11.3 kHz, $\delta_{ansio}^{H_3}$=4.0 kHz. *J-couplings:* $J_{iso}^{C_1H_2}$=130 Hz, $J_{aniso}^{C_1H_2}$=200 Hz, $J_{iso}^{C_1H_3}$=140 Hz, $J_{aniso}^{C_1H_3}$=200 Hz. *Dipolar couplings:* $R_{DD}^{C_1H_1}$=3.4 kHz, $R_{DD}^{C_1H_2}$=23.1 kHz, $R_{DD}^{C_1H_3}$=23.3 kHz, $R_{DD}^{H_1H_2}$=8.5 kHz, $R_{DD}^{H_1H_3}$=8.4 kHz, $R_{DD}^{H_2H_3}$=23.1 kHz. (The heteronuclear dipolar couplings were just used for the third spectrum of this figure. The other values are also valid for *Figure 4.31*.)

This is also illustrated by the projections of these spectra which are given in *Figure 4.32* in better quality. The three peaks at 6400 Hz, 6800 Hz and 8100 Hz correspond roughly to the chemical shifts specified in the input script, when a scaling factor of 0.57 is included. This factor gives theoretic shift values of 6469 Hz, 6765 Hz, and 7982 Hz, respectively. This is in very good agreement with the value in [2], which was a scaling factor of 0.5.
Additionally, a projection of a simulation is depicted which has all dipolar couplings enabled, including the heteronuclear ones. The heteronuclear dipolar couplings have a big impact on the spectrum. It is decreased in intensity and more importantly, the peaks of the CH_2 group are not that cleanly separated due to an additional splitting caused by not fully decoupled heteronuclear dipolar couplings. Hence, higher MAS rates would probably improve the outcome of this simulation.
As the basic 2D pulse sequence also the improved one was implemented, tested and optimised

(offset, varying pulse lengths and acquisition times) on the spectrometer. The resulting spectra, however, did not significantly improve, which can be seen in *Figure 4.33*. Only by processing using window functions all three glycine resonances were observable. Also the use of inserts in the rotor to reduce the sample volume showed no effect. Further a different symmetry, $\mathcal{R}14_2^7$, was tested without improvement.

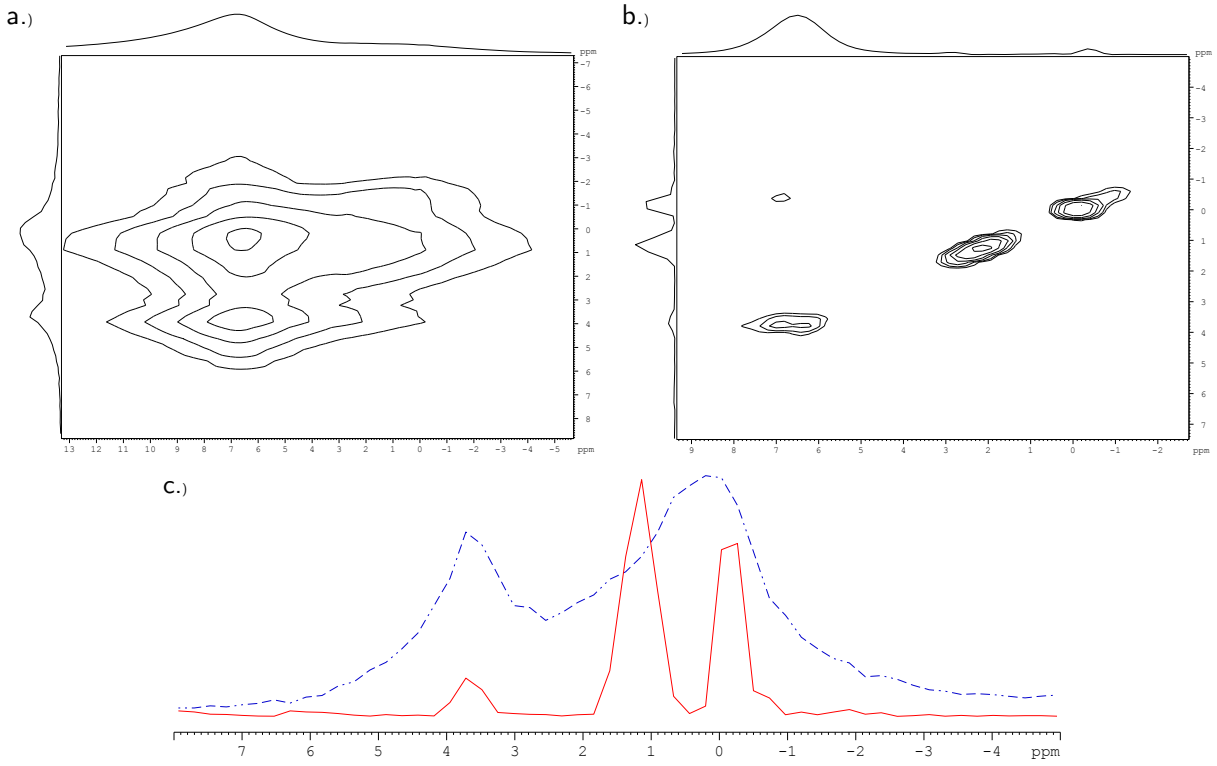

Figure 4.33.: Experimental 500 MHz ^{1}H NMR spectra (20 kHz MAS, Offset: 14.96 kHz, $\mathcal{R}6_1^3$) acquired with the enhanced pulse sequence described in [3]. TPPI was not enabled. a.) shows a spectrum of α-glycine without a window function and b.) shows the same spectrum processed with the QSINE window function in both dimensions. c.) compares the resulting projections directly (solid: QSINE window function; dashed and dotted: no window function).
Generally no big improvements compared to the basic pulse sequence were achieved.

As a result, the high resolution ^{1}H experiment was successfully implemented and tested. Nevertheless, it still needs to be investigated and optimized further, using both simulations and real life experiments.

4.2.2. $\mathcal{R}$ Decoupled ^{13}C Spectroscopy

A further use of $\mathcal{R}$ decoupling is ^{13}C spectroscopy. With the pulse sequence published in [2, 47] these decoupling schemes can be used to conduct experiments which lead to carbon spectra, which show the effects of heteronuclear J couplings but not the ones of dipolar couplings. [2, 47] (For details see *Section* 1.2.3.2.) As in the case of high resolution $\mathcal{R}$-decoupled proton experiments, the $\mathcal{R}$ decoupled ^{13}C experiment was initially simulated using the pulse sequence stated in [2] (see *Section 1.2.3.2*). For that purpose three spin systems modelling CH_2 groups (Details: see *Figure 4.34* and *Figure 4.37*) were used. The simulations were carried out under

various conditions, mostly enabling or disabling specific dipolar couplings in order to investigate their influence on the spectral lineshapes. The resulting spectra can be seen in *Figure 4.34*. When just the homonuclear dipolar coupling is enabled the spectrum is almost identical to the one without dipolar couplings. This means that the $\mathcal{R}$ sequence effectively decouples homonuclear dipolar couplings as it is supposed to. However, with only heteronuclear dipolar couplings this scheme has no effect as the spectra with those enabled do not exhibit the desired splittings, which originate from heteronuclear J-coupling (which is also in accordance with theory). Increasing the MAS rate improves the situation a bit although still no real splittings can be observed.

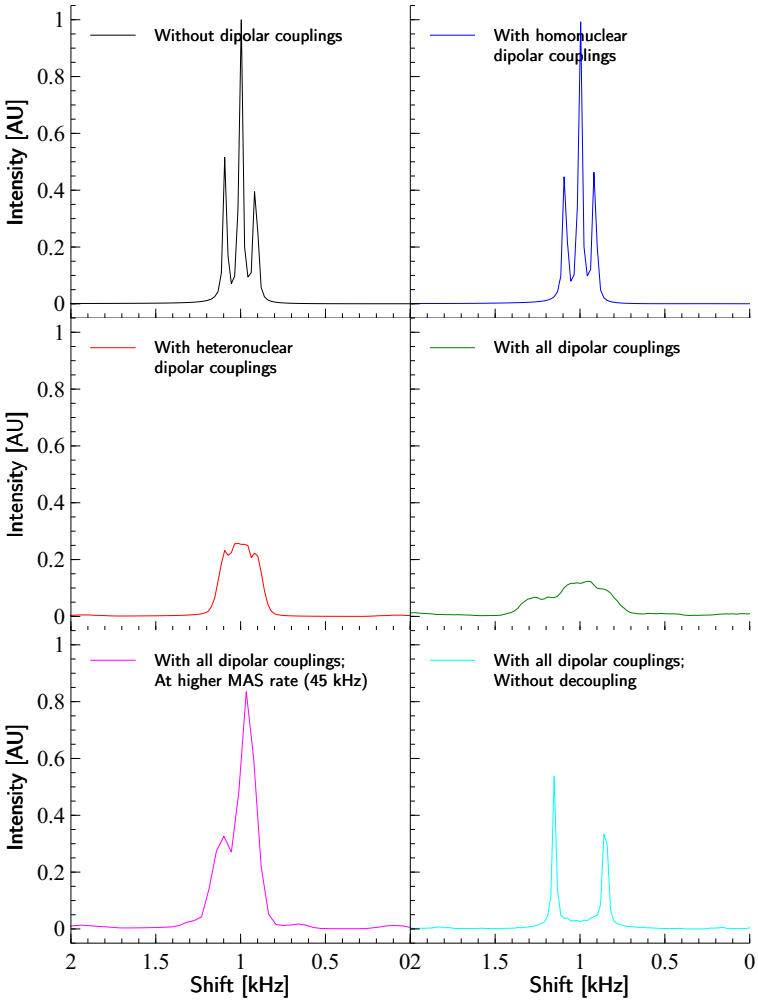

Figure 4.34.: Simulated spectra of the model CH_2 group using the $\mathcal{R}$ decoupled ^{13}C experiment with $\mathcal{R}6_1^3$ symmetry at 20 kHz MAS (except for the one at 45 kHz). The spectra show that this decoupling scheme is effectively suppressing homonuclear dipolar couplings. However, heteronuclear dipolar couplings are not removed. This can be partly achieved by increasing the MAS rate. For comparison a spectrum without any decoupling is also depicted (decoupling power is set to zero). It exhibits an interesting line shape pattern. Two peaks are separated by the added heteronuclear J-coupling constants. It can be viewed as a triplett with the central line missing. This shape is observed only when one homonuclear and at least one heteronuclear dipolar coupling is present in the spin system. An identical spectrum is produced with a standard pulse-acquire simulation. However, further investigations to this phenomenon were not undertaken.

Spin System Details: *Nuclei:* $\delta_{iso}^{C_1}$=1.0 kHz, $\delta_{ansio}^{C_1}$=2.5 kHz, $\delta_{iso}^{H_1}$=1.5 kHz, $\delta_{ansio}^{H_1}$=3.5 kHz, $\delta_{iso}^{H_2}$=2.0 kHz, $\delta_{ansio}^{H_2}$=2.5 kHz. *J-couplings:* $J_{iso}^{C_1H_1}$=150 Hz, $J_{aniso}^{C_1H_1}$=10 Hz, $J_{iso}^{C_1H_2}$=150 Hz, $J_{aniso}^{C_1H_2}$=15 Hz. *Dipolar couplings:* $R_{DD}^{C_1H_1}$=15.0 kHz, $R_{DD}^{C_1H_2}$=15.0 kHz, $R_{DD}^{H_1H_2}$=20.0 kHz.

As the simulations showed that the ^{13}C pulse sequence was generally functional, a corresponding pulse program on the NMR spectrometer was implemented. The experiment was realized in the form of a composite pulse decoupling program (cpd-program). This has the advantage that the cpd-program can be used with different standard pulse sequences such as 'cp' or 'hpdec' (These two were employed in this work.). The disadvantage in this approach is that the length of one decoupling pulse, τ_{Pulse}, has to be calculated manually depending on the MAS frequency

and symmetry[4.6]. This is done via this formula:

$$\tau_{Pulse} = \frac{n \cdot \tau_{rot}}{N \cdot i_{Pulses}} \tag{4.1}$$

N and n are the symmetry numbers, τ_{rot} is the MAS rotation period ($\tau_{rot} = \frac{1}{\nu_{rot}}$) and i_{Pulses} is the number of pulses per $\mathcal{R}$ block (In this experiments it was 3 as a composite π-pulse was used.)

The cpd program was initially tested on an adamantane sample. With this sample the splittings from heteronuclear J-couplings could be observed already at MAS frequencies as low as 7 kHz (*Figure 4.35a.)*). The prerequisite for that was the optimisation of the transmitter offset. In case the offset is not optimal the splittings dissapear and instead line narrowing occurs (*Figure 4.36*). The effect of the off resonant irradiation is explained by changing the effective angle of the rf induced magnetic field, which at a specific range causes the spin diffusion induced self decoupling of the heteronuclear J-coupling to be removed. This leads to the observation of the J-splittings [70].

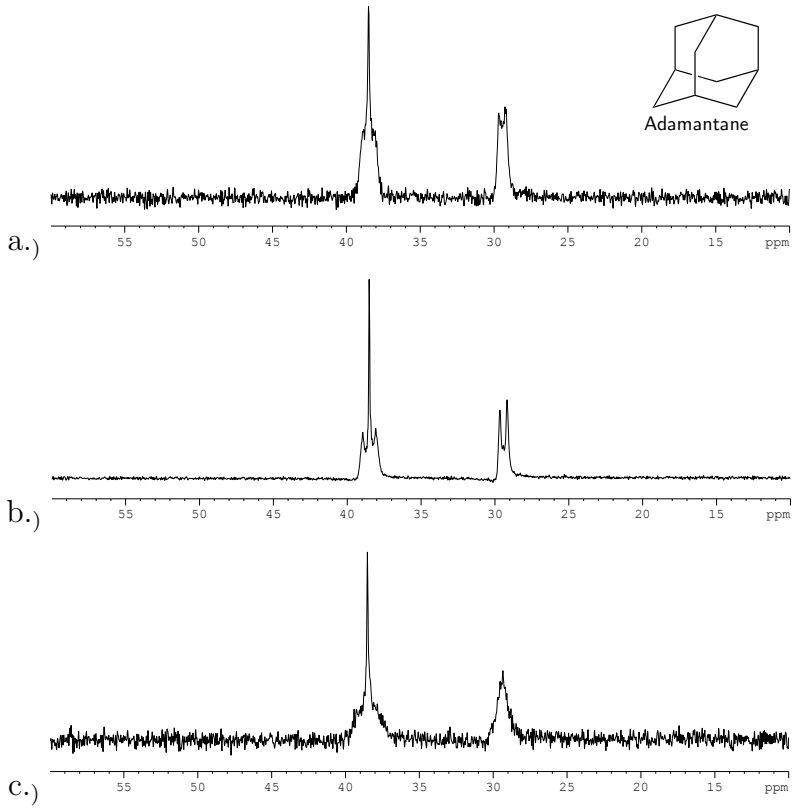

Figure 4.35.: Experimental 125.76 MHz $\mathcal{R}$ decoupled ($\mathcal{R}6_1^3$) ^{13}C NMR spectra of adamantane. a.) shows a spectrum at 7 kHz MAS and at already optimized 13 kHz transmitter offset. Even at this low spinning speed the splittings due to heteronuclear J-couplings are rudimentary present. Further the chemical structure of adamantane is depicted. b.) displays a spectrum at 18 kHz MAS with the transmitter offset optimised to 14.75 kHz. Here the splittings are nicely visible. c.) displays for comparison a 18 kHz MAS spectrum without decoupling. It exhibits the peakshapes typical for the self decoupling of the heteronuclear J-couplings as it is described in [70].

[4.6]The corresponding pulse amplitude has to be deduced anyway from a reference pulse.

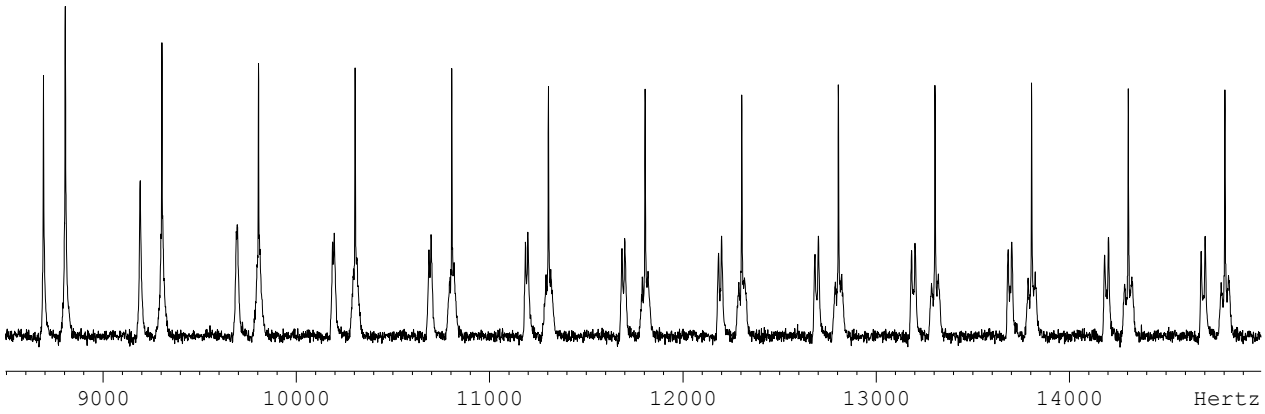

Figure 4.36.: A series of experimental 125.76 MHz $\mathcal{R}$ decoupled ^{13}C NMR spectra (18 kHz MAS, $\mathcal{R}6_1^3$) of admantane at different transmitter offsets. It displays a transition from very sharp singlets to peaks split by heteronuclear J-coupling at about 15 kHz.

Simulations with varying transmitter offset also exhibited a similar behaviour as illustrated in *Figure 4.37*. The peaks change their shape with increasing offset from sharper to broader lines. Nevertheless, the actual heteronuclear J-coupling cannot be seen due to too slow spinning (18 kHz) for the magnitude of the heteronuclear dipolar couplings (20 kHz and 21 kHz).

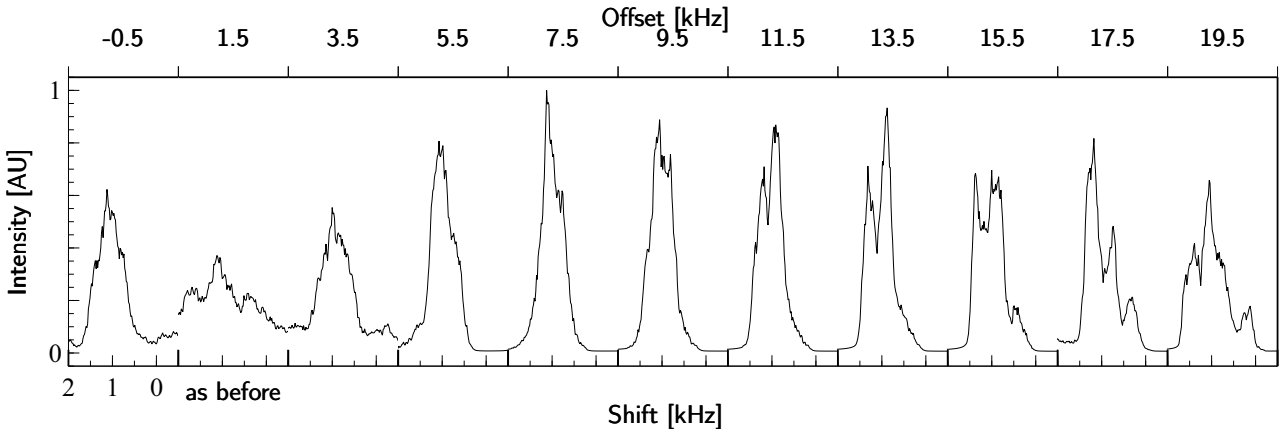

Figure 4.37.: Simulated $\mathcal{R}$ decoupled ^{13}C NMR spectra (18 kHz MAS, $\mathcal{R}6_1^3$) of a CH_2 spin system with varying transmitter offsets. A change in peak shape can be observed.

Spin System Details: *Nuclei:* $\delta_{iso}^{C_1}$=1.0 kHz, $\delta_{ansio}^{C_1}$=3.1 kHz, $\delta_{iso}^{H_1}$=1.5 kHz, $\delta_{ansio}^{H_1}$=3.5 kHz, $\delta_{iso}^{H_2}$=2.0 kHz, $\delta_{ansio}^{H_2}$=2.5 kHz. *J-couplings:* $J_{iso}^{C_1H_1}$=145 Hz, $J_{aniso}^{C_1H_1}$=10 Hz, $J_{iso}^{C_1H_2}$=150 Hz, $J_{aniso}^{C_1H_2}$=15 Hz. *Dipolar couplings:* $R_{DD}^{C_1H_1}$=15.0 kHz, $R_{DD}^{C_1H_2}$=21.0 kHz, $R_{DD}^{H_1H_2}$=21.0 kHz.

In spite of the good results for the adamantane sample, for other samples such as glycine the corresponding splittings were not observed.[4.7] The reason for that is probably the magnitude of the heteronuclear dipolar couplings. In adamantane it is scaled down due averaging effects caused by the rotation of the adamantane molecules in the crystal lattice [70]. In most crystaline samples rotational dynamics are not present. Hence, heteronuclear dipolar couplings are not

[4.7]For these samples cross polarisation was used to enhance the signal intensity.

fully averaged out by MAS and splittings are obscured. In order to improve the spectra higher MAS rates might increase the decoupling efficiency.

4.2.3. $\mathcal{R}$ Decoupled INEPT

Inspired by a paper on a solid state NMR version of the well-known INEPT polarisation transfer experiment using the eDUMBO homonuclear decoupling [4], the applicability of a $\mathcal{R}$ decoupled version of this experiment was implemented. Simulations and experiments on the spectrometer were performed.

The pulse sequences which were implemented, consisted of the basic or refocussed INEPT schemes (*Figure 1.38*), with a number, i, of full $\mathcal{R}$ sequences per delay $\frac{\tau}{2}$. One full $\mathcal{R}$ sequence is composed of $\frac{N}{2}$ $\mathcal{R}\mathcal{R}'$ blocks per n rotational periods (*i.e.* a full $\mathcal{R}$ sequence has a duration of $n \cdot \tau_{rot}$). The pulse sequences (in the simulations as well as experiments) were implemented in such a way that varying the parameter i adjusted the length of the delays $\frac{\tau}{2}$. Illustrations of these pulse sequences are shown in *Figure 4.38*.

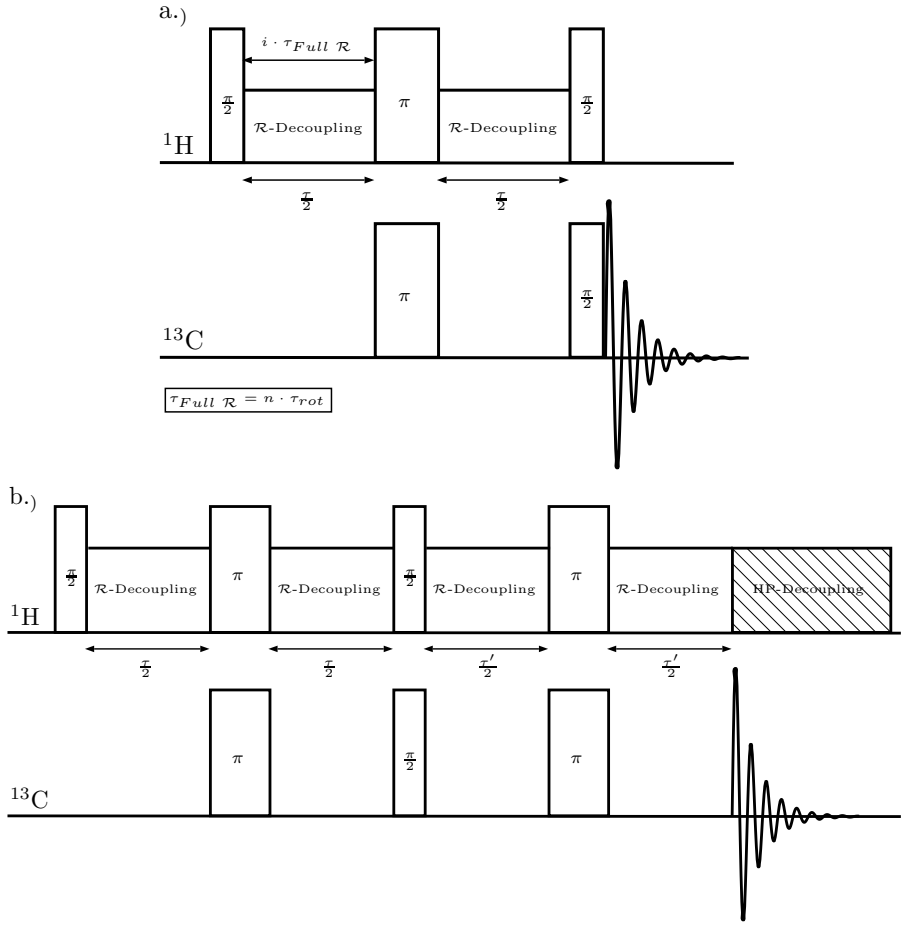

Figure 4.38.: Schematic representation of the $\mathcal{R}$ decoupled INEPT pulse sequences. a.) shows the basic version of the INEPT experiment and b.) the refocussed one, which allows for decoupling during acquisition. In both pulse sequences $\mathcal{R}$ decoupling is performed during the delay periods $\frac{\tau}{2}$ (and $\frac{\tau'}{2}$) via i full $\mathcal{R}$ sequences that consist of $\frac{N}{2}$ $\mathcal{R}\mathcal{R}'$ blocks per n rotational periods.

Simulations used the basic variant of the INEPT experiment (*Figure 4.38* a.)) as it was compu-

tationally faster than the refocussed one. Nevertheless, the refocussed variant (*Figure 4.38* b.)) was also simulated. The simulations were conducted with CH, CH_2 and CH_3 spin systems. Performance of the ^{1}H to ^{13}Cpolarisation trnasfer was assessed assuming the carbon atom to possess no polarisation at the start of the simulation. This allows to exclusively observe magnetisation that had been transferred from the H spins. Simulations with varying delays, τ, showed that the delay times under $\mathcal{R}$ decoupling needed to be much longer than $\tau = \frac{1}{2J_{CH}}$, which is the optimal value in liquid state NMR [5]. For example a CH coupling constant of $J_{CH} = 140\,Hz$ requires in liquid state NMR a total delay $\tau \approx 3.6$ ms to achieve maximal magnetisation transfer. Under $\mathcal{R}$ decoupling ($\mathcal{R}6_1^3$, 17.92 kHz MAS, spectral width: 20 kHz) the optimal length of the delay τ was found to be between 19.5 ms and 19.6 ms which is more than five times longer. This optimal delay was the same for CH, CH_2 and CH_3 spin systems with $J_{CH} = 140$ Hz. Remarkably, the optimal delay, τ, for the eDUMBO based experiment is also independent of the number of hydrogen atoms bonded to the carbon. Additionally, the optimal τ is longer with eDUMBO decoupling compared to the ideal (liquid) case, however, just about 1.6 times. [4] *Figure 4.39* shows the results for such a optimisation of τ, a mesh plot of all the simulations at different delays. The simulations were performed on a CH_2 spin system without dipolar couplings and two heteronuclear J-couplings of 140 Hz magnitude. As pulse sequence the basic INEPT was used, which is why an antiphase signal is observed. In further simulations it was found that the length of the delay strongly depended on the used symmetry as well as the MAS frequency. Both parameters have an impact on the pulse amplitudes.
When performing delay variation simulations with the refocussed INEPT pulse sequence it was found that the length of the refocussing delay, τ', was optimal when it was identical to the optimized one of the initial delay τ. This is in contrast to [4], where τ' is strongly dependent on the number of bonded hydrogens.

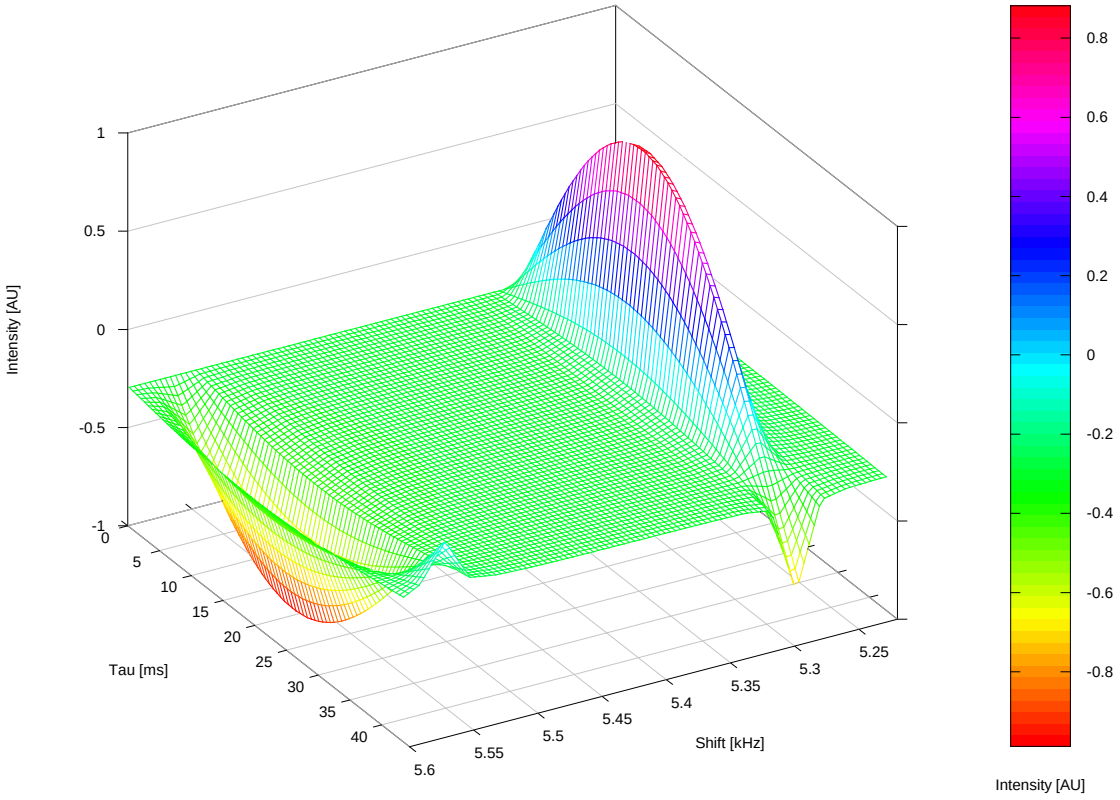

Figure 4.39.: Surface plot of simulated $\mathcal{R}$ decoupled INEPT spectra (17.92 kHz MAS, $\mathcal{R}6_1^3$, SW=20 kHz) of a CH_2 spin system (no dipolar couplings, $J_{CH} = 140\,Hz$, no magnetisation on carbon) with varying delays τ. The basic INEPT sequence was used. A maximum in signal intensity is reached at 19.5 ms, which is much longer than in liquid state NMR with a comparable J-coupling constant.

Spin System Details: *Nuclei:* $\delta_{\text{iso}}^{C_1}$=5.4 kHz, $\delta_{\text{ansio}}^{C_1}$=0.0 kHz, $\delta_{\text{iso}}^{H_1}$=11.9 kHz, $\delta_{\text{ansio}}^{H_1}$=0.0 kHz, $\delta_{\text{iso}}^{H_2}$=11.3 kHz, $\delta_{\text{ansio}}^{H_2}$=0.0 kHz. *J-couplings:* $J_{\text{iso}}^{C_1H_1}$=140 Hz, $J_{\text{aniso}}^{C_1H_1}$=0 Hz, $J_{\text{iso}}^{C_1H_2}$=140 Hz, $J_{\text{aniso}}^{C_1H_2}$=0 Hz.

Simulations assessing the actual decoupling efficiency of the pulse sequence were performed with the optimal τ values. Exemplary results can be seen in *Figure 4.40*. It was shown that the $\mathcal{R}$ decoupling itself does not disturb the INEPT transfer, because the spectrum with and without $\mathcal{R}$ decoupling are almost identical when no dipolar couplings are present. Further, decoupling of homonuclear dipolar couplings worked to some extent. Comparing the integrals of the decoupled spectra with homonuclear dipolar coupling it was found that in this particular case the integrals of the peaks with homonuclear dipolar coupling were 32.7% smaller. When now using heteronuclear dipolar couplings instead, the integrals become 86.2% smaller. This gets even worse when both heteronuclear and homonuclear dipolar couplings are simulated together. The peaks are even smaller and interestingly, their sign is switched. Hence, it can be concluded that the heteronuclear dipolar couplings were again not completely removed by MAS and interfered with the $\mathcal{R}$ decoupling. Nevertheless, some signal is preserved by the decoupling. Without any decoupling no signal was obtained at all, which can be seen in the last spectrum of the series.

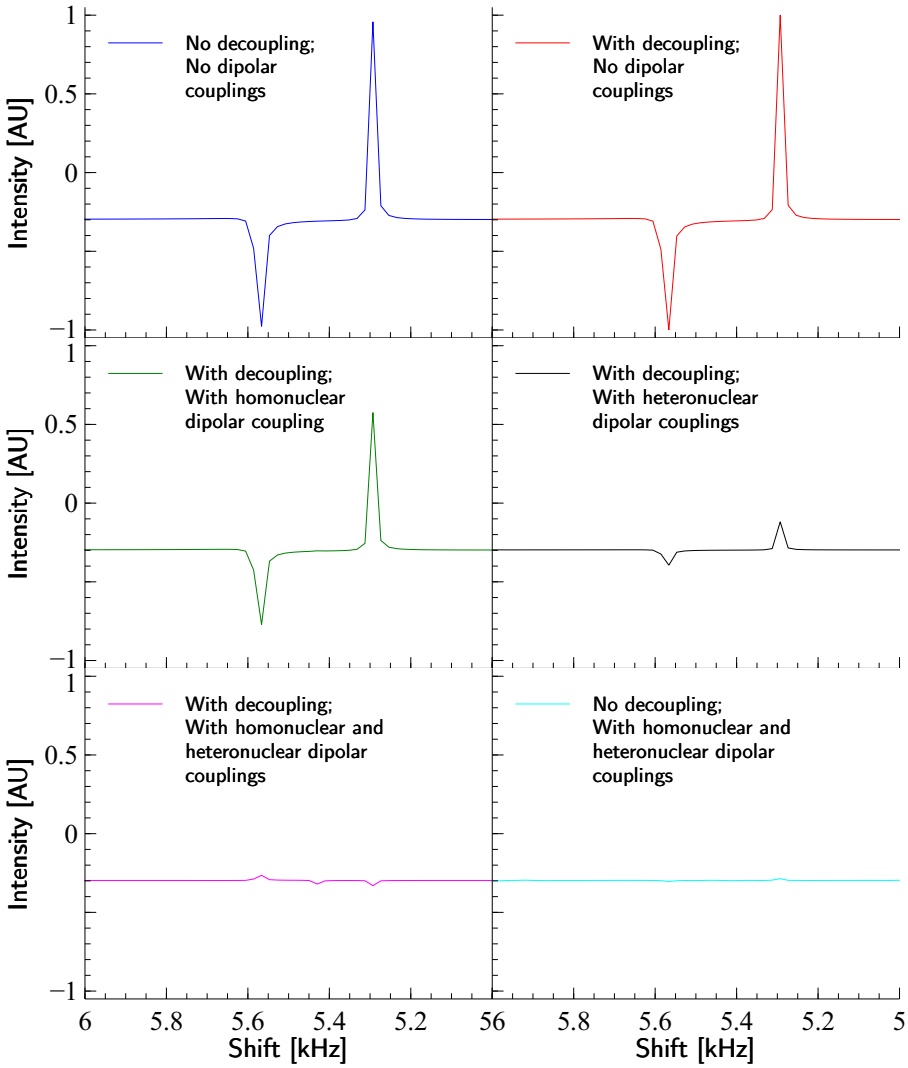

Figure 4.40.: Simulated INEPT spectra (17.92 kHz MAS, SW=20 kHz) of a CH_2 spin system ($J_{CH} = 140\,Hz$, no magnetisation on carbon) with the dipolar couplings set up in different ways. If decoupling was employed, it was done with the the $\mathcal{R}6_1^3$ symmetry. The spectra show that homonuclear dipolar couplings are decoupled efficiently, whereas heteronuclear ones are not. The spectra without decoupling are depicted for comparison.

Spin System Details: *Nuclei:* $\delta_{\text{iso}}^{C_1}$=5.4 kHz, $\delta_{\text{ansio}}^{C_1}$=0.0 kHz, $\delta_{\text{iso}}^{H_1}$=11.9 kHz, $\delta_{\text{ansio}}^{H_1}$=0.0 kHz, $\delta_{\text{iso}}^{H_2}$=11.3 kHz, $\delta_{\text{ansio}}^{H_2}$=0.0 kHz. *J-couplings:* $J_{\text{iso}}^{C_1H_1}$=140 Hz, $J_{\text{aniso}}^{C_1H_1}$=0 Hz, $J_{\text{iso}}^{C_1H_2}$=140 Hz, $J_{\text{aniso}}^{C_1H_2}$=0 Hz. *Dipolar couplings:* $R_{DD}^{C_1H_1}$=23.1 kHz, $R_{DD}^{C_1H_2}$=23.3 kHz, $R_{DD}^{H_1H_2}$=23.1 kHz. (The dipolar couplings were set up for the individual simulations as stated in the figures.)

In order to test the performance of the pulse sequence on the spectrometer and because it was shown to suppress homonuclear dipolar couplings, a real NMR experiment based on the mentioned simulations was implemented. For that, the refocussed INEPT pulse sequence was chosen because it allows for decoupling during acquisition. The experiments were carried out with an adamantane sample at the same spinning speed (17,92 kHz) and the value of τ =19.5 ms, which was optimal according to the simulations. The first spectra looked very promising (see *Figure 4.41 a.)*). Upon varying the delay τ (in concert with τ') it was found that in the experiments a value of 0.68 ms gave maximal signal intensity. This value is even lower than expected for a liquid state INEPT experiment. This probably shows the impact of relaxation,

which is not taken into account by the simulations.
These experiments, however, did not filter out the magnetisation initially coming from the ^{13}C spins. To find out how much magnetisation was actually transferred by the INEPT experiment the pulse sequence was slightly modified with a two step phase cycle, whereby the first proton pulse and the receiver phase were cycled in 180° steps. This results in a cancellation of the signal coming from thermal equilibrium carbon magnetisation, which is not cycled. *Figure 4.41 b.)* exhibits the resulting spectrum, which is basically just noise. This indicates that no magenetisation transferred from the proton spins to the carbon ones was detectable at the end of the INEPT pulse sequence. The most likely explaination is, that the magnetisation from the protons relaxed during the pulse sequence due to the much longer τ (compared to liquid state NMR) leading to the absence of signals. In the simulations this effect was not observed because relaxation is not treated explicitly by SIMPSON.
Due to time restrictions this issue was not investigated further. It would be, however, worth trying to tackle the problem because the simulations showed that the INEPT transfer under $\mathcal{R}$ decoupling is feasible. Maybe changing or omitting the refocussing delay might be a starting point for future improvements.

a.)

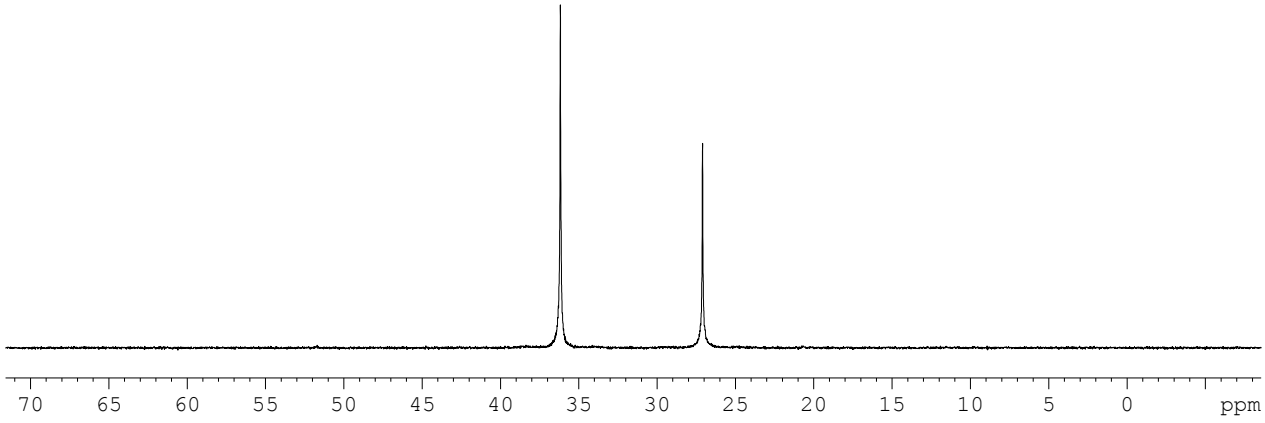

b.)

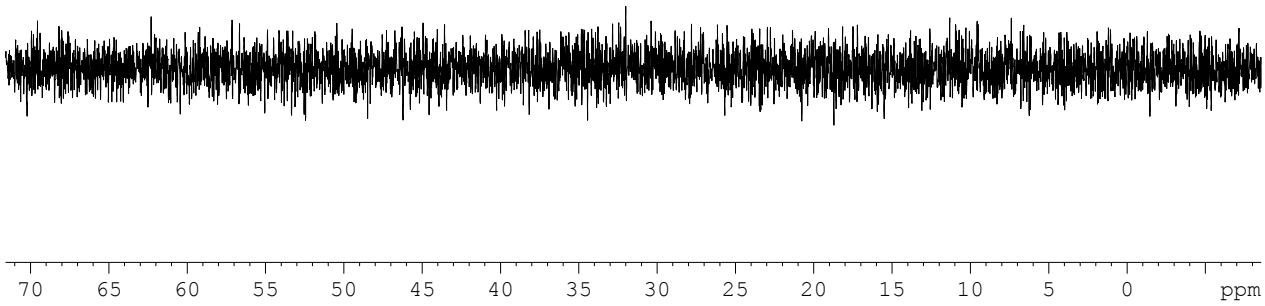

Figure 4.41.: Experimental spectra of adamantane recorded using the refocussed $\mathcal{R}$ decoupled INEPT sequence (17920 Hz MAS, $\mathcal{R}6_1^3$). a.) exhibits a spectrum with the delay τ set to 19.6 ms. It shows both characteristic adamantane peaks. In b.) a spectrum, which was recorded with a pulse sequence using a two step phase cycle to filter out signal coming from the initial polarisation of carbons. As this spectrum consists entirely of noise, it can be inferred that no magnetisation transferred from the protons is detectable.

5. Conclusions

5.1. Syntheis of fMLF

Summing up, a thorough examination of the possibilities of synthesizing fMLF, a chemotactic tripeptide used as reference substance in solid state NMR [1], via solid phase peptide synthesis was performed. Thereby special attention was turned to the requirements for using of isotopically labelled compounds, because the final product should be produced with ^{13}C and ^{15}N labelling.

First of all an efficient way to protect the *N*-termini of the needed amino acids (Phe, Leu and Met) with the Fmoc group was sought. The procedure described in [24, p.24-25] proved to be very useful for that task, giving very pure products in yields up to 95%.

With the amino acids protected the first attempt in synthesizing fMLF was undertaken according to the route described in [1]. It was found that the formylation step, which employed ethylformate, did not afford satisfying results. After testing the ethylformate approach several times in solution phase Route II was planned with the formylation reaction relying on the acetic formic anhydride approach. Although, abandoned at this point it still would be interesting to examine the ethylformate method. Ultrasonic sound irradiation or the basic conditions used for one of the solution phase test reactions (*Section 3.1.4.5*) may be promising starting points for further investigations.

After the test reactions for Route II had been successfully conducted, the actual sequence was carried out. On the resin the molecule was intact as indicated by the colour tests. After cleavage and subsequent treatments the formyl group, however, could not be detected. Hence, the group was reintroduced by formylation in solution giving some of the desired product. In a subsequent NMR study it was then shown that the TFA, used for the cleavage reaction, readily removes the formyl group.

As a result Route III and IV, which circumvent this issue by introducing the formyl group after cleavage in solution, were devised. These routes require Fmoc deprotection in solution and coupling reactions without *C*-terminal protection. To achieve the latter transformation the standard DCC/HOBt method [17] was successfully tested, albeit further investigations on the effectivity need to be done still. Moreover, an approach using benzotriazole derivatives of Fmoc-amino acids was tried [57]. This gave no useful product, however due to a mistake in conducting the reaction. Hence, repeating this reaction is necessary to assess the usefulness of this method.

The second transformation, the solution phase Fomc deprotection, initially gave promising results using the standard base mediated procedure [24, p.185-186] in an alternative solvent. Following experiments with protected peptides instead of single amino acids, however, were unsuccessful. Hence, for Route II and IV to be feasible, alternatives for the Fmoc deprotection have to be found. Promising candidates for that may be deprotection by TBAF or catalytic hydrogenation, as it is described in [26, p.23 (Note 3)].
One further topic, that was examined for Route III and IV, was the acetic formic anhydride mediated formylation reaction. It was optimised so that it did not require formic acid in large excess, which would be problematic in an a isotopically labelled synthesis. This was achieved by substiuting the excess of formic acid with acetic acid. For sterically unhindered compounds such as Gly-Gly the protocol needs further improvement to reduce acetylation. However, for Met, the amino acid that needs to be formylated for fMLF, it works already. Thereby just two equivalents of formic acid are consumed (instead of the 21 equivalents needed before).
Another option to avoid the destruction of the formyl group would be to alter the cleavage procedure. One approach would be using catalytic transfer hydrogenation with palladium acetate and ammoniumformate as it is described in [71]. The only flaw in this scheme is the presence of potentially catalyst poisoning methionine. Nevertheless, there are procedures, which use catalytic transfer hydrogenation, to remove protecting groups from Met containing peptides [23, 72, 73], which makes it an approach worth examining.
One last point for future synthesis investigations is the choice of the apparatus. Although the custom built apparatuses (*Section 3.1.3*) served their purpose, both had their drawbacks. Therefore it is recommended to use the conventional peptide synthesis vessels, whereby the Merrifield type glass reactors are probably to be more suitable for this task as it seems easier to work under fully inert conditions (necessary for avoiding oxidation of Met) with this kind apparatus. Moreover, these are reusable, which is more sustainable than syringe reactors.
In the end no synthesis with labelled compounds could be carried out. Nevertheless, the whole synthesis sequence was thoroughly examined and several issues were found and investigated. This lays the foundations for future work on establishing a highly efficient synthesis route for fMLF that can also be applied to reactions with isotopically labelled compounds.

5.2. $\mathcal{R}$ Decoupled Pulse Sequences

In short, pulse sequences that employ decoupling schemes based on the $\mathcal{R}$ symmetry, were implemented and examined using simulations as well as real world NMR experiments. Two of these sequences, namely the $\mathcal{R}$ decoupled proton and carbon experiments were already published in the literature [2, 3, 47]. Their function could be verified by simulations and experiments.
For the proton experiment this was done for a basic and an enhanced version of the pulse sequence. Both variants showed that the experiments are highly dependent on a optimal choice

of the transmitter offset. Another point is that the spectra were extremely influenced by processing parameters, especially window functions proved to be useful in getting clear spectra. Although these pulse sequences were shown to be functional, there is still much room for improvement, in order to make them experiments suitable for routine measurements. One step in this direction may be the proper implementation of the TPPI scheme, which was only preliminarily tested during this work. It would shift the central transmitter spike to the edge of the spectrum, probably making peaks better identifiable.

The carbon experiment was also found to be functional, however, just for samples such as adamantane, which exhibit extensive self decoupling due to rotation of the molecules in the crystal lattice. Interestingly, already a fairly low MAS frequency of 7 kHz allowed observation of the splittings caused by heteronuclear J-coupling. Also for this experiment a big dependence on the transmiter offset was observed.

With other samples such as glycine the heteronuclear J coupling was not observed. The reason for this are very large heteronuclear dipolar couplings (for glycine in the range of 20 kHz, as derived from the crystal structure), whose contributions to the signal have to be removed by MAS alone. To fully average out the contribution of an (anisotropic) interaction by MAS the spinning rate has to be about three times bigger than the interaction [40] (For the glycine example this would be at least 60 kHz, a speed in the range of modern MAS probes). In this work, however, speeds up to 20 kHz were possible, which is not enough to fully decouple the heteronuclear dipolar coupling of glycine. Hence, in order to record useful spectra for other samples than anamantane going to higher MAS rates or a means of heteronuclear dipolar decoupling via additional rf irradiation is necessary.

The third experiment under examination was a $\mathcal{R}$ decoupled INEPT experiment, similar to the one using eDUMBO decoupling described in [4]. The advantage of $\mathcal{R}$ decoupling compared to eDUMBO should be the easier set-up of the experiment as excessive optimisation procedures are not needed.

The experiment was initially designed using simulations based on the basic liquid state INEPT [5] pulse sequence. It was found that the actual INEPT transfer took place under $\mathcal{R}$ decoupling but compared with the liquid state with a slower transfer rate, which was dependent on the MAS frequency and the used symmetry. Further it was shown that homonuclear dipolar couplings were decoupled, whereas heteronuclear ones were not unless fast enough MAS was performed. This findings are similar to the ones for the previous carbon experiment.

Hence, adamantane was chosen for first experiments on the spectrometer. The initial experiments showed a typical adamantane peak pattern. Upon optimizing the delays crucial for the transfer a much shorter value than in the simulations was obtained, although the experimental set-up was almost the same.

Testing if the adamantane peaks arose from transferred proton magnetisation, using a two step phase cycle, gave a negative result. This means that the peaks were just observed due to magnetisation originating at the carbon atoms. The proton polarisation fully relaxed during

the pulse sequence affording no measurable signal.
Although it was shown that theoretically such an experiment is feasible, it is clear that further work is needed to be able to get useful spectra from it, which may be worth the effort as there are many useful pulse sequences based on the INEPT experiment.

Bibliography

[1] S. T. Breitung, J. J. Lopez, G. Dürner, C. Glaubitz, M. W. Göbel, M. Suhartono, "A practical synthesis of the $^{13}C/^{15}N$-labelled tripeptide N-Formyl-Met-Leu-Phe, useful as a reference in solid-state NMR spectroscopy", *Beilstein J. Org. Chem.* **2008**, *4*, DOI 10.3762/bjoc.4.35.

[2] S. Paul, R. S. Thakur, P. K. Madhu, "^{1}H homonuclear dipolar decoupling at high magic-angle spinning frequencies with rotor-synchronised symmetry sequences", *Chem. Phys. Lett.* **2008**, *456*, 253–256.

[3] S. Paul, R. S. Thakur, M. Levitt, P. Madhu, "^{1}H homonuclear dipolar decoupling using rotor-synchronised pulse sequences: Towards pure absorption phase spectra", *J. Magn. Reson.* **2010**, *205*, 269–275.

[4] B. Elena, A. Lesage, S. Steuernagel, A. Böckmann, L. Emsley, "Proton to Carbon-13 INEPT in solid-state NMR spectroscopy", *J. Am. Chem. Soc.* **2005**, *127*, 17296–17302.

[5] G. A. Morris, R. Freeman, "Enhancement of nuclear magnetic resonance signals by polarization transfer", *J. Am. Chem. Soc.* **1979**, *101*, 760–762.

[6] J. M. Berg, J. L. Tymoczko, L. Stryer, *Biochemistry*, W. H. Freeman, **2007**, 1120 pp.

[7] M. Bodanszky, *Principles of Peptide Synthesis*, Springer Berlin Heidelberg, Berlin, Heidelberg, **1993**.

[8] I. Ando, S. Kuroki, "Solid Biopolymers" in *eMagRes*, (Ed.: R. K. Harris), John Wiley & Sons, Ltd, Chichester, UK, **2007**.

[9] R. Hancock, M. Schaap, H. Pfister, G. Wells, "Peptide inhibitors of the Keap1-Nrf2 protein-protein interaction with improved binding and cellular activity", *Org. Biomol. Chem.* **2013**, *11*, 3553.

[10] L. Gentilucci, A. Tolomelli, F. Squassabia, "Peptides and Peptidomimetics in Medicine, Surgery and Biotechnology", *Curr. Med. Chem.* **2006**, *13*, 2449–2466.

[11] C. A. G. N. Montalbetti, V. Falque, "Amide bond formation and peptide coupling", *Tetrahedron* **2005**, *61*, 10827–10852.

[12] E. Fischer, "Synthese von Derivaten der Polypeptide", *Ber. Dtsch. Chem. Ges.* **1903**, *36*, 2094–2106.

[13] T. Curtius, "Synthetische Versuche mit Hippurazid", *Ber. Dtsch. Chem. Ges.* **July 1, 1902**, *35*, 3226–3228.

[14] *Hydrazine* in *GESTIS Substance database*, (Ed.: T. Smola), Institut für Arbeitsschutz der Deutschen Gesetzlichen Unfallversicherung, **Mar. 3, 2016**.

[15] M. M. Joullié, K. M. Lassen, "Evolution of amide bond formation", *Arkivoc.* **2010**, *8*, 189–250.

[16] A. El-Faham, F. Albericio, "Peptide Coupling Reagents, More than a Letter Soup", *Chem. Rev.* **2011**, *111*, 6557–6602.

[17] W. König, R. Geiger, "Eine neue Methode zur Synthese von Peptiden: Aktivierung der Carboxylgruppe mit Dicyclohexylcarbodiimid unter Zusatz von 1-Hydroxy-benzotriazolen", *Chem. Ber.* **1970**, *103*, 788–798.

[18] *Hexamethylphosphoric triamide* in *GESTIS Substance database*, (Ed.: T. Smola), Institut für Arbeitsschutz der Deutschen Gesetzlichen Unfallversicherung, **Apr. 2, 2016**.

[19] A. Abdelmajeid, S. Tala, M. Amine, A. Katritzky, "Tri-, Tetra- and Pentapeptidoylbenzotriazoles: Novel Synthetic Intermediates", *Synthesis* **2011**, *2011*, 2995–3005.

[20] A. R. Katritzky, P. Angrish, K. Suzuki, "The efficient preparation of di- and tripeptides by coupling *N*-(cbz- or Fmoc-α-aminoacyl) -benzotriazoles with unprotected amino acids", *Synthesis* **2006**, *2006*, 411–424.

[21] A. Isidro-Llobet, M. Álvarez, F. Albericio, "Amino Acid-Protecting Groups", *Chem. Rev.* **2009**, *109*, 2455–2504.

[22] R. P. Patel, S. Price, "Synthesis of Benzyl Esters of α-Amino Acids", *J. Org. Chem.* **1965**, *30*, 3575–3576.

[23] B. ElAmin, G. M. Anantharamaiah, G. P. Royer, G. E. Means, "Removal of benzyl-type protecting groups from peptides by catalytic transfer hydrogenation with formic acid", *J. Org. Chem.* **1979**, *44*, 3442–3444.

[24] M. Bodanszky, A. Bodanszky, *The practice of peptide synthesis*, Springer, Berlin ua, **1984**, xvii+284.

[25] G. B. Fields, R. L. Noble, "Solid phase peptide synthesis utilizing 9-fluorenylmethoxycarbonyl amino acids", *Int. J. Pept. Protein Res.* **1990**, *35*, 161–214.

[26] G. B. Fields, "Methods for removing the Fmoc group" in *Peptide Synthesis Protocols*, Springer, **1995**, pp. 17–27.

[27] J. C. Sheehan, D.-D. H. Yang, "The Use of N-Formylamino Acids in Peptide Synthesis", *J. Am. Chem. Soc.* **1957**, *80*, 1154–1158.

[28] R. B. Merrifield, "Solid phase peptide synthesis. I. The synthesis of a tetrapeptide", *J. Am. Chem. Soc.* **1963**, *85*, 2149–2154.

[29] P. H. Toy, Y. Lam, *Solid-Phase Organic Synthesis: Concepts, Strategies, and Applications*, 1st ed., John Wiley & Sons, Hoboken, New Jersey, **2012**, 636 pp.

[30] A. Ganesan, "Wang Resin" in *e-EROS*, John Wiley & Sons, Ltd, **2001**.

[31] B. Blankemeyer-Menge, M. Nimtz, R. Frank, "An efficient method for anchoring fmoc-anino acids to hydroxyl-functionalised solid supports", *Tetrahedron Lett.* **1990**, *31*, 1701–1704.

[32] K. Sandhya, B. Ravindranath, "A protocol for racemization-free loading of Fmoc-amino acids to Wang resin", *Tetrahedron Lett.* **2008**, *49*, 2435–2437.

[33] B. A. Burkett, R. C. D. Brown, M. M. Meloni, "A simple colorimetric test for the detection of polymer-supported tertiary alcohols", *Tetrahedron Lett.* **2001**, *42*, 5773–5775.

[34] W. Troll, R. K. Cannan, "A Modified Photometric Ninhydrin Method for the Analysis of Amino and Imino Acids", *J. Biol. Chem.* **1953**, *200*, 803–811.

[35] E. Kaiser, R. L. Colescott, C. D. Bossinger, P. I. Cook, "Color test for detection of free terminal amino groups in the solid-phase synthesis of peptides", *Anal. Biochem.* **1970**, *34*, 595–598.

[36] M. A. Panaro, V. Mitolo, "Cellular responses to FMLP challenging: a mini-review", *Immunopharmacol. Immunotoxicol.* **1999**, *21*, 397–419.

[37] K. H. Yang, H. Fang, J. S. Ye, J. Z. Gong, J. T. Wang, W. F. Xu, "The main functions and structural modifications of tripeptide N-formyl-methionyl-leucyl-phenylalanine (fMLP) as a chemotactic factor", *Pharmazie* **2008**, *63*, 779–783.

[38] W. A. Marasco, S. H. Phan, H. Krutzsch, H. J. Showell, D. E. Feltner, R. Nairn, E. L. Becker, P. A. Ward, "Purification and identification of formyl-methionyl-leucyl-phenylalanine as the major peptide neutrophil chemotactic factor produced by Escherichia coli.", *J. Biol. Chem.* **1984**, *259*, 5430–5439.

[39] S. Bréchard, C. Melchior, S. Plançon, V. Schenten, E. J. Tschirhart, "Store-operated Ca_2^+ channels formed by TRPC1, TRPC6 and Orai1 and non-store-operated channels formed by TRPC3 are involved in the regulation of NADPH oxidase in HL-60 granulocytes", *Cell Calcium* **2008**, *44*, 492–506.

[40] M. J. Duer, *Introduction to Solid-State NMR Spectroscopy*, Wiley, **2008**, 374 pp.

[41] R. E. Wasylishen, "Dipolar and Indirect Coupling: Basics" in *eMagRes*, (Eds.: R. K. Harris, R. Wasylishen), John Wiley & Sons, Ltd, Chichester, UK, **2009**.

[42] M. H. Levitt, "Symmetry-Based Pulse Sequences in Magic-Angle Spinning Solid-State NMR" in *eMagRes*, John Wiley & Sons, Ltd, **2007**.

[43] L. Euler, *Theoria motus corporum solidorum seu rigidorum ex primis nostrae cognitionis principiis stabilita et ad omnes motus qui in huiusmodi corpora cadere possunt accommodata*, A.F. Röse, Rostock and Greifswald, **1765**, 742 pp.

[44] E. Wigner, *Gruppentheorie und ihre Anwendung auf die Quantenmechanik der Atomspektren*, Vieweg + Teubner Verlag, Wiesbaden, **1931**.

[45] E. R. Andrew, "Magic Angle Spinning" in *eMagRes*, John Wiley & Sons, Ltd, **2007**.

[46] W. Magnus, "On the exponential solution of differential equations for a linear operator", *Communications on Pure and Applied Mathematics* **1954**, *7*, 649–673.

[47] P. K. Madhu, X. Zhao, M. H. Levitt, "High-resolution ^{1}H NMR in the solid state using symmetry-based pulse sequences", *Chem. Phys. Lett.* **2001**, *346*, 142–148.

[48] D. P. Burum, R. R. Ernst, "Net polarization transfer via a J-ordered state for signal enhancement of low-sensitivity nuclei", *J. Magn. Reson.* **1980**, *39*, 163–168.

[49] P. Friedrich, D. J. Darley, B. T. Golding, W. Buckel, "The Complete Stereochemistry of the Enzymatic Dehydration of 4-Hydroxybutyryl Coenzyme A to Crotonyl Coenzyme A", *Angew. Chem. Int. Ed.* **2008**, *47*, 3254–3257.

[50] G. R. Fulmer, A. J. M. Miller, N. H. Sherden, H. E. Gottlieb, A. Nudelman, B. M. Stoltz, J. E. Bercaw, K. I. Goldberg, "NMR Chemical Shifts of Trace Impurities: Common Laboratory Solvents, Organics, and Gases in Deuterated Solvents Relevant to the Organometallic Chemist", *Organometallics* **2010**, *29*, 2176–2179.

[51] Curly Arrow: Let's talk about TLCs Part 4 - Ninhydrin Stain, `http://curlyarrow.blogspot.com/2008/08/lets-talk-about-tlcs-part-4-ninhydrin.html` (visited on 04/26/2016).

[52] M. B. Gawande, P. S. Branco, "An efficient and expeditious Fmoc protection of amines and amino acids in aqueous media", *Green Chem.* **2011**, *13*, 3355.

[53] M. Nardi, N. H. Cano, P. Costanzo, M. Oliverio, G. Sindona, A. Procopio, "Aqueous MW eco-friendly protocol for amino group protection", *RSC Advances* **2015**, *5*, 18751–18760.

[54] I. Menzl, "Präparative RP-HPLC von Oligo-Peptiden", Bachelor Thesis, Johannes Kepler Universität, Linz, **2009**, 31 pp.

[55] I. Muramatsu, M. Murakami, T. Yoneda, A. Hagitani, "The Formylation of Amino Acids with Acetic Formic Anhydride", *Bull. Chem. Soc. Jpn.* **1965**, *38*, 244–246.

[56] K. Alfonsi, J. Colberg, P. J. Dunn, T. Fevig, S. Jennings, T. A. Johnson, H. P. Kleine, C. Knight, M. A. Nagy, D. A. Perry, M. Stefaniak, "Green chemistry tools to influence a medicinal chemistry and research chemistry based organisation", *Green Chem.* **2008**, *10*, 31–36.

[57] A. R. Katritzky, P. Angrish, D. HüR, K. Suzuki, "N-(Cbz- and Fmoc-α-aminoacyl)-benzotriazoles: Stable derivatives enabling peptide coupling of Tyr, Trp, Cys, Met, and Gln with free amino acids in aqueous media with complete retention of chirality", *Synthesis* **2005**, *2005*, 397–402.

[58] B. Kantharaju, V. Babu, "Ultrasound accelerated synthesis of proteinogenic and α, α-dialkylamino acid ester salts", *Indian J. Chem.* **2006**, *45*, 1942–1944.

[59] M. Bak, J. T. Rasmussen, N. C. Nielsen, "SIMPSON: A General Simulation Program for Solid-State NMR Spectroscopy", *Journal of Magnetic Resonance* **2000**, *147*, 296–330.

[60] M. Bak, R. Schultz, T. Vosegaard, N. C. Nielsen, "Specification and Visualization of Anisotropic Interaction Tensors in Polypeptides and Numerical Simulations in Biological Solid-State NMR", *J. Magn. Reson.* **2002**, *154*, 28–45.

[61] K. Srinivasan, "Crystal growth of α and γ glycine polymorphs and their polymorphic phase transformations", *J. Cryst. Growth* **2008**, *311*, 156–162.

[62] M. E. Peter, P. Ramasamy, "Growth of gamma glycine crystal and its characterisation", *Spectrochim. Acta Part A* **2010**, *75*, 1417–1421.

[63] H. Foerster, J. Struppe, S. Steuernagel, F. Aussenacc, F. Benevelli, P. Gierth, S. Wegner, Solid State NMR - AVANCE Solids User Manual, English, version 002, Rheinstetten, Germany, **2009**, p. 328.

[64] *Glycine (SDBS No.: 2482)* in *SDBS - Spectral Database for Organic Compounds*, (Ed.: H. Watanabe), National Institute of Advanced Industrial Science and Technology (AIST), Japan, **Aug. 14, 2015**.

[65] *Glycylglycine (SDBS No.: 1205)* in *SDBS - Spectral Database for Organic Compounds*, (Ed.: H. Watanabe), National Institute of Advanced Industrial Science and Technology (AIST), Japan, **Aug. 14, 2015**.

[66] Y. Nozaki, C. Tanford, "The solubility of amino acids and two glycine peptides in aqueous ethanol and dioxane solutions establishment of a hydrophobicity scale", *Journal of Biological Chemistry* **1971**, *246*, 2211–2217.

[67] M. S. Dunn, F. J. Ross, "Quantitative investigations of amino acids and peptides IV. The solubilities of the amino acids in water-ethyl alcohol mixtures", *Journal of Biological Chemistry* **1938**, *125*, 309–332.

[68] F.-X. Schmid, "Biological Macromolecules: UV-visible Spectrophotometry" in *eLS - Encyclopedia of Life Sciences*, John Wiley & Sons, Ltd, Chichester, UK, **2001**.

[69] P. P. Man, dumbod2: High power homonuclear dipole-dipole windowed-dumbo decoupling pulse program, **Sept. 9, 2015**, `http://www.pascal-man.com/pulseprogram/avance3/dumbod2-topspin.shtml` (visited on 09/09/2015).

[70] M. Ernst, A. Verhoeven, B. H. Meier, "High-Speed Magic-Angle Spinning ^{13}C MAS NMR Spectra of Adamantane: Self-Decoupling of the Heteronuclear Scalar Interaction and Proton Spin Diffusion", *J. Magn. Reson.* **1998**, *130*, 176–185.

[71] M. K. Anwer, A. F. Spatola, "A rapid non-acidolytic method for deprotection and removal of peptides from solid phase resins-applications of ammonium formate catalytic transfer hydrogenation", *Tetrahedron Lett.* **1981**, *22*, 4369–4372.

[72] Y. Okada, N. Ohta, "Amino Acids and Peptides. VII. Synthesis of Methionine-Enkephalin using Transfer Hydrogenation", *Chem. Pharm. Bull. (Tokyo)* **1982**, *30*, 581–585.

[73] K. M. Sivanandaiah, G. Sivashankarappa, "Catalytic Transfer Hydrogenation of Protected Peptides at Room temperature", *J. Chem. Research (S)* **1979**, 108–109.

List of Figures

List of Tables

Appendix

A. Detailed Experimental Procedures of Reactions with Unsatisfactory Results

A.1. Fmoc Protections in Ethanol/Water

Prot - I: Synthesis of Fmoc-Phe *According to [52].* To the mixture of Fmoc-chloride (0.290 g, 1.1 mmol) and phenylalanine (0.166 g, 1 mmol) a mixture of ethanol and water (EtOH:H_2O =1:3) was added (1.5 mL). This reaction suspension was heated with an oil bath to 60°C under stirring. The reaction was monitored with TLC (mobile phase EtOAc:heptanes=1:4). After 2.5 days of stirring at this temperature under N_2 atmosphere, the reaction mixture was cooled on an ice/water bath. As its pH was already acidic, the reaction solution was immediately extracted three times with 10 mL ethylacetate. Thereby, a saturated salt solution was used to aid phase separation. The organic phase was dried over Na_2SO_4 and evaporated *in vacuo* at 60°C. The crude product was analysed with NMR (solvent: deuterated methanol). Further purification was done by normal phase column chromatography. The mobile phase was initially EtOAc:heptanes=1:6, which was changed firstly to EtOAc:heptanes=1:3 and finally to 10% vol. methanol in ethylacetate. The evaporated fractions too were analysed by NMR (solvent: deuterated methanol and $CDCl_3$). The desired product could not be identified.

Prot - II: Synthesis of Fmoc-Leu *According to [52].* This reaction was performed in the same way as *Prot - I*, with leucine (0.131 g, 1 mmol) instead of phenylalanine. The amount of Fmoc-Cl was 0.285 g (1.1 mmol). The reaction was stirred just for 22 hours. Also column chromatography was performed. For packing the column and the first fractions, the same mobile phase (EtOAc:heptanes=1:6) was used. For the rest of the run 15% vol. methanol were added to this mobile phase. For the final fractions EtOAc:MeOH=1:1 was used. The NMR solvent to analyse the fractions was deuterated acetone. The desired product could not be identified.

Prot - III: Synthesis of Fmoc-Met *According to [52].* The reaction again was performed similarly to *Prot - I*, however with slight variations. Firstly, the methionine (0.155 g, 1 mmol) was dissolved in 2.5 mL of the water/ethanol mixture and under stirring heated to 60°C before the addition of Fmoc-Cl (0.289 g, 1.1 mmol). Secondly, the reaction mixture was heated and

stirred for four days. Rotary evaporation of the reaction mixture was performed at 40°C. The crude product was analysed with NMR (solvent: deuterated DMSO) and MS (solvent: methanol). No column chromatography was performed.

Yield	
Fmoc-Met (Prot - III)	*Only detectable in traces by MS*

Characterisation - Fmoc-Met (Prot - III)

Appearance: yellowish solid

MS (ESI, positive ion mode, qTOF, m/z): 150.0582 ($C_5H_{12}NO_2S^+$, Met), 178.0897 ($C_7H_{16}NO_2S^+$, Met-OEt), 286.1439 ($C_{17}H_{16}O_3NH_4^+$, Fmoc-OEt), 372.1265 ($C_{20}H_{22}NO_4S^+$, Fmoc-Met), 400.1578 ($C_{22}H_{26}NO_4S^+$, Fmoc-Met-OEt), 422.1395 ($C_{22}H_{25}NO_4SNa^+$, Fmoc-Met-OEt)

A.2. Microwave assisted Fmoc Protections

Prot - IV: Synthesis of Fmoc-Phe, Microwave assisted *According to [53].* Fmoc-Cl (0.568 g, 2.2 mmol) was added to 2 mL H_2O under stirring. Next, phenylalnine (0.334 g, 2 mL) was added. A TLC for reaction monitoring was done (mobile phase: EtOAc:heptanes=1:4), whereby detection was done with an UV lamp and the Ninhydrin stain. The suspension was irradiated with microwaves (600 Watt) for five minutes. After a further reaction TLC, one more mL was introduced and irradiation at 600 Watt was continued for 30 seconds. After a final TLC the product was dried and analysed with NMR (solvent: deuterated acetone) and MS (solvent: methanol).

Yield	
Fmoc-Phe (Prot - IV)	*Only detectable in traces by MS as methyl ester*

Characterisation - Fmoc-Phe (Prot - IV)

Appearance: light brown solid

MS (ESI, positive ion mode, qTOF, m/z): 166.0862 ($C_9H_{12}NO_2^+$, Phe), 180.1019 ($C_{10}H_{14}NO_2^+$, Phe-OMe), 402.1700 ($C_{25}H_{24}NO_4^+$, Fmoc-Phe-OMe), 424.1516 ($C_{25}H_{23}NO_4Na^+$, Fmoc-Phe-OMe), 549.2379 ($C_{34}H_{33}N_2O_5^+$, Fmoc-Phe-Phe-OMe)

Prot - V: Synthesis of Fmoc-Leu, Microwave assisted *According to [53].* Generally, this experiment was performed similarly to *Prot - IV*. Fmoc-Cl (0.289 g, 1.1 mmol) was stirred in 1 mL H_2O together with leucine (0.134 g, 1 mmol) in order to homogenize the substances. Then the suspension was irradiated with microwaves under stirring for 5 minutes. The reaction was monitored with TLC (see *Prot - IV*). The resulting crude product was thoroughly washed with water and dried. It was examined with NMR (solvent: deuterated acetone) and MS (solvent: methanol).

Yield	
Fmoc-Leu (Prot - V)	*Only detectable in traces by MS as methyl ester*

Characterisation - Fmoc-Leu (Prot - V)

Appearance: brownish solid

MS (ESI, positive ion mode, qTOF, m/z): 132.1021 ($C_6H_{14}NO_2^+$, Leu), 146.1176 ($C_7H_{16}NO_2^+$, Leu-OMe), 272.1281 ($C_{16}H_{14}O_3NH_4^+$, Fmoc-OMe), 368.1866 ($C_{22}H_{26}NO_4^+$, Fomc-Leu-OMe), 390.1682 ($C_{22}H_{25}NO_4Na^+$, Fomc-Leu-OMe), 481.2697 ($C_{28}H_{37}N_2O_5^+$, Fomc-Leu-Leu-OMe)

A.3. Formylation: Test Reactions

R_{II} - I, II and III: Test Reactions - Formylation of Met using Ethylformate *On the basis of the formylation reaction described in [1].*

R_{II} - I Methionine (0.149 g, 1.0 mmol) was treated with 2 mL of ethylformate. Under stirring, formic acid was dropped in until all Met dissolved completely (1 mL). The mixture was stirred at room temperature under N_2(g) over night. After that the solvents were evaporated *in vacuo* at 40°C. The residue was examined by NMR (solvent: deuterated acetone).

R_{II} - II 2 mL of ethylformate were heated to 50°C. Under stirring, Met (0.150 g, 1.0 mmol) was added. Next, the Met was dissolved by the addition of formic acid (0.5 mL). The mixture was stirred over night at 50°C. Subsequently, the liquids were evaporated *in vacuo* (40°C) and the remaining solid was analysed by NMR (solvent: deuterated acetone).

R_{II} - III 0.149 g Met (1.0 mmol) were treated with 2 mL of ethylformate and stirred at r.t. under N_2(g) for two days. The ethylformiate was evaporated *in vacuo* at r.t. and the residue examined by NMR in D_2O.

Yield	
R_{II} - I, II and III	*None of the reactions afforded useful amounts of product*

$R_{III\,IV}$ - IV Formylation of Met in One Equivalent of Formic acid *Based on [27].* Methionine (0.149 g, 1.0 mmol) was treated first with formic acid (38 µL, 1.01 mmol) and acetic anhydride (94 µL, 0.99 mmol) on an ice/water bath. After keeping the mixture at 0°C for 10 minutes, stirring was continued at room temperature. In order to enhance stirring 0.2 mL of acetic acid were added after ten minutes at r.t. (this was initially not intended). After stirring for one hour, 0.5 mL of ice cooled water were introduced. Subsequently the solvents were evaporated at 30°C *in vacuo*, dried and inspected by NMR in D_2O. No useful amount of product was obtained.

(For a reaction scheme see *R_{II} - V, VI and VII*)

A.4. Solution Phase Peptide Synthesis Reactions

Sol - III: Coupling of Phe-OBz with Fmoc-Leu Followed by Deprotection *According to [24, p.145;185-186] and [56].* Phe-OBz (0.148 g, 0.51 mmol), Fmoc-Leu(0.193 g, 0.55 mmol) and HOBt (0,067 g, 0.50 mmol) were suspended in 0.7 mL dry THF under N_2. Eventually, 62.5 µL *N*-ethylmorpholine (0.50 mmol) were added. The mixture was cooled to 0°C and DCC (0.109 g, 0.53 mmol) was added portion-wise under stirring. Residual DCC was washed into the mixture with 0.1 mL THF. The reaction is stirred for one hour at 0°C and 1.5 hours at room temperature. Subsequently the DCU is filtered off. For this purpose, further 6.2 mL of THF were used. The solvent was then removed under reduced pressure at 30°C. The residue was then dissolved in 5 mL of ethylacetate and 2.5 mL of saturated aqueous $NaHCO_3$ solution. The phases were separated and the organic layer was washed with 10% citric acid in water (1.25 mL) and with $NaHCO_3$ solution (1.25 mL). The combined aqueous layers were reextracted with 2 mL ethylacetate. The joined organic layers were dried over Na_2SO_4 and evaporated at 30°C *in vacuo*. The dried residue is examined by NMR in deuterated methanol.

For deprotection, the residue was dissolved in 10 mL of acetonitrile and treated at room temperature under nitrogen with 1 mL of diethylamine. The mixture was stirred for 1.5 hours and the solvents were evaporated subsequently at 30°C under vacuum. The residue was triturated with 12.5 mL of diethylether and washed two times with 10 mL of diethylether. The ether phase was evaporated. Both fractions, the precipitate and the evaporated ether phase were examined by NMR in deuterated methanol or DMSO.
No product could be isolated.

B. Pulse Programs

B.1. $\mathcal{R}$-decoupled ^{1}H Experiment - Basic Version

```
1  ;RtypeHomoDecSolid
2  ;Matthias Guggenberger
3  ;$COMMENT=Homonuclear Decoupling 1H experiment for Solids (MAS). Based on R type
       symmetry
4  ;$CLASS=Solid
5  ;$TYPE=R-Symetry
6  ;$SUBTYPE=Homonuclear decoupling
7  ;$DIM=2D
8
9  define loopcounter count
10 "count=td1"
11
12 define delay dwellf1
13
14 "p1=(cnst11/cnst12)*(1.0s/cnst31)/3.0"
```

```
"inf1=p1*6"
"dwellf1=inf1"
"cnst18= 1000000/(2*inf1)"
1 ze
2 d1

;R block
3 p1 ph11
  p1 ph12
  p1 ph13

;R' block
  p1 ph21
  p1 ph22
  p1 ph23
lo to 3 times l0

;detection pulse
  p1 ph25

;acquisition
  go=2  ph31    ;acquire
  1m
  100m wr #0 if #0 zd
  1m iu0
  lo to 2 times count
HaltAcqu, 1m    ;jump address for protection files

exit

ph11=  (360) 45
ph12= (360) 135
ph13= (360) 45

ph21= (360) -45
ph22= (360) -135
ph23= (360) -45

ph25= (360) 0 90 180 270
ph31= (360) 90 180 270 0

;cnst11: R-Symmetry parameter n
;cnst12: R-Symmetry parameter N
;cnst13: R-Symmetry parameter ny
;inf1: dwelltime t1 dim.
;cnst18: SW t1 dim.
;cnst31: Spinning Speed
```

```
62
63 ;d1: recycle delay
64 ;p1: length of 90 degree pulse corresponding to the chosen symmetry
65 ;l0: loop counter that goes for the indirect dimension
66 ;iu0: increments l0 till td1
67
68 ;ph11: Pulse phase of the first pulse in the R block
69 ;ph12: Pulse phase of the second pulse in the R block
70 ;ph13: Pulse phase of the third pulse in the R block
71
72 ;ph21: Pulse phase of the first pulse in the R' block
73 ;ph22: Pulse phase of the second pulse in the R' block
74 ;ph23: Pulse phase of the third pulse in the R' block
75
76 ;ph25: Phase cycle of the detection pulse
77 ;ph31: Phase cycle of the receiever
```

B.2. $\mathcal{R}$-decoupled ^{1}H Experiment - Improved Version

```
1  ;RtypeHomoDecSolid
2  ;Matthias Guggenberger
3  ;$COMMENT=Homonuclear Decoupling 1H experiment for Solids (MAS). based on R type
       symmetry Improved by several pulses.
4  ;$CLASS=Solid
5  ;$TYPE=R-Symetry
6  ;$SUBTYPE=Homonuclear decoupling
7  ;$DIM=2D
8
9  define loopcounter count
10 "count=td1"
11
12 define delay dwellf1
13
14 "p1=(cnst11/cnst12)*(1.0s/cnst31)/3.0" ;
15 "inf1=p1*6"
16 "dwellf1=inf1"
17 "cnst18= 1000000/(2*inf1)"
18 1 ze
19 2 d1
20
21   ; pulse sandwiching the r blocks
22   p1 ph1
23
24 ;R block
25 3 p1 ph11
26   p1 ph12
27   p1 ph13
28
```

```
;R' block
  p1 ph21
  p1 ph22
  p1 ph23

lo to 3 times l0

  ;pulse finishing the sandwich
  p1 ph2

;pre detection pulse
  p1 ph3
;detection pulse
  p1 ph25

;acquisition
  go=2  ph31
  1m
  100m wr #0 if #0 zd
  1m iu0
  lo to 2 times count
HaltAcqu, 1m            ;jump address for protection files

exit

ph1=  (360) 0
ph2=  (360) 270
ph3=  (360) 180

ph11=  (360) 45 135 225 315
ph12= (360) 135 225 315 45
ph13= (360) 45 135 225 315

ph21= (360) -45 45 135 225
ph22= (360) -135 -45 45 135
ph23= (360) -45 45 135 225

ph25= (360) 0 90 180 270
ph31= (360) 90 180 270 0


;cnst11: R-Symmetry parameter n
;cnst12: R-Symmetry parameter N
;cnst13: R-Symmetry parameter ny
;inf1: dwelltime t1 dim.
;cnst18: SW t1 dim.
;cnst31: Spinning Speed
```

```
76
77 ;d1: recycle delay
78 ;p1: length of 90 degree pulse corresponding to the chosen symmetry
79 ;l0: loop counter that goes for the indirect dimension
80 ;iu0: increments l0 till td1
81
82 ;ph1: Phase of first sandwich pulse
83 ;ph2: Phase of second sandwich pulse
84 ;ph3: Pulse of the pre-detection pulse
85
86 ;ph11: Pulse phase of the first pulse in the R block
87 ;ph12: Pulse phase of the second pulse in the R block
88 ;ph13: Pulse phase of the third pulse in the R block
89
90 ;ph21: Pulse phase of the first pulse in the R' block
91 ;ph22: Pulse phase of the second pulse in the R' block
92 ;ph23: Pulse phase of the third pulse in the R' block
93
94 ;ph25: Phase cycle of the detection pulse
95 ;ph31: Phase cycle of the receiever
```

B.3. $\mathcal{R}$-decoupled ^{13}C Experiment - cpd-Program

```
1  ;$OWNER=GUGGENBERGER
2  ;RType Decoupling sequence for Solid State MAS NMR
3
4   0.3u fq=cnst21
5   0.5u pl=pl12
6  ;the length has to be calculated and the power level has to be derived from a
       normal 1h reference pulse
7
8  ;R
9  1 pcpd:45
10   pcpd:135
11   pcpd:45
12 ;R'
13   pcpd:-45
14   pcpd:-135
15   pcpd:-45
16 jump to 1
```

B.4. $\mathcal{R}$-decoupled INEPT Experiment

```
1 ;RTypeINEPT
2 ;Matthias Guggenberger
3 ;$COMMENT=Homonuclear Decoupling INEPT experiment for Solids (MAS). based on R
      type symmetry
4 ;$CLASS=Solid
```

```
;$TYPE=R-Symetry
;$SUBTYPE=Homonuclear Decoupling
;$DIM=1D
;f2 1H channel
;f1 13C/X Channel


"cnst30=1.0s/cnst31"
"p1= (1.0s*cnst30*(cnst11/cnst12))/ cnst14"
"p2=(1.0s*cnst30*(cnst11/cnst12))/ cnst14"
"p11= p1*2"
"p22= p2*2"
"cnst25= cnst17*cnst12/2.0"
"cnst26=cnst18*cnst12/2.0"

"cnst22 = 2.0*(6.0*p1*(cnst12/2))*cnst17+p11"
"cnst23 = 2.0*(6.0*p1*(cnst12/2))*cnst18+p11"

define loopcounter loop1
"loop1 = cnst25"
define loopcounter loop2
"loop2 = cnst26"

1 ze
1u pl1:f1
1u pl2:f2
2 d1 do:f2

        ;first INEPT pulse
        (p2 ph25):f2

                        ;delay tau with R decoupling
                          ;R block
                  3 (p2 ph11):f2
                          (p2 ph12):f2
                          (p2 ph13):f2

                          ;R' block
                          (p2 ph21):f2
                          (p2 ph22):f2
                          (p2 ph23):f2
                   lo to 3 times loop1


        ;Second Inept pulses
        (p22 ph26):f2 (p11 ph27):f1

```

```
                        ;delay tau with R decoupling
                          ;R block
                  4 (p2 ph11):f2
                          (p2 ph12):f2
                          (p2 ph13):f2

                          ;R' block
                          (p2 ph21):f2
                          (p2 ph22):f2
                          (p2 ph23):f2
                   lo to 4 times loop1

       ;final INEPT pulses
       (p2 ph28):f2 (p1 ph29):f1

;now refocussing part in order to be able to doi a hp decoupling

                        ;delay tau1 with R decoupling
                          ;R block
                  5 (p2 ph11):f2
                          (p2 ph12):f2
                          (p2 ph13):f2

                          ;R' block
                          (p2 ph21):f2
                          (p2 ph22):f2
                          (p2 ph23):f2
                   lo to 5 times loop2

       ;Further INEPT refocussing pulses
       (p22 ph26):f2 (p11 ph27):f1

                        ;delay tau1 with R decoupling
                          ;R block
                  6 (p2 ph11):f2
                          (p2 ph12):f2
                          (p2 ph13):f2

                          ;R' block
                          (p2 ph21):f2
                          (p2 ph22):f2
                          (p2 ph23):f2
                   lo to 6 times loop2


         ;acquisition at 13C channel with total decoupling(=DDC as well as J)
            in the style of hpdec, using a cpd program
```

```
          (1u cpds2):f2
          go=2 ph31
          1m do:f2
          wr #0
          HaltAcqu, 1m
exit

ph11= (360) 45
ph12= (360) 135
ph13= (360) 45

ph21= (360) -45
ph22= (360) -135
ph23= (360) -45

ph25= (360) 0
ph26= (360) 0
ph27= (360) 0
ph28= (360) 90
ph29= (360) 90

ph31= (360) 90

;cnst11: R-Symmetry parameter n
;cnst12: R-Symmetry parameter N
;cnst13: R-Symmetry parameter ny
;cnst14: Number of pulses in one R (R OR R') block
;cnst15: Repetitions of the R-sequence per Delay
;cnst16: Estimated JCH
;cnst17: parameter i which denotes the number of repetitions of the R sequence
;cnst18: parameter i_ref which denotes the number of repititions of the R
   sequence the refocussing period
;cnst22: Length of full INEPT delay (between the two 90 degree pulses)
;cnst23: length of the full refocussing delay (between the last 90 degree pulse
   and acquuisition
;cnst25: Number of RR' blocks of each of  the first two delay periods
;cnst26: Number of RR' blocks of each of the second two refocussing  delay
   periods
;cnst30: rotational period
;cnst31: Spinning Speed

;loop1: loopcounter for the first two delay periods
;loop2: loopcounter for the second two delay periods (refocussing)

;d1: recycle delay
;p1: pulselength of a 90 Degree pulse corresponding to the symmetry for the 13C
   channel
```

```
;p11: pulselength of a 180 Degree pulse corresponding to the symmetry for the 13
    C channel
;p2: pulselength of a 90 Degree pulse corresponding to the symmetry for the 1H
    channel
;p22: pulselength of a 180 Degree pulse corresponding to the symmetry for the 1H
     channel
;pl1: power level of f1 channel (13C/X)
;pl2: power level of f2 channel (1H)

;ph11: Pulse phase of the first pulse in the R block
;ph12: Pulse phase of the second pulse in the R block
;ph13: Pulse phase of the third pulse in the R block

;ph21: Pulse phase of the first pulse in the R' block
;ph22: Pulse phase of the second pulse in the R' block
;ph23: Pulse phase of the third pulse in the R' block

;ph25: Pulse phase of the first 1H pulse (90 degrees)
;ph26: Pulse phase of the second 1H pulse (180 degrees)
;ph27: Pulse phase of the first 13C pulse (180 degrees)
;ph28: Pulse phase of the third 1H pulse (90 degrees)
;ph29: Pulse phase of the second 13C pulse (90 degrees)

;ph31: Receiver Phase
```

C. Additional Spectra

C.1. Organic Synthesis

C.1.1. R_I - V: MLP

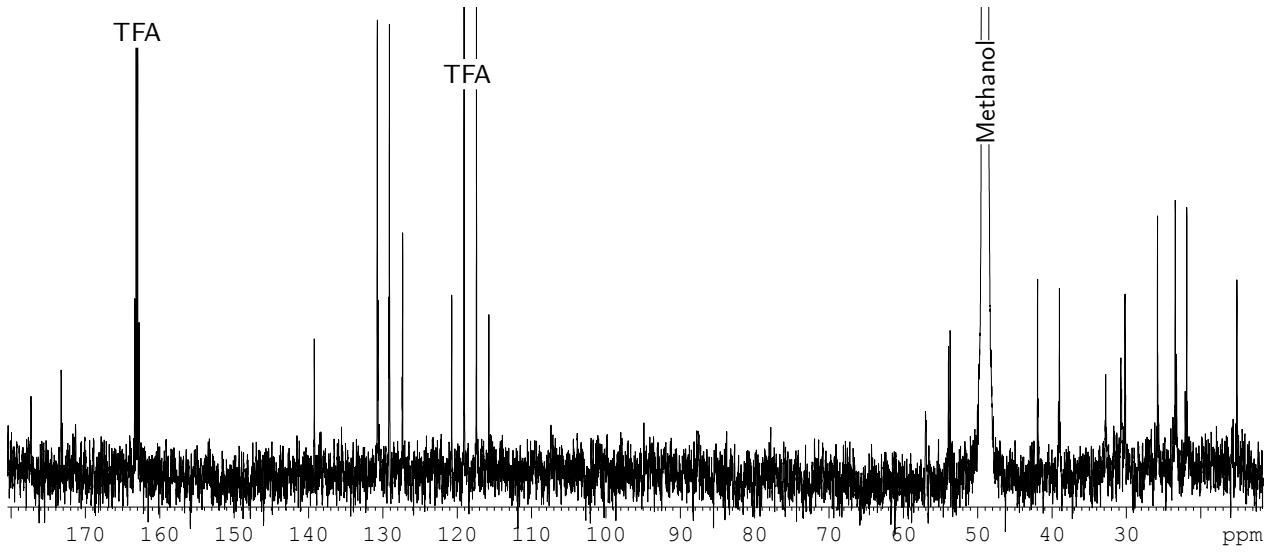

Figure C.1.: 176 MHz ^{13}C NMR spectrum of Met-Leu-Phe, the final product of Route I. The quartets at 136.1 ppm and 118.2 ppm and belong to TFA impurities. (Solvent: Methanol-d_4)

C.1.2. R_{II} - VIII: formyl-Met-Phe-OCH_3

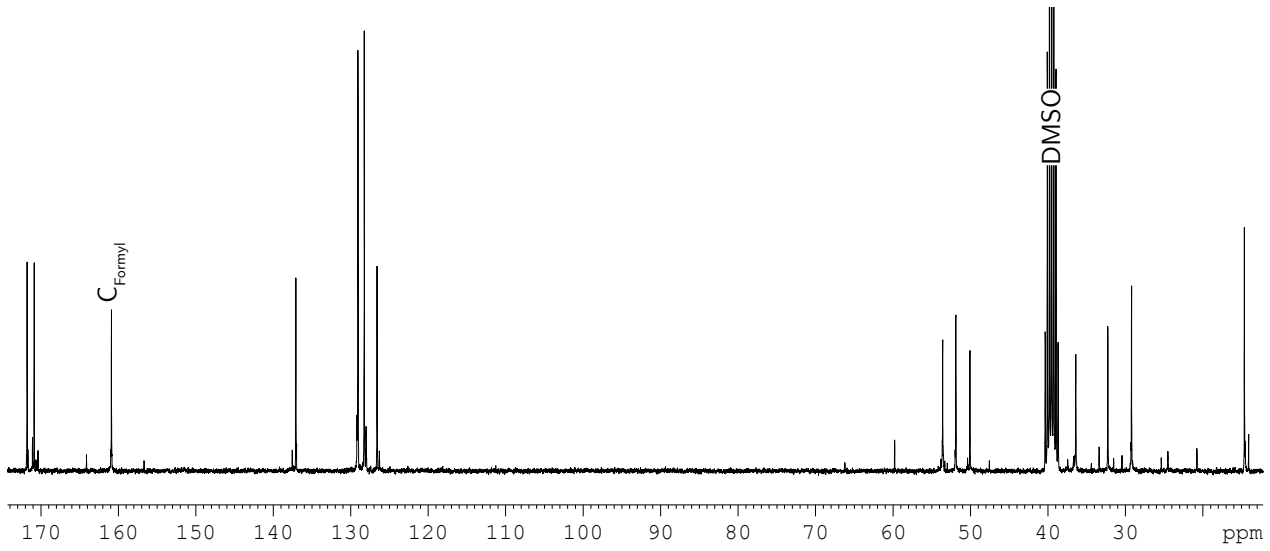

Figure C.2.: 75.45 MHz ^{13}C NMR spectrum of formyl-Met-Phe-OCH_3, the product of R_{II} - VIII. The peak corresponding to the formyl group is at 161.1 ppm (Solvent: DMSO-d_6)

C.1.3. The Stability of the formyl-Gly-Gyl Dipeptide

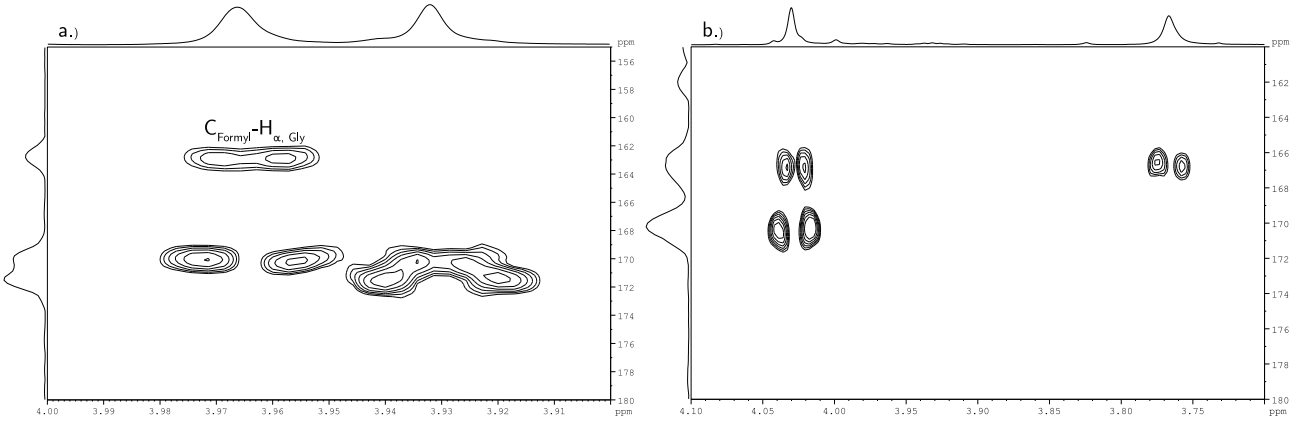

Figure C.3.: 300 MHz / 75.45 MHz HMBC NMR spectra of formyl-Gly-Gly (R_{II} - VIII) before the TFA addition (a.)) and after it (b.)). These spectra further confirm the cleavage of the formyl group upon TFA treatment, as the corresponding correlation peak vanishes. Additionally, the integrity of the peptide backbone is shown by the other correlations. (Solvent: DMSO-d_6)

C.1.4. $R_{III\,IV}$ - V: Deprotection of Leu in Solution

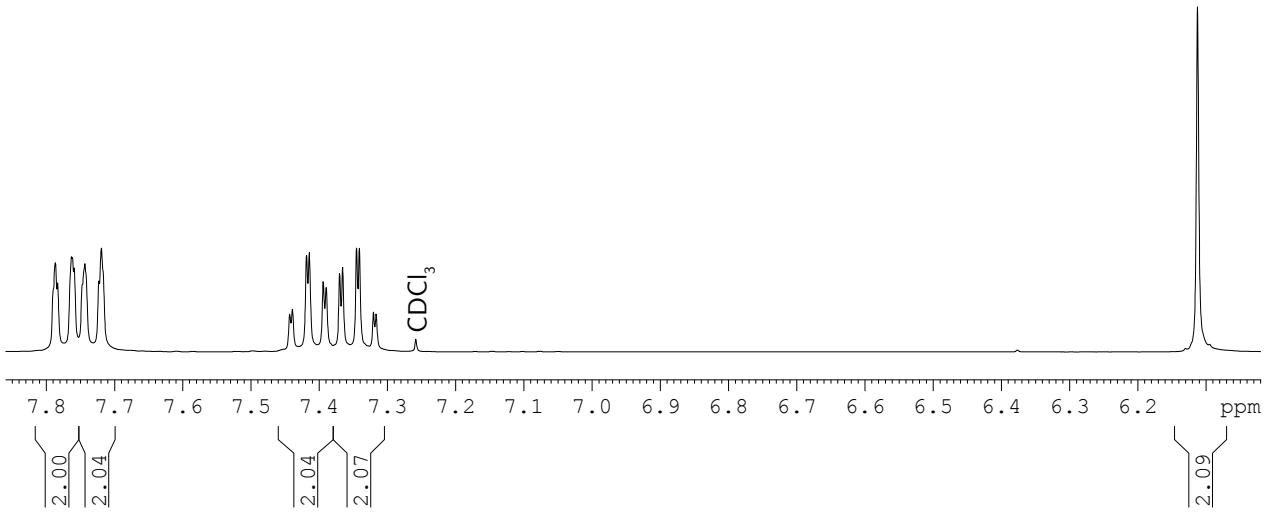

Figure C.4.: 300 MHz NMR ^{1}H spectrum of 9-Methylene-9H-flourene, the by-product of $R_{III\,IV}$ - V. This sample was not purified in any way. (Solvent: $CDCL_3$)

C.1.5. $R_{III\,IV}$ - VI: Solution Phase Coupling of Fmoc-Leu with Phe

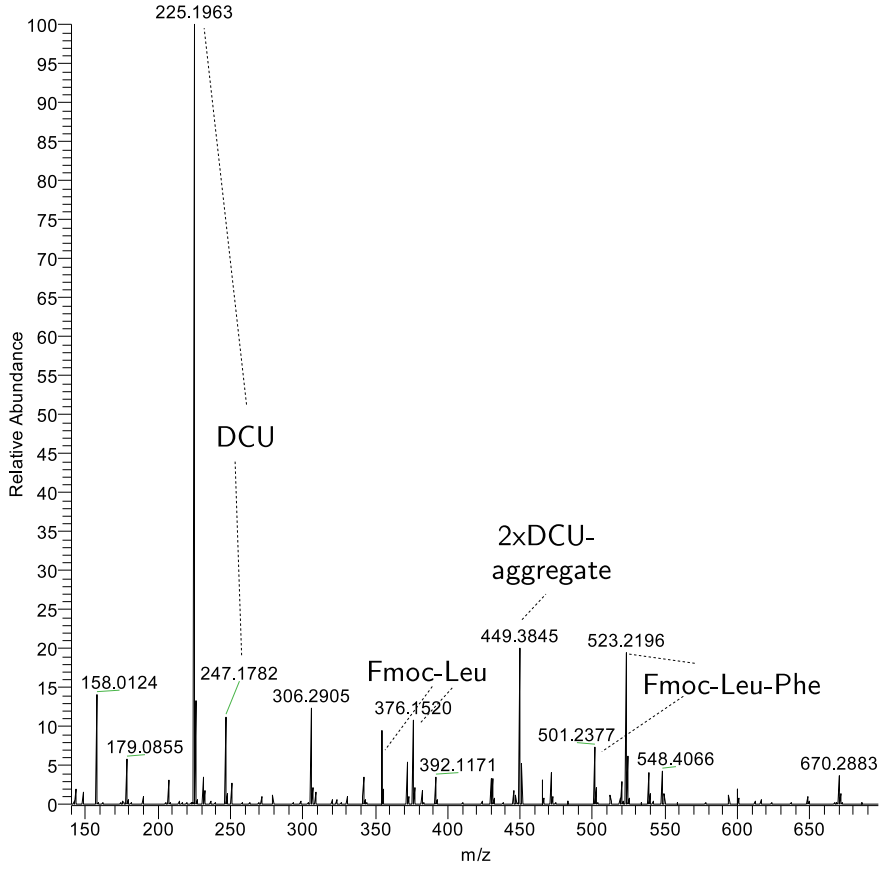

Figure C.5.: MS spectrum (ESI ion source, positive mode; qTOF mass analyser) of the crude product $R_{III\,IV}$ - VI. It contains the desired compound Fmoc-Leu-Phe as well as impurities and the educt. (Solvent: Methanol)

C.1.6. Sol - IV Solution Phase Coupling of Fmoc-Leu with Phe-OBz, Alternative procedure

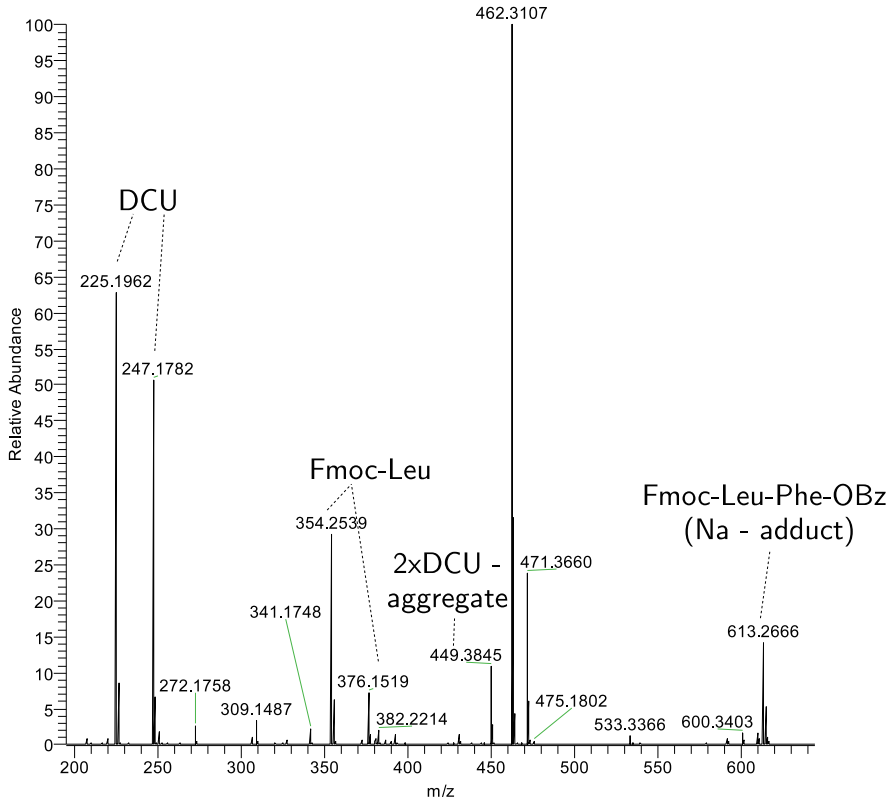

Figure C.6.: MS spectrum (ESI ion source, positive mode; qTOF mass analyser) of the crude product Sol - IV. It contains the desired compound Fmoc-Leu-Phe-OBz as well as the educt Fmoc-Leu and impurities, including the by-product DCU. (Solvent: Methanol)

D. Exemplary SIMPSON Input Scripts

D.1. $\mathcal{R}$ decoupled ^{1}H Spectroscopy - Fast Variant

```
spinsys {
channels 1H
nuclei 1H 1H
shift 1 3p 7p 1 0 0 0
shift 2 8p 3p 0.5 0 0 0
dipole 1 2 -20000 0 0 0
jcoupling 1 2 7 15 0.5 0 0 0
}
par {
spin_rate 20000
proton_frequency 500e6
crystal_file rep10
gamma_angles 5
verbose 1101
```

```
start_operator -Inz
detect_operator Inz
np 512
#Symmetry Numbers and Derived Parameters
variable n 1.0
variable N 6.0
variable ny 3.0
variable NumberPulsesRRp 6.0
variable tauRot 1.0e6/spin_rate
variable tRblock (n/N)*tauRot
variable tPulse90  tRblock/(NumberPulsesRRp*0.5)
variable tPulse360 tPulse90*4.0
variable ampPulse90 ((1/tPulse360)*1.0e6)
variable tdwell (tPulse90*6)
variable phi (180/N)*ny
sw 1.0e6/tdwell
}
proc pulseq {} {
global par
maxdt 1
 acq
 for {set j 1 } { $j < $par(np) } { incr j } {
  #R block
  pulse $par(tPulse90) $par(ampPulse90) [ expr -45 + $par(phi) ]
  pulse $par(tPulse90) $par(ampPulse90) [ expr +45 + $par(phi) ]
  pulse $par(tPulse90) $par(ampPulse90) [ expr -45 + $par(phi) ]
  #R' block
  pulse $par(tPulse90) $par(ampPulse90) [ expr +45 - $par(phi) ]
  pulse $par(tPulse90) $par(ampPulse90) [ expr -45 - $par(phi) ]
  pulse $par(tPulse90) $par(ampPulse90) [ expr +45 - $par(phi) ]
  acq
 }
}
proc main {} {
global par
 set f [fsimpson]
 fsave $f $par(name)_$par(detect_operator).fid
 fsave $f $par(name)_$par(detect_operator).dat -xreim
 funload $f
}
```

D.2. $\mathcal{R}$ decoupled ^{1}H Spectroscopy - Basic 2D Variant

```
spinsys {
channels 1H
nuclei 1H 1H
shift 1 3p 7p 1 0 0 0
shift 2 8p 3p 0.5 0 0 0
```

```
dipole 1 2 -20000 0 0 0
jcoupling 1 2 7 15 0.5 0 0 0
}
par {
spin_rate 20000
proton_frequency 500e6
crystal_file rep10
gamma_angles 5
verbose 1101
start_operator Inz
detect_operator Inp
np 1024
ni 512
sw 60000
#Symmetry Numbers and Derived Parameters
variable n 1.0
variable N 6.0
variable ny 3.0
variable NumberPulsesRRp 6.0
variable tauRot 1.0e6/spin_rate
variable tRblock (n/N)*tauRot
variable tPulse90  tRblock/(0.5*NumberPulsesRRp)
variable tPulse360 tPulse90*4.0
variable ampPulse90 ((1/tPulse360)*1.0e6)
variable tdwell 1.0e6/sw
variable tidwell 6*tPulse90
sw1 int(1.0e6/tidwell)
variable phi (180/N)*ny
variable PhaseCyclingStep 0
}
proc pulseq {} {
global par
maxdt 1
for {set j 1 } { $j <= $par(ni) } { incr j } {
 for {set s 1 } { $s <= $j } { incr s } {
  #R block
  pulse $par(tPulse90) $par(ampPulse90) [ expr -45 + $par(phi) ]
  pulse $par(tPulse90) $par(ampPulse90) [ expr +45 + $par(phi) ]
  pulse $par(tPulse90) $par(ampPulse90) [ expr -45 + $par(phi) ]
  #R' block
  pulse $par(tPulse90) $par(ampPulse90) [ expr +45 - $par(phi) ]
  pulse $par(tPulse90) $par(ampPulse90) [ expr -45 - $par(phi) ]
  pulse $par(tPulse90) $par(ampPulse90) [ expr +45 - $par(phi) ]
 }
 #Acquisition
 pulse $par(tPulse90) $par(ampPulse90) $par(PhaseCyclingStep)
 acq [ expr $par(PhaseCyclingStep) + 90 ]
```

```
 for {set i 1} {$i < $par(np)} {incr i } {
  delay $par(tdwell)
  acq
 }
reset
}
}
proc main {} {
global par
set PhasesDetectionPulse {0 90 180 270}
variable Sum
 foreach k $PhasesDetectionPulse {
  set par(PhaseCyclingStep) $k
  set f [fsimpson]
  if {$k ==  [ lindex $PhasesDetectionPulse 0 ] } {
   set Sum [ fdup $f ]
  } else {
   fadd $Sum $f
  }
  fsave $f $par(name)_$k.fid
  fsave $f $par(name)_$k.dat -xyreim
  fzerofill $f 2048 2048
  fft $f 0 0 0 0
  fsave $f $par(name)_$k.spe
  fsave $f $par(name)_$k.fdat -xyreim
  funload $f
 }
 fsave $Sum Sum_$par(name).fid
 fsave $Sum Sum_$par(name).dat -xyreim
 fzerofill $Sum 2048 2048
 fft $Sum 0 0 0 0
 fsave $Sum Sum_$par(name).spe
 fsave $Sum Sum_$par(name).fdat -xyreim
}
```

D.3. $\mathcal{R}$ decoupled ^{1}H Spectroscopy - Improved 2D variant

```
spinsys {
channels 1H 13C
nuclei   13C 1H 1H 1H
#dipolar coupling constants extracted from the crystal structure of Gly
#Heteronuclear Dipolar Couplings
#dipole 1 2 -3371.73 0 144.03 -169.9
#dipole 1 3 -23119 0 109.5 -41.066
#dipole 1 4 -23293 0 103.85 70.641
#Homonuclear Dipolar Couplimgs
dipole 2 3 -8470.6 0 57.065 -13.174
dipole 2 4 -8389.4 0 54.213 38.01
```

```
12 dipole 3 4 -23103 0 86.558 104.26
13 #13C (C_Alpha)
14 shift 1 43.21p 0p 1 0 0 0
15 #1H ( one amino H spin )
16 shift 2 28.0079p 15p 0.1 0 90 0
17 #1H (H_Alpha)
18 shift 3 23.7382p 10p 0.5 350 0 80
19 shift 4 22.6974p 8p  0.8 0 0 80
20 #C-H
21 jcoupling 1 3 130 200 0.1 20 50 0
22 jcoupling 1 4 140 200 0.2 170 120 99
23 }
24 par {
25 spin_rate 20000
26 proton_frequency 500e6
27 crystal_file rep10
28 gamma_angles 5
29 verbose 1101
30 start_operator Inz
31 detect_operator I2p+I3p+I4p
32 np 512
33 ni 512
34 sw 30000
35 variable n 1.0
36 variable N 6.0
37 variable ny 3.0
38 variable NumberPulsesRRp 6.0
39 variable tauRot 1.0e6/spin_rate
40 variable tRblock (n/N)*tauRot
41 variable tPulse90  tRblock/(0.5*NumberPulsesRRp)
42 variable tPulse360 tPulse90*4.0
43 variable ampPulse90 ((1/tPulse360)*1.0e6)
44 variable tdwell 1.0e6/sw
45 variable tidwell 6*tPulse90
46 sw1 int(1.0e6/tidwell)
47 variable phi (180/N)*ny
48 variable PhaseCyclingStep 0
49 }
50 proc pulseq {} {
51 global par
52 maxdt 1
53 for {set j 1 } { $j <= $par(ni) } { incr j } {
54  #x pulse to improve the sequence
55  pulse $par(tPulse90) $par(ampPulse90) x 0 0
56  for {set s 1 } { $s <= $j } { incr s } {
57   #R block
58   pulse $par(tPulse90) $par(ampPulse90) [ expr -45 + $par(phi) + $par(
```

```
    PhaseCyclingStep)] 0 0
  pulse $par(tPulse90) $par(ampPulse90) [ expr +45 + $par(phi) + $par(
    PhaseCyclingStep)] 0 0
  pulse $par(tPulse90) $par(ampPulse90) [ expr -45 + $par(phi) + $par(
    PhaseCyclingStep)] 0 0
  #R' block
  pulse $par(tPulse90) $par(ampPulse90) [ expr +45 - $par(phi) + $par(
    PhaseCyclingStep)] 0 0
  pulse $par(tPulse90) $par(ampPulse90) [ expr -45 - $par(phi) + $par(
    PhaseCyclingStep)] 0 0
  pulse $par(tPulse90) $par(ampPulse90) [ expr +45 - $par(phi) + $par(
    PhaseCyclingStep)] 0 0
 }
 #-y pulse to improve the sequence
 pulse $par(tPulse90) $par(ampPulse90) -y 0 0
 #-x pulse in front of the detection pulse
 pulse $par(tPulse90) $par(ampPulse90) -x 0 0
 #Acquisition
 pulse $par(tPulse90) $par(ampPulse90) $par(PhaseCyclingStep) 0 0
 acq [ expr $par(PhaseCyclingStep) + 90 ]
 for {set i 1} {$i < $par(np)} {incr i } {
  delay $par(tdwell)
  acq [ expr $par(PhaseCyclingStep) + 90 ]
 }
 reset
}
}
proc main {} {
global par
set PhasesDetectionPulse {0 90 180 270}
variable Sum
foreach k $PhasesDetectionPulse {
 set par(PhaseCyclingStep) $k
 set f [fsimpson]
 if {$k ==  [ lindex $PhasesDetectionPulse 0 ] } {
  set Sum [ fdup $f ]
 } else {
  fadd $Sum $f
 }
 faddlb $f 1 0 1 0
 fsave $f $par(name)_$k.fid
 fsave $f $par(name)_$k.dat -xyreim
 #fzerofill $f 1024 512
 fft $f 0 0 0 0
 fsave $f $par(name)_$k.spe
 fsave $f $par(name)_$k.fdat -xyreim
 funload $f
```

```
}
faddlb $Sum 1 0 1 0
fsave $Sum Sum_$par(name).fid
fsave $Sum Sum_$par(name).dat -xyreim
#fzerofill $Sum 1024 512
fft $Sum 0 0 0 0
fsave $Sum Sum_$par(name).spe
fsave $Sum Sum_$par(name).fdat -xyreim
}
```

D.4. $\mathcal{R}$ decoupled ^{13}C Spectroscopy

See *Section 3.2.1.1.*

D.5. $\mathcal{R}$ decoupled INEPT

```
spinsys {
channels 1H 13C
nuclei   13C 1H 1H
dipole 1 2 -23119 0 109.5 -41.066
dipole 1 3 -23293 0 103.85 70.641
 #heteronuclear dipolar coupling is switched off:
#dipole 2 3 -23103 0 86.558 104.26
#13C
shift 1 43.21p 0 0 0 0 0
#1H
shift 2 23.7382p 0 0 0 0 0
shift 3 22.6974p 0 0 0 0 0
#C-H
jcoupling 1 2 140 0 0 0 0 0
jcoupling 1 3 140 0 0 0 0 0
}
par {
spin_rate 17920.0
proton_frequency 500e6
crystal_file rep168
gamma_angles 8
verbose 1101
start_operator I2z+I3z
detect_operator I2p
np 1024
sw 20000
}
proc pulseq {} {
global par
maxdt 1
pulseid $par(tpulse90) $par(PulseAmp) x 0 0
  #first R decoupling block
```

```
  for { set o 1} { $o <= $par(i) } { incr o } {
   for { set d 1  } { $d <= [ expr $par(N)/2 ] } { incr d } {
    #R
    pulse $par(tpulse90) $par(PulseAmp) [ expr -45 + $par(phi) ] 0 0
    pulse $par(tpulse90) $par(PulseAmp) [ expr +45 + $par(phi) ] 0 0
    pulse $par(tpulse90) $par(PulseAmp) [ expr -45 + $par(phi) ] 0 0
    #R'
    pulse $par(tpulse90) $par(PulseAmp) [ expr +45 + $par(phi) ] 0 0
    pulse $par(tpulse90) $par(PulseAmp) [ expr -45 + $par(phi) ] 0 0
    pulse $par(tpulse90) $par(PulseAmp) [ expr +45 + $par(phi) ] 0 0
   }
  }
pulseid $par(tpulse180) $par(PulseAmp) x $par(PulseAmp) x
  #Second R decoupling block
  for { set m 1} { $m <= $par(i) } { incr m } {
   for { set p 1  } { $p <= [ expr $par(N)/2 ] } { incr p } {
    #R
    pulse $par(tpulse90) $par(PulseAmp) [ expr -45 + $par(phi) ] 0 0
    pulse $par(tpulse90) $par(PulseAmp) [ expr +45 + $par(phi) ] 0 0
    pulse $par(tpulse90) $par(PulseAmp) [ expr -45 + $par(phi) ] 0 0
    #R'
    pulse $par(tpulse90) $par(PulseAmp) [ expr +45 + $par(phi) ] 0 0
    pulse $par(tpulse90) $par(PulseAmp) [ expr -45 + $par(phi) ] 0 0
    pulse $par(tpulse90) $par(PulseAmp) [ expr +45 + $par(phi) ] 0 0
   }
  }
pulseid $par(tpulse90) $par(PulseAmp) y $par(PulseAmp) y
  #Acquisition
  turnoff dipole_1_2 dipole_1_3
  acq
  for {set q 1} {$q < $par(np)} {incr q } {
    delay $par(tdwell)
    acq
  }
  turnon dipole_1_2 dipole_1_3
}
proc main {} {
global par
global spinsys
#for { set ll 0 } { $ll < 501 } { incr ll } {
set par(tdwell) [ expr 1.0e6 /$par(sw) ]
set par(JCH) [ lindex $spinsys(jcoupling) 2 ]
set par(tauOriginal) [ expr  (1.0 / (2.0*double($par(JCH))))*1.0e6 ]
set par(N) 6.0
set par(n) 1.0
set par(ny) 3.0
set par(PulsesPerR) 3.0
```

```
set par(taurot) [ expr (1.0/$par(spin_rate))*1.0e6 ]
set par(tpulse90) [ expr ($par(taurot)*($par(n)/$par(N))) / $par(PulsesPerR) ]
set par(tpulse180) [ expr 2.0*$par(tpulse90) ]
set par(PulseAmp) [ expr 1.0/ (2*$par(tpulse180)*1.0e-6)]
set par(phi) [ expr (180.0/$par(N))*$par(ny) ]
 #Number of Full R sequences during tau/2
set par(i) 176
set par(WholeTau) [ expr 2*6*$par(tpulse90)*($par(N)/2)*$par(i)+$par(tpulse180)
   ]
set par(detection) { I2p+I3p I1p }
for {set jj  0 } { $jj < 2 } { incr jj } {
 set par(detect_operator) [ lindex $par(detection) $jj ]
 set f [fsimpson]
 faddlb $f 10 0
 fsave $f $par(name)_np$par(np)_$par(detect_operator)_Ieff$par(i).dat -xreim
 fsave $f $par(name)_np$par(np)_$par(detect_operator)_Ieff$par(i).fid
 #fzerofill $f 512 512
 fft $f
 fsave $f $par(name)_np$par(np)_$par(detect_operator)_Ieff$par(i).fdat -xreim
 fsave $f $par(name)_np$par(np)_$par(detect_operator)_Ieff$par(i).spe
 funload $f
}
}
```